

**THE CHARACTERIZATION OF ACETONE FRACTIONATED AND  
UNFRACTIONATED, CHEMICALLY MODIFIED LIGNIN-ECOFLEX™  
THERMOPLASTIC BLENDS**

by

Kim Bessler

B.Sc., Colorado School of Mines, 2018

A THESIS SUBMITTED IN PARTIAL FULFILLMENT OF  
THE REQUIREMENTS FOR THE DEGREE OF

MASTER OF APPLIED SCIENCE

in

THE FACULTY OF GRADUATE AND POSTDOCTORAL STUDIES  
(Forestry)

THE UNIVERSITY OF BRITISH COLUMBIA  
(Vancouver)

May 2021

© Kim Bessler, 2021

The following individuals certify that they have read, and recommend to the Faculty of Graduate and Postdoctoral Studies for acceptance, the thesis entitled:

The Characterization of Acetone Fractionated and Unfractionated, Chemically Modified  
Lignin-Ecoflex™ Thermoplastic Blends

---

submitted by Kim Bessler in partial fulfillment of the requirements for

the degree of Master of Applied Science

---

in Forestry

---

**Examining Committee:**

Scott Renneckar, Professor, Faculty of Forestry, UBC  
Supervisor

Emily Cranston, Professor, Faculty of Forestry, UBC  
Supervisory Committee Member

Feng Jiang, Professor, Faculty of Forestry, UBC  
Supervisory Committee Member

Johan Foster, Professor, Chemical and Biological Engineering, UBC  
Additional Examiner

## Abstract

There is a growing demand to replace non-renewable fossil-based materials like many one use plastics with renewably sourced alternatives that fit within the circular bioeconomy model and demonstrate a favourable end of life. One such option is lignin, found in all woody plants with its desirable aromatic polymeric structure and potential utilization as a byproduct in the pulping and paper industry. However, complications arise because of lignins' complex non-uniform heterogenous structure which is often remedied through harsh carcinogenic chemical pathways. In this study softwood kraft lignin was fractionated in a one step process using acetone, modified first with ethylene carbonate, then with propionic acid, and finally melt-blended with completely biodegradable Ecoflex<sup>TM</sup> in order to develop an alternative to thermoplastics like non-degradable polyethylene and polypropylene.

The acetone fractionation separated the lignin by molecular weight. The reaction with ethylene carbonate etherified the lignin creating a more uniform structure. Finally, the reaction with propionic acid esterified the lignin thus masking reactive hydroxyl groups. Nine lignin powders ready for blend with Ecoflex<sup>TM</sup> were developed using green chemistry practices: unfractionated (UF), acetone soluble (ASKL) and acetone insoluble (AIKL) fractions each unmodified (UN) and modified via hydroxyethyl ether (HE) and esterification (E).

The lignin samples were melt-blended, extruded, mould injected and underwent extensive tensile testing to determine how each fraction with or without modification behaved in comparison to the as received softwood kraft lignin. In addition, detailed thermal and structural testing was carried out using DSC, TGA, and FT-IR analysis. The acetone soluble fraction without modification (ASKL\_UN) increased the tensile properties (tensile strength and toughness) at lower lignin loadings (5-10 wt%) in comparison to neat Ecoflex<sup>TM</sup> and the acetone

insoluble fraction. The acetone soluble esterified lignin (ASKL\_E) maintained tensile properties up to a 40 wt% lignin loading in comparison to neat Ecoflex<sup>TM</sup> and the acetone insoluble fraction.

In summary, this work used green chemistry practices to develop lignins that were processible with the biodegradable polyester Ecoflex<sup>TM</sup> and found an improvement in tensile properties. This has great implication in valorizing lignin-based polymeric materials as this work showed a simple acetone fractionation is capable of improving mechanical properties.



## Lay Summary

Lignin is a renewable aromatic polymer found in all woody plants. As plastic pollution issues climax, lignin based plastics have gained attention as an alternative to petroleum based plastics. However, a deeper understanding of how fractionated modified lignin behaves in melt-processed blends with polyesters like biodegradable Ecoflex<sup>TM</sup> in comparison to their unfractionated unmodified counterparts is necessary for valorization. Here, we develop a process which follows the principles of green chemistry and blends different lignins at varying weight percentages with Ecoflex<sup>TM</sup> to determine how the thermal and mechanical properties of the subsequent thermoplastic blends are affected. We found that the unmodified lower molecular weight fraction improved the tensile properties of Ecoflex<sup>TM</sup>, while the lower molecular weight esterified lignin showed great potential in blend with Ecoflex<sup>TM</sup>. This may extend the working knowledge of lignins behavior in two system polymeric blends and help to alleviate the excessive use of non-renewable resources like petroleum.

## Preface

With the guidance of my supervisor (Scott Renneckar), all of the research work reported in this thesis was planned, conducted, and analyzed by Kim Bessler in the Advanced Renewable Materials Lab in the Wood Science department of the Faculty of Forestry at University of British Columbia, Vancouver campus with only minor exceptions. In chapter 4.1, Liyang Liu advised me on experimental set up and  $^{31}\text{P}$  NMR protocols, and Mijung Cho and Muzaffer Karaaslan advised me on DSC, TGA and FT-IR protocol. The GPC testing in chapter 4.1 was performed by Liyang Liu who ran samples that I prepared and provided data that I analyzed. The SEM in chapter 4.2 was performed by Muzaffer Karaaslan who imaged samples I prepared. The  $^{13}\text{C}$  NMR in Appendix B was performed under the supervision of Liyang Liu and Qi Hua. A version of chapter 3.5.1 has been published in the European Polymer Journal as indicated below. Liyang Liu was the lead investigator, responsible for all major areas of concept formation, experimental design, and manuscript composition. Siwei Chen, Mijung Cho, Qi Hua, and myself contributed to data collection and analysis under the supervision of Liyang Liu and Scott Renneckar.

Liu, L.U., Bessler, K., Chen, S., Cho, M.J., Hua, Q., and Renneckar, S., (2020). In-situ real time monitoring of hydroxyethyl modification in obtaining uniform lignin derivatives. *Eur. Polym. J.*:

1-10

## Table of Contents

<b>Abstract.....</b>	<b>iii</b>
<b>Lay Summary .....</b>	<b>v</b>
<b>Preface.....</b>	<b>vi</b>
<b>Table of Contents .....</b>	<b>vii</b>
<b>List of Tables .....</b>	<b>xiv</b>
<b>List of Figures.....</b>	<b>xvii</b>
<b>List of Abbreviations .....</b>	<b>xxx</b>
<b>Acknowledgements .....</b>	<b>xxxiv</b>
<b>Dedication .....</b>	<b>xxxv</b>
<b>Chapter 1: Introduction .....</b>	<b>1</b>
1.1    Thesis objectives .....	2
<b>Chapter 2: Literature review .....</b>	<b>5</b>
2.1    Lignin.....	5
2.1.1    Biosynthesis and structure .....	5
2.1.2    Softwood and hardwood .....	10
2.1.3    Structure and function.....	13
2.1.4    Chemical pulping .....	14
2.1.4.1    Organosolv .....	15
2.1.4.2    Soda.....	17
2.1.4.3    Sulfite .....	18
2.1.4.4    Kraft .....	19

vii

2.1.4.4.1	Advances in extraction techniques of lignin from black liquor .....	23
2.1.5	Molecular weight and thermal properties of technical lignins.....	24
2.1.6	Lignin compostability .....	25
2.1.7	Lignin potential .....	26
2.2	Petroleum based synthetic polymers.....	26
2.2.1	The basics.....	26
2.2.2	Statistics .....	28
2.2.3	Toxicity .....	29
2.2.4	Plastic ban in Canada .....	32
2.2.5	Ecoflex <sup>TM</sup> .....	33
2.2.5.1	Biodegradability.....	35
2.2.6	Potential for biobased thermoplastic blends .....	36
2.3	Modifications for technical lignin utilization .....	36
2.3.1	Fractionation .....	37
2.3.1.1	Single step solvent extraction .....	39
2.3.1.2	Sequential solvent extraction .....	42
2.3.2	Chemical modification.....	45
2.3.2.1	Lignin depolymerization.....	46
2.3.2.2	New active sites .....	48
2.3.2.2.1	Hydroxyalkylation.....	48
2.3.2.2.2	Nitration .....	50
2.3.2.2.3	Amination.....	51
2.3.2.2.4	Other methods .....	52

2.3.2.2.5	Modification of existing hydroxyl groups.....	54
2.3.2.2.6	Esterification .....	54
2.3.2.2.7	Etherification.....	61
2.4	Polymeric lignin blends for thermoplastic materials .....	68
2.4.1	Early work.....	69
2.4.2	Recent work .....	71
2.4.3	Key studies.....	73
2.4.4	Green solutions .....	80
<b>Chapter 3: Materials and methods.....</b>		<b>81</b>
3.1	Materials .....	81
3.2	Preparation of as received technical lignin .....	81
3.3	Acetone fractionation of technical lignin.....	82
3.4	Elemental analysis .....	83
3.5	Synthesis of technical hydroxyethyl lignin.....	83
3.5.1	Real time control.....	84
3.6	Synthesis of esterified technical lignin .....	86
3.7	<sup>31</sup> P NMR characterization of unmodified and modified technical lignin powders.....	88
3.7.1	Sample preparation .....	88
3.7.2	Sample analysis.....	89
3.8	As received Ecoflex™ F blend C1200 .....	89
3.8.1	Storage .....	90
3.8.2	Characterization using <sup>13</sup> C NMR.....	91
3.9	Preparation of lignin-Ecoflex™ thermoplastic blends .....	91

3.9.1	Melt compounding .....	92
3.9.2	Mould injection .....	96
3.9.3	Mechanical testing .....	96
3.9.3.1	Sample measurements .....	97
3.9.3.2	Tensile testing .....	98
3.9.3.3	Quantitative data analysis .....	99
3.10	Differential scanning calorimetry (DSC) analysis .....	99
3.10.1	Lignin powders .....	100
3.10.2	Lignin-Ecoflex™ thermoplastic blends .....	100
3.10.2.1	Degree of crystallinity .....	101
3.11	Thermal gravimetric analysis (TGA) .....	102
3.12	Fourier – transform infrared spectroscopy (FT-IR) .....	102
3.13	Gel permeation chromatography (GPC) analysis .....	103
3.13.1	Sample preparation .....	103
3.13.2	Sample analysis .....	103
3.14	Scanning electron microscopy (SEM) .....	104
<b>Chapter 4: Results and discussion .....</b>		<b>105</b>
4.1	Characterization of technical lignin powders for thermoplastic blends .....	105
4.1.1	Background .....	105
4.1.2	Acetone fractionation of grade A Lignoforce™ softwood kraft lignin .....	105
4.1.2.1	T <sub>g</sub> of lignin as a function of molecular weight and chemical functionality ....	112
4.1.2.2	Thermal degradation of fractionated moieties .....	116
4.1.2.3	FT-IR analysis of fractionated and unfractionated lignin powders .....	118

4.1.3	Hydroxyethyl ether modification of fractionated and unfractionated lignins.....	120
4.1.3.1	Background .....	120
4.1.3.2	Molecular weight and chemical functionality of HE lignin fractions.....	121
4.1.3.3	FT-IR structural analysis of HE lignin powders .....	123
4.1.3.4	T <sub>g</sub> for HE lignin derivatives .....	127
4.1.3.5	Thermal degradation for HE lignin derivatives .....	128
4.1.4	Esterification of hydroxyethyl ether lignin powders .....	130
4.1.4.1	Background .....	130
4.1.4.2	Molecular weight and chemical functionality of esterified lignin fractions ...	131
4.1.4.3	FT-IR structural analysis of esterified HE lignin powders .....	132
4.1.4.4	T <sub>g</sub> reduction for esterified HE lignin powders .....	136
4.1.4.5	Thermal degradation for esterified lignin powders.....	139
4.1.5	Concluding remarks .....	143
4.2	Characterization of lignin-Ecoflex <sup>TM</sup> thermoplastic blends .....	144
4.2.1	Background .....	144
4.2.2	Tensile properties of lignin-Ecoflex <sup>TM</sup> thermoplastic blends .....	145
4.2.2.1	Ultimate tensile strength (UTS) .....	145
4.2.2.2	Young's modulus (E) .....	151
4.2.2.3	Elongation at break .....	155
4.2.2.4	Toughness .....	158
4.2.3	Analysis of tensile properties of lignin-Ecoflex <sup>TM</sup> thermoplastic blends .....	163
4.2.3.1	Unmodified lignin-Ecoflex <sup>TM</sup> thermoplastic blends .....	166
4.2.3.2	Hydroxyethyl ether lignin-Ecoflex <sup>TM</sup> thermoplastic blends .....	174

4.2.3.3	Esterified lignin-Ecoflex™ thermoplastic blends.....	176
4.2.4	Thermal properties of lignin-Ecoflex™ blends .....	182
4.2.4.1	Degree of crystallinity.....	200
4.2.4.2	Thermogravimetric analysis of lignin-Ecoflex™ blends.....	205
4.2.5	Fourier transform infrared spectroscopy for thermoplastic blends.....	207
4.2.6	Melt processing temperature comparison for ASKL_E – Ecoflex™ blends.....	217
4.2.7	Mechanical property comparison of lignin thermoplastic blends.....	222
4.2.8	Concluding highlights.....	225
<b>Chapter 5: Conclusions and future work .....</b>		<b>226</b>
5.1	Conclusions.....	226
5.2	Future work.....	229
5.2.1	Acetone soluble unmodified and esterified lignin-Ecoflex™ films .....	229
5.2.2	Small angle X-ray scattering of developed thermoplastic blends.....	229
5.2.3	Biodegradation testing .....	230
5.2.4	Improving lignin powder chemistries .....	230
5.2.5	Techno-economic analysis.....	230
5.2.6	Crystallization kinetics of lignin-Ecoflex™ thermoplastic blends.....	230
5.2.7	Carbon spun fibres from acetone insoluble lignin fraction.....	231
<b>Bibliography .....</b>		<b>232</b>
<b>Appendices.....</b>		<b>258</b>
Appendix A Supporting calculations .....		258
A.1	Moisture content .....	258
A.2	Ethylene carbonate.....	258



A.3	Real time control.....	259
A.4	<sup>31</sup> P NMR functional groups .....	260
Appendix B	<sup>13</sup> C NMR spectrum for as received Ecoflex™ blend F C1200.....	261
Appendix C	Melt processing equipment and sample imagery .....	262

## List of Tables

Table 1 Relative frequencies <sup>a</sup> of common linkages in softwood and hardwood lignin.....	8
Table 2 General classification of technical lignins adapted from ref. <sup>37</sup> .....	15
Table 3 Chemical linkages and functional groups of milled wood lignin (MWL) and different technical lignins per 100 Ar <sup>37,54–58,59</sup> .....	22
Table 4 Characteristics for oxidized and unoxidized black liquor in the Lignoforce <sup>TM</sup> process <sup>62,63</sup> .....	24
Table 5 M <sub>w</sub> , M <sub>n</sub> , PDI, and T <sub>g</sub> of technical lignins using similar light scattering techniques <sup>58, 59, 61- 65</sup> .....	25
Table 6 Mechanical property comparison for Ecoflex and low-density polyethylene for a 50 μm blown film using similar standardized test methods <sup>93-98</sup> .....	34
Table 7 Physical properties and toxicity of commonly used organic solvents in lignin fractionation methods <sup>118-120</sup> .....	44
Table 8 Reaction details for new chemical active sites added to technical lignin.....	53
Table 9 Mechanical property literature comparison of lignin based thermoplastic blends .....	76
Table 10 Elemental composition of SWKL and its acetone fractionated counterparts .....	83
Table 11 Composition of lignin-Ecoflex <sup>TM</sup> thermoplastic blends .....	92
Table 12 Type V sample measurements following standard dimensions.....	98
Table 13 Molecular weight (GPC), functional group content ( <sup>31</sup> P NMR), and thermal properties (DSC and TGA) for unfractionated (UF), acetone soluble (ASKL), acetone insoluble (AIKL), unmodified (UN), hydroxyethyl ether (HE), and esterified (E), lignin powders.....	108

Table 14 The ultimate tensile strength of neat Ecoflex <sup>TM</sup> (ECO) and the percent increase (+) or decrease (-) of the nine lignin powders loaded in melt (5-40 wt%) in comparison to the Ecoflex <sup>TM</sup> control.....	163
Table 15 The Young's modulus of neat Ecoflex <sup>TM</sup> (ECO) and the percent increase (+) or decrease (-) of the nine lignin powders loaded in melt (5-40 wt%) in comparison to the Ecoflex <sup>TM</sup> control.....	163
Table 16 The total percent elongation at break of neat Ecoflex <sup>TM</sup> (ECO) and the percent increase (+) or decrease (-) of the nine lignin powders loaded in melt (5-40 wt%) in comparison to the Ecoflex <sup>TM</sup> control.....	164
Table 17 The toughness of neat Ecoflex <sup>TM</sup> (ECO) and the percent increase (+) or decrease (-) of the nine lignin powders loaded in melt (5-40 wt%) in comparison to the Ecoflex <sup>TM</sup> control ....	164
Table 18 DSC results of neat Ecoflex <sup>TM</sup> (ECO) and unfractionated (UF) unmodified (UN), hydroxyethyl ether (HE), and esterified (E) lignin-Ecoflex <sup>TM</sup> blends at different lignin loadings (wt %)......	182
Table 19 DSC results of neat Ecoflex <sup>TM</sup> (ECO) and acetone soluble (ASKL) unmodified (UN), hydroxyethyl ether (HE), and esterified (E) lignin-Ecoflex <sup>TM</sup> blends at different lignin loadings (wt %)......	183
Table 20 DSC results of neat Ecoflex <sup>TM</sup> (ECO) and acetone insoluble (AIKL) unmodified (UN), hydroxyethyl ether (HE), and esterified (E) lignin-Ecoflex <sup>TM</sup> blends at different lignin loadings (wt %)......	183
Table 21 TGA data for acetone soluble unmodified and esterified lignin powders (ASKL_UN and ASKL_E) and acetone insoluble esterified lignin powder (AIKL_E) at a 30 wt% lignin loading in comparison to neat Ecoflex <sup>TM</sup> (ECO).....	205

Table 22 DSC results for neat Ecoflex <sup>TM</sup> (ECO) and acetone soluble esterified lignin (ASKL_E) blended from 5-30 wt% lignin loading at 135 °C and 180 °C melt processing temperatures ....	220
Table 23 Literature comparison of the Ultimate tensile strength (UTS) of lignin-Polymer blends .....	223
Table 24 Chemical shifts used for qualitative <sup>31</sup> P NMR analysis of lignin functional groups...	260

## List of Figures

Figure 1 Overview of the three step chemical process used to make lignin powders for melt processed thermoplastic blend with Ecoflex <sup>TM</sup> ; acetone fraction (1) etherification using ethylene carbonate (2) and esterification using propionic acid (3) .....	3
Figure 2 Mechanical properties analysis of lignin-Ecoflex <sup>TM</sup> thermoplastic blends begins with extrusion and mould injection.....	4
Figure 3 Basic lignin monomeric units or lignin precursors <sup>8-11</sup> .....	6
Figure 4 Example of resonance stabilized coniferyl monolignol radicals <sup>9</sup> .....	7
Figure 5 Common linkages found in softwood and hardwood lignin <sup>8, 11, 18</sup> .....	9
Figure 6 Schematic of a softwood lignin structure Reprinted with permission from ref <sup>7</sup> Copyright 2010 American Chemical Society .....	12
Figure 7 Schematic of a hardwood lignin structure Reprinted with permission from ref <sup>7</sup> Copyright 2010 American Chemical Society .....	12
Figure 8 Petrochemicals obtained from fossil fuels after oil refining and the materials they produce <sup>70</sup> .....	28
Figure 9 The Ecoflex <sup>TM</sup> copolymer composed of the three monomers 1,4-butanediol, terephthalic acid, and adipic acid <sup>92,93</sup> .....	33
Figure 10 Overview flow chart for technical lignins that either undergo or do not undergo chemical .....	46
Figure 11 Scheme for hydroxymethylation of lignin using formaldehyde to make LPF wood adhesives Reprinted with permission from ref <sup>130</sup> Copyright 2019 Royal Society of Chemistry.	49

Figure 12 Lignin nitration scheme using tetranitromethane or nitric acid with acetic anhydride Reprinted with permission from ref <sup>65</sup> Copyright 2016 Royal Society of Chemistry .....	50
Figure 13 Lignin amination scheme using formaldehyde and dimethylamine Reprinted with permission from ref <sup>65</sup> Copyright 2016 Royal Society of Chemistry .....	51
Figure 14 Esterification reaction of lignin with acetic anhydride via nucleophilic substitution Reprinted with permission from ref <sup>130</sup> Copyright 2019 Royal Society of Chemistry .....	55
Figure 15 Greener solvent and catalyst free lignin esterification compared to traditional lignin esterification involving toxic reagents, solvents, and catalysts Reprinted with permission from ref <sup>153</sup> Copyright 2019 Royal Society of Chemistry .....	61
Figure 16 Oxypropylation reaction involving lignin and propylene oxide and the hazard rating of PO Reprinted with permission from ref <sup>161</sup> Copyright 2012 American Chemical Society .....	63
Figure 17 Methylation of softwood kraft lignin using dimethyl sulfate (a) and methyl iodide (b) where L represents lignin <sup>162</sup> .....	64
Figure 18 Cyclic carbonate structures and the nomenclature of the carbonate ring; ethylene carbonate (EC), propylene carbonate (PC), vinyl ethylene carbonate (VEC), and glycerol carbonate (GC) <sup>166</sup> .....	66
Figure 19 Potential reactions between ethylene carbonate and deprotonated hydroxyl functional groups Reprinted with permission from ref <sup>167</sup> Copyright 2018 American Chemical Society.....	67
Figure 20 Real time control laboratory set-up schematic .....	85
Figure 21 As received Ecoflex <sup>TM</sup> F blend C1200 lens pellets with average diameter .....	90
Figure 22 Effect of extruder torque on melt stability at a 30 wt% lignin loading for unfractionated and acetone fractionated unmodified lignins (UF_UN and ASKL_UN) (a) hydroxyethyl ether lignins (UF_HE, ASKL_HE and AIKL_HE) (b) and esterified lignins (UF_E,	

ASKL_E and AIKL_E (c) Neat Ecoflex™ (ECO) is the baseline reference and time 0 minutes is when lignin is added to the top feeder .....	95
Figure 23 ASTM D638-14 standard type V dumbbell shape dimensions <sup>195</sup> .....	97
Figure 24 GPC traces of unfractionated (UF), acetone soluble (ASKL), and acetone insoluble (AIKL) lignin fractions for unmodified (UN) (a), hydroxyethyl ether (HE) (b), and esterified (E) (c) lignin powders .....	106
Figure 25 <sup>31</sup> P NMR spectra for unfractionated, acetone soluble, and acetone insoluble unmodified (UF_UN, ASKL_UN, AIKL_UN) lignin powders (a) and accompanying quantitative functional group content (b).....	109
Figure 26 A schematic of the chemical structure of acetone soluble softwood kraft lignin (a) and acetone insoluble softwood kraft lignin (b) shows a difference in fragmented portions of pulped moieties, hydroxyl content and molecular weight Reprinted with permission from ref <sup>205</sup> Copyright 2017 Royal Society of Chemistry .....	112
Figure 27 The glass transition temperatures for unmodified (UN) acetone insoluble (AIKL), unmodified unfractionated (UF), and unmodified acetone soluble (ASKL) lignin powders (a) and the correlating DSC curves (b) .....	113
Figure 28 Linear relationships between aromatic hydroxyl functional groups ArOH and glass transition temperature T <sub>g</sub> (a) aliphatic hydroxyl functional groups AlOH and T <sub>g</sub> (b) number average molecular weight M <sub>n</sub> and T <sub>g</sub> (c) and the classic Flory-Fox relationship (d) for unfractionated unmodified (UF_UN), acetone soluble unmodified (ASKL_UN), and acetone insoluble unmodified (AIKL_UN) lignin powders.....	115
Figure 29 TGA analysis for unfractionated unmodified (UF_UN), acetone soluble unmodified (ASKL_UN), and acetone insoluble unmodified (AIKL_UN) lignin powders weight % loss	

curves (a) maximum derivative weight % as a function of temperature curves (b) average values with standard deviation error bars for  $T_{D5\%}$  (c)  $T_{max}$  (d) and char yield (e)..... 117

Figure 30 FT-IR spectrum for unmodified unfractionated (UF\_UN), acetone soluble (ASKL\_UN), and acetone insoluble (AIKL\_UN) softwood kraft lignins (a) the lignin fingerprint region (b) and zoomed in signals at  $1454\text{ cm}^{-1}$  and  $1079\text{ cm}^{-1}$  with absorbance readings (c).... 119

Figure 31  $^{31}\text{P}$  NMR spectra for hydroxyethyl ether unfractionated UF\_HE, acetone soluble ASKL\_HE and acetone insoluble AIKL\_HE lignin powders (a) the amount (mmol/g) of aliphatic hydroxyl groups (AlOH) present in each fraction (b) and the spectra plot for all nine lignin powders (c)..... 122

Figure 32 FT-IR spectra for unfractionated unmodified (UF\_UN) and unfractionated hydroxyethyl ether (UF\_HE) (a) acetone soluble unmodified (ASKL\_UN) and acetone soluble hydroxyethyl ether (ASKL\_HE) (b) acetone insoluble (AIKL\_UN) and acetone insoluble hydroxyethyl ether (AIKL\_HE) (c) and the carbonate linkages at  $1740\text{ cm}^{-1}$  (1) and aryl-alkyl ether formation at  $1000\text{--}1270\text{ cm}^{-1}$  (2)..... 126

Figure 33 The glass transition temperatures for unmodified (UN) and hydroxyethyl ether (HE), acetone insoluble (AIKL), unfractionated (UF), and acetone soluble (ASKL) lignin powders (a) and the correlating DSC curves (b)..... 127

Figure 34 TGA analysis for unfractionated hydroxyethyl ether (UF\_HE), acetone soluble hydroxyethyl ether (ASKL\_HE), and acetone insoluble hydroxyethyl ether (AIKL\_HE) lignin powders weight % loss curves (a) maximum derivative weight % as a function of temperature curves (b) average values with standard deviation error bars for  $T_{D5\%}$  (c)  $T_{max}$  (d) and char yield (e) ..... 129



Figure 35 The complete chemical reaction with conditions, where step one is the etherification of lignin fractions using ethylene carbonate and step two is the esterification of the synthesized HE lignin powders using propionic acid .....	131
Figure 36 Complete FT-IR spectra for unfractionated (UF) (a) acetone soluble (ASKL) (b) and acetone insoluble (AIKL) (c) unmodified (UN), hydroxyethyl ether (HE), and esterified (E) lignin powders.....	133
Figure 37 FT-IR spectra for unfractionated unmodified (UF_UN), unfractionated hydroxyethyl ether (UF_HE) and unfractionated esterified (UF_E) (a) acetone soluble unmodified (ASKL_UN) , acetone soluble hydroxyethyl ether (ASKL_HE) and acetone soluble esterified (ASKL_E) (b) acetone insoluble (AIKL_UN), acetone insoluble hydroxyethyl ether (AIKL_HE) and acetone insoluble esterified (AIKL_E) (c) and the ester bond signal increase at $1740\text{ cm}^{-1}$ (1) and C-O expansion in ester groups at $1000\text{-}1300\text{ cm}^{-1}$ (2) .....	135
Figure 38 The glass transition temperatures for unmodified (UN), hydroxyethyl ether (HE), and esterified (E) acetone insoluble (AIKL), unfractionated (UF), and acetone soluble (ASKL) lignin powders (a) and the correlating DSC curves (b).....	137
Figure 39 DSC curves for unfractionated (UF) (a) acetone soluble (ASKL) (b) and acetone insoluble (AIKL) (c) unmodified (UN), hydroxyethyl ether (HE) modified, and esterified (E) modified lignin powders .....	138
Figure 40 TGA analysis for unfractionated esterified (UF_E), acetone soluble esterified (ASKL_E), and acetone insoluble esterified (AIKL_E) lignin powders weight % loss curves (a) maximum derivative weight % as a function of temperature curves (b) average values with standard deviation error bars for $T_{D5\%}$ (c) $T_{\text{max}}$ (d) and char yield (e).....	140

Figure 41 TGA weight % loss curves and maximum derivative weight % as a function of temperature curves for unfractionated (UF) (a) acetone soluble (ASKL) (b) and acetone insoluble (AIKL) (c) unmodified (UN), hydroxyethyl ether (HE) modified, and esterified (E) modified lignin powders..... 142

Figure 42 Ultimate tensile strength for neat Ecoflex<sup>TM</sup> (ECO), unfractionated unmodified (UF\_UN), unfractionated hydroxyethyl ether (UF\_HE), unfractionated esterified (UF\_E), acetone soluble unmodified (ASKL\_UN), acetone soluble hydroxyethyl ether (ASKL\_HE), acetone soluble esterified (ASKL\_E), acetone insoluble unmodified (AIKL\_UN), acetone insoluble hydroxyethyl ether (AIKL\_HE), and acetone insoluble esterified (AIKL\_E) at a lignin loading of 5, 10, 20, and 30 wt% with ASKL\_E blended to 40 wt% ..... 146

Figure 43 Ultimate tensile strength as a function of wt% lignin loading for unfractionated unmodified, hydroxyethyl ether, and esterified samples (UF\_UN, UF\_HE, UF\_E) (a) acetone soluble unmodified, hydroxyethyl ether, and esterified samples (ASKL\_UN, ASKL\_HE, ASKL\_E) (b) and acetone insoluble unmodified, hydroxyethyl ether, and esterified samples (AIKL\_UN, AIKL\_HE, AIKL\_E) (c) with the neat Ecoflex<sup>TM</sup> (ECO) control at 23.1 MPa.... 149

Figure 44 Ultimate tensile strength as a function of wt% lignin loading for unfractionated, acetone soluble, and acetone insoluble, unmodified, hydroxyethyl ether, and esterified (UF\_UN, UF\_HE, UF\_E, ASKL\_UN, ASKL\_HE, ASKL\_E, AIKL\_UN, AIKL\_HE, and AIKL\_E) samples with the neat Ecoflex<sup>TM</sup> (ECO) control at 23.1 MPa ..... 150

Figure 45 Young's modulus for neat Ecoflex (ECO), unfractionated unmodified (UF\_UN), unfractionated hydroxyethyl ether (UF\_HE), unfractionated esterified (UF\_E), acetone soluble unmodified (ASKL\_UN), acetone soluble hydroxyethyl ether (ASKL\_HE), acetone soluble esterified (ASKL\_E), acetone insoluble unmodified (AIKL\_UN), acetone insoluble hydroxyethyl

ether (AIKL_HE), and acetone insoluble esterified (AIKL_E) at a lignin loading of 5, 10, 20, and 30 wt% with ASKL_E blended to 40 wt% .....	152
Figure 46 Young's modulus as a function of wt% lignin loading for unfractionated, acetone soluble, and acetone insoluble, unmodified, hydroxyethyl ether, and esterified (UF_UN, UF_HE, UF_E, ASKL_UN, ASKL_HE, ASKL_E, AIKL_UN, AIKL_HE, and AIKL_E) samples with the neat Ecoflex™ (ECO) control at 31.6 MPa .....	153
Figure 47 Young's modulus as a function of ultimate tensile strength for unfractionated, acetone soluble, and acetone insoluble, unmodified, hydroxyethyl ether, and esterified (UF_UN, UF_HE, UF_E, ASKL_UN, ASKL_HE, ASKL_E, AIKL_UN, AIKL_HE, AIKL_E) samples with the neat Ecoflex™ (ECO) control at 23.1, 31.6 MPa .....	154
Figure 48 Elongation at break for neat Ecoflex™ (ECO), unfractionated unmodified (UF_UN), unfractionated hydroxyethyl ether (UF_HE), unfractionated esterified (UF_E), acetone soluble unmodified (ASKL_UN), acetone soluble hydroxyethyl ether (ASKL_HE), acetone soluble esterified (ASKL_E), acetone insoluble unmodified (AIKL_UN), acetone insoluble hydroxyethyl ether (AIKL_HE), and acetone insoluble esterified (AIKL_E) at a lignin loading of 5, 10, 20, and 30 wt% with ASKL_E blended to 40 wt% .....	156
Figure 49 Percent elongation at break as a function of wt% lignin loading for unfractionated, acetone soluble, and acetone insoluble, unmodified, hydroxyethyl ether, and esterified (UF_UN, UF_HE, UF_E, ASKL_UN, ASKL_HE, ASKL_E, AIKL_UN, AIKL_HE, and AIKL_E) samples with the neat Ecoflex™ (ECO) control at 1745% .....	157
Figure 50 Toughness for neat Ecoflex (ECO), unfractionated unmodified (UF_UN), unfractionated hydroxyethyl ether (UF_HE), unfractionated esterified (UF_E), acetone soluble unmodified (ASKL_UN), acetone soluble hydroxyethyl ether (ASKL_HE), acetone soluble	

esterified (ASKL_E), acetone insoluble unmodified (AIKL_UN), acetone insoluble hydroxyethyl ether (AIKL_HE), and acetone insoluble esterified (AIKL_E) at a lignin loading of 5, 10, 20, and 30 wt% with ASKL_E blended to 40 wt% .....	159
Figure 51 Toughness as a function of wt% lignin loading for unfractionated, acetone soluble, and acetone insoluble, unmodified, hydroxyethyl ether, and esterified (UF_UN, UF_HE, UF_E, ASKL_UN, ASKL_HE, ASKL_E, AIKL_UN, AIKL_HE, and AIKL_E) samples with the neat Ecoflex™ (ECO) control at 271 J/cm <sup>3</sup> .....	160
Figure 52 Total elongation at break as a function of toughness for unfractionated, acetone soluble, and acetone insoluble, unmodified, hydroxyethyl ether, and esterified (UF_UN, UF_HE, UF_E, ASKL_UN, ASKL_HE, ASKL_E, AIKL_UN, AIKL_HE, AIKL_E) samples with the neat Ecoflex™ (ECO) control at 271 J/cm <sup>3</sup> , 1745% .....	162
Figure 53 Tukey simultaneous 95% confidence intervals (CIs) difference of means for ultimate tensile strength (UTS) of acetone soluble unmodified softwood kraft lignin powders (ASKL_UN) at different lignin loadings (0, 5, 10, 20, 30 wt%) where 0 wt% ASKL_UN is the neat Ecoflex™ control (ECO) .....	168
Figure 54 Engineering stress strain curves (average of five samples) with inset Young's modulus (average of five samples) for acetone soluble unmodified samples (ASKL_UN) at 5, 10, 20, 30 wt% lignin loading as compared to neat Ecoflex™ (ECO).....	171
Figure 55 SEM images of neat Ecoflex (ECO) blended with 5 and 20 wt% acetone soluble unmodified lignin powders (ASKL_UN) frozen and fractured (a) and a cross section of the fractured surface after tensile testing is carried out (b).....	173

Figure 56 Engineering stress strain curves (average of five samples) with inset Young's modulus (average of five samples) for UF_HE, ASKL_HE, and AIKL_HE at 30 wt% lignin loading as compared to neat Ecoflex <sup>TM</sup> (ECO) .....	175
Figure 57 Engineering stress strain curves (average of five samples) with inset Young's modulus (average of five samples) for UF_E at 5, 10, 20, 30 wt% lignin loading as compared to neat Ecoflex <sup>TM</sup> (ECO).....	177
Figure 58 Engineering stress strain curves (average of five samples) with inset Young's modulus (average of five samples) for ASKL_E at 5, 10, 20, 30, 40 wt% lignin loading as compared to neat Ecoflex <sup>TM</sup> (ECO).....	179
Figure 59 Tukey simultaneous 95% confidence intervals (CIs) difference of means for ultimate tensile strength (UTS) of acetone soluble esterified softwood kraft lignin powders (ASKL_E) at different lignin loadings (0, 5, 10, 20, 30, 40 wt%) where 0 wt% ASKL_E is the neat Ecoflex <sup>TM</sup> control (ECO).....	180
Figure 60 DSC scans for second heating cycle showing the glass transition temperatures for neat Ecoflex <sup>TM</sup> at 0 wt% lignin loading and all lignin powders at 30 wt% loading in lignin-Ecoflex <sup>TM</sup> blend with AIKL_UN reported at 20 wt% loading because of inability to blend at 30 wt% .....	184
Figure 61 DSC scans for second heating cycle showing the glass transition temperatures for neat Ecoflex <sup>TM</sup> at 0 wt% lignin loading and acetone soluble esterified (ASKL_E) lignin powder at 5-40 wt% loading in lignin-Ecoflex <sup>TM</sup> blend .....	186
Figure 62 Glass transition temperature ( $T_g$ ) as a function of lignin loading (wt %) for unmodified (UN), hydroxyethyl ether (HE) and esterified (E) unfractionated lignin powders (UF) (a) acetone soluble lignin powders (ASKL) (b) and acetone insoluble lignin powders (AIKL) (c) as compared to neat Ecoflex <sup>TM</sup> (ECO) with theoretical Fox equation (FOX) linear fit.....	187

Figure 63 DSC scans for second heating cycle showing the melting endotherm peaks for neat Ecoflex <sup>TM</sup> (ECO) at 0 wt% lignin loading and all lignin powder samples loaded at 30 wt% in lignin-Ecoflex <sup>TM</sup> blend with AIKL_UN reported at 20 wt% loading because of an inability to blend at 30 wt% .....	189
Figure 64 Melting temperature ( $T_m$ ) as a function of lignin loading (wt %) for unfractionated (UF), acetone soluble (ASKL), and acetone insoluble (AIKL), unmodified (UN) lignin powders (a), hydroxyethyl ether lignin powders (HE) (b) and esterified (E) lignin powders (c) as compared to neat Ecoflex <sup>TM</sup> (ECO).....	191
Figure 65 DSC scans for cooling cycle showing the crystallization exothermic curves for neat Ecoflex <sup>TM</sup> (ECO) at 0 wt% lignin loading and all lignin powder samples loaded at 30 wt% in lignin-Ecoflex <sup>TM</sup> blend with AIKL_UN reported at 20 wt% loading because of inability to blend at 30 wt% .....	193
Figure 66 The temperature difference between the onset crystallization temperature $T_c$ and the peak crystallization temperature $T_{os}$ as a function of lignin loading (wt %) for unmodified (UN), hydroxyethyl ether (HE) and esterified (E) unfractionated lignin powders (UF) (a) acetone soluble lignin powders (ASKL) (b) and acetone insoluble lignin powders (AIKL) (c) as compared to neat Ecoflex <sup>TM</sup> (ECO).....	195
Figure 67 Crystallization peak temperature ( $T_c$ ) as a function of lignin loading (wt %) for unfractionated (UF), acetone soluble (ASKL), and acetone insoluble (AIKL), unmodified (UN) lignin powders (a), hydroxyethyl ether lignin powders (HE) (b) and esterified (E) lignin powders (c) as compared to neat Ecoflex <sup>TM</sup> (ECO) .....	197

Figure 68 DSC scans for cooling cycle showing the crystallization exothermic curves for unmodified (UN) (a), hydroxyethyl ether (HE) (b), and esterified (E) (c) acetone soluble lignin powders (ASKL) at lignin loading 5-40 wt% as compared to neat Ecoflex™ (ECO).....	199
Figure 69 Degree of crystallinity ( $X_c$ ) as a function of lignin loading (wt %) for unfractionated (UF), acetone soluble (ASKL), and acetone insoluble (AIKL), unmodified (UN) lignin powders (a), hydroxyethyl ether lignin powders (HE) (b) and esterified (E) lignin powders (c) as compared to neat Ecoflex™ (ECO).....	202
Figure 70 Glass transition temperature ( $T_g$ ) of lignin-Ecoflex™ blends at weight percentage lignin loading (wt%) where 0 wt% is neat Ecoflex™ (ECO), as a function of degree of crystallinity (%) for unmodified (UN), hydroxyethyl ether (HE) and esterified (E) lignin modification for unfractionated (UF) (a), acetone soluble (ASKL) (b), and acetone insoluble (AIKL) (c) lignin fractions.....	204
Figure 71 TGA weight % loss curves and maximum derivative weight % as a function of temperature curves (DTG) for esterified acetone soluble, esterified acetone insoluble, and unmodified acetone soluble (ASKL_E, AIKL_E, ASKL_UN) samples in blend with Ecoflex™ as compared to neat Ecoflex™ (ECO).....	206
Figure 72 FT-IR spectrum for unmodified acetone soluble (ASKL_UN) powder, neat Ecoflex™ (ECO), and 5-30 wt% ASKL_UN – Ecoflex™ blends (a) the fingerprint region (b) and enlarged signals at 1709 and 1269 $\text{cm}^{-1}$ (c) .....	209
Figure 73 FT-IR spectrum for unfractionated unmodified lignin powder (UF_UN) (a) and acetone soluble unmodified lignin powder (ASKL_UN) (b) melt processed with neat Ecoflex™ (ECO) in blend with 5-30 wt% with signals 1512 and 1594 $\text{cm}^{-1}$ belonging to aromatic skeletal	

vibrations in lignin and signals 1504 and 1577 $\text{cm}^{-1}$ belonging to skeletal vibrations of the benzene ring in Ecoflex <sup>TM</sup> .....	211
Figure 74 Lignin loading (wt%) as a function of wavenumber ( $\text{cm}^{-1}$ ) for the neat Ecoflex <sup>TM</sup> (ECO) peak at 1709 $\text{cm}^{-1}$ and the subsequent peak shift for unfractionated unmodified (UF_UN) and acetone soluble unmodified (ASKL_UN) samples in blend with Ecoflex <sup>TM</sup> .....	212
Figure 75 FT-IR spectrum for esterified acetone soluble (ASKL_E) powder, neat Ecoflex <sup>TM</sup> (ECO), and 5-40 wt% ASKL_E – Ecoflex <sup>TM</sup> blends (a) and enlarged signals from 1660-1780 and 1220-1300 $\text{cm}^{-1}$ (c).....	214
Figure 76 Lignin loading (wt%) as a function of wavenumber ( $\text{cm}^{-1}$ ) for neat Ecoflex (ECO) peak 1709 $\text{cm}^{-1}$ and the subsequent peak shift for unfractionated esterified (UF_E), acetone soluble esterified (ASKL_E), and acetone insoluble esterified (AIKL_E) lignin powders in blend with Ecoflex <sup>TM</sup> .....	215
Figure 77 Lignin loading (wt%) as a function of wavenumber ( $\text{cm}^{-1}$ ) for neat Ecoflex <sup>TM</sup> (ECO) peak 1709 $\text{cm}^{-1}$ and the subsequent peak shift for acetone soluble unmodified (ASKL_UN) and acetone soluble esterified (ASKL_E) lignin powders in blend with Ecoflex <sup>TM</sup> .....	216
Figure 78 Ultimate tensile strength (a) Young's modulus (b) percent elongation at break (c) and toughness (d) for neat Ecoflex <sup>TM</sup> (ECO) at a 180 °C and 135 °C melt processing temperature blended with acetone soluble esterified (ASKL_E) at a lignin loading of 5, 10, 20, and 30 wt% .....	218
Figure 79 Engineering stress strain curves with inset Young's modulus for ASKL_E at 30 wt% lignin loading as compared to neat Ecoflex <sup>TM</sup> (ECO) at processing temperatures 135 °C and 180 °C .....	219



Figure 80 Degree of crystallinity ( $X_c$ ) as a function of lignin loading (wt %) for acetone soluble esterified lignin (ASKL_E) powders, and neat Ecoflex <sup>TM</sup> (ECO) at a 135 °C and 180 °C processing temperatures .....	221
Figure 81 Comparison of the tensile strength and Young's modulus (stiffness) for lignin based thermoplastic blends .....	224
Figure 82 Complete <sup>13</sup> C NMR spectra for as received Ecoflex <sup>TM</sup> (a), the enlarged region 1 with structures and specific carbons pointed out (b) and the enlarged region 2 with structures and specific carbons pointed out (c) used to confirm the Ecoflex <sup>TM</sup> chemical structure prior to melt-processing .....	261
Figure 83 Overall equipment set up used to make lignin-Ecoflex <sup>TM</sup> thermoplastic blends (a), the twin screws used for melt processing (b), and the mould used for dumbbell shaped specimens (c) .....	262
Figure 84 Instron load frame used for tensile testing (a), the grips elongating neat Ecoflex <sup>TM</sup> in vertical test direction (b) neat Ecoflex <sup>TM</sup> type V dumbbell shaped specimen (c), 10 wt% ASKL_UN – Ecoflex <sup>TM</sup> thermoplastic blend after mould injection (d), 40 wt% ASKL_E – Ecoflex <sup>TM</sup> thermoplastic blend after mould injection and removed from top piece (e), fracture of 40 wt% ASKL_E – Ecoflex <sup>TM</sup> thermoplastic blend after tensile testing (f) and fracture of 40 wt% ASKL_E – Ecoflex <sup>TM</sup> thermoplastic blend after tensile testing .....	263

## List of Abbreviations

AFEX	Ammonia fibre expansion
AH	Acid Hydrolysis
AIKL	Acetone insoluble softwood kraft lignin
AIKL_UN	Acetone insoluble unfractionated lignin powder
AIKL_HE	Acetone insoluble hydroxyethyl ether lignin powder
AIKL_E	Acetone insoluble esterified lignin powder
AlOH	Aliphatic hydroxyl functional group
ASKL	Acetone soluble softwood kraft lignin
ASKL_UN	Acetone soluble unfractionated lignin powder
ASKL_HE	Acetone soluble hydroxyethyl ether lignin powder
ASKL_E	Acetone soluble esterified lignin powder
ArOH	Aromatic hydroxyl functional group
BL	Black liquor
$^{13}\text{C}$ NMR	Carbon-13 nuclear magnetic resonance
COOH	Carboxylic acid hydroxyl functional group
DC	Degree of condensation
DSC	Differential scanning calorimetry
E	Young's modulus
EC	Ethylene carbonate
ECO	Ecoflex <sup>TM</sup> F blend C1200

FT IR	Fourier-transform infrared spectroscopy
G	Guaiacyl unit
GPC	Gel permeation chromatography
H	<i>p</i> -hydroxyphenyl unit
HDPE	High density polyethylene
HMW	High molecular weight
HWKL	Hardwood kraft lignin
IS	Internal standard
LCC	Lignin-carbohydrate complexes
LDPE	Low density polyethylene
LMW	Low molecular weight
Me	Methyl group (CH <sub>3</sub> )
MeOH	Methanol
Mt	Metric tons
M <sub>n</sub>	Number average molecular weight
M <sub>w</sub>	Weight average molecular weight
MWL	Milled wood lignin
NMR	Nuclear magnetic resonance spectroscopy
O	Oxygen atom
OH	Hydroxyl group (alcohol)
<sup>31</sup> P NMR	Phosphorus-31 nuclear magnetic resonance
PBAT	Polybutylene adipate terephthalate

PC	Polycarbonate
PDI	Polydispersity index
PET	Polyethylene terephthalate
PLA	Poly(lactic acid)
PP	Polypropylene
PS	Polystyrene
PVC	Polyvinyl chloride
PW	Primary wall
S	Syringyl unit
SE	Steam explosion
SEM	Scanning electron microscopy
SW	Secondary wall
SWKL	Softwood kraft lignin
TGA	Thermal gravimetric analysis
$T_c$	Crystallization peak temperature
$T_g$	Glass transition temperature
$T_m$	Melting temperature
$T_{D5\%}$	Temperature at 5 wt% weight loss
$T_{max}$	Derivative weight peak temperature
$T_{os}$	Onset crystallization temperature
UF_UN	Unfractionated unmodified lignin powder
UF_HE	Unfractionated hydroxyethyl ether lignin powder

UF_E	Unfractionated esterified lignin powder
UTS	Ultimate tensile strength
$X_c$	Degree of crystallinity
$\Delta H_c$	Crystallization enthalpy
$\Delta H_m$	Enthalpy of fusion

## Acknowledgements

I offer my gratitude to the faculty, staff, and my teammates in wood science, who have inspired me over the past several years to continue my work in this field. I owe particular thanks to my advisor Dr. Scott Renneckar, whose guidance and encouragement helped me attain all research goals. I thank Dr. Emily Cranston for being a strong female role model and a friend whose door was always open. I thank Dr. Feng Jiang for raising excellent questions that helped to round out my project. Working with these professors developed me into a successful researching scientist.

Without my colleagues and lab mates Dr. Mijung Cho, Dr. Liyang Liu, Dr. Muzaffer Karaaslan, and PhD candidate Amanda Johnson, I could not have completed my research project at the University of British Columbia. Dr. Cho, Dr. Liu, Dr. Karaaslan, and PhD candidate Amanda Johnson trained me on laboratory equipment, processes, and procedures and guided me through my master program. They were always there to lend a helping hand, an ear to listen, and a shoulder to lean upon. To my office mates Lun Ji, Ricky Hua and Li Ting whom I shared a tiny space with no windows, thank you for always making me laugh and helping me with Microsoft word formatting issues. I will never forget my time with you in the middle of the Forestry building.

Lastly, I would like to acknowledge the Forestry staff, particularly Diane Hastings, Gayle Kosh, Robin Poirier-Vasic, and Ivy Fung who helped me navigate the international student paperwork and funding process and kept all of us safe on the fourth floor.

Research cannot be done without a team and I am so grateful for the family I became a part of over the last several years. Thank you.

## **Dedication**

To my loving father, who never stopped believing I could. To my caring my mother, who always had kind words of encouragement. To my enthusiastic brother who might be my biggest supporter. To the beautiful North Shore mountains for being a personal sanctuary during my most difficult days. I love, care, and connect deeply to this planet and that is ultimately what motivated and kept my research moving forward.

## Chapter 1: Introduction

In 1997, Captain Charles Moore was sailing home to Los Angeles from Honolulu when he discovered the “North Pacific Garbage Patch.” He said, “I could stand on deck for five minutes seeing nothing but the detritus of civilization in the remotest part of the great Pacific Ocean.”<sup>1,2</sup> The debris pile that Captain Moore referred to is comprised of durable human-made single-use plastics that require a fossil-based feedstock for synthesis.

After World War II, petroleum-based resources became readily available and chemists polymerized these feedstocks into synthetic polymers like polypropylene, polyvinyl chloride, polyethylene terephthalate, and polystyrene. These materials can then be moulded into items like milk jugs, flexible bags, drinking cups, and foam packaging. These new materials were inexpensive, convenient, versatile, and safe for food storage. Amongst the most heavily produced is the prototypical plastic, polyethylene; a tough material that can be stretched hundreds of times beyond its proportional limit and can hold both water and gasoline without being dissolved. Durability is the main challenge with plastics like polyethylene, which after initial break down take thousands of years to degrade. In the process, these materials can turn into micro-plastics that persist in the environment and this is dangerous to marine life and the oceans that regulate our biosphere.<sup>1,3</sup>

With now more than 380 million tons of plastic produced each year and 60-75% used once and thrown into landfills or the natural environment, scientists predict that plastic in the ocean will outweigh fish pound for pound by 2050.<sup>1,4</sup> As such, there is a demand for an environmentally compatible, mechanically sound plastic that fits within a circular bioeconomy. One potential solution that does not intensify agricultural land development is to use



lignocellulosic biomass for plastics. Lignin is one major component of plants, is underutilized as a raw renewable material resource, and is the main focus of this thesis.

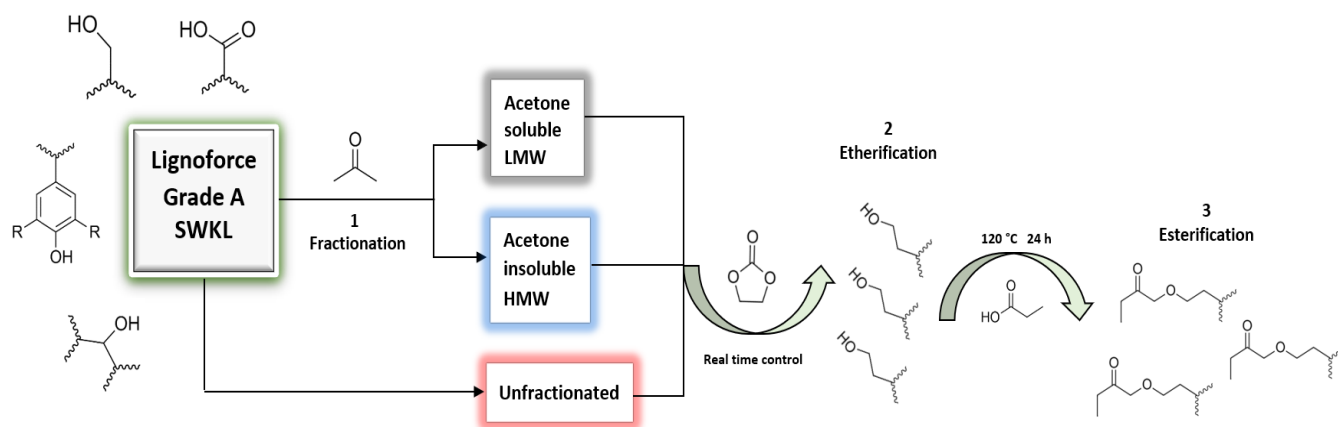
## **1.1 Thesis objectives**

When engineering a lignin-based thermoplastic meant to replace a petro-chemical based thermoplastic, many considerations must be taken into account. In 2021, it is not adequate to substitute one problematic material for another and cost, efficiency and toxicity are more important than if the material simply works. However, for progression to be made it is necessary to continue research and development into how technical modified lignins perform in polymeric matrices under different conditions. This study aims to fill a gap in literature and develop a simple, clean process for lignin modification capable of scale-up and to form a miscible blend with a renewable polymer such as Ecoflex<sup>TM</sup>, thus creating a mechanically sound thermoplastic material comparable to neat polyethylene, but with an environmentally sound end of life (i.e. compostability). The results and discussion are organized into two sections with the first focusing on the acetone fractionation, etherification, esterification, and subsequent characterization of the unmodified and modified softwood kraft lignin powders. The second section focuses on melt compounding, mould injection, and a detailed mechanical analysis of the resulting lignin-Ecoflex<sup>TM</sup> thermoplastic blends. The sections are summarized below to prepare the reader.

*Section 4.1:* How does an acetone fractionation combined with an etherification (hydroxyethylation) and esterification (propionate derivative) using green reagents effect the thermal properties, molecular weight, and chemical structure of the resulting lignin powders?

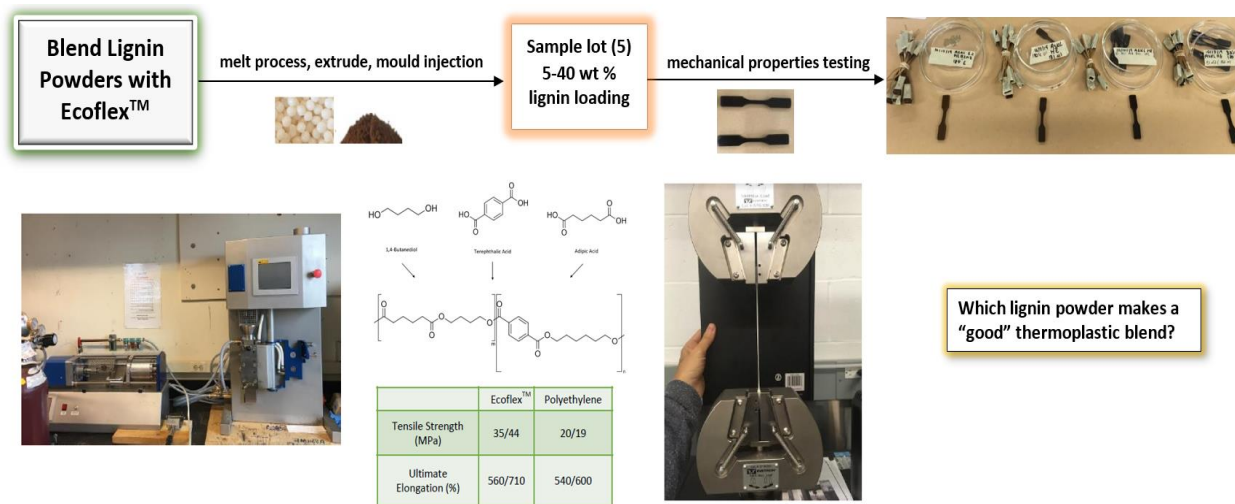
Softwood kraft lignin was chosen because it is commercially sourced from kraft pulp producers. Acetone is a simple ketone, inexpensive, easily recoverable, and proven to effectively

fractionate lignin in one step. Ethylene carbonate was chosen as the green reagent for the etherification because it has the simplest side chain of all the cyclic carbonates making it the most reactive to form primary aliphatic hydroxyl derivatives. The process was carried out under real time control to reduce side reactions and maximize time efficiency and reagent consumption. The resulting hydroxyethyl ether lignin possesses uniform functionality and the resulting hydroxyl groups are readily esterified using propionic acid as both solvent and catalyst. It was hypothesized that acetone soluble esterified lignin would have the lowest  $T_g$  value, be the most thermally stable in melt and would favorably interact with Ecoflex<sup>TM</sup>. Figure 1 is a basic overview of the three-step chemical process described above.



**Figure 1 Overview of the three step chemical process used to make lignin powders for melt processed thermoplastic blend with Ecoflex<sup>TM</sup>; acetone fraction (1) etherification using ethylene carbonate (2) and esterification using propionic acid (3)**

Ecoflex<sup>TM</sup>, is a mixed aliphatic and aromatic polyester that is certified compostable, readily available, reasonably cost efficient, and previously used with naturally occurring polymers. In addition, the monomers can be sourced from biobased feedstocks. In the current study a laboratory sized extruder was used to synthesize standard dumbbell shaped specimens with various loadings of lignin which were mechanically tested in five sample lots. It was hypothesized that the acetone soluble esterified lignin powder would be stable in melt and the ester modification would result in a miscible blend with Ecoflex<sup>TM</sup>. The thermoplastic blends underwent detailed characterization with Instron load frame mechanical testing, FT-IR, DSC, TGA, and SEM and comparisons were made. Figure 2 summarizes the thrust of this research project and asks the important question, what makes a “good” thermoplastic blend?



## Chapter 2: Literature review

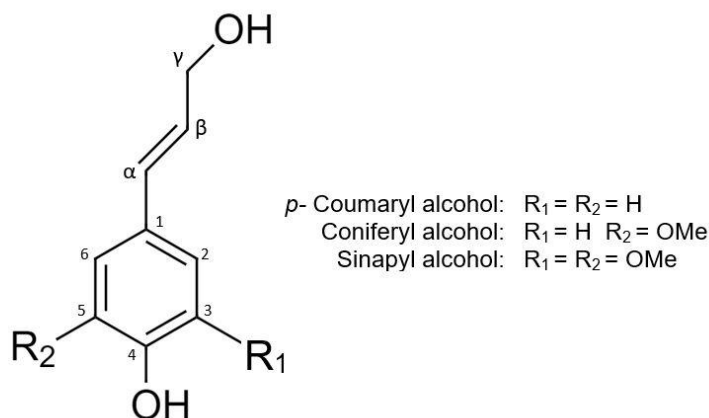
### 2.1 Lignin

Lignin is the second most abundant terrestrial biopolymer making up 30% of organic carbon in the biosphere.<sup>5,6</sup> Cellulose, the most abundant cell wall polymer, together with lignin and hemicellulose comprise lignocellulosic biomass that constitute the cell walls in all vascular plants. Depending on the plant species, cellulose accounts for 30-50% of the biomass, hemicellulose 20-35%, and lignin 15-30% by weight or 40% by energy.<sup>6,7</sup> Lignin is a crosslinked heteropolymer and a naturally occurring source of aromatic compounds. Because lignin synthesis is carbon negative and occurs during plant photosynthesis it has become a raw material of interest in high end structural applications such as polymer blends. Understanding native lignin formation and the complexity of the structure-function relationship in combination with the availability of industrial lignins and the process by which they are isolated is crucial in developing a robust lignin-biobased thermoplastic blend to address the shortcomings of current single-use plastic materials.

#### 2.1.1 Biosynthesis and structure

Over a century of scientific research has been dedicated to developing an understanding of how lignin is synthesized in the cell walls of vascular plants. In general, native lignin begins its journey as phenylalanine, a neutral, non-polar, essential  $\alpha$  - amino acid found in the cytosol of xylem cells.<sup>5,8-10</sup> A plethora of enzymes catalyze the deamination of phenylalanine and subsequent addition of a hydroxyl group (OH) to the aromatic ring, followed by an alkylation reaction or *O*-methylation which introduces a methyl group (Me) to the phenol.<sup>5,8,11</sup> The final step is the side chain conversion of a carboxyl group to an alcohol group resulting in lignin

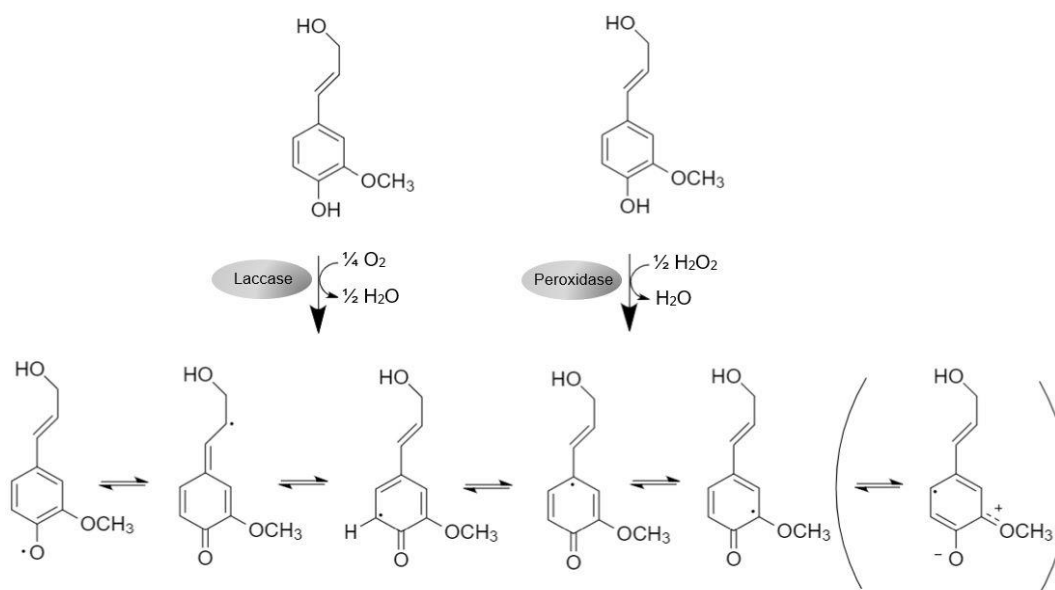
precursors, or C6-C3 (sometimes referred to as C9) phenylpropanoids also known as monolignols.<sup>5,8,10</sup> Monolignols are the hydroxycinnamyl alcohol monomeric building blocks for lignification and vary in degree of methoxylation.<sup>8,10,12</sup> Figure 3 illustrates the basic monomeric units (*p*- coumaryl alcohol, coniferyl alcohol, and sinapyl alcohol) which are derived in the first steps of in vivo lignin biosynthesis. Monolignol biosynthesis has been extensively studied and reviewed. The reader can reference the accompanying literature for a more detailed view of the known enzymes and regulated pathways by which monolignols are derived.<sup>5,8,11–17</sup> It is important to note that while these processes have been a major focus in the study of lignin and are well understood, with advances in technology, especially within the field of genetic engineering, new discoveries are made each year.<sup>17–20</sup>



**Figure 3 Basic lignin monomeric units or lignin precursors**<sup>8-11</sup>

After synthesis the monolignols are transported to the plant cell wall where they undergo dehydrogenation and finally polymerization. The exact mode of transportation between cytosol and cell wall, and whether it is active, or passive is still under investigation.<sup>10,21,22</sup>

The precise processes by which native lignification occurs and the corresponding structure varies with plant species and is not fully understood. However, there is a generally accepted theory that lignin formation occurs through dehydrogenative polymerization and renders radical resonance stabilized monolignols which can couple in various ways.<sup>23,24</sup> The monolignols are oxidized by the enzyme peroxidase which uses hydrogen peroxide or by the enzyme laccase which is an O<sub>2</sub> dependent catalyst in the polymerization.<sup>25,26</sup> Figure 4 illustrates the resulting resonance stabilized radicals due to electron delocalization. An end wise polymerization will occur, and covalent bonds can form between monolignol radicals, one monolignol radical and an end group radical, or two end group radicals.<sup>5,9</sup> What type of linkage forms is dependent on the monomer's degree of methoxylation. For example, Figure 4 is representative of a coniferyl alcohol which is the guaiacyl unit (G) and has a methoxy group on the third carbon position leaving the fifth carbon open to bond. All possible covalent bonds are



**Figure 4** Example of resonance stabilized coniferyl monolignol radicals <sup>9</sup>

not present in lignin because of steric hindrance and chemical instability. Despite the monomer composition or ratio, the most common linkage in both softwood and hardwood lignin is the  $\beta$  – aryl ether bond or the  $\beta$  – O – 4 linkage.<sup>11,27</sup> Table 1 shows the frequencies and differences between linkages found in softwoods and hardwoods, while Figure 5 illustrates common linkages formed between monolignols during the polymerization process.

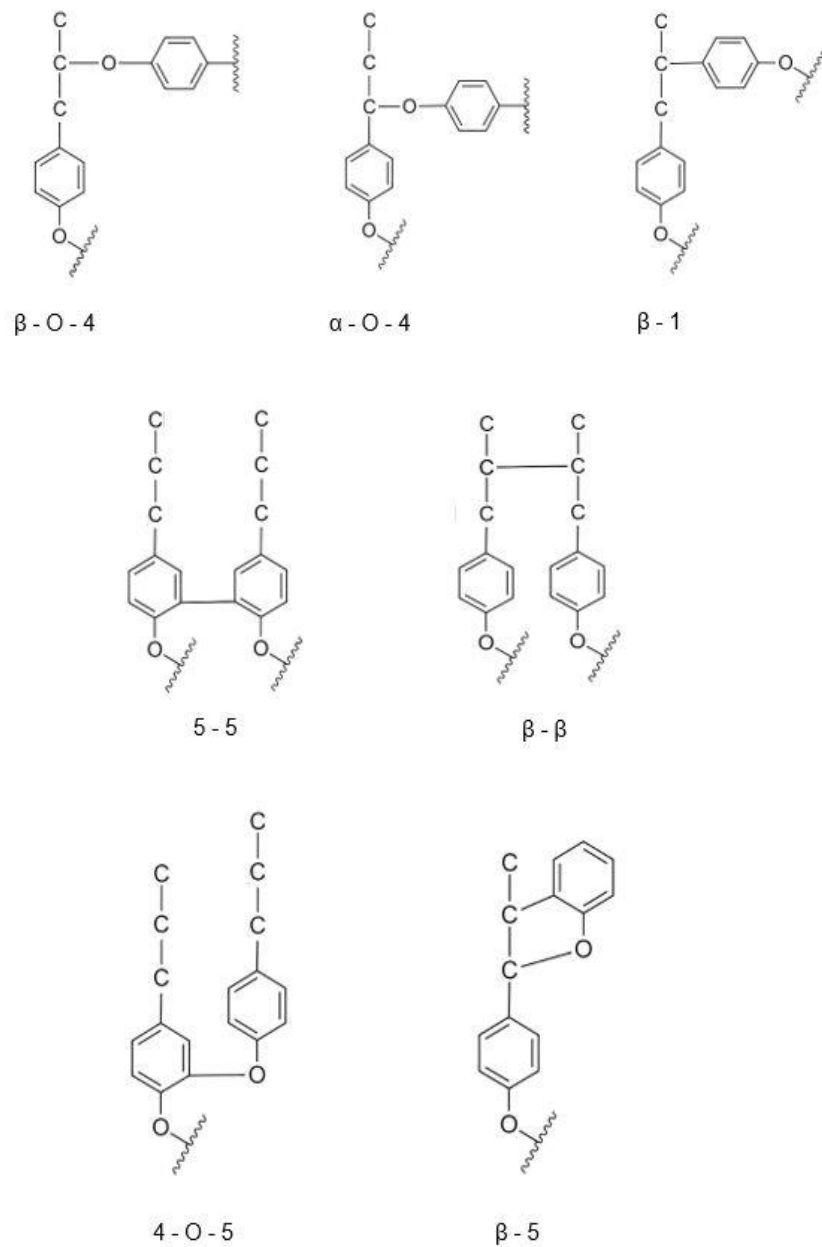
Lignin is racemic, containing two enantiomers which are chiral molecules that are mirror images of one another. Because enantiomers are non-superimposable (cannot be stacked on top of one another to give the same molecule) there is zero optical rotation and therefore no optical activity.<sup>7</sup> This is interesting as it proves lignification is not a protein controlled biological process but instead a chemical process.<sup>7</sup>

**Table 1 Relative frequencies<sup>a</sup> of common linkages in softwood and hardwood lignin per 100 monomeric C6-C3 units<sup>8,11,18</sup>**

Linkage type <sup>b</sup>	Dimer structure	Softwood	Hardwood
$\beta$ -O-4	$\beta$ -aryl ether	45-50	50-70
$\alpha$ -O-4	$\alpha$ -aryl ether	6-8	6-8
$\beta$ -1	Diarylpropane	7-9	7
5-5	Biphenyl	19-22	9
$\beta$ - $\beta$	Pinoresinol	2-4	3
4-O-5	Diarylether	4-7	9
$\beta$ -5	Phenylcoumaran	9-12	6

<sup>a</sup> Approximate values based on Adler (1977) data for Milled Wood Lignin from spruce and birch woods.

<sup>b</sup> See Figure 5 for related structures.



**Figure 5 Common linkages found in softwood and hardwood lignin** <sup>8, 11, 18</sup>

A more detailed investigation into the differences between softwood and hardwood lignin is needed to gain an in depth understanding of the polymeric variation between species.



### 2.1.2 Softwood and hardwood

Lignin content varies within species of vascular plant. In general, softwoods contain approximately 27-33% lignin, hardwoods 18-25%, and grasses 17-24%.<sup>11,24</sup> This however, is a generalization and lignin content will vary with the plant age, type of wood within the plant, environment, and season.

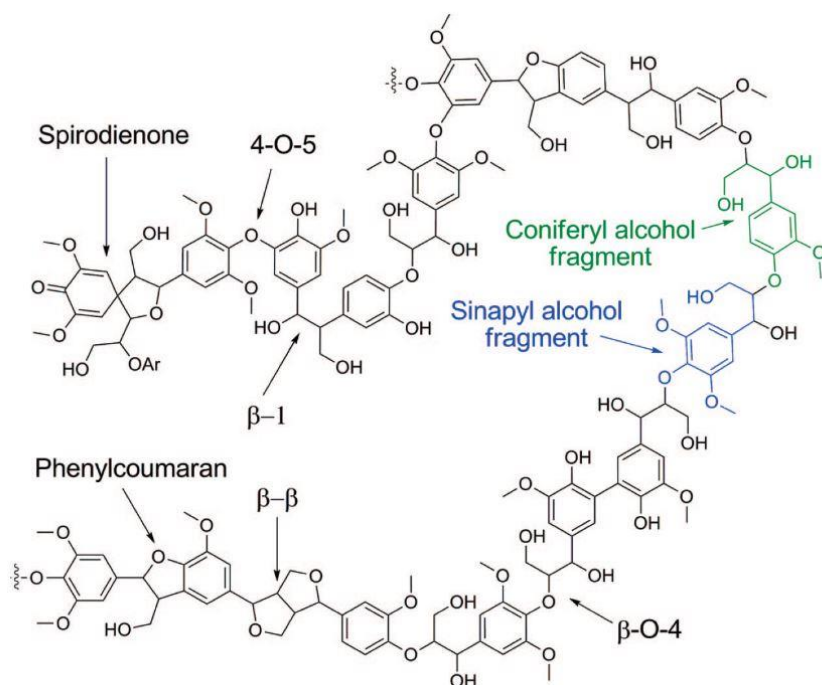
Gymnosperms like pines, cedars, spruces, and firs are considered softwoods which contain 90-95% tracheid cells that conduct water in the xylem.<sup>20,28</sup> Softwood trees can have compression wood, a type of reaction wood which is highly lignified and found in the secondary cell wall (S2) on the underside of the curved stem.<sup>18,29</sup> Coniferyl alcohol or the G unit is the most abundant monolignol in gymnosperms.<sup>18</sup> Because the C5 position is available softwoods can form strong carbon-carbon linkages (Figure 3).<sup>16,18</sup> Therefore, softwoods tend to have more 5-5 and  $\beta$ -5 linkages than hardwoods (Table 1).<sup>11,16</sup> Although there are no condensation reactions taking place these are often called condensed bonds and they are harder to cleave in the delignification process during wood pulping.<sup>30</sup> *P*-coumaryl alcohol (H unit) may be found which can lead to other types of linkages in the final polymer.<sup>16,18</sup>

Softwood pulps tend to have higher lignin content, meaning delignification can be more difficult. In locations like British Columbia where gymnosperms dominate harvestable wood and pulp and paper making is a major industry this must be addressed. Wood scientists have spent centuries studying and refining the processes by which lignin is removed from the lignocellulosic cell wall.

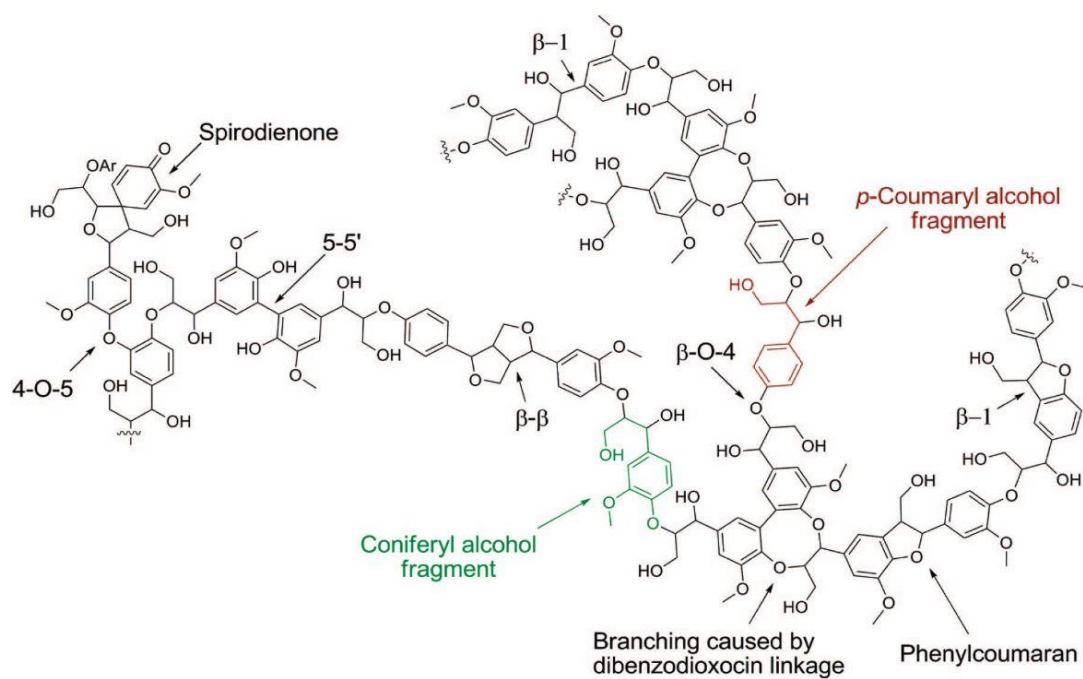
Angiosperms, like birch, oak, maple, and dogwood are considered hardwoods and are composed of vessels, fibres, ray parenchyma cells, and may contain tracheid and axial parenchyma cells.<sup>28,30</sup> Hardwood trees have a different type of reaction wood referred to as

tension wood which contains lower amounts to no amounts of lignin compared to the compression wood found in softwoods.<sup>28</sup> Hardwood contains coniferyl alcohol and sinapyl alcohol monolignols or guaiacyl-syringyl lignin (G-S units) and a small amount of *p*-coumaryl alcohol (H).<sup>16,18</sup> Because the S unit is found in higher proportions in angiosperms and has a methoxy group on both the third and fifth carbon in the aromatic ring it cannot form as many 5-5 linkages for this type of monolignol, therefore, there are more  $\beta$ -O-4 linkages which are easier to cleave during delignification (Table 1).<sup>16,18</sup> Figure 6 and Figure 7 are schematics which highlight the differences between softwoods and hardwoods.<sup>7</sup>

In recent years, using advanced nuclear magnetic resonance spectroscopy (NMR) techniques, scientists have been able to quantify linkages and the structure of lignin has been extensively examined to develop structural models. However, this is technically impossible because lignin is a very complex polymer. Therefore Figures 6 and 7 are merely pictorial representations of softwood and hardwood lignins meant to show how the methoxylation of differing monolignols and the subsequent amount of each monolignol effect the type and amount of linkages (Table 1) and therefore structure arising after polymerization of these monolignols. Generally, hardwood lignin has the potential to form a more linear polymer with more  $\beta$ -O-5 linkages than softwood lignin because of the additional methoxy group present on the fifth carbon of the aromatic group in the S unit.<sup>7,26,28</sup> Meanwhile, softwood lignin will show more cross linking because the fifth carbon on the aromatic ring of the G unit is available to form more 5-5 and  $\beta$ -5 linkages.<sup>7,26,28</sup> These structural differences will affect how the pulp and papermaking industry processes the lignocellulosic cell wall, which will be discussed in following sections.



**Figure 6 Schematic of a softwood lignin structure** Reprinted with permission from ref <sup>7</sup>  
 Copyright 2010 American Chemical Society



**Figure 7 Schematic of a hardwood lignin structure** Reprinted with permission from ref <sup>7</sup>  
 Copyright 2010 American Chemical Society

### 2.1.3 Structure and function

The structure-function relationship is important in understanding how lignin will behave in a polymeric blend. Imagine lignin as the glue that holds cellulose, pectin, and hemicellulose sugars together in the cell wall giving it the strength and rigidity necessary for upward growth. Lignin is not deposited in the secondary cell wall until these carbohydrates have first been deposited.

The primary cell wall (PW) is approximately 30% cellulose, 30% hemicellulose, 30% pectin, and 10% proteins.<sup>5,18</sup> The secondary wall (SW) consists of three layers and is where lignin deposition begins: the outer layer (S1), the middle layer (S2), and the inner layer (S3). Lignin will begin to polymerize in the cell corner but rapidly spread after cellulose microfibrils have been deposited. The SW has the highest lignin content despite lignin concentration being greater in the middle lamella and cell corners because the SW takes up more volume in the plant.<sup>18,31</sup>

Lignin has many important functions in the life and overall health of vascular plants, especially trees. Every person directly benefits from the incredibly complex polymer that is lignin. While most of the other components in the plant cell wall are hydrophilic, lignin is more hydrophobic which makes water transport possible. This aspect was key in the evolution of plants to a harsh land environment. Lignin provided mechanical support to plants which allowed stems to grow and compete for sunshine while acting as a glue keeping woody tissue intact. Because lignin has an aromatic structure, it also protects the plant against microbial and UV degradation. Lignin is a major source of naturally occurring aromatic carbons and has a high energy density. Aside from allowing vascular plants to survive and release oxygen, which is necessary to sustain human life, lignin is the reason that trees grow so large. Since the beginning

of human civilization, wood has been a crucial material for survival. So, if lignin is such an amazing biopolymer, why has it customarily been an annoyance to the wood processing industry?

#### **2.1.4 Chemical pulping**

Lignin has great potential as a renewable resource in polymeric blends but in the paper product industry it is viewed as a nuisance since it must be removed for high quality pulp. Cellulosic fibres are the key ingredient in papermaking and the main objective is to remove lignin without damaging cellulose, so lignin is often burned off as an energy source during the chemical recovery process in kraft pulping. There is potential to produce 140 million tons of technical lignin each year, yet lignin is underutilized in material applications.<sup>13,32</sup>

All industrial lignin isolation methods depend on conditions and will change the structure of native lignin. Two laboratory isolation methods were developed decades ago. In 1890 Peter Klason developed the Klason technique which used strong acidic conditions to isolate native lignin.<sup>33,34</sup> The main issue was the harsh chemicals that greatly altered the linkages and functional groups of native lignin.<sup>33,34</sup> In 1956 Anders Björkman used a ball milling technique to grind the lignocellulosic material and then extracted the milled wood lignin (MWL) in a dioxane/water solution.<sup>33,32</sup> Under mild conditions there was only a slight change to the native lignin. Although MWL yield was low in comparison to Klason lignin, this is a standard and often used laboratory method to determine structure.<sup>32,33</sup> Both processes have been improved upon and are well cited in literature.<sup>13,24,32–36</sup> For the sake of relevance this review will focus on the four most common types of technical lignins; organosolv, soda, sulfite, and kraft.

There are other types of chemical pulping techniques, but most are in the early stages of development and working towards industrial scaling. Table 2 provides an overview of the

different types of lignins, the general chemistry, and the scale at which they are produced. For the most part, organosolv, acid hydrolysis (AH), steam explosion (SE), and ammonia fibre expansion lignin (AFEX), are all techniques still in their pilot stage and are not readily available on the market. A higher demand for lignin-based materials could create a demand for the availability of cleaner and more consistent technical lignins.

**Table 2 General classification of technical lignins adapted from ref. <sup>37</sup>**

Lignin Type	Scale	Chemistry	Sulphur content	Purity
Kraft	Industrial	Alkaline	Moderate	Moderate
Soda	Industrial	Alkaline	Free	Moderate-low
Lignosulfonate	Industrial	Acid or Alkaline	High	Low
Organosolv	Pilot/demo	Acid	Low-free	High
AH	Industrial/pilot	Acid	Low-free	Moderate-low
SE	Demo/pilot	Acid	Low-free	Moderate-low
AFEX	Pilot	Alkaline	Free	Moderate-low

#### 2.1.4.1 Organosolv

In general, organosolv is a term that specifies delignification carried out in organic solvents. Pulping with organic solvents dates back as early as 1931 but it was the Alcell process at the Repap Alcell pilot plant in New Brunswick, Canada that gained traction from 1989 to 1996 and in 2000, the UPM-Kymmene Corporation acquired the process.<sup>7,38</sup> In its prime, the demonstration plant produced over 5,000 tons of pulp from northern hardwoods and was competitive with the Kraft process.<sup>38</sup> Despite the environmentally friendly technique and its

great potential for producing high quality technical lignin, these organosolv mills have limited commercial success when competing in pulp production.

A low weight organic solvent like methanol or ethanol is used in the cook. The cook is heated to 180-195 °C for 30-90 minutes and an extensive amount of lignin is removed with a minimal loss of cellulose.<sup>39</sup> This is done through the cleavage of the  $\beta$ -ether linkages. An acid catalyst can be used but is not necessary as its absence leads to a better retention of the native  $\beta$ -ether linkages.<sup>39</sup> Normally the process streams (lignin, cellulose, and hemicellulose) are easily isolated. Solvent recovery and lignin isolation are required because the organosolv liquor cannot be burned without destruction of the solvent. The lignins produced are low molecular weight, sulfur free (if sulfuric acid is not used as a catalyst) and are a great source of phenols and aromatics.

The organosolv process comes at a higher cost because the organic solvent must be recovered. This poses potential difficulties when trying to implement the process into a pre-existing mill where the pulping liquor is used as fuel. The organosolv process is diverse in the types of wood it can handle but must be tweaked at a local level depending on available species. Therefore, it would be difficult to sell this process and the resulting product as “one size fits all” since it produces very different lignins with very different properties.<sup>37-40</sup> Although the technical lignins produced tend to be of higher quality with less impurities, a more consistent stream of availability is required before organosolv high end lignin products are researched, produced, and considered economically feasible.

#### 2.1.4.2 Soda

Soda pulping was industrialized in 1853 and uses a mostly non-wood fibre feedstock from straw, bamboo, sugarcane, and flax. The pulp is digested in sodium hydroxide at a processing temperature of 160 °C because the structure of non-wood fibres are less rigid and have lower lignin content.<sup>10,41</sup> Delignification occurs through the cleavage of non-phenolic  $\beta$ -aryl ether units and quinone methide structures common in kraft pulping are less likely.<sup>10,34,41</sup> Hardwoods processed via soda pulping make packaging, papers, and boards. At higher processing temperatures the hydroxyl ion,  $\text{OH}^-$  can break down the ether bonds in lignin and NaOH will react with the fragmented phenolic hydroxyls forming a lignin salt that is soluble in an aqueous solution.<sup>34,42</sup> This is a well-established process that produces low molecular weight, sulfur free, and low ash lignins.

Soda lignins are sulfur free and closer to the native lignin structure than most other technical lignins.<sup>41,42</sup> Because there is no sulfur used in the process the smell and volatile sulfur compounds are eliminated. However, the lack of sulphides leads to a greater amount of lignin condensation when compared to the Kraft process.<sup>42</sup> In addition, soda pulps tend to have higher amounts of carboxylic acid.<sup>42</sup>

Soda pulping works on hardwoods, but it is primarily used on easy to pulp materials like straw which yield lower tear strengths. The soda pulping process is not often used on softwoods, a prominent feedstock in British Columbia. Regardless, soda lignin is used in thermoset binding applications, animal feed, and as a phenol replacement in resins used as binders.<sup>41</sup>



### 2.1.4.3 Sulfite

Eighty years ago, the sulfite pulping process was dominant with around twenty million tons of lignosulfonates produced annually. With a steady decline, today only about seven million tons are produced per year.<sup>7,41</sup> Lignosulfonates act as a concrete water reducer which is the largest current application of any technical lignin.<sup>41</sup> Despite lignosulfonates important role as dispersing and binding agents in building materials it is unlikely these lignins will ever be used in new applications because of limited global supply.

Wood is digested in an aqueous solution of sulphite or bisulphite salt such as sodium, ammonium, magnesium or calcium at a temperature range of 140-170 °C.<sup>16,43</sup> Solubility will be the result of the type of salt (pulping agent) used which determines the pH. For example, calcium bisulphite is highly acidic and sodium sulphite is highly alkaline. The negatively charged sulphite or bisulphite will carry out a nucleophilic attack and if the pH is low the  $\alpha$  position is sulfonated and if the pH is high the quinone methide structures are sulfonated.<sup>7,16,43</sup> In the former situation intermediates form condensed structures which are undesirable and problematic in production so pulping conditions should be adjusted accordingly. In acidic conditions condensation occurs between the C $_{\alpha}$  and C $_6$  carbons but can be regulated with bisulphite ions.<sup>7,16,43</sup> During digestion linkages between lignins and carbohydrates and the carbon-oxygen bonds between lignin units are cleaved. In addition, the aliphatic chains of native lignin are sulphonated to the highest degree of any of the technical lignins. Approximately 4-8% sulfur is incorporated into lignin preventing recondensation and a greater preservation of lignin side chains when compared to kraft lignins. Lignosulfonates tend to be soluble in water and insoluble in organic solvents.<sup>16,43</sup>

The sulfite pulp must be purified by ultrafiltration or alcohol fermentation because of a clutter of sugars and pulping chemicals that are difficult to separate by solubility differences. The relationship between lignin and the sulphite species render a complicated polymer. As mentioned above, lignosulfonates make great dispersing and binding agents but because of their dwindling availability, impurity and wide range of molecular weight distribution, lignosulfonates are not a good candidate as a base resource for polymeric composites. However, for now, the largest lignin demand is for lignosulfonates which play an important role in the building and construction industry.

#### **2.1.4.4 Kraft**

Today, kraft pulping is the dominant global process generating approximately 130 million tons of black liquor (BL) lignin per year but only 1-2% of that is utilized in higher value products while the remainder is burned to generate steam and energy within the system.<sup>44-46</sup> In that sense, lignin is an important biofuel with the black liquor playing a key role in providing energy to recover pulping chemicals. These black liquors produce approximately 700 million tons of high-pressure steam per year building up an energy surplus which can be sold back to electrical companies.<sup>44,47</sup> But is that the most efficient and economically valuable use of this carbon rich renewable resource? It is estimated that by 2030 kraft lignin production will increase from 130 million tons to 225 million tons annually.<sup>45-47</sup> An increasing demand for high end lignin-based materials would serve as the foundation for existing kraft mills to place focus not only on cellulose production but lignin production. This could result in the development of successful biorefineries which fall into an environmentally conscious circular bioeconomy model.

The conventional kraft cook is carried out in three successive steps. The initial step is diffusion controlled and wood chips are placed in an aqueous sodium hydroxide and sodium sulfide solution as the temperature is brought up to approximately 150 °C.<sup>48,49</sup> The second step called the bulk step is controlled by chemical reactions at a temperature of 170 °C and lasts approximately two hours.<sup>48-50</sup> Most of the lignin is removed during the bulk step, with about 50-60% in the black liquor.<sup>48-50</sup> There is poor selectivity in the final or residual step and the rate of delignification decreases. The chemical reactions in the bulk step lead to degradation and condensation of the lignin. Degradation is desirable and occurs via cleavage of the  $\alpha$ -aryl or  $\beta$ -aryl ether bonds while condensation is undesirable.<sup>48-51</sup>

It is generally accepted that depolymerization of native lignin occurs via nucleophilic attack and that during the kraft pulping process aliphatic double bonds (stilbene structures) are introduced while many terminal gamma hydroxyl groups of the side chain are released as formaldehyde. The cleavage of  $\beta$ -O-4 and  $\beta$ -5 linkages fragment the native lignin forming new phenolic hydroxyl groups, an important characteristic for later chemical modification.<sup>32,44,48-51</sup> New 5-5 linkages are formed and stubbornly survive the pulping process.<sup>48,49</sup> Thiol groups are introduced but kraft lignins still have a lower sulfur content than sulfite lignins.<sup>48,49</sup>

If the alkalinity is high (~pH 10) then the lignin will be soluble in the black liquor because of the free phenolic hydroxyl groups, allowing it to leach from the wood.<sup>50,51</sup> Subsequently, the black liquor is concentrated by evaporation to 40-50% solids and then burned.<sup>50,51</sup> The heat released is used for steam and power which recovers nearly all the pulping chemicals. To recover some kraft lignin from the process the pH must be lowered, and the lignin precipitated out, washed, and filtered prior to the recovery burner.

The kraft process is rather insensitive to wood species however, softwood kraft lignin (SWKL) has a higher reactivity than hardwood kraft lignin (HWKL).<sup>49,52,53</sup> As previously discussed, softwoods have one predominant monolignol (G-unit) as the building block for synthesis. Therefore, softwoods behave more uniformly during pulping whereas there is greater variability amongst hardwoods which require a change in pulping conditions.<sup>49,53</sup> Regardless, the native lignin structure is chemically changed and varies from wood species to species.<sup>53</sup> The resulting issue is a difficulty in transforming lignin into high end economically feasible materials because of a lack of consistency and homogeneity in its structure.

Table 3 gives a more detailed comparison of the differing industrial lignins and their most relevant chemical linkages and functional groups. Milled wood lignin (MWL) is structurally closer to native lignin than any other type of technical lignin. It can be observed that the degree of condensation (DC) for softwood and hardwood kraft lignin nearly doubles, and most  $\beta$ -O-4 linkages are lost while  $\beta$ - $\beta$  and  $\beta$ -5 linkages persist during the pulping process. Organosolv lignin maintains a low degree of condensation and it is considered the most pure.

**Table 3 Chemical linkages and functional groups of milled wood lignin (MWL) and different technical lignins per 100 Ar <sup>37,54-58,59</sup>**

	Milled wood lignin		Softwood kraft lignin		Hardwood kraft lignin	Lignosulfonate lignin <sup>a</sup>	Organosolv lignin	Soda lignin
	Spruce	Birch	Indulin AT <sup>b</sup>	BioChoice <sup>b</sup>	Birch	Eucalyptus	Alcell <sup>b</sup>	Bamboo
β-O-4	45	66	6-8	2	2	45	8	3
β-β	4	11	4-5	6	3	8	3	0.7
β-5	9	2	0.3-4	2	2	6	3	0
AlOH	107	129	49-51	44	26	117	32	1
ArOH	31	20	63-67	66	80	44	72	3
OCH <sub>3</sub>	95	177	68-80	63	141	142	117	140
DC	38	16	65	71	65	n.a. <sup>c</sup>	33	n.a. <sup>c</sup>

<sup>a</sup> Residual lignin isolated from unbleached acid sulfite pulp

<sup>b</sup> Indulin AT and BioChoice are pulping processes for softwood kraft lignins and Alcell is a pulping process for organosolv lignins

<sup>c</sup> n.a. - not available

#### 2.1.4.4.1 Advances in extraction techniques of lignin from black liquor

Work is being done to improve the efficiency of the kraft pulping process and the purity of resulting technical kraft lignins. Two processes, “Lignoboost<sup>TM</sup>” and “Lignoforce<sup>TM</sup>” emerged and challenged the quality of the traditional WestRock recovery process trade named Indulin AT.

The Lignoboost<sup>TM</sup> process was developed by Future Resource Adapted Pulp Mill or FRAM in Sweden where approximately 4,000 tons of Lignoboost<sup>TM</sup> lignin was produced per year in a demonstration plant owned and operated by Metso.<sup>60,61</sup> Carbon dioxide was used to acidify the lignin, precipitate it out and then the lignin was filtered.<sup>60,62</sup> After filtration the lignin was re-dispersed and acidified instead of being washed. After redispersion the lignin was filtered for a final time and then went through displacement washing which reduces the concentration gradient and improves filterability.<sup>60,61</sup> The result is a higher lignin yield, a lower ash and carbohydrate content, and a higher number of dry solids.<sup>60,61</sup>

The Lignoforce<sup>TM</sup> process was jointly developed by FPInnovations and NORAM who constructed a demo plant in Thunder Bay, Ontario in 2012.<sup>63,64</sup> The Lignoforce<sup>TM</sup> system produced 100 kg of lignin per day.<sup>63,64</sup> The major difference between the Lignoboost<sup>TM</sup> process is the Lignoforce<sup>TM</sup> process uses O<sub>2</sub> to oxidize the lignin before the addition of carbon dioxide.<sup>62–64</sup> The oxidation step addresses the totally reduced sulfur (TRS) compounds (hydrogen sulfide, methyl mercaptan, dimethyl sulfide, and dimethyl disulfide) which are odorous and toxic to humans.<sup>63,64</sup> The oxidation step converts these volatile compounds to nonvolatile species. In addition, there is an increase in lignin content, filtration rate, particle size and total solids, and a decrease in ash content, sulfur content, and chemical requirements.<sup>63,64</sup> Table 4 shows a significant reduction in ash content and an increase in lignin content using the Lignoforce<sup>TM</sup> system which is sufficiently pure for a biopolymeric blend.

**Table 4 Characteristics for oxidized and unoxidized black liquor in the Lignoforce™ process** <sup>62,63</sup>

	With BL oxidation	Without BL oxidation
Filtration rates (kg lignin/h.m <sup>2</sup> )	100-200	0-80
Total solids (%)	60-62	30-58
Ash content (%)	0.1-0.7	0.2-15
UV lignin (%)	97-98	50-98
Lignin particle size (μm)	5-10	0.2-1

### 2.1.5 Molecular weight and thermal properties of technical lignins

In general, technical lignins have varying molecular weights with sulfonated lignins like kraft and liginosulfonates having a larger molecular weight and a greater distribution or higher polydispersity index (PDI) than non-sulfonated organosolv lignin. High glass transition temperatures along with polarities arising from polyfunctionality affect technical lignins melt flow properties and therefore ability to blend uniformly in a polymer matrix. For example, the phenolic hydroxyl groups in technical kraft lignins can cause thermal induced crosslinking which results in higher glass transition temperatures ( $T_g$ ) which is why kraft lignin modification is necessary for processibility.<sup>59,65,66</sup> Based on light scattering data collected and averaged from various sources, Table 5 provides the weight average molecular weight ( $M_w$ ), the number average molecular weight ( $M_n$ ), the PDI, and  $T_g$  values for different technical lignins.<sup>59,62-66</sup> It should be noted that the PDI ranges from 1.5 to 6.7 depending on what pulping process delignified the lignocellulosic biomass. PDI occurs because of size distribution or aggregation/agglomeration and is a unitless measurement of heterogeneity based on  $M_w/M_n$  (PDI=1 being homogenous). As discussed, lignin is a heterogenous polymer, so high PDI values are expected however, organosolv lignins are sulfur free and show greater uniformity in

comparison to more readily available industrial counterparts.<sup>40</sup> The new Lignoboost<sup>TM</sup> and Lignoforce<sup>TM</sup> technologies have improved SWKL uniformity but chemical modifications are still necessary for success in a blend.<sup>63,64</sup>

**Table 5**  $M_w$ ,  $M_n$ , PDI, and  $T_g$  of technical lignins using similar light scattering techniques<sup>58, 59, 61-65</sup>

	SW kraft			Organosolv	Lignosulfonates	Soda
	Lignoboost <sup>TM</sup>	Lignoforce <sup>TM</sup>	Indulin AT			
$M_w$ (kDa)	11.4	11.2	14	9	38	19
$M_n$ (kDa)	3.2	5.3	6.0	3.3	5.7	3.6
PDI	3.6	2.2	2.4	1.5	6.7	5.3
$T_g$ (°C)	165-176	162-185	140-150	90-110	130-150	140-150

### 2.1.6 Lignin compostability

One of the roles of native lignin in the living tree is to protect against microbial degradation and other forms of rot. When a plant dies the carbohydrates will readily breakdown leaving lignin as the last compound to decompose. White rot fungus or *Basidiomycotina* is one of the most well-known degraders of native lignin.<sup>67,68</sup> Technical lignins used in materials experience processing and chemical modifications which change the structure adding in potentially toxic and volatile compounds. Janshekar et al. found that white rot fungus will break down kraft lignin at a slower rate than native lignin. Any chemical modifications carried out on kraft lignin will affect its end of life. When modifying kraft lignin for thermoplastic blends a focus should be placed on green chemistry practices.<sup>67,68</sup>



### **2.1.7 Lignin potential**

Lignin is a carbon rich renewable material that has great potential for valorization. What types of existing materials could lignin successfully supplement or replace? Scientific research must justify that lignin is a viable material of the future and then create a demand for lignin-based materials to provoke pulping mills to focus on producing consistent and clean lignin streams.

## **2.2 Petroleum based synthetic polymers**

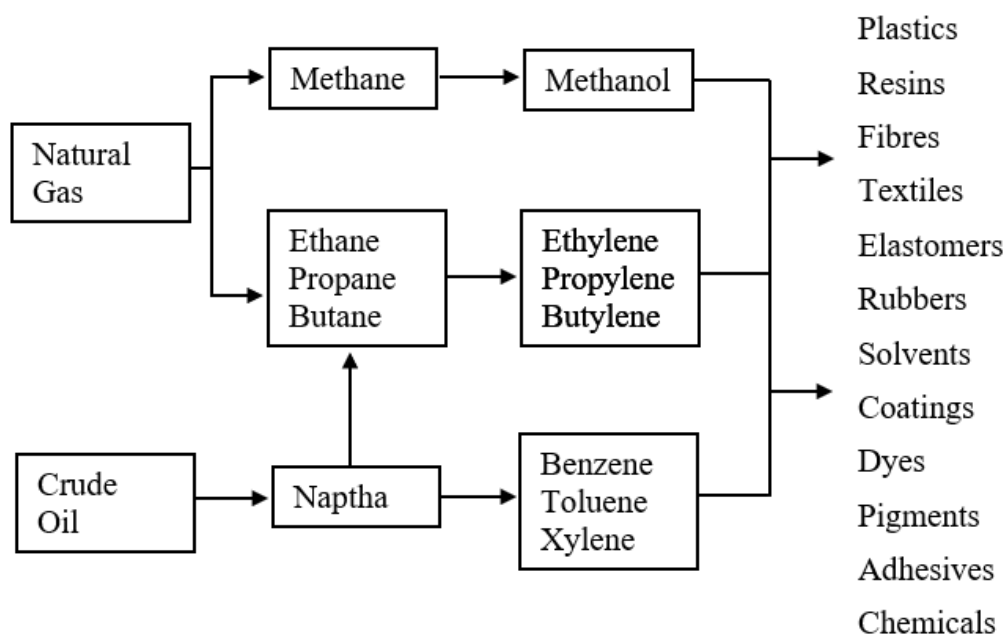
Synthetic plastics are made from crude oil, natural gas, and coal feedstocks. Fossil fuel is a non-renewable resource unlike wood which is a widespread, abundant, and replaceable biomass. The world has, “almost run out of oil” several times since 1950.<sup>69</sup> Because the oil and gas industries are so tight lipped, there is little information on how much fossil fuel remains but there is an understanding that conventional oil is running out. Conventional or easy to extract oil costs around 10-15 dollars per barrel to produce, while less conventional and more difficult methods like shale oil extraction costs 30-90 dollars per barrel to produce.<sup>69</sup> Oil shales require hydraulic fracturing or fracking to extract. It is likely that oil production costs and environmental risk will become too high in the next century and a drastic shift towards renewable resources for material production will be necessary.

### **2.2.1 The basics**

There is a plethora of plastics divided into two categories; thermoplastics which can be reformed upon heating and thermosets which once moulded will not reform. Some commonly used petroleum based synthetic thermoplastics are polycarbonate (PC), polyethylene, both high and low density (HDPE and LDPE), polyethylene terephthalate (PET), polytetrafluoroethylene (PTFE), polystyrene (PS), polyvinyl chloride (PVC), nylon 6,6, polymethyl methacrylate

(PMMA), and polypropylene (PP).<sup>1,4</sup> These plastics have a wide range of use from plastic bags to eyeglass inserts, piping, non-woven textiles, and containers for nearly all food applications . Some commonly used petroleum based synthetic thermosets are epoxy (EP), phenol-formaldehyde (PF), and polyurethane (PUR). Epoxy resins are used in many construction applications like primers, sealers, and flooring and PURs have been used for cable sheathing since the 1960's.<sup>1,4</sup> It is impossible to exist in today's climate and not regularly utilize fossil fuel based plastics. It is important to recognize how dependent humans have become on plastics and how imbedded they are in modern society.

Synthetic plastic comes from petrochemicals which must be extracted from beneath the earth's surface on either land or ocean. After extraction and pipeline transportation, crude oil or natural gas is refined via fractional distillation. Both crude oil and natural gas are combinations of carbon, hydrogen, nitrogen, sulfur, and oxygen, with crude oil having extra minerals.<sup>70</sup> A temperature gradient in the distillation tower separates fractions of the hydrocarbons by weight and boiling point.<sup>70</sup> The lightest fractions which are vapour gases flow to the top becoming petroleum gas and gasoline.<sup>70</sup> The intermediate weight liquid fractions become naphtha, paraffin, and diesel. Paraffin and diesel are used as fuels for air and heavy truck travel while naphtha undergoes high temperature steam cracking to become aromatics like xylene, toluene, and benzene and olefins like ethylene, propylene, and butane.<sup>70,71</sup> These petrochemicals are linked together to make polymer chains which undergo either addition or condensation polymerization and blend with plasticizers and other additives to become well known plastics like polyethylene and polypropylene. The heavier gas oils will condense at the lowest temperatures of the column and become lubricating oils and fuel oil for factories.<sup>70,71</sup> Figure 8 is a flow chart showing the transition from raw material, to petrochemical, to eventual use.<sup>70</sup>



**Figure 8 Petrochemicals obtained from fossil fuels after oil refining and the materials they produce** <sup>70</sup>

### 2.2.2 Statistics

As of 2015, 8.3 billion metric tons (Mt) of fossil derived plastics were used on planet earth with 6.3 billion Mt becoming waste.<sup>1,4,72</sup> Approximately 79% of this plastic waste builds up in landfills or the natural environment while 12% is incinerated with only 9% being recycled.<sup>1,4,72</sup> A tremendous amount of this plastic escapes containment and finds its way to the ocean each year.<sup>1,4,73</sup> This is an obvious mismanagement of resources and a waste of limited fossil fuel feedstocks. HDPE, LDPE, PP, PS, PVC, PET, polyester polyamide, and acrylic fibres account for 92% of all plastics made and of that 42% is some form of packaging which has the shortest life cycle, often used once and then discarded.<sup>4,73-75</sup> 80% of plastic found in household trash are PP food containers, HDPE soda bottles and milk jugs, LDPE carrier bags, PET textiles,

PS rigid foam packaging, and PVC piping.<sup>73-75</sup> If plastic consumption follows the compound annual growth rate, approximately 12 billion Mt of plastic waste should exist by 2050 and pound for pound there will be more plastic in the ocean than there are fish.<sup>4,74</sup> These plastics are problematic not only because they draw from a non-renewable source, but they accumulate in the natural environment at potentially catastrophic rates.

### **2.2.3 Toxicity**

It has been three decades since scientists took notice of macroplastics accumulating on land and subsequently in water. Poor waste management systems have caused worldwide leakage of these plastics into aquatic habitats. Plastic debris accumulation has been documented in the deep sea, coastlines, pelagic areas, estuaries, sandy beaches, seagrass beds, arctic sea ice, coral reefs, fresh water sources like rivers and lakes, soil, ground water, indoor air, and outdoor air.<sup>4,74</sup> There have been obvious effects on habitat and animals like sea turtles, birds, whales, and fish but the question remains, why should humans care?

It is easy to forget that plastics are a relatively new material and because of this scientists are only beginning to document and understand microplastic accumulation in natural environments. Microplastics are degraded plastic materials under the size of 5 mm (length) but invisible contaminants ranging in size from 5-20  $\mu\text{m}$  have been found in drinking water and wastewater.<sup>1,4</sup> Challenges in the relative size of oceans and landmasses and an agreement on a standardized method for data collection make microplastic accumulation based studies difficult to carry out. It is unlikely the effects of microplastic accumulation in the gut and tissues of aquatic animals will be fully understood in the next decade, however, it is known that petroleum-based plastics have entered our food chain and water filtration systems.

Rochman and her research group have extensively studied the absorption of dangerous chemicals into microplastics, the leaching of additives out of microplastics, and the subsequent effects on sea life and aquatic habitat.<sup>76,77</sup> Microplastics can be found in industrial abrasives, facial scrubs, and pellets known as nurdles but the majority slowly break down from macroplastics due to ultraviolet (UV) radiation and abrasive wave action.<sup>78</sup> Plastics are mixed with additives like stabilizers, fillers, flame retardants, pigments, and plasticizers to enhance performance.<sup>79,80</sup> A staggering 50% of plastics contain known carcinogenic and endocrine disrupting monomers like styrene, polyvinyl chloride, and Bisphenol A (BPA) and these plastics slowly break down into toxic monomers, while additives and solvents are shed.<sup>77,79</sup>

Aside from the obvious entanglement issues that aquatic animals and sea birds face from encountering discarded macroplastics, the toxicity of microplastic ingestion is now a major concern of scientists like Rochman. The Stockholm convention states that persistent organic pollutants or POPs are “harmful organic compounds that resist environmental degradation through chemical, biological and photolytic processes.” While fragmented plastics can be classified as POPs, the Stockholm convention is referring to persistent bioaccumulative toxins like pesticide DDT, polychlorinated biphenyls (PCBs), polybrominated diphenyl ethers (PBDEs), and polycyclic aromatic hydrocarbons (PAHs).<sup>76–80</sup> For example, in the 1980’s General Electric in Niskayuna, New York dumped PCBs directly into the Mohawk River without regulation and with time these toxins spread throughout water sources. Today, dumping such toxins into a water source is illegal but the long-lasting damage remains. Toxins like PCBs, DDT, PBDEs, and PAHs are found accumulating on land and in water sources worldwide.<sup>78–80</sup> This issue is of interest because alongside microplastics, these POPs are hydrophobic. As macroplastics fragment into infinitesimally smaller pieces surface area increases and the plastic

debris soak up these toxins far more efficiently than naturally occurring materials like algae. Microplastics can concentrate POPs and other metal pollutants from the environment one-million-fold relative to their dilute concentration in sea water.<sup>77-80</sup> At first glance this seems like a solution to remove toxins from water sources, but the reality is microplastics are nearly impossible to locate and remove. The unfortunate outcome has been transportation at high concentrations into the food chain via plankton, filter feeders, and deposit feeders to fish, seabirds, crabs, marine animals, whales and eventually humans.

Rochman studied the long-term sorption of these organic contaminants and found that PP, LDPE, and HDPE account for 62% of petroleum based plastics that are most commonly leaked into the ocean and are known to be concentrators of PCBs.<sup>73,75-77</sup> Plastic ingestion affects at least 208 species and although more time is needed to understand the full consequence of bioaccumulation, negative impacts are already being seen.<sup>73,75-77</sup> Because microplastics are so small there is a high capacity for transfer across tissue and cell boundaries. Toxicology reports on mussels, crabs, fish, and seabirds in Brazilian waters show an exposure to PE and PS particles absorbed with pyrene and these animals demonstrate a reduction in feeding, reproductive success, and a decrease in survival rates.<sup>73,75-77</sup> Plastic ingestion in adult fish and seabirds as low as 1% can effect enzyme, immune and gene function.<sup>73,75-77</sup> While no study points directly to how this effects humans, it is known that ingestion of microplastics drenched in POPs cause reduced growth, reproductive distress, and a decrease in population of animals within the food chain and this should be cause for concern.

In a second study Rochman examines the effects of plastic additives like BPA, adipates, phthalates and flame retardants in marine environments. BPA is an estrogen mimicking chemical that is found in PC water bottles and receipt ink.<sup>73,75-77</sup> Adipates and phthalates mimic some

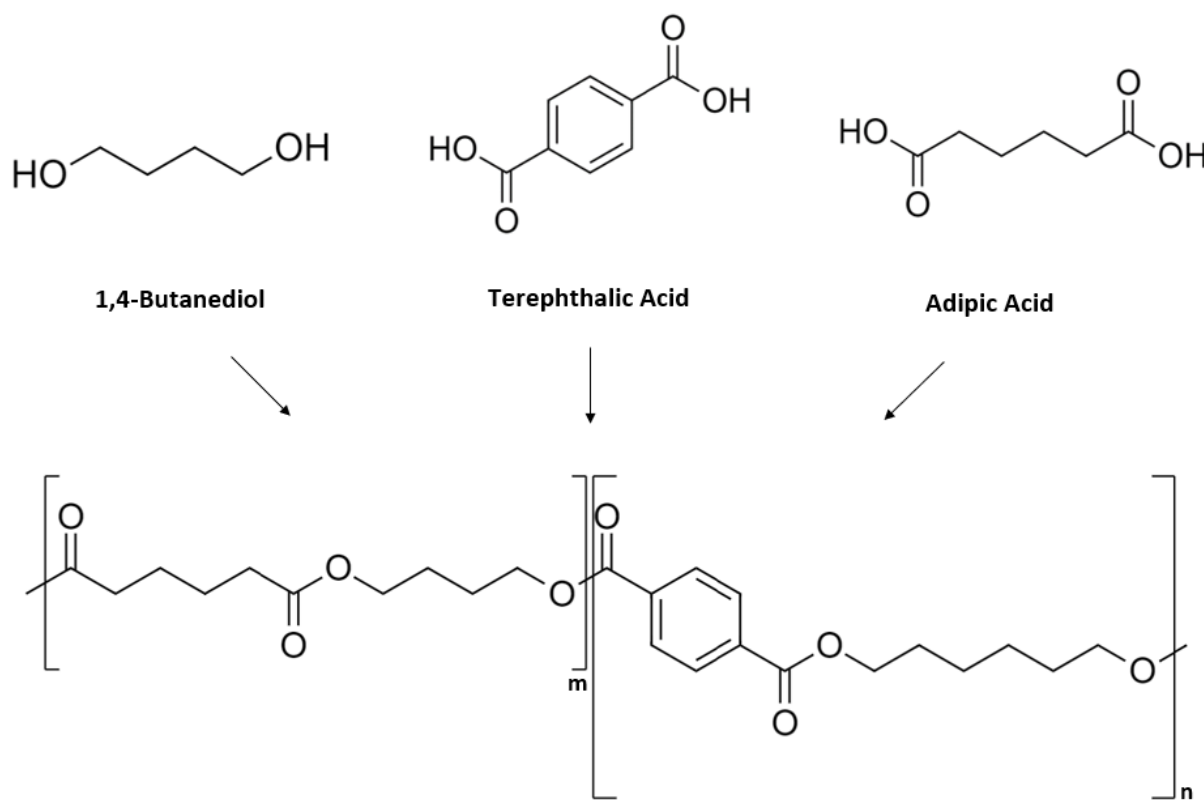
human hormones and are added to PVC to make it more pliable for use in food packaging and children's toys.<sup>73,75-77</sup> Rochman sampled a population of exposed medaka, a Japanese fish and found early warning signs of endocrine disruption. Once again, stunted growth, suppressed reproduction and malformed offspring were all the result of contaminated microplastic indigestion. Other works have been published to back Rochman's claims and can be referred to for further study.<sup>81-86</sup> If plastic use continues to increase which is likely, it is expected a higher frequency of physical effects will be seen in the human population.

#### **2.2.4 Plastic ban in Canada**

In October of 2020 the Canadian government revealed a plan to ban six one use plastic items (straws, stir sticks, cutlery, takeout containers, carrier bags, and six pack rings) by the end of 2021 citing harm to the environment, difficult or costly recycling, and potential of available alternatives as the cause. In addition, the companies who produce these plastics will have to help pay for their end of life. This will act as an incentive for corporations to look towards making better plastics which is exciting news for the valorization of lignocellulosic materials. Environment and Climate Change Canada, a sector of Health Canada created a detailed draft science assessment of plastic pollution and the harm it causes to the environment and the potential human affect as a revolutionary study revealed the first evidence of microplastics found in human placentas.<sup>87,88</sup> It clearly stated more research is needed to develop an in depth understanding of the damage petroleum based plastics cause but sufficient evidence demands an immediate and necessary change in use, life cycle and alternatives to the petroleum based plastics discussed earlier.

### 2.2.5 Ecoflex™

Ecoflex™ is the brand name for polybutylene adipate terephthalate (PBAT), a semi crystalline completely biodegradable aliphatic-aromatic polyester produced by the chemical company BASF. Structurally, Ecoflex™ is composed of three fossil-based monomers: 1,4-butanediol, a primary alcohol, terephthalic acid, and adipic acid. It should be noted that all three monomers can be biobased but in this study, PBAT or Ecoflex™ was supplied as a synthetic polymer from BASF.<sup>89-91</sup> Figure 9 shows the aliphatic polyester region which helps biodegradability and the aromatic polyester region which is good for rigidity.<sup>92,93</sup>



**Figure 9** The Ecoflex™ copolymer composed of the three monomers 1,4-butanediol, terephthalic acid, and adipic acid<sup>92,93</sup>



Ecoflex™ has a high toughness and is strong, flexible, tear resistant, resistant to fluctuations in humidity and water, compostable, approved for food contact, and processible on conventional blow film plants.<sup>92,94</sup> Hence, Ecoflex™ is similar to LDPE films but because of moderate water vapour permeability, Ecoflex™ is more breathable. Much like LDPE, Ecoflex™ is optimal for packaging food like vegetables and fruits. Proper packaging will keep perishable foods fresh for longer thus minimizing food waste. However, because of its structure Ecoflex is more versatile and can be extruded into foam trays, hygiene films, shampoo bottles, coatings, and rigid packaging containers.<sup>92,93</sup> What makes Ecoflex™ so interesting is its ability to blend with biobased and biodegradable polymers that do not exhibit good mechanical properties or melt processability on their own. Because Ecoflex™ is certified compostable worldwide and approved for food contact it is a great candidate to blend with technical lignin which is notoriously unstable in a melt on its own. Table 6 gives a side by side comparison of some mechanical properties of Ecoflex™ C1200 and LDPE for a 50 µm blown film.<sup>94-98</sup>

**Table 6 Mechanical property comparison for Ecoflex and low-density polyethylene for a 50 µm blown film using similar standardized test methods**<sup>93-98</sup>

	Test Method	Unit	Ecoflex	LDPE
Transparency	ASTM D 1003	%	79-82	55-79
Tensile Strength	ISO 527	N/mm <sup>2</sup>	32-44	20-19
Ultimate Strength	ISO 527	N/mm <sup>2</sup>	36-45	26-31
Ultimate Elongation	ISO 526	%	560-710	540-600

### 2.2.5.1 Biodegradability

Biodegradability is a function of chemical structure and biodegradable plastics can be sourced from petroleum or biobased resources. While plastics like PE or PS will degrade by fragmentation, they persist indefinitely in the environment in the form of microplastics. Some polymers can be metabolized by microorganisms and standardized testing will confirm biodegradability. The biodegradation processes usually carried out by yeast, fungi or bacteria is aerobic if degradation takes place in the presence of oxygen and generally occurs in soil or compost or anaerobic if there is a lack of oxygen which generally occurs in landfills or the ocean.<sup>92,93</sup>

There are a series of standards that any new material must complete to be considered compostable and biodegradable under certain conditions. The European standard is the EN 13432, the American standard is the ASTM D 6400-04, and the Japanese standard is the GreenPla.<sup>99–101</sup> The American and European standard make the international standard, the ISO 17088 which was created in 2008. Ecoflex™ is certified through the ISO 17088 and the ISO 14855 composting test.<sup>102</sup> Ecoflex™ has also undergone the EN 13432 Amex E plant growth test which tests plants grown from seeds in compost which Ecoflex™ was degraded.<sup>92,94</sup> These plants were compared with untreated compost plants and showed no negative side effects.<sup>92–94</sup> Ecoflex™ passed the Daphnia test in accordance with standard DIN 38412 Part 30 which demonstrates a low toxicity in water-soluble intermediates meaning ground water is safe if contaminated.<sup>92,103</sup> In addition, the earthworm test was performed following OECD guideline 207.<sup>92</sup> Earthworms were placed in a control soil and an Ecoflex™ treated soil and there was no deaths in either of the soils after 7 and 14 days concluding that compost exposed to Ecoflex™ is safe for plants, earthworms, and groundwater.<sup>92</sup> Siegenthaler et al. summarized the life cycle

assessment of Ecoflex<sup>TM</sup> concluding it is a viable and more valuable alternative to PE from the standpoint of a circular bioeconomy and the end life of a plastic.<sup>92</sup> Ecoflex<sup>TM</sup> has undergone standardized testing for biodegradability to receive its certification for compostability.

### **2.2.6 Potential for biobased thermoplastic blends**

Given the evidence of an increasing amount of fossil based macro and microplastic pollution in the environment and the subsequent harm caused to animals and habitat, it is understood that if solutions are not developed, impacts will be felt for decades to come. The advantage of sourcing polymeric feedstock from a renewable material like lignin will help with decarbonization, resource management, and the improved life cycle of plastic materials. Currently and for reasons that will be discussed in detail, lignin alone does not meet the requirements of a “good” plastic. It is necessary to blend lignin with a more thermally stable partner like Ecoflex<sup>TM</sup>. If the blend ratio of lignin to Ecoflex<sup>TM</sup> is significant and mechanical properties are not compromised then an increased demand for lignin in biodegradable plastics will occur. The benefit is that lignin is sourced from a waste stream and does not compete with a food source. A higher demand for lignin will drive incentive for pulping plants to transition into biorefineries that better utilize the lignin waste stream, and this will boost the forest products economy. There is no denying we need plastics, but we need better plastics.

### **2.3 Modifications for technical lignin utilization**

Much like petrochemicals that must be refined from crude oil before polymerization into the well-known plastics previously discussed, technical lignins need modification to reach their full potential as building blocks in novel materials like biobased plastics. Scientists have extensively studied the reactivity of different technical lignins and while the chemical non-uniformity is dependent on plant species and pulping process it is well understood that technical

lignins have a plethora of reactive sites based on their many functional groups. Amongst the functional groups, phenolic hydroxyls are the most prominent in kraft lignins. These groups are centers of high polarity which effect stability in a blend with a hydrophobic polyester like Ecoflex™. These polar groups lead to hydrogen bonding which produce aggregated domains that need to be better blended when considering plastics. It is important to understand heterogenous technical lignin and what makes it difficult to work with while simultaneously understanding its potential.

The easiest way to control lignins structure would be during the pulping process (lignin first approach) but lignin is not the priority and pulping conditions which affect cellulose, the target product, would have to be changed. This leaves scientists and engineers with a unique problem to solve, what are the most efficient, environmentally sound, scale-up chemistries available to transform an “as is lignin waste stream” into a viable and economically feasible material? Researchers have studied and applied fractionation and/or chemical derivitization to develop a variety of solutions.

### **2.3.1 Fractionation**

Fractionation separates lignin into different portions based on solubility differences or molar mass. The two common lignin fractionation methods are solvent extraction and membrane extraction.<sup>104</sup> Ultra and nano filtration by means of ceramic or polymeric membranes has been quite successful in size exclusion of lignin fractions by sequentially increasing or decreasing the membrane pore size. However, ultrafiltration has several drawbacks in fouling, cleaning, price, service, and durational use of the membranes. Because of this, most research focuses on solvent based fractionation methods like single step extraction, sequential extraction, pH dependent

precipitation, and fractional precipitation. Of these four methods currently, single step and sequential extraction are the most common types of lignin fractionations.<sup>104</sup>

A series of studies by Morck et al. introduced the concept of solvent fractionation of lignin in the 1980's and these were followed in the 2000's with interest in solution spinning for carbon fibre precursors.<sup>105,106,107</sup> A pivotal study that emphasized the importance of fractionation was performed by Cui et al. using a fractionation-precipitation method. Using three softwood kraft species the research group separated the soluble and insoluble portions of lignin with polar solvent acetone and continued to subject the soluble portion to increased amounts of the nonpolar solvent hexane.<sup>108</sup> The results yielded narrowly dispersed fractions with PDI values  $\leq 1.5$ . The group distinguished a linear correlation between  $M_n$  or the ratio of aliphatic to aromatic hydroxyl groups to the volume of hexane which proved a relationship between chemical structure and the molecular weight of lignin fractions.<sup>108</sup> As mentioned, wood species and pulping conditions will change the structure of resulting lignin making it difficult to develop a, "one size fits all" homogenous building block for blends. This group used three softwood kraft lignins; KL1, southern pine aimed for bleachable grade pulp, KL2, southern pine aimed for linear board pulp, and KL3, Norway spruce with an undisclosed pulp type.<sup>108</sup> The most revealing outcome of this study was the consistency and reproducibility of the narrow isolates even though the three lignins were produced under different pulping conditions. This holds major significance in potentially commercializing lignin fractionation into preexisting pulp mills.

This study opened the door for many other research groups to build upon, refine, and improve processing for efficiency and limiting toxicity (Table 7) however, fractional precipitation methods require large volumes of solvent. With each step, volume of solvent increases while the concentration of lignin in solution decreases. This could make a scale up

operation in a large facility difficult as an increase in solvent and an increase in protocol steps, means an increase in operational cost.<sup>109</sup>

### **2.3.1.1 Single step solvent extraction**

The ability to alter the  $T_g$  is an important processing parameter and critical when blending lignin in polymeric products. Using both kraft processed softwood and hardwood Saito et al. carried out a lignin fractionation with methanol (MeOH) and successfully separated out the low molecular weight (LMW) fraction. An important finding was the  $T_g$  change of the as received lignin (153°C) after the MeOH fractionation.<sup>110</sup> The LMW fraction or the soluble portion had a  $T_g$  of 117°C and the high molecular weight portion (HMW) or the insoluble portion had a  $T_g$  of 211°C. Using  $^{13}\text{C}$  nuclear magnetic resonance ( $^{13}\text{C}$  NMR) Saito's group found that the MeOH-soluble portion contained more aliphatic C-C than the as received or insoluble portions which would impact free volume expansion and a decrease in  $T_g$ .<sup>110</sup>

Using  $^{31}\text{P}$  nuclear magnetic resonance ( $^{31}\text{P}$  NMR) Saito's group determined the soluble portion had more aromatic hydroxyl groups than aliphatic hydroxyl groups which led to less hydrogen bonding interactions and therefore a lower  $T_g$  value.<sup>110</sup> A low  $T_g$  value is one consideration for lignin in melt processing but aromatic hydroxyl groups of high reactivity need modification for stability. An increase in carbon content due to aromatic rings in the MeOH-insoluble portion correlates to a higher  $T_g$  value and char yield than the soluble or as received portions. The insoluble portion could be highly beneficial as a carbon precursor in carbon fibres or activated carbons.<sup>110</sup> This study demonstrates that a simple fractionation created uniform lignin portions with different thermal properties and different potentials in value added products.

Using softwood kraft lignin from the Lignoboost process, Duval et al. carried out a solvent screening experiment to separate Kraft lignin fractions using a variety of industrial

solvents in relation to Hansen solubility parameters (for polar systems) which consider dispersion forces, polar interactions, and hydrogen bonding.<sup>111</sup> In contrast, the Hildebrand solubility for non-polar systems does not account for hydrogen bonding. All three parameters represent the cohesive energy of a mixture and are interdependent meaning they should be considered together instead of individually when choosing a solvent system.

An important part of Duval's research focused on sustainable chemistry practices and for that reason hexane, diethyl ether, dichloromethane, dioxane, and chlorinated solvents were eliminated.<sup>111</sup> The solvents of interest had low boiling points and would be easy to recover in an industrial setting (Table 7). In today's climate, taking into consideration the potential for industrializing any process is an important experimental parameter. The above considerations limit solvent choice to alcohols like methanol and ethanol, 1-propanol, iso-propanol, and tert-butanol, ketones like acetone and methyl ethyl ketone, and esters like ethyl acetate (EtOAc).<sup>111</sup>

Duval et al. confirmed a decrease in lignin solubility with an increase in carbon chain length and so it was the acetone fractionation and the methanol fractionation that produced the highest yield of the LMW portion.<sup>111</sup> However, EtOAc was the most selective in terms of separating LMW fragments. Using the Hansen solubility parameters and single solvent analysis, Duval's group was able to define a reproduceable solvent sequence involving EtOAc which separated five lignin fractions with polydispersity lower than two.<sup>111</sup>

A recent study by Jiang et al. used BioChoice pine Kraft Lignoboost lignin in a one stage fractionation using multiple solvents for comparison and then an economic analysis to determine if a scale-up operation was feasible.<sup>109</sup> Taking into consideration all of the previously discussed parameters, six solvents were chosen (acetone, ethyl acetate, methyl ethyl ketone (MEK), methanol, ethanol, and isopropanol) and EtOAc and isopropanol produced low extraction yields

and were eliminated from further analysis.<sup>109</sup> The group framed the scale-up based on solvent consumption in relation to lignin yield and acetone and MEK were economically feasible.<sup>109</sup>

Using gel permeation chromatography (GPC) the research team constructed detailed molecular weight plots for the soluble and insoluble fractionated lignin portions.<sup>109</sup> The soluble portions showed a narrower distribution and much lower molecular weight than the insoluble portions. Insoluble fractions still contained some residual low molecular weight fragments. The insoluble portion is capable of additional washing with fresh solvent for further purification to give a residual high  $T_g$  material to be used in different applications.

Further, hydroxyl group content was analyzed using  $^{31}\text{P}$  NMR and it was found the soluble fraction contained less aliphatic hydroxyls than the insoluble portion.<sup>109</sup> In addition, the soluble LMW portions had a higher amount of 5-free phenolic hydroxyls. For utilization that requires free C5 aromatic ring positions the LMW soluble portions have more potential such as in hydroxymethylation for adhesives. Molecular weight correlates to degradation indicating the soluble portion undergoes more aryl ether cleavage during pulp processing causing a decrease in molecular weight but an increase in phenolic hydroxyl group content. The same logic would infer that the insoluble or higher molecular weight portion contained more intact lignin side chains and therefore more aliphatic hydroxyl groups. These are very important processing parameters for lignin when making thermoplastic or thermosetting materials.

Many research groups have studied solvent/water extractions which can lead to reduced cost and environmental pressure in production. Boeriu et al. fractionated five different technical lignins in green solvents like acetone/water at different ratios and showed the maximum solubility for all types of lignins was reached at 70-90% acetone.<sup>112</sup> Solubility parameters are important in optimizing a procedure and predicting how lignin will behave in a solvent (Table 7).



This group calculated the solubility of lignin was 13.5-14.4 (cal/cm<sup>3</sup>)<sup>1/2</sup> and the mixture of 70-90% acetone was 12-15.7 (cal/cm<sup>3</sup>)<sup>1/2</sup> which show similarities.<sup>112</sup>

Ajao et al. built on Duval's research by using solubility parameters to study the potential of large-scale fractionation for Lignoboost softwood kraft lignin in eight pure solvents and four solvent mixtures. Ajao et. al showed that an acetone water mixture of 70:30 was successful in producing high yield and high purity lignin which agrees with Boeriu et al.<sup>111-113</sup>

### **2.3.1.2 Sequential solvent extraction**

Sequential step extraction involves the use of multiple solvents and while the goal is to get a more uniform or pure product, the question of necessity should arise. Can the same results be gained from a single solvent extraction?

Ropponen et al. analyzed both softwood and hardwood organosolv and kraft lignins in a three-step fractionation process that used diethyl ether, diethyl ether/acetone, and acetone sequentially as the solvents.<sup>114</sup> Diethyl ether is a highly volatile flammable liquid used as a starting fluid for some engines (Table 7). When comparing the final and most pure (PDI 2.16) of the fractionated softwood kraft lignin residue to Jiang et al. acetone soluble softwood kraft lignin portion after one simple fractionation (PDI 2.2), there is no significant difference.<sup>109,114</sup> It would be revealing to compare molecular structure and functional group content of these two products. Ropponen et al. found only minor differences between soluble fractions in the sequence but common differences between the soluble and insoluble portions, i.e. thermal properties, molecular weight and functional group content.<sup>114</sup> One interesting finding showed that hardwood syringyl type lignin preferred dissolution in acetone while organosolv lignins did not.<sup>114</sup>








Greener more sustainable sequences have been developed like, Robles et al. who used aqueous fraction methods on Kraft, organosolv, and soda lignins in successive steps starting with 60% acetone (v/v) and then 40% acetone (v/v).<sup>115</sup> The chemical make-up of the unfractionated technical lignins differed but upon completion of the fractionation process the chemical composition and carbon content of all insoluble portions were similar.<sup>115</sup> All three soluble portions produced good yields, but the lignin origin defined the chemical structure with kraft and organosolv showing promise in applications that require high reactivity.<sup>115</sup> Using a succession of steps that started with 60% acetone, 10% acetone and finally the evaporation of acetone, Jaaskelainen et al. improved upon this research and developed a novel approach that requires less solvent.<sup>116</sup>

Recently, a study by Majdar et al. revealed that by targeting specific hydrogen bonding affinities, trends in glass transition temperatures can be observed and  $T_g$  values are a product of both molecular weight and hydroxyl group type and amount.<sup>117</sup> This approach involved sequentially fractionated Lignoboost softwood kraft lignin using aprotic acetone and protic methanol.<sup>117</sup> The fractionation took advantage of the hydroxyl groups present in lignin and their ability to hydrogen bond with the solvents. Further refinement filtered out oligomeric structures that polluted the methanol soluble and acetone insoluble fraction by using a dialysis membrane.<sup>117</sup> By harnessing differences in polarity and hydrogen bonding characteristics the team was able to study the soluble fractions on a more tertiary level in comparison to previous studies. This work could have great implications towards a more precise structure for both fractions which have different value-added applications.

In conclusion, Table 7 gives a general overview of the more commonly used solvents and their hazard rating, boiling point (b.p.) and Hildebrand solubility parameter ( $\delta$ ).<sup>118–120</sup> As

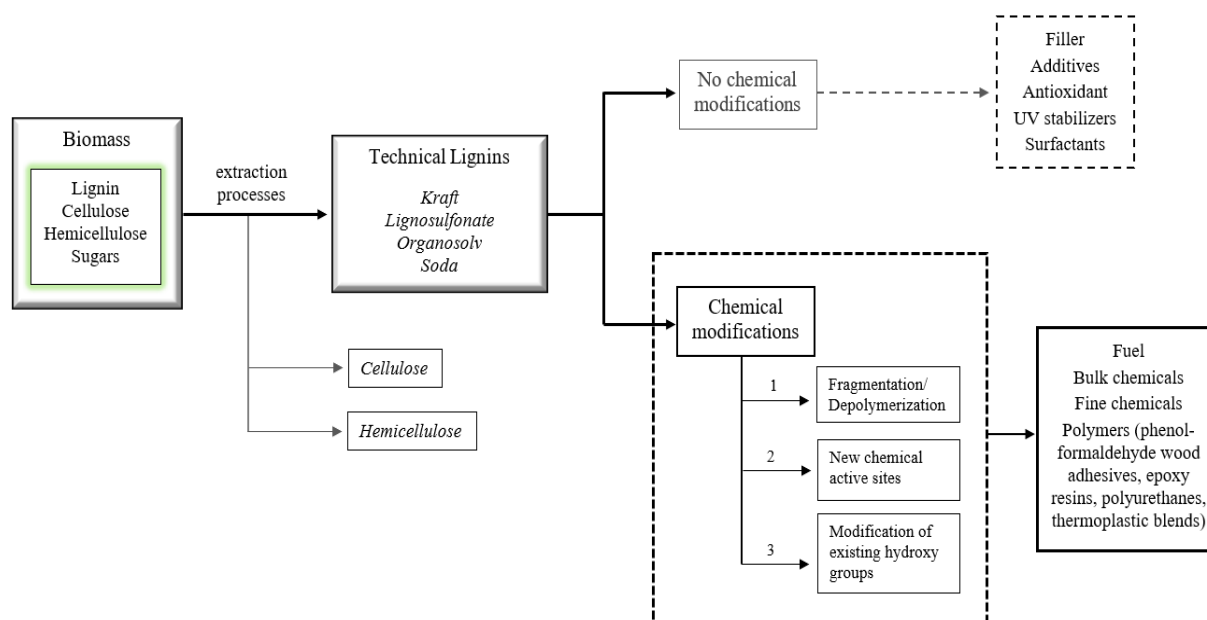
discussed, these are important criterion when choosing an appropriate solvent. The solubility parameter of lignin is 13.5-14.4 (cal/cm<sup>3</sup>)<sup>1/2</sup>.<sup>112</sup>

**Table 7 Physical properties and toxicity of commonly used organic solvents in lignin fractionation methods**<sup>118-120</sup>

	Hazard rating	$\delta$ (cal/cm <sup>3</sup> ) <sup>1/2</sup>	b.p. (°C)
Acetone		9.77	56
Diethyl ether		7.62	34.6
Ethanol		12.7	78.5
Ethyl acetate		9.10	77
Hexane		7.24	68.7
Methanol		14.5	64.6
Methyl ethyl ketone		9.27	79.6

### 2.3.2 Chemical modification

Technical lignins vary in homogeneity and functionality which make them difficult and somewhat unpredictable to work with and these differences lead to great variability. Depending on the intended use, lignin can be functionalized to meet desired material requirements. Unmodified lignins tend to aggregate because of hydrogen bonding,  $\pi$ - $\pi$  stacking of the aromatic rings, and Van der Waals interactions.<sup>6,121</sup> Instability of functional groups leads to crosslinking at higher temperatures which is desirable when using as a stiffening agent in phenol-formaldehyde binders but undesirable when blending in a polymer matrix where poor flow properties hinder miscibility thus diminishing mechanical properties. It is important to note that unmodified lignin is utilized in various materials but fine-tuning technical lignin with applicable chemical modifications will improve polymer-lignin compatibility in thermoset and thermoplastic blends. Figure 10 is an overview flowchart of the uses of lignin with and without chemical modifications.<sup>121,122</sup> The three main ways to modify technical lignin are by fragmentation or depolymerization, introduction of new active sites or modification of existing functional groups. These methods and chemistries will be examined in upcoming sections.



**Figure 10 Overview flow chart for technical lignins that either undergo or do not undergo chemical modifications**<sup>121,122</sup>

### 2.3.2.1 Lignin depolymerization

Lignin depolymerization, also called lignin fragmentation has potential to produce aromatic chemicals like benzene, toluene, and xylene through two major thermochemical routes; oxidation or hydrogenolysis. Other degradation techniques are beyond the scope of this review. Benzene, toluene, and xylene are three aromatics commonly derived from petroleum and used as building blocks in a plethora of chemicals. The potential to synthesize these aromatics from lignin instead of petroleum exists and is beneficial because lignin is renewable and there is a high demand for these starting molecules.

Hydrogenolysis, also called hydrogenation is a form of pyrolysis where hydrogen is present, but air is absent. It serves to mimic hydrocracking, a successful high pressure, high temperature process in petroleum refining. The Noguchi Process was established in Japan in

1952 and Crown-Zellerbach in the United States tried to improve upon it in 1961.<sup>123,124</sup> The two-step process utilized a metal catalyst, typically iron (II) sulfide with one co-catalyst like copper, silver or tin.<sup>123,124</sup> It is a high temperature process (between 300-600 °C) and the hydrogen source acts as a radical scavenger.<sup>123,124</sup> The Noguchi Process produced 44% monophenol products while the Crown-Zellerbach process only yielded 21%.<sup>123,124</sup> There have been research groups like Hartwig et al. who developed a nickel-catalyzed system that operates under milder conditions and Sels et al. who studied reductive catalytic fractionation methods to produce lignin derived phenolic monomers used in printing ink but overall, these methods are not commercially available.<sup>125,126</sup>

Oxidation is the other major technical lignin depolymerization technique but often produces a more complex product than hydrogenolysis. Typical oxidants include nitrobenzene, metallic oxides, air, oxygen, and hydrogen peroxide. Vanillin, most known in the food industry, is also a chemical feedstock in the pharmaceutical industry and is the most valuable and well-known product of oxidation. A strong market for vanillin exists, and although its isolation is complex, the process has been refined throughout the years especially by Borregaard.<sup>127,128</sup>

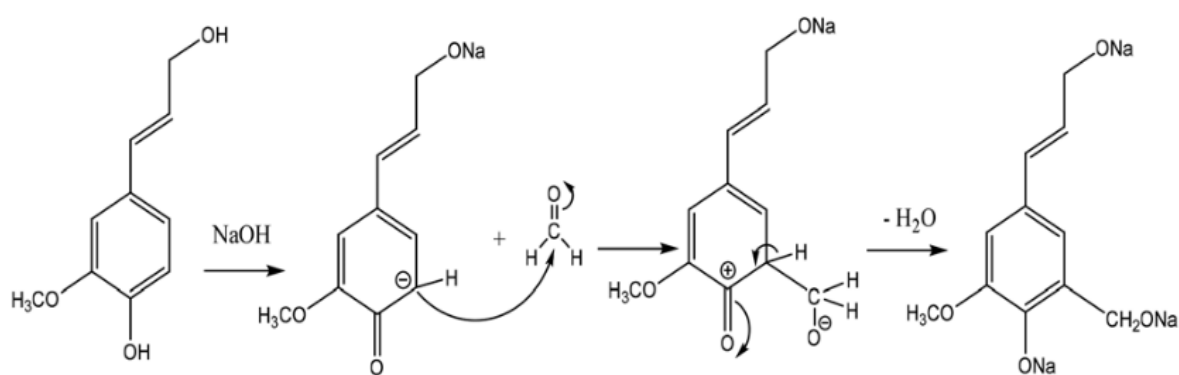
It would be ideal to acquire aromatic monomers by depolymerizing technical lignin, but a combination of high cost, poor yield, and extreme conditions make it nearly impossible to compete economically with petroleum counterparts. For compounds like benzene, lignin aromatics need to be completely deoxygenated and that is difficult because technical lignins are riddled with phenolic hydroxyls. Radicals are produced via cleavage during pulping and this leads to new stable C-C bonds which need to be broken to produce pure chemical products. Fragmenting lignin down to fine chemicals is possible but perhaps not the most efficient use of this abundant renewable resource.

### **2.3.2.2 New active sites**

As discussed, lignin has many functional sites including the phenolic hydroxyl group in the para position of the aromatic ring, but these active sites can be sterically hindered due to cross linking. If lignin is functionalized by either enhancement or addition of a new active site this can increase reactivity, decrease brittleness, and improve solubility. There are many chemical pathways towards synthesizing new chemical active sites, i.e. hydroxyalkylation, nitration, and amination. These modifications will improve the mechanical and thermal properties of polyurethanes (PU) and phenolic resins (PF) which contain lignin.

#### **2.3.2.2.1 Hydroxyalkylation**

Unmodified lignin can replace petroleum sourced phenol in phenol-formaldehyde (PF) resins with some success although reactivity and effectiveness are limited. Similarities in structure, function and reactivity between lignin and petro-based phenols make lignin a good biobased alternative in this popular wood adhesive. Methylolation (hydroxymethylation) can be utilized to improve lignins reactivity with formaldehyde by adding an active site at open positions on the ring. This modification has led to success in industry for lignin-phenol-formaldehyde resins (LPF). Figure 11 shows a scheme for a common methylolation reaction where lignin is reacted with formaldehyde in a strong base environment to introduce a hydroxymethyl group ( $-\text{CH}_2\text{OH}$ ) at the para and/or ortho position of the aromatic ring via electrophilic aromatic substitution.<sup>129,130</sup>



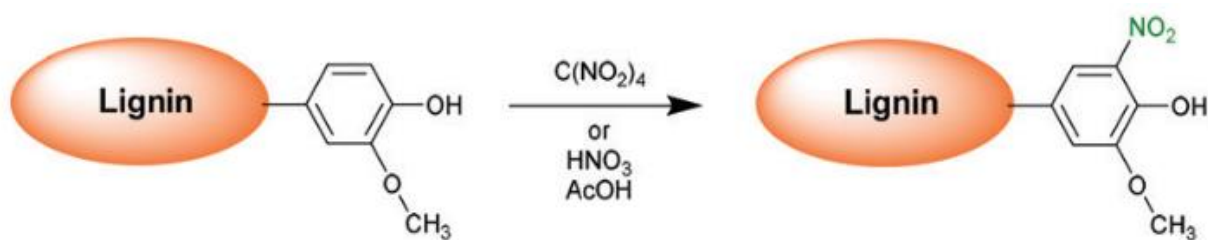
**Figure 11 Scheme for hydroxymethylation of lignin using formaldehyde to make LPF wood adhesives** Reprinted with permission from ref <sup>130</sup> Copyright 2019 Royal Society of Chemistry

In 1984 Glasser et al. carried out an extensive study that characterized (molecular weight, thermal properties, chemical structures, and solubilities) hydroxyalkyl lignin derivatives from several lignin sources.<sup>131</sup> This very extensive and important study ultimately determined that hydroxyalkyl lignin derivatives are good prepolymers for thermoset adhesives like PF resin. Glasser's early work was inspiration for future wood scientists to build upon. In 1994, Peng and Riedl studied hydroxymethylation which is one of the most common and easy ways to produce lignin derivatives for wood adhesives like PFs.<sup>132</sup> Recently, Talabi et al. thermally treated kraft lignin in a non-oxidizing environment and through ether link cleavage lowered the molecular weight making the lignin more reactive.<sup>133</sup> The derivatized lignin was able to replace petroleum-based phenols up to 30%.<sup>133</sup> The team went on to carbonize the 30% LPF resin in the presence of boric acid which generated graphitic carbon. This LPF resin showed promise as a binder in carbon-containing bricks.<sup>133</sup> Even with advances in research, hydroxymethylation remains a versatile and simple way to add a chemical site to lignin.<sup>130,134</sup>



#### 2.3.2.2.2 Nitration

Nitro lignins are made by adding an electron withdrawing nitro group onto the aromatic ring in a non-aqueous solvent with nitrating reagents like nitric acid with acetic anhydride.<sup>65,121</sup> Nitration improves the reactivity of technical lignin which can then be incorporated into a polyurethane (PU) network where it will act as a hardening segment that enhances the physical strength of the thermoset.<sup>135</sup> Polyurethanes are flexible or rigid foams with a variety of uses in construction, automotive, furniture, bedding, appliances, packaging, and textiles. Lignins phenolic structure and aliphatic hydroxyl functional groups make it possible to replace a portion of the polyol in polyurethanes resulting in improved degradability. Figure 12 presents a scheme of a lignin nitration reaction.<sup>65</sup>



**Figure 12 Lignin nitration scheme using tetranitromethane or nitric acid with acetic anhydride**  
Reprinted with permission from ref <sup>65</sup> Copyright 2016 Royal Society of Chemistry

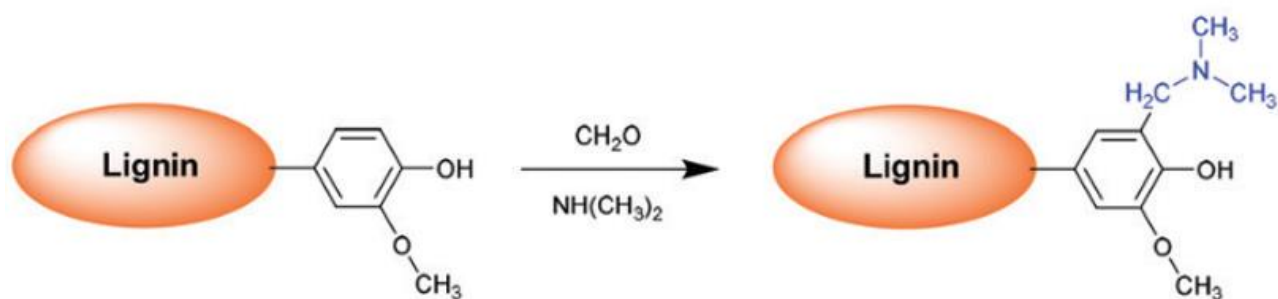
In 2002, Zhang and Huang ran a comprehensive study with polyurethane foams and revealed how the nitrolignin effects the mechanical properties. Polyurethane-nitrolignin films were synthesized with nitric acid, acetic anhydride, alkali lignin and a polyurethane prepolymer.<sup>136</sup> At various lignin ratios, the material was cast on a Teflon plate to form a film which then underwent mechanical property testing. The group found that the films infused with

up to 6% nitrolignin showed an increase in tensile strength and break at elongation demonstrating that the lignin enhanced cross-link density.<sup>136</sup>

Graglia et al. used beech wood nitrolignin obtained by the same straight forward aromatic nitration process to prepare an efficient nitrogen-doped carbon (NDC) electrocatalyst.<sup>137</sup> The nitrolignin precursors were synthesized with porous carbon via ionothermal carbonization.<sup>137</sup> The nitrogen doping from the lignin precursor improved the catalytic activity of the electrochemical oxygen reduction reaction (ORR) in comparison to their unmodified lignin counterparts.<sup>137</sup> Nitrolignin is a sustainable and cheaper alternative with comparable performance to more expensive non-noble metal catalysts.

#### 2.3.2.2.3 Amination

In general, amination introduces amine groups to the lignin backbone via the Mannich reaction with an amination agent like dimethyl amine and a solvent like formaldehyde via a nucleophilic substitution ( $S_N2$ ) reaction mechanism.<sup>65,135</sup> This is a simple and selective but toxic process that creates high surface activity cationic surfactants and heavy metal adsorbents. Figure 13 presents a general scheme for lignin amination.



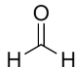

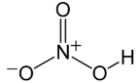

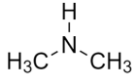

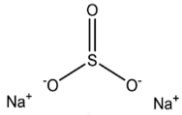



**Figure 13 Lignin amination scheme using formaldehyde and dimethylamine Reprinted with permission from ref <sup>65</sup> Copyright 2016 Royal Society of Chemistry**

Lindstrom et al. subjected Lignoboost softwood kraft lignin with and without phenolation pretreatment to the Mannich reaction to determine the amount of amine groups introduced. As suspected the Mannich reaction occurred selectively at the C-5 position on the G unit aromatic ring. SWKL that underwent the phenolation pretreatment had a greatly increased reactivity and a higher molecular mass due to an increase of incorporated amine groups.<sup>138</sup> However, both phenolated and non-phenolated lignin were hydrophilic, dispersed, and highly protonated with a positive charge under acidic conditions.<sup>138</sup> This group showed the potential for many practical applications like surfactants and polycationic materials for waste water treatment.

#### **2.3.2.2.4 Other methods**

There are several other methods to add chemical active sites to technical lignins. Sulfomethylation adds a methylene sulfonate group to the ortho position of the aromatic lignin ring using formaldehyde as a solvent.<sup>139</sup> Halogenation introduces a halogen group like bromine to the lignin molecule via an electrophilic aromatic substitution using a polar protic solvent like acetic acid. Halogenated lignin compounds can be used as fungicides, herbicides, and insecticides.<sup>140</sup> Lastly, dealkylation methods like demethylation remove a methyl group from the lignin molecule and are well known in DMSO (polar solvent used in polymer synthesis) production.<sup>141</sup> Table 8 highlights active site addition reactions for the mechanisms described above and the diversity in property improvement and application.

**Table 8 Reaction details for new chemical active sites added to technical lignin**

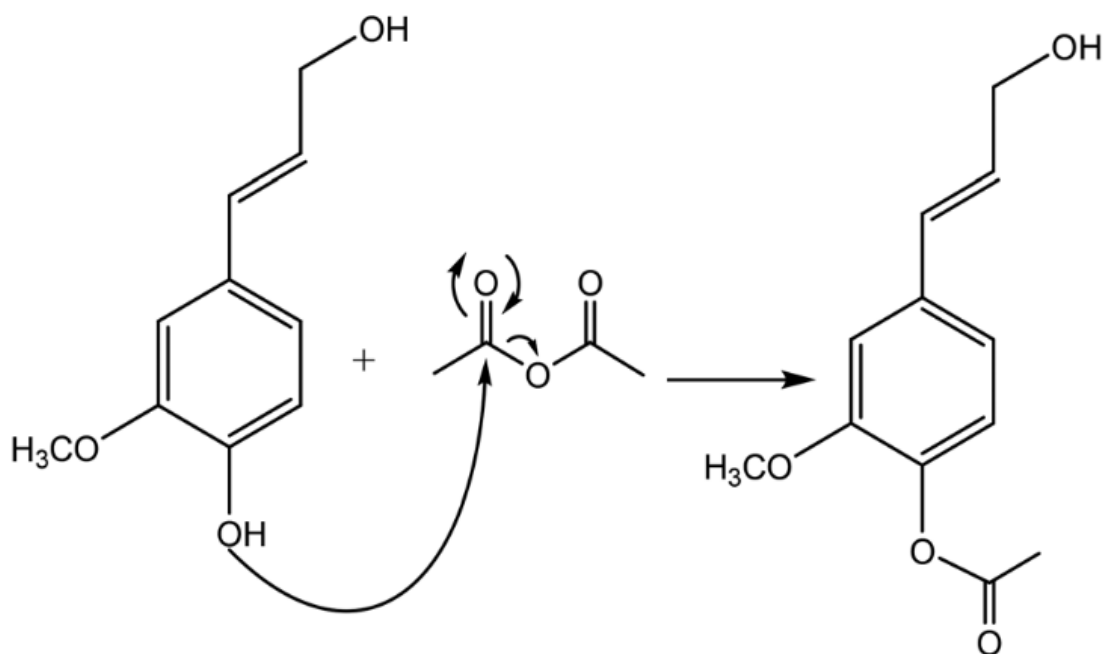
Modification	Reagent	Hazard rating	Lignin Source	Solvent	Temp./Time	Improvement	Application	Ref.
Hydroxymethylation			SWKL	Water	20-25 °C 72 h	Crosslinking Thermal stability	Adhesives Resins	132
Nitration	 and Acetic anhydride		Bamboo alkali lignin	n.a.	Ice bath 12 h	Crosslinking Tensile strength	Films	136
Amination			Lignoboost SWKL	Dioxane Formaldehyde	60 °C 4 h	Molecular weight Nitrogen Content	Surfactant Slow release fertilizer	138
Sulfomethylation			Alkali extracted corn stalk	Formaldehyde	75 °C 2-9 h	Surface activity Dispersibility	Dispersant for dye	139
Halogenation	Br-Br		HWKL SWKL	Acetic acid	163-164 °C 2h	Aggregation	Fungicides	140
Dealkylation	Molten sulfur		SWKL	NaOH	n.a.	Strength Water resistance	Adhesives	141

#### **2.3.2.2.5 Modification of existing hydroxyl groups**

Functionalization of technical lignin hydroxyl groups has proved a valuable and rather simple modification in the progression of lignin valorization. Native and technical lignins possess phenolic hydroxyl groups located on the aromatic ring and aliphatic hydroxyl groups found on the  $\alpha$  and  $\gamma$  side chain carbons. Technical lignins typically have more phenolic hydroxyl groups than native lignins due to  $\beta$ -aryl bond cleavage during pulping. Phenolic hydroxyl groups have higher reactivity because they have a lower pKa value and are more acidic meaning they have higher nucleophilicity compared to aliphatic hydroxyl groups. Therefore, nucleophilic substitution reactions are more favourable for phenolic hydroxyl groups. These hydroxyl groups are targeted by esterification or etherification to enhance technical lignins performance.

#### **2.3.2.2.6 Esterification**

Esterification reactions convert alcohol functional groups to ester functional groups and are relatively simple to carry out by nucleophilic substitution (Figure 14).<sup>130</sup> The pair of electrons belonging to the aromatic hydroxyl group attack the reagent, more specifically the carbon of the carbonyl group which can be (1) a monocarboxylic like acetic or propionic acid, (2) a dicarboxylic like maleic, phthalic, or fumaric acid, or (3) a fatty acid like oleic or lauric, and their anhydrides or acid chlorides.<sup>142</sup> On the carboxylic group, the hydroxyl group is replaced with a carbonyl group.<sup>142</sup> Esterification reactions are applied to technical lignins to decrease brittleness, increase solubility, and decrease intramolecular hydrogen bonding forces in order to increase miscibility with other polymers.<sup>130</sup>



**Figure 14 Esterification reaction of lignin with acetic anhydride via nucleophilic substitution**  
 Reprinted with permission from ref <sup>130</sup> Copyright 2019 Royal Society of Chemistry

Thielemans and Wool developed a pivotal study on modified lignin ester solubility in styrene which is a common additive in unsaturated thermosets like epoxide resins. The researchers started with softwood and hardwood kraft lignin and under a closed nitrogen system stirred vigorously at 50 °C for 24 hours with different anhydrides (acetate, propionic, butyric, methacrylic, and maleic) and 1 MIM as the catalyst.<sup>143</sup> The acetate, propionic and butyric anhydrides were reacted without solvent at a 2:1 anhydride/lignin ratio while the methacrylic and maleic anhydrides were reacted with 1,4-dioxane as the solvent to reduce polymerization.<sup>143</sup> The lignin esterified with maleic anhydride showed no solubility in styrene while acetylated, methacrylated and propionated esterified lignins were soluble with the latter being the most soluble of the three.<sup>143</sup> Both softwood and hardwood butyrated lignin were completely soluble in

styrene and the addition of butyrate kraft lignin reinforced and plasticized the material thus improving fracture properties.<sup>143</sup>

Later Dehne et al. used Thielemans esterification process (acetic, propionic, and butyric anhydrides) and various types of lignin (SWKL, HWKL, organosolv, soda, and hydrolysis) to study how the type of technical lignin effected the esterification. It was demonstrated that various lignins showed chemical differences based on plant origin and pulping process.<sup>144</sup> The anhydride used during esterification effected thermal properties as the best results came from the butyrate lignins.<sup>144</sup> In fact, melt blend properties progressively enhanced with an increase in length of ester carbon chains because a higher number of backbone carbons will decrease the density and hydrogen bonding of lignin chains. All melt blends with esterified lignins showed improved properties in comparison to unmodified lignins. The esterification worked to lower the  $T_g$ , sugar and ash content and make the lignin molecule less polar thus improving miscibility despite its species of origin.<sup>144</sup>

Luo et al. esterified Indulin AT SWKL and agriculture fibre soda lignin with similar anhydrides and then blended the resulting modified lignins with poly(3-hydroxybutyrate-co-3-hydroxyvalerate) PHBV, or polypropylene at a weight ratio of 3:7 (30 wt% lignin held constant in all blends). These samples were blended for five minutes at 180-190°C and 60 rpm before being mould injected to form dog bone type testing specimens.<sup>145</sup> The subsequent blended samples showed an increase in tensile strength and elongation at break as compared to their unmodified lignin counterparts. The lignin esterified with acetate showed two  $T_g$  values during characterization demonstrating partial miscibility.<sup>145</sup>

Chiappero et al. blended Indulin AT SWKL and eucalyptus HWKL lignin esterified with acetic anhydride and N-methylimidazole using the methods described thus far with linear low-

density polyethylene (LLDPE). LLDPE was chosen for its low cost, good tensile strength, and impact strength. The lignin/LLDPE blends underwent melt extrusion at 185 °C and 60 rpm and blown films were synthesized.<sup>146</sup> Unmodified HWKL could not be processed because of low compatibility and a 41° C difference in  $T_g$  values between the two components.<sup>146</sup> Esterified lignin was blended up to 10 wt% and the esterified SWKL/LLDPE films showed greater stiffness.<sup>146</sup> However, tensile strength and elongation at break decreased with an increase in lignin.<sup>146</sup> This group used acetic anhydride to esterify the lignin which has been shown by other groups to have reduced miscibility in blends as compared to other esters due to the shorter carbon chain.

Dai et al. synthesized an in house organosolv waste lignin derived from poplar chips using ethanol as the solvent. The recovered lignin was esterified using butyric anhydride (well known for effectiveness) and 1- methylimidazole. This esterified lignin was added to form a spinning solution with polyacrylonitrile dissolved in DMF. Using electrospinning methods, the group synthesized a nitrogen-oxygen co-doped esterified lignin/polyacrylonitrile based carbon nanofibre (E-CNF).<sup>147</sup> Detailed characterization showed higher heteroatom (N,O) lowered  $T_g$  values, improved wettability and led to superior electrochemical performance in comparison to CNFs without esterified lignin.<sup>147</sup>

Teramoto et al. esterified organosolv lignin with acetate, butyric, valeric and propionate anhydrides and then blended the modified lignins with poly( $\epsilon$ -caprolactone) PCL to form films at different blend ratios by solvent evaporation using chloroform. The butyric and valeric esterified lignins showed excellent miscibility and good mechanical properties up to 50% lignin.<sup>148</sup> The group found that simple lignin derivatives allowed blends with aliphatic polymers (PCL) even though lignin is an aromatic rich polymer.<sup>148</sup>



Hult et al. esterified Indulin AT SWKL and PC-1369 HWKL with palmitic and lauric chloride derived fatty acids using DMF and pyridine as solvents. Five grams of lignin were dissolved in 30 ml DMF, 7.6 ml pyridine was added and then 8 ml of the chloride derived fatty acid was slowly added via syringe.<sup>149</sup> The reaction took place at room temperature under Ar gas for 20 hours of stirring. The esterified lignin was characterized with FTIR, <sup>31</sup>P NMR, and GPC before being applied as a coating material on paperboard.<sup>149</sup> Usually, fibre based packaging materials are laminated with aluminum or petro-based polymers. Lignin is hydrophobic with poor film-forming properties, but the esterification improved compatibility. The lignin treated with palmitic acid (16 carbon backbone) performed the best at improving barrier properties because of its longer carbon chain length.<sup>149</sup>

Gordobil et al. used Hult's esterification method as the foundation to manually blend fatty acid esterified spruce and eucalyptus organosolv lignins with commercial cellulose acetate and plasticizer triethyl citrate at 5-50 wt% lignin to make films. The films were characterized, and the esterified lignin increased in molecular weight and decreased in T<sub>g</sub>. The esterified eucalyptus lignin had a higher ability to deform and a more stable contact angle while the esterified spruce lignin was more rigid and tough.<sup>150</sup> The ratios showed less dependence on cellulose acetate content and more dependency on lignins intrinsic characteristics.<sup>150</sup>

Laurichesse et al. esterified Alcell organosolv lignin with oleic acid from sunflower oil. Under nitrogen, the oleic acid was dissolved in ethyl acetate, cooled and excess oxalyl chloride was added dropwise for fifteen minutes. The mixture was heated to 50 °C for five hours. The pre-esterification chlorination step produced oleoyl chloride which was characterized and then agitated with the dried lignin at 130 °C for fifteen hours under nitrogen.<sup>151</sup> The product was washed with methanol, characterized and the esterified lignin then underwent epoxidation with

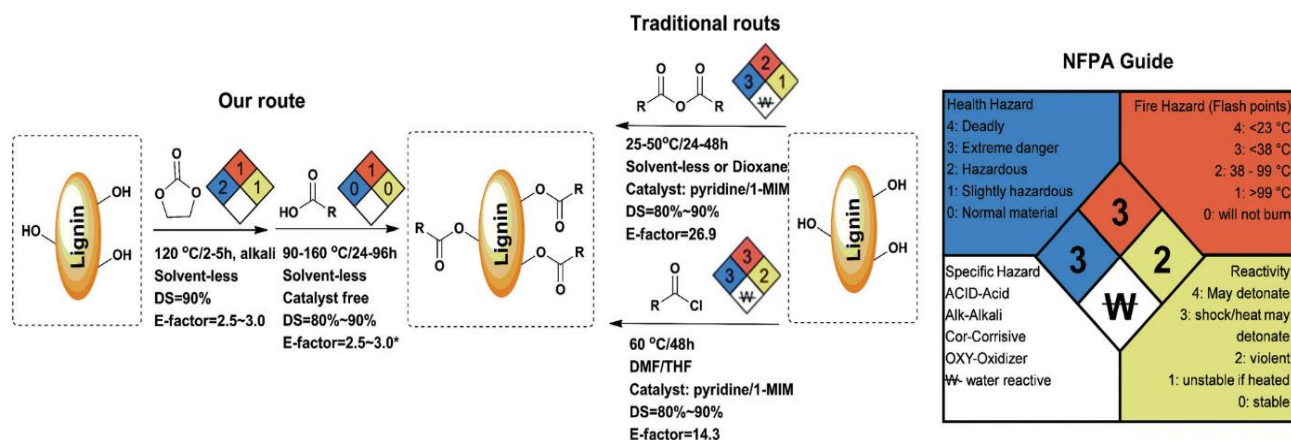
DCM and peracetic acid via an oxirane ring opening synthesis which made a lignin-oleic acid polyol (LOAP).<sup>151</sup> The LOAP is a bio-based building block (up to 89%) for polyurethane synthesis and was characterized by DSC, TGA, DMA, FTIR, and mechanical testing which showed advanced properties.<sup>151</sup>

Most methods described use anhydrides with added catalysts or halogenated compounds like acyl chlorides because they are very effective at modifying lignin. However, researching scientists in today's climate face a unique pressure in developing green chemistry practices that use less harsh solvents and catalysts that proceed through environmentally friendly reactions. The solvents and catalysts described above are mostly toxic and produce waste with separation issues making it difficult for industrial application scale-up and end of life cycle.

An et al. developed a green method at room temperature using oleic acid and water to esterify hardwood kraft lignin. The kraft lignin was dissolved in a surfactant solution of *p*-toluenesulfonic acid (TsOH) and 4-dodecylbenzenesulfonic acid (DBSA) followed by dispersal of oleic acid to form an emulsion which was stirred at reaction temperature for 48 hours.<sup>152</sup> Surfactant combined microreactors were formed which solubilized the kraft lignin and dispersed oleic acid.<sup>152</sup> Lignin esters were precipitated out in distilled water and the TsOH was recycled.<sup>152</sup> Characterization confirmed esterified lignin with improved thermoplasticity and hydrophobicity.

Potentially one of the most important developments was made by Liu et al. who used an organic acid as both the solvent and reagent without adding a strong acid to esterify Biochoice softwood kraft lignin (SKL) and Fibria Innovations organosolv HW lignin (OSHL). Liu's solution fits nicely into green chemistry practices but also produced quality esterified lignins. An issue arose regarding incomplete conversion because of the differences in reactivity between the phenolic and aliphatic hydroxyl groups. Liu's solution was a green etherification method of the

lignin using ethylene carbonate which played a major role in this current thesis and will be described in latter sections and the results and discussion portion of this work. The product hydroxyethyl (HE) lignin was comprised of aliphatic hydroxyl groups only and provided a more uniform chemical structure for esterification.<sup>153</sup> Liu esterified 5 grams of unmodified and HE lignin in 50 ml of propionic acid at temperature ranging from 90-120 °C for 24-48 hours in an oil bath.<sup>153</sup> The unmodified SKL and OSHL reacted with propionic acid at 120 °C for 24 hours showed a yield of 75-80% and a degree of substitution of 80% and 72% for both primary and secondary aliphatic hydroxyl groups but aromatic hydroxyl and carboxylic acid groups only showed a slight reduction.<sup>153</sup> The HESKL and HEOSHL showed a yield of 95-110% (based on original lignin mass) and a degree of substitution of 91% and 87% for all groups.<sup>153</sup> This confirmed that the etherification step was effective in unifying the lignin molecule for successful esterification.<sup>153</sup> Further characterization showed a significant reduction in  $T_g$ , a higher molecular weight and a narrower PDI. Liu recovered 90% of the propionic acid with roto evaporation and adhered to the principles of green chemistry. These esterified lignins could be used in polymer blends, as hydrophobic coatings, and in copolymerization with other polymers. Figure 15 as a side by side view of Liu's green esterification compared to some of the previous methods discussed.<sup>153</sup> The center figure shows the esterified lignin which is the goal, with Liu's work on the left harboring no solvent or catalyst and rather benign reagents reacted. The right side of Figure 15 shows the traditional route which uses a plethora of toxic and volatile reagents, solvents, and catalysts.



**Figure 15 Greener solvent and catalyst free lignin esterification compared to traditional lignin esterification involving toxic reagents, solvents, and catalysts Reprinted with permission from ref <sup>153</sup> Copyright 2019 Royal Society of Chemistry**

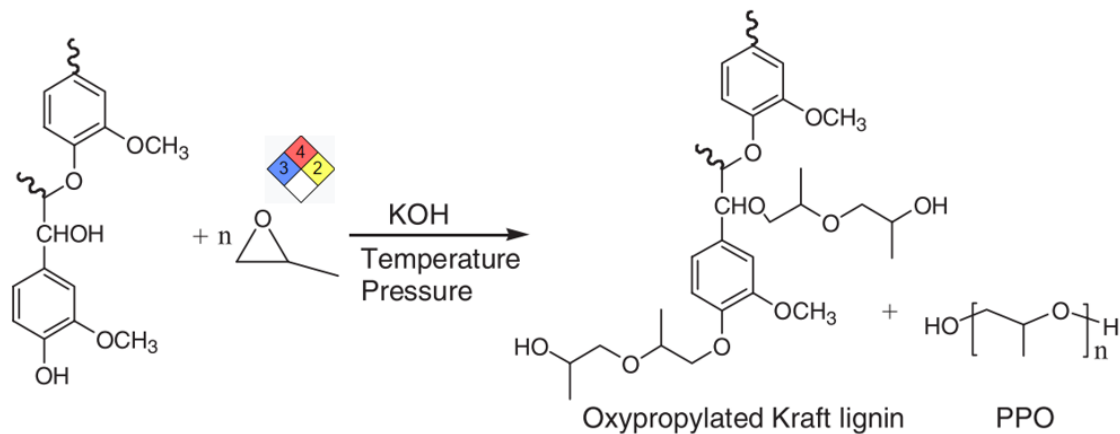
#### 2.3.2.2.7 Etherification

In general, a wide variety of etherification reactions exist in which alcohols dehydrate to form ethers. More specifically, etherification reactions performed on lignin will functionalize either the aromatic hydroxyl groups or both the aliphatic and aromatic groups (depending on reaction conditions) forming lignin-polyethers. The most well-known lignin etherification is the “oxypropylation” reaction with propylene oxide which was extensively studied and developed by Glasser and co-workers.

In the 1984 Glasser et al. prepared different technical lignins with various oxides (ethylene, propylene and butylene) to produce hydroxyalkyl lignin derivatives.<sup>131,154</sup> Using potassium hydroxide as the catalyst the reactions took place in toluene at 180 °C in a pressurized reactor.<sup>131,154</sup> Thermal analysis revealed a drastic reduction (50-100 °C from parent lignin) in  $T_g$  values which is indicative of lower amounts of hydrogen bonding and an increase in free volume.<sup>131,154</sup> The functionalized lignin showed an increase in solubility in organic solvents

which made it possible to characterize using NMR and GPC techniques. Using propylene oxide Glasser prepared SWKL epoxy resins and star like copolymers with polycaprolactone.<sup>155,156</sup> The epoxy copolymers showed a narrow molecular weight distribution, chemical uniformity, good solubility, and an improvement in mechanical properties particularly modulus.<sup>155</sup> This epoxy resin was comparable or superior to diglycidyl ether bis-phenol A (DGEBA) base resins.<sup>155</sup> Glasser coined this hydroxypropylated lignin (HPL) via the oxypropylation reaction and went on to develop a patented melt blown compostable polyester with these lignin building blocks.<sup>157</sup> Glasser's methods were utilized by other researching scientists to develop novel materials which have quite the presence in modern day literature.<sup>156,158-160</sup>

Figure 16 is a general schematic of the chain extension reaction that is accompanied by the homopolymerization of polypropylene oxide (PPO) which produces propylene glycol derivatives.<sup>154,161</sup> The transfer reaction results in a polyol which is a mix of both oxypropylated lignin and PPO oligomers.<sup>154,161</sup> These reaction are often carried out at high temperatures and pressures and propylene oxide is highly volatile without a solvent. The anionic ring opening polymerization is carried out through nucleophilic reactions and the phenolic hydroxyl group is extended.<sup>154,161,162</sup> By utilizing the existing phenolic hydroxyl groups within lignins chemical structure and converting them to aliphatic hydroxyl groups, a polyol is created and urethane linkages form with introduced isocyanate groups.

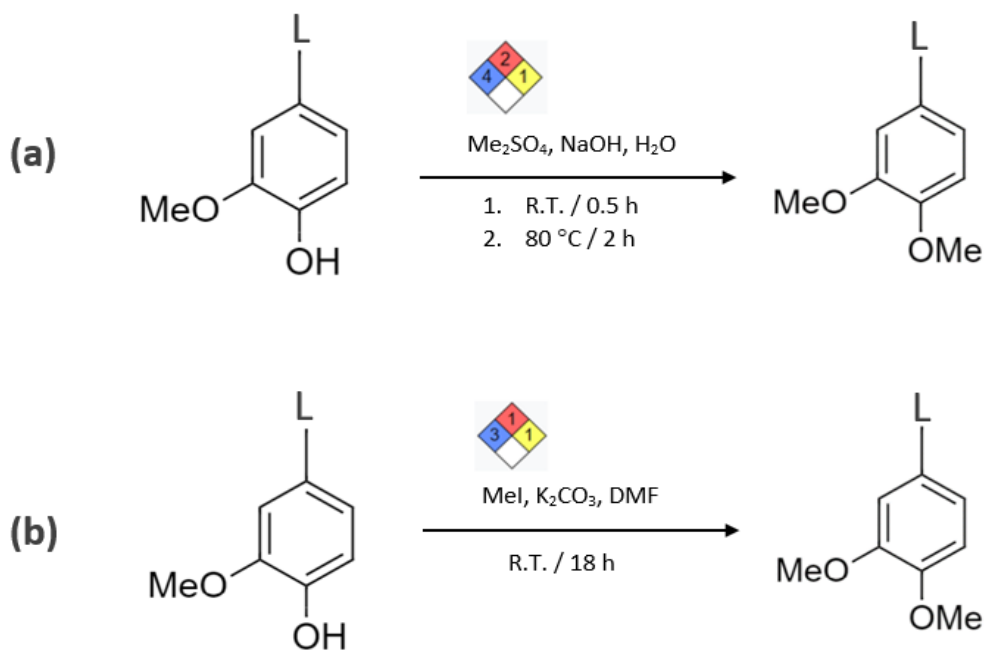


**Figure 16 Oxypropylation reaction involving lignin and propylene oxide and the hazard rating of PO** Reprinted with permission from ref <sup>161</sup> Copyright 2012 American Chemical Society

Sadeghifar et al. performed a selective masking of the phenolic hydroxyl group on Indulin AT SWKL using a mild oxypropylation in 0.5M aqueous NaOH at room temperature for 18 hours. Results monitored by <sup>31</sup>P NMR showed effective masking of the phenolic hydroxyl groups but no substitution on the aliphatic hydroxyl groups.<sup>162</sup> Despite the milder conditions, propylene oxide is considered a volatile and toxic reagent and should be avoided and replaced with greener chemistry practices. In earlier research by Professor Knut Lundquist at Chalmers University the exothermic decomposition of propylene oxide during a reaction with lignin led to an explosion and it was only by chance that no one was injured.<sup>163</sup>

Another reaction that leads to etherification is the methylation of lignin, considered an alkylation where a hydrogen atom replaces a methyl group. Methylation of lignin occurs by nucleophilic aromatic substitution and masks the phenolic hydroxyl groups of lignin creating a phenyl methyl ether that is less reactive.<sup>130</sup> This functionalization will lower the  $T_g$  value because intramolecular hydrogen bonding will be eliminated. It is yet another route to make lignin a more uniform molecule for valorization and is typically carried out with methyl iodine or dimethyl sulfate.

In 2012 Sadeghifar et al. performed an important experiment on Indulin AT SWKL that selectively methylated the phenolic hydroxyl groups using two different methods. Method one used dimethyl sulfate ( $\text{Me}_2\text{SO}_4$ ) and method two used methyl iodide ( $\text{MeI}$ ).  $\text{Me}_2\text{SO}_4$  was reacted with 0.7M NaOH at room temperature and slowly heated up, while  $\text{MeI}$  was reacted with DMF at room temperature, and upon completion both reactions were acidified with HCl to precipitate out the lignin (Figure 17).<sup>162</sup> At an optimal mol ratio the conversion was quantitative and the phenolic hydroxyl groups were selectively masked based on the  $\text{pK}_a$  differences between phenolic hydroxyl and aliphatic hydroxyl groups.<sup>162</sup> Above the optimal mol ratio, methyl iodide was less reactive because methylation leveled off at 60% and selectivity dropped as 38% of aliphatic hydroxyl groups were methylated.<sup>162</sup>



**Figure 17 Methylation of softwood kraft lignin using dimethyl sulfate (a) and methyl iodide (b) where L represents lignin**<sup>162</sup>

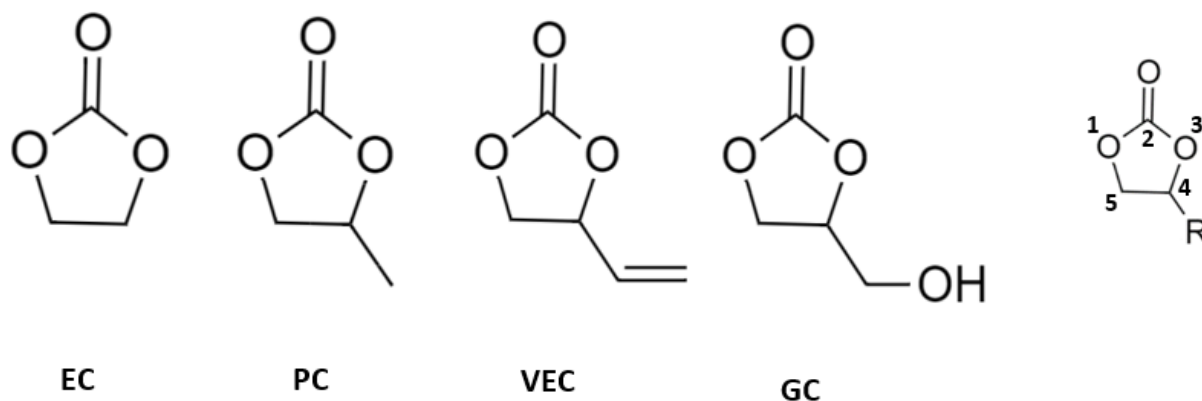
Thermal analysis showed that using  $\text{Me}_2\text{SO}_4$  the fully methylated lignin had remarkable thermal stability upon heating at  $148\text{ }^\circ\text{C}$  which is  $20\text{ }^\circ\text{C}$  above the  $T_g$  value.<sup>164</sup> There was no molecular weight increase which demonstrated that phenoxy radical formation was avoided preventing thermally induced radical coupling reactions which demonstrates that methylated SWKL could be used as a thermoplastic.<sup>164</sup> This was excellent work but much like using toxic propylene oxide to etherify lignin, it does not address the issue of using toxic dimethyl sulfate to do the same.

Five membered cyclic organic alkyene carbonates have a high boiling point, flash point solvency, low odor level, toxicity, evaporation rate, better biodegradability properties and can be used as both a solvent and a reagent.<sup>165</sup> Such cyclic carbonates like ethylene carbonate (EC) and propylene carbonate can replace chemicals like propylene oxide while dimethyl carbonate is an organic carbonate ester and considered a green reagent for methylating compounds.<sup>165</sup>

In 2017, Duval et al. did an extensive study with cyclic carbonates and soda lignin from wheat straw. The research group reacted different cyclic carbonates; EC, propylene carbonate, vinyl ethylene carbonate (VEC), and glycerol carbonate (GC) with the soda lignin and potassium carbonate a benign catalyst in an oil bath at  $150\text{ }^\circ\text{C}$ .<sup>166</sup> The lignin to carbonate to catalyst ratio was determined via NMR techniques prior to the experiment.<sup>166</sup>

The group found that ethylene carbonate was the most reactive and full conversion was achieved in only fifteen minutes.<sup>166</sup> The difference in conversion times are based on the cyclic carbonate side chain with EC being the simplest (hydrogen atom) and all others tested having a substituent in position four which reduces reactivity.<sup>166</sup> Figure 18 represents the structure and nomenclature of the different cyclic carbonates.<sup>166</sup>





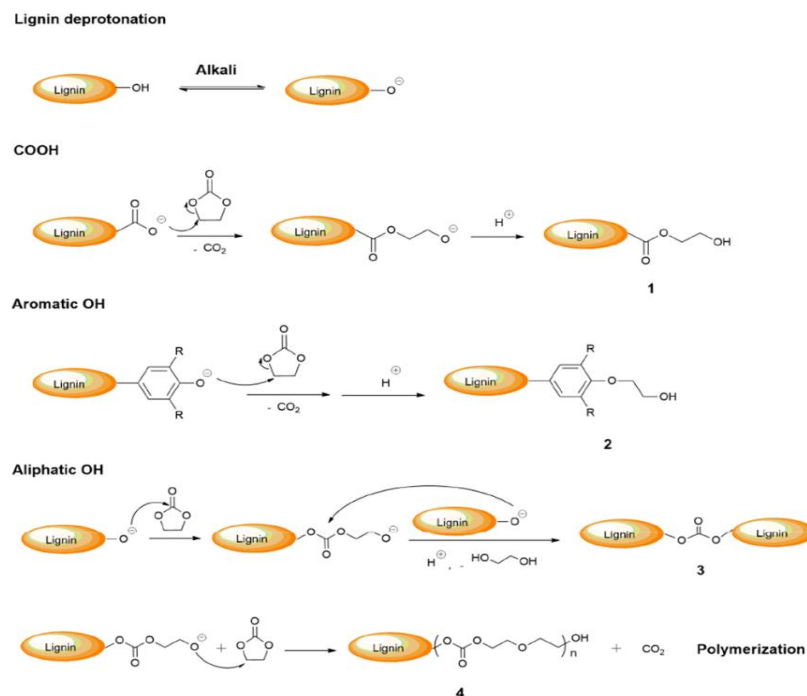
**Figure 18 Cyclic carbonate structures and the nomenclature of the carbonate ring; ethylene carbonate (EC), propylene carbonate (PC), vinyl ethylene carbonate (VEC), and glycerol carbonate (GC) <sup>166</sup>**

Carboxylic acid (COOH) groups also reacted and were converted into esters because of  $pK_a$  values lower than phenolic hydroxyl groups. In addition, the research group found that reaction time could be extended to achieve chain extension which forms ether linkages and releases carbon dioxide (CO<sub>2</sub>). This is a much greener alternative to oxyethylation or oxypropylation reaction because it is easier to control grafting as chain length increases linearly with reaction time.<sup>166</sup> Thermal characterization showed an increase in stability and these lignin building blocks showed real promise as a greener alternative.

In 2018, Liu et al. reacted ethylene carbonate with Indulin AT acetone soluble SWKL and sodium carbonate (Na<sub>2</sub>CO<sub>3</sub>) and converted phenolic hydroxyl and carboxylic acid groups to aliphatic hydroxyls thus synthesizing a uniform chemically functional hydroxyethyl ether with enhanced thermal stability under strict green chemistry practices.<sup>167</sup> In a similar method to Duval's, <sup>31</sup>P NMR was used to calculate molar ratios and determine the amount of reagent and catalyst needed for conversion. Dried lignin, EC, and the benign catalyst were purged under nitrogen and reacted in an oil bath at temperatures ranging from 60-170 °C for 1-20 hours and

the product was precipitated out using HCl.<sup>167</sup> Liu optimized the reaction at two hours and 120 °C where 95% of phenolics were converted to hydroxyalkyl ethers.<sup>167</sup> The functionalized lignin was characterized, and Liu went on to react it with propionic acid resulting in a green lignin ester which was discussed in the previous section.<sup>153,167</sup> These uniform green lignin building blocks have been used to develop polyurethane foams and have great potential in lignin polymeric blends.

Figure 19 shows possible reactions between ethylene carbonate and the phenolic hydroxyls, aliphatic hydroxyls and carboxylic acid functional groups that make up technical lignins. Sodium carbonate is necessary to deprotonate hydroxyl groups which catalyzes the reactions. Figure 19 highlights various attacks on the cyclic carbonate which produce CO<sub>2</sub> as a byproduct.



**Figure 19** Potential reactions between ethylene carbonate and deprotonated hydroxyl functional groups Reprinted with permission from ref <sup>167</sup> Copyright 2018 American Chemical Society

Lastly, Sen et al. successfully methylated acetone soluble softwood kraft lignin using dimethyl carbonate (DMC) with DMSO as the solvent and either sodium hydroxide or cesium carbonate as the catalytic base which produced CO<sub>2</sub> and methanol as a byproduct, the latter which can be recycled.<sup>168</sup> Characterization showed an improvement in thermal stability for the methylated lignin and GPC data showed similar results for the starting lignin and methylated version, meaning no crosslinking or degradation took place during the reaction.<sup>168</sup>

These pivotal studies show the progress made in lignin chemistry over the last decade. A shift in what is important to industry has begun to focus on green chemistry practices that use fewer starting materials and reagents that are non-toxic, easily recoverable, and show improved biodegradability. To this point, chemically functionalizing lignin for utilization has been the focus, but utilization of what? We have discussed various uses for lignin as a surfactant, an adhesive in PF resins, a blend component in polyurethane foams and spun fibres but is it possible for lignin to be more? To what extent does lignin have the potential to replace the petroleum based synthetic plastics we use every day?

## **2.4 Polymeric lignin blends for thermoplastic materials**

Previous sections have led the reader to the conclusion that some technical lignin derivatives are a waste product of the pulping industry and could serve as renewable building blocks in biobased thermoplastic blends that potentially replace petroleum-based thermoplastics like LDPE, PP, and PET. It has been shown that petro-plastics are a necessary commodity for modern society but a serious threat to the environment. Blending lignin with petro-based polymers or biodegradable polymers would harness an underutilized less damaging material.

### 2.4.1 Early work

The first detailed report of polymeric blends with high lignin contents was published in 1997 when Sarkanen et al. blended unmodified SWKL fractionated by ultrafiltration with poly(vinyl acetate) and several plasticizers up to 85% using solvent casting methods.<sup>169</sup> In 1999, Glasser et al. consecutively alkylated ultrafiltrated SWKL with dialkyl sulfates in dioxane solution and then methylated with diazomethane chloroform.<sup>170</sup> The 100% ethylated methylated derivatives were solvent cast and for the first time a tensile strength was recorded for 100% lignin.<sup>170</sup> The esterified lignin derivatives showed similar tensile properties to polystyrene, but both were quite brittle and had to be plasticized for injection moulding.<sup>170</sup> That same year Glasser esterified organosolv lignin with anhydrides and then blended the product with biodegradable thermoplastics, cellulose acetate butyrate, starch caprolactone, and poly(hydroxybutyrate).<sup>24</sup> The blends were melt processed and mould injected to make dog bone specimens. The acetate and butyrate esterified lignin showed good compatibility with the cellulose acetate butyrate at 20 wt% lignin.<sup>24</sup> In 2000, Kosikova et al. blended prehydrolysis beechwood lignin with polyethylene or polypropylene using a single screw extruder.<sup>171</sup> The group found that at 10 wt% lignin the blend was stabilized against degradation reactions and at 30 wt % lignin tensile strength began to decrease.<sup>171</sup> In 2001, Nitz et al. blended unmodified Alcell organosolv lignin, and abaca and sisal lignin from annual plants with a commercial polyester amide (BAK<sup>TM</sup>) or commercial polyester Ecoflex<sup>TM</sup>.<sup>172</sup> The group blended at a melt temperature of 200 °C with a co-rotating twin screw extruder at 200 rpm and mould injected test bars that underwent mechanical testing.<sup>172</sup> At 40 wt%, Alcell lignin blended with Ecoflex<sup>TM</sup> showed a high impact strength while sisal lignin blended with Ecoflex<sup>TM</sup> did not impair mechanical properties.<sup>172</sup> In 2002, Sarkanen et al. built off of Glasser's work on alkylated kraft

lignin based polymeric materials to complete the first comprehensive study on the characterization of the recently developed ethylated methylated lignin derivatives blended with poly (butylene adipate) (PBA), an aliphatic polyester.<sup>170,173</sup> The blends were solvent casted in a Teflon mould and filed into 1mm thick dog bone shaped specimens. Using an Instron load frame for tensile testing, strain hardening was detected at 55 wt% lignin.<sup>173</sup> With DSC and X-ray powder diffraction, the group discovered the interactions between polyester chains and alkylated SWKL are most favourable when the CH<sub>2</sub>/COO ratio is between 2.5 and 3.0.<sup>173</sup>

In commercial application, Arboform<sup>TM</sup> was developed by Nägele and Pfitzer and in 2002 was patented and sold in pea sized thermoplastic granules that can be moulded into desired shapes.<sup>174</sup> Arboform is 30% native aquasolv lignin, 60% cellulose fibres, and natural additives that consist of plasticizers, dyes, antioxidants and fillers with mechanical properties similar to a polyamide.<sup>174</sup> Toriz et al. blended unmodified Indulin AT SWKL with polypropylene by melt mixing at 170 °C and 120 rpm and then mould injecting specimens from 10-60 wt% lignin.<sup>175</sup> Tensile strength, flexural strength and impact strength decreased as lignin content increased, but by adding mineral fillers the strength properties were improved however, at 60 wt% lignin the blend was brittle.<sup>175</sup> This research group went on to subject the blend to plasma treatments which improved mechanical properties.<sup>175,176</sup> Finally, in 2005 Sarkanen et al. further expanded their work by extensively studying molecular weight fractions separated by ultrafiltration of ethylated methylated SWKL blended with poly(ethylene glycol) or poly(butylene adipate).<sup>177</sup> It was determined that low molecular weight (LMW) lignin components will improve interactions selectively at peripheral regions and improve plasticizing efficiency.<sup>177</sup>

### 2.4.2 Recent work

In 2009 Teramoto et al. esterified organosolv lignin with various anhydrides and blended different ratios with poly ( $\epsilon$ -caprolactone) or PCL to make films by solvent evaporation.<sup>148</sup> Atomic force microscopy showed that organosolv-butyrate was miscible with PCL and decent mechanical properties were attained up to 50 wt% lignin.<sup>148</sup> In 2010 Sailaja et al. also used lignin esterified with various anhydrides but blended with LDPE and then grafted with the compatibilizer maleic anhydride.<sup>178</sup> By adding the compatibilizer mechanical properties improved making the material comparable to neat LDPE.<sup>178</sup> Aradoaei et al. was able to blend secondary PET and LDPE which is usually immiscible by adding esterified lignin as a compatibilizing agent which not only combined the PET and LDPE but created a new material with new properties.<sup>179</sup> In 2011 Feng et al. blended bromododecane alkylated unbleached hardwood kraft lignin with polypropylene by melt mixing thus improving the thermal resistance by 25 °C while also increasing compatibility of the matrix because of the alkylation.<sup>180</sup> In addition, impact strength of the blend was enhanced by adding 40 wt% alkylated lignin.<sup>180</sup> In 2012 Yue et al. performed a sequential extraction on soda lignin and blended it with PVC by melt compounding. The low molar mass fractions accelerated plasticization of the blends which resulted in better mechanical properties in comparison to unfractionated lignin portions.<sup>181</sup> The high molecular fraction improved the decomposition temperature of the blends.<sup>181</sup> In 2015 Gordobil et al. acetylated SWKL and blended with poly(lactic acid) (PLA) using a double screw extruder. The blend with up to 20 wt% modified lignin showed an increase in thermal stability.<sup>182</sup> In 2016, Tran et al. developed a new class of elastomers by nanodispersing lignin in nitrile rubber creating a material similar to acrylonitrile-butadiene-styrene (ABS) copolymers but with lignin replacing the styrene fraction.<sup>183,184</sup> The blended elastomer showed a tensile strength

of 30 MPa, a high yield stress of 45 MPa, and good miscibility. In addition, the material had a significantly higher toughness than nonrenewable styrene based (ABS) copolymers. In 2019 Dias et al. esterified Indulin AT SWKL using maleic anhydride and then blended 10-50 wt% esterified lignin with PP by twin screw extrusion compounding at 180 °C and 150 rpm. The esterified lignin showed good blendability and no significant loss of mechanical properties up to 40 wt% lignin.<sup>185</sup> Beyond that the material was much stiffer however, this could be of interest to the automotive industry where more rigid materials with good thermal characterization are needed.<sup>185</sup> Beaucamp et al. first fractionated organosolv hardwood lignin with 2-propanol and then modified the fractions to synthesize hydroxypropyl lignin. Various ratios of the fractionated modified lignin were blended with biobased PET using an Xplore microcompounder and carbon fibres were spun.<sup>186</sup> As expected, the lignin structure and amount of phenolic hydroxyl groups and crosslinking effected miscibility and spinnability of the blend.<sup>186</sup> The high molecular weight fraction which contained more aliphatic hydroxyl groups showed good crosslinking resulting in ether type bonds and this made for better fibres.<sup>186</sup> In 2020 Ge et al. blended hardwood acid hydrolysis lignin with PLA by melt compounding at 170 °C and 60 rpm to make 1mm thick film sheets. The group used either dicumyl peroxide (DCP), maleic anhydride (MA), or biphenyl peroxide (BPO) to modify the blend and found that the MA/BPO modified blend had reinforcing effect while the DCP modification reduced tensile strength of the material; at 40 wt% lignin mechanical properties deteriorated for all blends.<sup>187</sup> Chiappero blended Indulin AT SWKL esterified using acetic anhydride with LLDPE by twin screw melt extrusion at temperatures varying from 170-185 °C and a speed of 60 rpm. Up to 10 wt% esterified lignin was blended to make films for agriculture mulch application with enhanced opacity, thermal and biodegradable properties.<sup>146</sup>

### 2.4.3 Key studies

There are several studies that have influenced this work and stand out regarding developed materials and unique findings. Dehne et al. examined the effects of different technical lignins and their anhydride esterified modification counterparts on lignin - high density polyethylene blends. The research group took five types of technical lignin; HWKL, SWKL, organosolv, soda, and acid hydrolysis and esterified each using the Thielemans and Wool technique previously discussed.<sup>143,144</sup> Using a torque rheometer the blends were melt mixed at a constant 1:1 ratio (50 wt% lignin) for 15 minutes at 160 °C and 50 rpm. Both modified and unmodified lignin in powder form was added to the HDPE in pellet form after the torque curve stabilized and then samples were mould injected and lubricated with 1% paraffin wax.<sup>144</sup> While the chemical characterization of unmodified lignin was distinctly different with regard to plant species and pulping process, lignin source did not influence or effect the mechanical properties of resulting blends.<sup>144</sup> There was a comparable difference between unmodified and esterified lignin performance in blend with esterified lignins showing 45% higher tensile strengths when compared to its unmodified lignin counterpart.<sup>144</sup> This important study shows that chemical modification trumps lignin source when examining mechanical properties of blends with non-polar polymers.<sup>144,188</sup> It is more effective to mask polarity of the lignin in order to improve blendability then worry about where the lignin is sourced from.

Sadeghifar and Argyropoulos first fractionated Lignoboost SWKL with acetone to obtain high and low molecular weight portions and then methylated the fractions using dimethyl sulfate via the previously discussed chemistries developed by the group.<sup>162,189</sup> Using a laboratory scale twin screw compounder the group blended polyethylene and the fractionated modified and unmodified lignin from 5-25 wt% at 170 °C and 100 rpm.<sup>189</sup> The torque was measured and used



to draw the conclusion that unfractionated unmodified lignin blends significantly increase torque because of melt crosslinking while soluble and insoluble unfractionated portions have a lower initial torque with improved melt stability.<sup>189</sup> Overall, the methylation improved the stability of the thermal melt with the acetone soluble methylated lignin showing a reduction in torque and plasticizing effects.<sup>189</sup> This study demonstrates that by measuring something as simple as compounder torque output conclusions can be drawn about melt stability and as expected the modified lignin performs best in blend when compared to its unmodified counterpart.

Glasser and co-workers oxyalkylated SWKL to make hydroxypropyl lignin (HPL) via methods he previously developed and then blended it with pelletized Ecoflex™ using a twin-screw compounder. Samples were processed from 0-40 wt% pelletized HPL lignin at 185-190 °C and 200 rpm.<sup>154,157</sup> From this material blown films were created ranging in thicknesses from 12-93 µm. During the melt process, a malodorous odor typical to kraft pulping arose from the samples, and the melt became unstable around 30 wt% lignin.<sup>157</sup> Overall, as more lignin was added the modulus increased and the tensile strength of the films decreased. Films 12-14 µm thick containing 20 wt% lignin were processed and showed good mechanical properties.<sup>157</sup> This material was scaled up and made commercially available as Xylobag products for rubbish bags, plastic cutlery, and shopping baskets.<sup>157</sup>

Recently, Xiong et al. methylated eucalypt hydrothermal lignin with dimethyl carbonate (DMC) and then blended with compatibilizer maleic anhydride (MAH) and PBAT.<sup>190</sup> The group used a twin-screw melt extruder to blend 40-60 wt% unmodified lignin or methylated lignin with MAH-g-PBAT to make films. Thorough characterization revealed outstanding improvements in elongation at break and a reduction in lignin agglomerates for 60 wt% methylated lignin and MAH-g-PBAT blends.<sup>190</sup> Mechanical properties met the requirement of Chinese National

Standard for packaging and this material could be used in the future as rubbish bags and thin soil agricultural films.<sup>190</sup>

Table 9 is a summary of the discussed works for blended lignin thermoplastics.

**Table 9 Mechanical property literature comparison of lignin based thermoplastic blends**

Preparation method	Lignin type	Lignin content (wt%)	Polymer matrix	Additives	Mechanical properties			Ref.
					Young's modulus (MPa)	Tensile strength (MPa)	Elongation at break (%)	
Solvent casting	Unmodified fractionated SWKL	85%	Poly(vinyl acetate)	Plasticizers	Increased linearly w/ $M_w$	Increased linearly w/ $M_w$	n.a.	169
Solvent casting	Anhydride esterified organosolv	Up to 20%	Cellulose acetate butyrate	None	Increased	Reduced	Reduced	24
Melt processing	Prehydrolysis beechwood	Up to 30%	PP PE	None	Increased	Reduced	n.a.	171
Solvent casting	Ethylated methylated SWKL	100%	None	None	Reduced	Reduced	Reduced	170
Melt processing	Unmodified organosolv from Abaca	Up to 40%	Ecoflex™	None	No change	No change	No change	172
Solvent casting	Ethylated methylated SWKL	Up to 70%	PBA	PBA	Increased	Reduced	Reduced	170 173

Preparation method	Lignin type	Lignin content (wt%)	Polymer matrix	Additives	Mechanical properties			Ref.
					Young's modulus (MPa)	Tensile strength (MPa)	Elongation at break (%)	
Melt processing	Native aquasolv	30%	Cellulose	Plasticizers, dyes, fillers	n.a.	n.a.	n.a.	174
Melt processing	Unmodified Indulin AT SWKL	Up to 60%	PP	Mineral fillers and MAPP	Increased	Reduced	Reduced	175
Solvent evaporation and melt moulding	Anhydride esterified organosolv	Up to 75%	PCL	None	Increased	Reduced	$\leq 500\%$	148
Melt processing	Anhydride esterified	Up to 40%	LDPE	Maleic anhydride compatibilizer	Increased	Reduced	n.a.	178
Melt processing	Bromododecane alkylated unbleached HWKL	Up to 40%	PP	None	Increased	Reduced	n.a.	180
Melt processing	Fractionated soda	Up to 10%	PVC	Plasticizer	Increased	Reduced	Reduced	181

Preparation method	Lignin type	Lignin content (wt%)	Polymer matrix	Additives	Mechanical properties			Ref.
					Young's modulus (MPa)	Tensile strength (MPa)	Elongation at break (%)	
Melt processing	Acetylated esterified SWKL	Up to 20%	PLA	None	No change	No change	No change	182
Melt mixing	Methanol fractionated SWKL	Constant at 50%	Acrylonitrile butadiene rubbers	Polybutadiene copolymer rubber	n.a.	Increased compared to unfractionated	Increased compared to unfractionated	183
								184
Melt processing	Anhydride esterified HWKL, SWKL, organosolv, soda, hydrolysis	Constant at 50%	HDPE	Parafilm wax	No change	Increased	$\leq 45\%$	143
								144
Melt processing	Maleic anhydride Indulin AT esterified SWKL	Up to 50%	PP	None	Increased	No change	No change	185

Preparation method	Lignin type	Lignin content (wt%)	Polymer matrix	Additives	Mechanical properties			Ref.
					Young's modulus (MPa)	Tensile strength (MPa)	Elongation at break (%)	
Melt processing and electro-spinning	Fractionated hydroxypropylated etherified organosolv HW	Up to 40%	Biobased PET	None	Increased	No change	Increased	186
Melt processing	Methylated with DMC eucalypt hydrothermal lignin	Up to 60%	PBAT	Compatibilizer MAH	n.a.	Increased	≤ 800%	190
Melt processing	Unmodified hardwood acid hydrolysis	Up to 40%	PLA	DCP MA BPO	Increased	Reduced	Reduced	187
Melt processing	Acetic anhydride esterified SWKL and HWKL	Up to 10%	LLDPE	None	Increased	Reduced	Reduced	146
Melt processing	Oxyalkylated etherified SWKL	Up to 20%	Ecoflex™	None	Increased	Reduced	Reduced	157

#### **2.4.4 Green solutions**

This review has covered comprehensive research done in wood pulping processes to obtain technical lignin, technical lignin fractionation and modification, and the application of technical lignins in different materials specifically thermoplastic blends. Blending lignin in polymeric matrices is not a novel pursuit but when reviewing previous work there is a lack of applicable green chemistry practices when modifying and blending lignin-based thermoplastics. Section 2.2 details the danger and toxicity of materials made from petro-based chemicals, fillers, and additives and if a material is engineered to replace these plastics it must be “better” for the environment. But what constitutes a “better” plastic for everyday consumption? The previously described lignin-thermoplastic blends utilize harsh modifications involving toxic chemical anhydrides, oxides, additional plasticizers and compatibilizers, and lack evidence as to how the synthesized material will break down in the natural environment. Cyclewood’s commercial Xylo bags are made with propylene oxide and when tested sulfur containing volatiles were identified in the headspace films. Xiong et al. created a material using green reagent dimethyl carbonate to modify the lignin but then added a compatibilizer and revealed no evidence of biodegradation. Engineering a better plastic will involve the use of green reagents, recycling or reuse of chemicals and minimal consumption in the process while maintaining good mechanical properties in the final material.

## **Chapter 3: Materials and methods**

### **3.1 Materials**

West Fraser through Alberta Innovates kindly supplied the Lignoforce™ Grade A softwood kraft lignin from their mill in Hinton, Alberta. ACS grade acetone solvent for HPLC  $\geq$  99.9% was obtained from Sigma-Aldrich. ACS certified ethylene carbonate 99% and sodium carbonate were obtained from Fisher Scientific and 99% pure propionic acid was received from Acros Organics. Ecoflex F Blend C1200 was purchased from BASF. All chemicals were used as received.

### **3.2 Preparation of as received technical lignin**

The pH value of the as received lignin was tested with a pH meter and recorded at pH 3.0 when 1g lignin was placed in 10 mL water. In order to remove the acid and make the pH neutral (5.0-6.0) the as received lignin was thoroughly washed with distilled water, filtered, and dried prior to acetone fractionation. The as received lignin had a moisture content of 44.66% and the calculation to determine the distilled water to lignin ratio can be found in Appendix A.1. The calculated amount of distilled water (1,400 mL) was added to an 1800 mL Erlenmeyer flask and placed on a magnetic stir plate at room temperature. The distilled water began stirring and the correct amount lignin (150g) was slowly added and mixed for 24 hours. The washed lignin was vacuum filtered using a Büchner funnel with 150 mm Whatman qualitative filter paper and dried using a Labconco freeze dryer (-50°C) for 48 hours. All samples in this research were pre-frozen prior to lyophilization in order to maximize efficiency. Freeze drying was necessary to remove water and preserve samples. Due to equipment size restrictions this process was repeated four times.



### **3.3 Acetone fractionation of technical lignin**

In a fume hood the prepared lignin (dried) and acetone were mixed at a 1:10 ratio in an Erlenmeyer flask on a magnetic stir plate. The acetone was first added, and magnetic stirring began as the lignin was slowly scooped into a glass funnel to prevent clogging and clumping. The top of the flask was covered with parafilm to prevent evaporation and the solution was left to mix for 6 hours. A vacuum filtration was set up using a Büchner funnel with Whatman No. 1 filter paper which was rinsed with acetone prior to the filtration to ensure sealing of the filter. The mixture was poured into the funnel and the dissolved acetone soluble portion (ASKL) was recovered in the vacuum flask, while the insoluble portion was retained by the Büchner funnel. The acetone insoluble portion (AIKL) was washed with distilled water for 24 hours, filtered with 150 mm Whatman qualitative circle filter paper, and freeze dried for 48 hours. The soluble portion underwent rotoevaporation with a BUCHI Rotavapor R-200 at 475 millibars, 40°C, and a rotation of 20 rpm to recover acetone. The remaining acetone soluble solution was spread in a shallow glass tray and placed uncovered in a fume hood for 48 hours to allow complete evaporation of trace amounts of solvent. To meet the lignin powder demand for blending, five batches of 100 grams of lignin were fractionated and the yields averaged 61% soluble and 39% insoluble. The standard deviation of the five individual measurements was  $\pm 1.3$ . The coefficient of variation for fractionation yield was 2.1% for the soluble portion and 3.3% for the insoluble portion which demonstrated good repeatability and confirms a scale up fractionation with recovered solvent is possible.

### 3.4 Elemental analysis

Elemental analysis of the Lignoforce Grade A SWKL and its subsequent acetone fractionated portions were performed using a Carlo Erba Elemental Analyzer. The absolute content for carbon (C), hydrogen (H), nitrogen (N), and sulfur (S) were measured while oxygen (O) was calculated by subtracting the sum of the elements from 100. The resulting data is listed in Table 10.

**Table 10 Elemental composition of SWKL and its acetone fractionated counterparts**

	SWKL	ASKL	AIKL
Carbon (%)	63.7	66.7	62.7
Hydrogen (%)	5.9	6.2	5.8
Nitrogen (%)	0	0	0
Oxygen (%)	28.9	25.8	29.9
Sulfur (%)	1.5	1.3	1.6

### 3.5 Synthesis of technical hydroxyethyl lignin

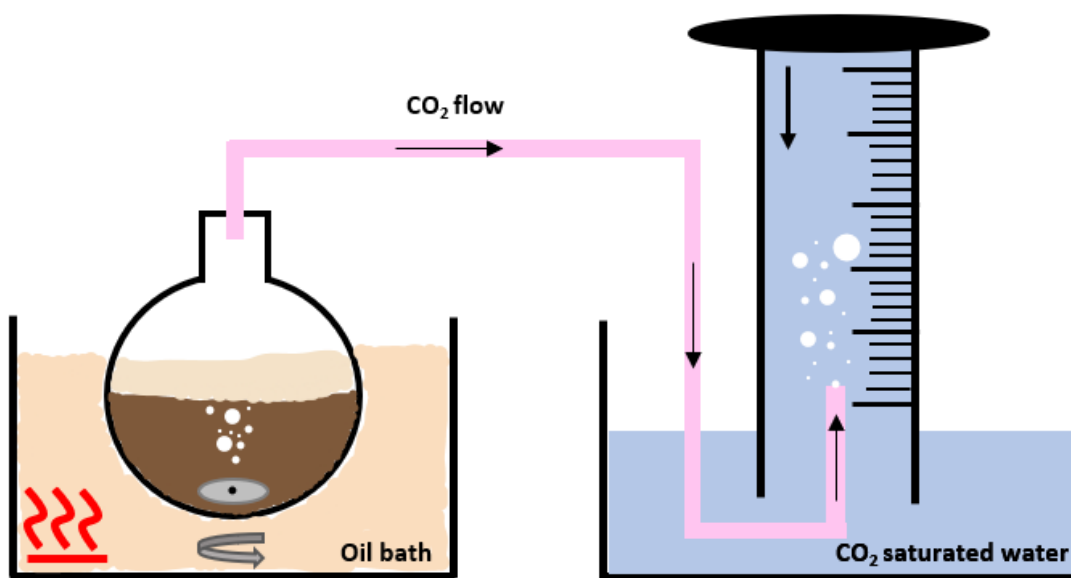
The original unmodified, ASKL, and AIKL lignin powders were hydroxyethylated with ethylene carbonate (EC) which would act as the reagent and solvent and sodium carbonate ( $\text{Na}_2\text{CO}_3$ ) which would act as the catalyst. All reactions were carried out in batches of 15 grams lignin powder in a 250 mL round bottom flask with a magnetic stir bar. Prior to reaction unmodified lignin powder was kept in a 40°C model 280A Isotemp vacuum oven for 24 hours to dry the lignin. The amount of EC and  $\text{Na}_2\text{CO}_3$  meant to react with a specific lignin powder was determined by quantitative  $^{31}\text{P}$ NMR analysis and sample calculations can be found in Appendix A.2. The EC was ground up in a mortar and pestle to increase surface area and added to the round bottom flask first. The catalyst and lignin were added to the top of the EC and air was removed from the reaction flask with nitrogen and then sealed with a rubber stopper, Teflon tape,

and parafilm to ensure there was no leakage. The reaction was placed into a 120 °C oil bath and stirred at 400 rpm on a hotplate, and closely monitored using real time control (RTC) as described below to detect evolved CO<sub>2</sub>. Upon completion the HE lignin was slowly added to 1500 mL distilled water and stirred for 24 hours. The precipitated HE lignin was vacuum filtered using a Büchner funnel with 150 mm Whatman qualitative filter paper and rewashed until the pH meter read between 5 and 6 and the pH strip showed a corroborating color (pale yellow). A Thermo Scientific Legend XTR Centrifuge was used to collect the remaining sample that was rinsed off of the filter paper to prevent product loss. The process avoided using strong acid washes like H<sub>2</sub>SO<sub>4</sub> or HCL to neutralize pH. The HE lignin was put in the laboratory freezer for 24 hours, freeze dried according to previous protocol for 48 hours, vacuum dried at 40 °C for another 24 hours, and stored in a blacked out vacuum bench desiccator.

### **3.5.1 Real time control**

Carbon dioxide is a byproduct of the EC/lignin reaction and so real time control was developed to optimize reaction time and avoid cumbersome side reactions that result in extensive structural modifications. Alongside laboratory partner Dr. Liyang Liu, data was collected to develop an in-situ monitoring technique which produced a series of equations that calculate volume displacement created by carbon dioxide (CO<sub>2</sub>) off gassing in order to stop the reaction before unnecessary side reactions that form carbonate linkages take place. Please refer to the published journal article for details.<sup>191</sup> Sodium carbonate was carefully chosen as the catalyst for the HE reaction because it is a carbonate salt and reduces the degradation of EC producing negligible amounts of CO<sub>2</sub>. The reaction temperature of 120 °C was carefully chosen because it promotes the reaction between EC and lignin rather than the degradation or self-polymerization of EC. Given the main goal was to derivatize ArOH and COOH to AIOH the CO<sub>2</sub> production

must come from that reaction alone to determine the maximum amount of derivatization. A schematic of the reaction set up can be viewed in Figure 20. A completely sealed pliable tube ran from the reaction pot to a 1000 mL graduated cylinder that was filled with water and turned upside down. As the reaction progressed and CO<sub>2</sub> was released the water in the graduated cylinder was saturated with CO<sub>2</sub> and displaced.



**Figure 20 Real time control laboratory set-up schematic**

Based on calculations of the molar quantity of phenolics and carboxylic acid when, 1,347 mL water was displaced for the UF\_HE reaction, it was complete. When 1,631 mL water was displaced for the ASKL\_HE reaction, it was complete and when 1,206 mL water was displaced for the AIKL\_HE reaction, it was complete. Please refer to the complete set of calculations in Appendix A.3. Because UF, ASKL, and AIKL contain different amounts of free phenolics, the conversion times for ArOH and COOH groups to ALOH will differ. The ASKL\_HE reaction required a higher volume of water displacement because there were more free phenolics to react.

The water volume displacement dependent reaction times varied between 90-130 minutes depending on the fraction.

### **3.6 Synthesis of esterified technical lignin**

The final HE lignin product was weighed and split into two parts, HE lignin to be blended and HE lignin to be esterified with propionic acid. The HE lignin that was meant for future blending was stored in a blacked-out bench Bel-art vacuum desiccator dedicated to lignin powders only. The remaining HE lignin was kept in a 40°C model 280A Isotemp vacuum oven for 24 hours prior to esterification. For this modification, lignin was added to propionic acid in a 250 mL round bottom flask at a ratio of one gram lignin to 10 mL propionic acid for 24 hours in a 120 °C oil bath. Aluminum foil was placed over the top of the reaction flask and small holes were poked through to allow ventilation into the fume hood. Typically, esterified batches were done with 7.5 grams of lignin and 75 mL propionic acid. For recovery of the esterified lignin, two wash stations were set up in 1000 mL corning Pyrex glass beakers each filled with 700 mL distilled water on magnetic stir plates. A small stir bar at low speeds was used and the esterified product was slowly added between the two. The esterified lignin was initially washed for 24 hours and then vacuum filtered using a Büchner funnel with 150 mm Whatman qualitative filter paper and rewashed until the pH meter read between 5 and 6 and the pH strip showed a corroborating color (pale yellow). A Thermo Scientific Legend XTR Centrifuge was used to collect the remaining sample off the rinsed filter paper to prevent product loss. The esterified lignin was put in the laboratory freezer for 24 hours, freeze dried according to previous protocol for 48 hours and finally vacuum dried at 40 °C for another 24 hours. The esterified lignin that was meant for future blending was stored in a blacked-out bench Bel-art vacuum desiccator dedicated to this studies lignin powders only.

The etherification followed by the esterification were carried out in a two-pot reaction. The purpose of synthesizing the hydroxyethyl ether (HE) lignin in a two-pot reaction (etherification followed by esterification) was to create a technical lignin that presents uniform functionality with primary alcohol groups. The HE lignin showed improved solubility in propionic acid for greener esterification. Towards the beginning of this research project a one pot reaction process was attempted but product loss was extensive, and it was impossible to consistently isolate the HE lignin. Because this project aims to comparatively study how HE lignin powders behave in a thermoplastic blend with Ecoflex<sup>TM</sup> versus their unmodified and esterified counterparts it was necessary to have the reliable product the two-pot reaction produced.

The weight percent lignin loading reported in the results and discussion section refers to the amount of hydroxyethyl ether or esterified lignin blended in relation to Ecoflex<sup>TM</sup>. In literature, modified lignin loading is often presented as a weight percentage without taking into full account the actual amount of lignin present after a chemical modification is carried out.<sup>10,188,190,192</sup> For example, after the etherification with ethylene carbonate two carbons are added to the lignin and after the esterification with propionic acid an additional six carbons are added. The formula weight for the coniferyl alcohol (G-unit) without the unsaturated bonds is 179 g/mol. After the hydroxyethylation the formula weight increases to 223 g/mol. After the esterification and addition of the propionate groups the formula weight increases to 335 g/mol. This should be considered when discussing weight percent lignin loading.

### 3.7 <sup>31</sup>P NMR characterization of unmodified and modified technical lignin powders

Lignin derivatization was carried out in small batches and all lignin powders were characterized using quantitative <sup>31</sup>P NMR analysis. Measurements were done in triplicate and the coefficient of variation for functional group analysis ranged from 1.6-7.3% for all powders showing good reproducibility. Error bars in section 4.1 Figures 25b and Figure 31b represent plus or minus the standard deviation of three individual measurements for both fractionated portions in comparison to their parent counterpart.

#### 3.7.1 Sample preparation

Prior to testing, the lignin powder sample was kept in a 40°C model 280A Isotemp vacuum oven for 24 hours. 20 mg of dried lignin was carefully weighed out and dissolved into 400 µL of solution A consisting of deuterated chloroform (CDCl<sub>3</sub>) and pyridine at a 1/1.6 v/v ratio in a 2 mL vial. The pyridine was protected from moisture with molecular sieves. The lignin and solution A were thoroughly stirred using a laboratory vortex mixer. The internal standard (IS) was prepared by mixing N-hydroxy-5-norbornene-2,3-dicarboximide (NHND) with solution A at 10 mg/mL. The relaxing agent was prepared by mixing chromium (III) acetylacetonate with solution A at 5.6 mg/mL. 100 µL of internal standard, 40 µL of relaxing agent, and 50 µL of phosphitylating reagent of 2-chloro-4,4,5,5-tetramethyl-1,3,2-dioxaphospholane (TMDP) were pipetted into the lignin solution and thoroughly mixed using the vortexer until absolute dissolution. The solution was transferred into a 5 mm NMR tube and immediately analyzed to prevent degradation. All solutions were made fresh for each test and all scientific grade chemicals were stored properly. This procedure follows a well-established and universally accepted protocol developed over decades of research.<sup>37,55,162,167,193–195</sup>

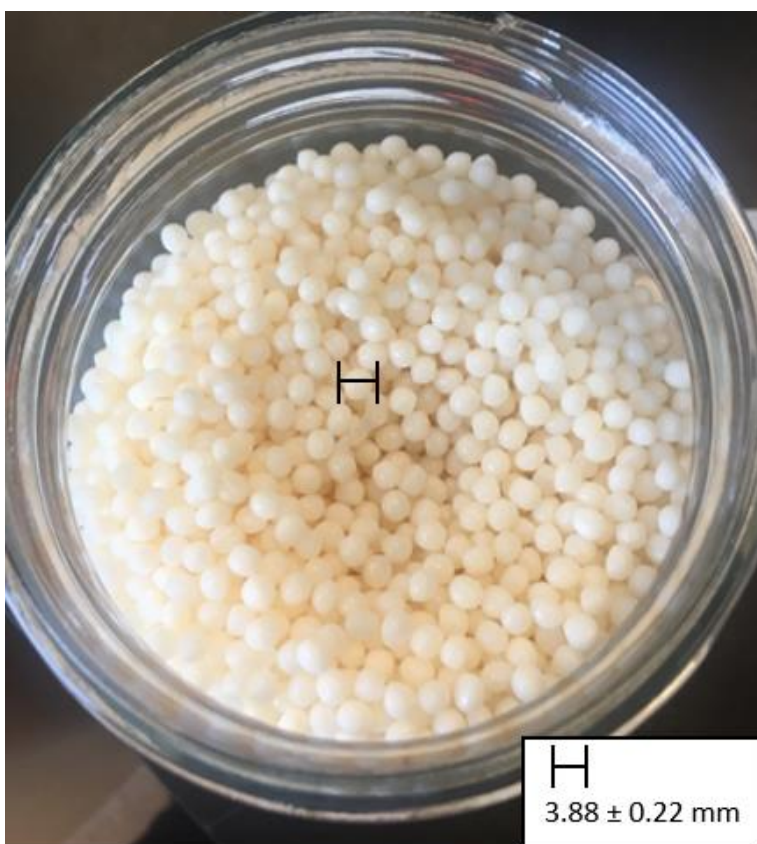
### 3.7.2 Sample analysis

Nuclear magnetic resonance Bruker Avance 300 MHz spectrometer at 25 °C equipped with BBO probe was used to analyze all lignin powder samples prepared in accordance to the previously discussed protocol. An inverse gated decoupling pulse was employed to obtain quantitative  $^{31}\text{P}$  NMR with the following parameters: number of scans 800, relaxation delay 5s, acquisition time 1.4s, pulse length 6  $\mu\text{s}$ , and 90° pulse width. The chemical shift of each phosphitylated product was calibrated with a product of TMDP with residual moisture which gave a sharp stable signal at 132.2 p.p.m. Different functional groups were assigned, and Bruker TopSpin 4.1.1 and Microsoft excel were used for analysis. The NMR peaks were integrated with respect to the internal standard NHND peak and a baseline correction was made to improve integration accuracy. This procedure along with integration regions for lignin was configured in accordance with reviewed literature and a sample calculation can be found in Appendix A.4.<sup>37,55,162,167,193–195</sup>

### 3.8 As received Ecoflex<sup>TM</sup> F blend C1200

Ecoflex<sup>TM</sup> F blend C1200 arrived in bulk as lens shaped pellets in a vacuum sealed bag made of UV light blocking material. Upon arrival, the pellets were sized for diameter with a micro caliper by taking five measurements of five individual pellets chosen at random. The measurements were recorded, and the average diameter was  $3.88 \pm 0.22$  mm. Figure 21 is an image of the as received Ecoflex<sup>TM</sup> pellets.





**Figure 21 As received Ecoflex™ F blend C1200 lens pellets with average diameter**

### **3.8.1 Storage**

In accordance with the safety data and product information sheets, Ecoflex™ must be protected against moisture, extreme heat, direct UV light and oxidizing reagents.<sup>94,95</sup> Four 1L amber glass bottles were filled with Ecoflex™ and placed in a blacked out bench desiccator dedicated to Ecoflex™ at room temperature (23°C). Before testing or blending Ecoflex™ was removed from these bottles, placed in a smaller amber glass bottle and vacuum dried at 40 °C for 24 hours. The remaining bulk Ecoflex™ was resealed in the UV radiation proof heavy-duty bag, placed back in its original box, and stored at room temperature away from other chemicals.

### 3.8.2 Characterization using $^{13}\text{C}$ NMR

The as received Ecoflex<sup>TM</sup> was characterized using  $^{13}\text{C}$  NMR to confirm its structure. A solubility test was carried out to check for miscibility in different solvents. Ecoflex<sup>TM</sup> did not dissolve in, DMSO, THF, or ethyl acetate but fully dissolved in chloroform-d ( $\text{CHCl}_3\text{-d}$ ). 99.8 mg of Ecoflex<sup>TM</sup> was dissolved into 500  $\mu\text{L}$   $\text{CHCl}_3\text{-d}$  in a 5 mm NMR tube followed by 60  $\mu\text{L}$  relaxation agent (50mg/mL) chromium III acetylacetonate and 15 mg 1,3,5 trioxane as the internal standard. The sample was tested by nuclear magnetic resonance spectroscopy on a Bruker Avance 300 MHz spectrometer at 25 °C equipped with BBO probe. An inverse gated decoupling sequence was applied with parameters: relaxation delay 2s, acquisition time 1.4s, pulse length 8.5  $\mu\text{s}$ , pulse angle 90°, and scan number 20,000. Results were analyzed and different functional groups were assigned using Bruker TopSpin 4.1.1 and Microsoft excel and the accompanying spectrum can be found in Appendix B.

### 3.9 Preparation of lignin-Ecoflex<sup>TM</sup> thermoplastic blends

By melt mixing, Ecoflex<sup>TM</sup> (ECO) was blended with the nine prepared lignin powders: unfractionated unmodified (UF\_UN), unfractionated hydroxyethyl ether (UF\_HE), unfractionated esterified (UF\_E), acetone soluble unmodified (ASKL\_UN), acetone soluble hydroxyethyl ether (ASKL\_HE), acetone soluble esterified (ASKL\_E), acetone insoluble unmodified (AIKL\_UN), acetone insoluble hydroxyethyl ether (AIKL\_HE), and acetone insoluble esterified (AIKL\_E). Table 11 gives an overview of the composition based thermoplastic blends. No dyes, additives, plasticizers, compatibilizers, stabilizers or lubricants were used. See Appendix C for equipment and sample imagery.

**Table 11 Composition of lignin-Ecoflex™ thermoplastic blends**

Sample	Composition (wt %)	
	Ecoflex™	Lignin Powder
ECO	100	0
UF_UN	95, 90, 80, 70	5, 10, 20, 30
UF_HE	95, 90, 80, 70	5, 10, 20, 30
UF_E	95, 90, 80, 70	5, 10, 20, 30
ASKL_UN	95, 90, 80, 70	5, 10, 20, 30
ASKL_HE	95, 90, 80, 70	5, 10, 20, 30
ASKL_E	95, 90, 80, 70, 60	5, 10, 20, 30, 40
AIKL_UN	95, 90, 80	5, 10, 20
AIKL_HE	95, 90, 80, 70	5, 10, 20, 30
AIKL_E	95, 90, 80, 70	5, 10, 20, 30

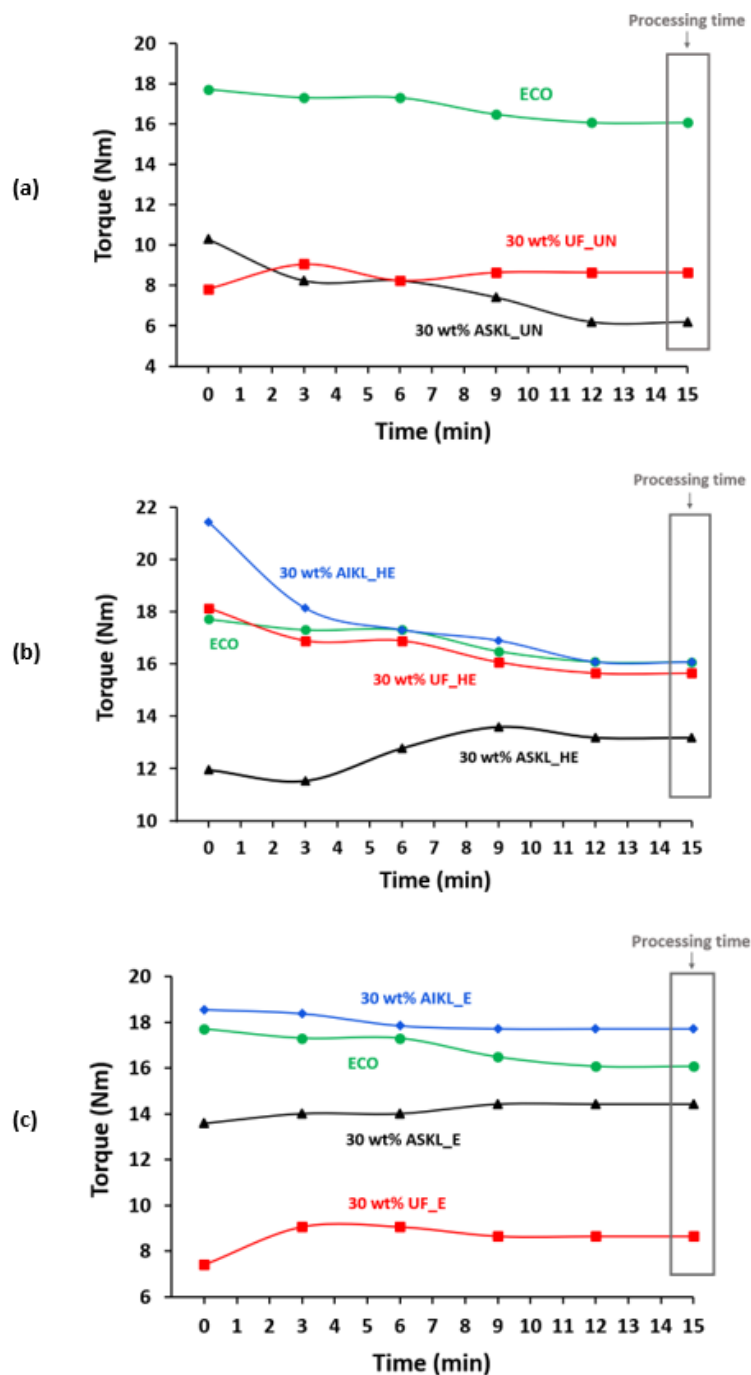
### 3.9.1 Melt compounding

A laboratory-scale Xplore MC 15 twin screw micro compounder was used for all melt mixing and extrusion. Ecoflex™ pellets and lignin powders were manually introduced in the top feeder by weight percent or mass fraction. The process began with 15 grams of total material and was blended according to composition (5, 10, 20, 30, 40) wt% lignin powder. The controlled or constant variables were melt temperature 179-181 °C (there was some mechanical fluctuation), screw speed 150 rpm, and processing time, 8 minutes for Ecoflex™ with an additional 15 minutes once lignin powder was added. During the process dry nitrogen was continuously purged into the mixture chamber at 5 psi to ensure minimum thermo-oxidative degradation. Pure Ecoflex™ (100 wt%) was extruded and set as the baseline reference material for this research

project. Unless otherwise specified, all samples were processed under these controls in a consistent and well monitored fashion to ensure repeatability.

Prior to establishing the boundaries, a set of experiments were carried out to determine processing times. Sadeghifar et al. reported on the melt stability of lignin powders in a synthetic polymer blend with PE in the barrel of a similar twin-screw extruder as a function of torque output.<sup>189</sup> On a macroscopic level, the group demonstrated there is a direct correlation between melt stability and torque output.<sup>189</sup> With this knowledge it was determined that processing time could be established by plotting torque measurements against time and observing where the curve flattened. Pure Ecoflex<sup>TM</sup> was extruded and torque values were recorded from the machine every 3 minutes for 15 minutes. It was noted that after 8 minutes the curve flattened and the Ecoflex<sup>TM</sup> was stable in the melt. At 8 minutes, lignin powder was added, and torque values were recorded from the machine every 3 minutes for 15 minutes. There was an expected variation in results based on lignin powder and wt% loading but at 15 minutes all lignin powders showed stability in torque output. Because the goal of this research was to compare unmodified/unfractionated lignin powders to modified/fractionated lignin powders it was crucial to develop a set of parameters that worked for all lignin powders at all lignin loadings. Figure 22 offers the graphical depiction of the described procedure (at 30 wt% lignin loading) and justifies the 15 minute lignin/Ecoflex<sup>TM</sup> processing time. The time of zero minutes represents when lignin was first introduced to the top feeder. At time zero, only the Ecoflex<sup>TM</sup> pellets have been processing for 8 minutes in the barrel of the machine. Neat Ecoflex<sup>TM</sup> (ECO) or 0 wt% lignin is shown as the baseline reference. The total processing time is 23 minutes but only the 15 minutes after lignins are added are shown in Figure 22. AIKL\_UN could not be blended at 30 wt% and is therefore absent from Figure 22a.

The independent variables were the lignin powder type and composition (wt%) and the dependent variables were the resulting thermal and mechanical properties which will be extensively discussed in the results section. No malodorous odor was observed by the researcher or other close working laboratory personal during processing. The machine was thoroughly cleaned between each sample extrusion (lignin powder and wt% lignin loading) to avoid contamination and there were no other users at the time.



**Figure 22** Effect of extruder torque on melt stability at a 30 wt% lignin loading for unfractionated and acetone fractionated unmodified lignins (UF\_UN and ASKL\_UN) (a) hydroxyethyl ether lignins (UF\_HE, ASKL\_HE and AIKL\_HE) (b) and esterified lignins (UF\_E, ASKL\_E and AIKL\_E) (c) Neat Ecoflex™ (ECO) is the baseline reference and time 0 minutes is when lignin is added to the top feeder

### **3.9.2 Mould injection**

The compounded material was moulded into standard dumbbell shaped test specimens using the Xplore IM 5.5 micro injection moulder. After melt mixing was complete the material was added to the transfer unit and then injected into Xplore mould 1202701 thickness 3.2 mm ASTM D638 type V. The three-step holding pressure and time were controlled and adjusted to avoid shrinkage or leakage of the moulded sample. If the sample showed leakage which presented as a thin outer film, pressures were lowered and if the sample showed shrinkage, pressures were increased, neither were of issue. The transfer unit was pre-heated to 180 °C to ensure consistency in melt temperature. No material was left to sit in the transfer unit between extrusions, meaning the blend went directly from the barrel of the compounder, to the transfer unit and into the mould. Once injected, the mould was left to sit for two minutes before careful removal of the sample. The mould was cooled between injections and a thermocouple was used to confirm the mould temperature was between 24-25 °C before the next injection. The machine was thoroughly cleaned between each sample injection (lignin powder and wt% lignin loading) and there were no other users at the time. Moulded samples were stored in parafilm sealed petri dish and kept in a blacked-out desiccator until mechanical testing.

### **3.9.3 Mechanical testing**

The American Society for Testing Materials (ASTM) standard ASTM D638 -14 was used for sample preparation, sample testing, and all subsequent calculations.<sup>196</sup> This standard addresses the same subject matter and is comparable to the International Standards Organization (ISO) standard ISO 527-1. The standard is meant to produce data for the control and specification of plastic materials and is useful for qualitative characterization and research and development. It is important to note that all samples in this research were prepared, tested, and

analyzed following the exact process outlined in chapter three. By carefully following the ASTM standard protocols, the samples can be successfully compared to one another.

### 3.9.3.1 Sample measurements

According to the standard for mould injected species, actual measurements should be taken from each sample lot and specimen variation in width of narrow section ( $W_c$ ) and thickness (T) should be less than 1%. In addition, all numbers shall be reported as averages to three significant figures. This was successfully carried out using a micro caliper and the thickness was averaged at 3.21 mm and the width was averaged at 3.36 mm. All other measurements shown in Figure 23 were taken and fell within the appropriate range for a Type V specimen size (Table 12). It is important to note the gauge length (G) was 7.73 mm as this will later be used to normalize strain. All samples were inspected for visible defects prior to mechanical testing.

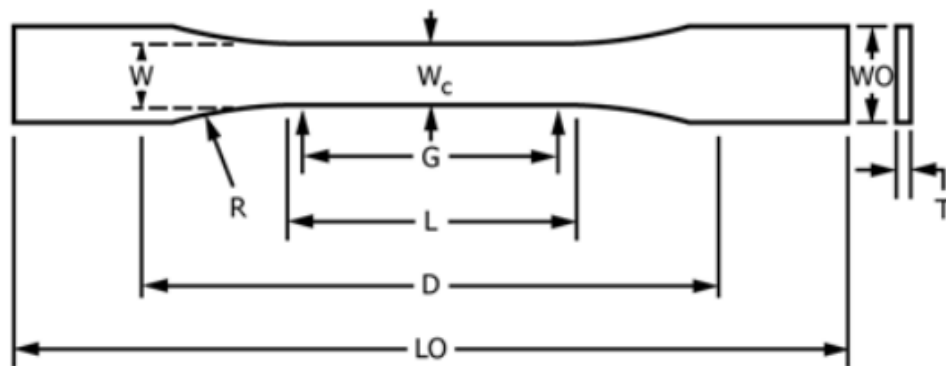


Figure 23 ASTM D638-14 standard type V dumbbell shape dimensions <sup>195</sup>



**Table 12 Type V sample measurements following standard dimensions**

	ASTM D638-14 <sup>a</sup> (mm)	Actual <sup>b</sup> (mm)
W <sub>c</sub>	3.18 ± 0.5	3.36
T	3.2 ± 0.4	3.21
G	7.62 ± 0.25	7.73
W <sub>o</sub>	9.53 ± 3.18	9.73
L	9.53 ± 0.5	9.82
LO	63.5 no max	63.8
D	25.4 ± 5	26.6

<sup>a</sup> Values from section 6 of the ASTM D638-14 standard <sup>195</sup>

<sup>b</sup> Measurements taken from each sample lot and averaged to three significant figures

### 3.9.3.2 Tensile testing

All mechanical testing was carried out using an Instron 5969 load frame with a 2 kN load cell at 23 °C and 50% humidity measured by a control connected to the machinery and recorded by Bluehill software. The lowest crosshead speed of testing was determined in an experiment that ensured a rupture time with 0.5 to 5 minutes of testing. At 5 mm/min and 10 mm/min the sample did not rupture before the maximum extension of the machine was reached and at 100 mm/min the sample ruptured too quickly. It was determined that 50 mm/min was the appropriate speed for testing and all ruptured samples did so within the gauge length. In accordance with the standard, each lot of samples contained five specimens. All samples were loaded according to standard requirements (section 5 apparatus of ASTM D638 -14) and Bluehill software recorded the load-extension curve of each specimen. The data rate was recorded at 5 points per second and time (seconds), extension (mm), force (N), humidity (%), and temperature (°C) were also recorded.

### 3.9.3.3 Quantitative data analysis

Because of take up slack or seating of the specimen, toe compensation was carried out in accordance with section 11.1 annex A1.1 of ASTM D638-14.<sup>196</sup> Force was normalized by division with cross sectional area ( $T \cdot W_c = 10.8 \text{ mm}$ ) which gave engineering stress ( $\sigma$ ) and strain was normalized by division with gage length ( $G = 7.73 \text{ mm}$ ) which gave engineering strain ( $\epsilon$ ). Engineering stress strain curves were processed for each specimen and an average curve was created by arithmetic mean of the 5 specimens in each sample lot by ASTM D638 -14 standard requirements (section 11 calculation).<sup>196</sup> In accordance with ASTM D638-14, all mechanical property values are therefore reported as averages to 3 significant figures and standard deviations are reported to 2 significant figures. All mechanical property data was presented as the average of five samples which fractured within the gauge length and the error bars in section 4.2.2 Figures 42-45 and Figure 78 represent plus or minus the standard deviation of the five individual samples. The coefficient of variation for the mechanical property analysis ranged from 1.1-13% showing good reproducibility. Relevant samples were analyzed statistically using a single factor one-way Analysis of Variance (ANOVA) test with a post hoc Tukey test in Origin Pro 64.

### 3.10 Differential scanning calorimetry (DSC) analysis

Thermal properties of lignin powders and lignin-Ecoflex<sup>TM</sup> thermoplastic blends were determined using a TA Q1000 differential scanning calorimeter from TA Instruments, USA. All data was recorded and processed using TA instruments Universal Analysis 2000 software and Microsoft Excel. To ensure all moisture was removed prior to testing, all samples were kept in a 40°C model 280A Isotemp vacuum oven for 24 hours. All samples were analyzed under a 50 mL/min nitrogen flow. It is well documented in literature that an annealing cycle prior to thermal property analysis is necessary to release stored thermal history.<sup>131,164</sup> In order to accomplish this

and avoid any changes to the lignin chemical structure 105 °C is a good annealing temperature.<sup>131,164</sup>

### **3.10.1 Lignin powders**

Approximately 5 mg of dried lignin powder was sealed in a 40  $\mu$ L aluminum crucible, run through a 5-cycle process. The  $T_g$  values were determined as the midpoint of the heat capacity change during the second heating cycle. Because a large amount of lignin powder was necessary for blending, multiple batches of each lignin powder were synthesized, and duplicates of each batch were run. For example, there were five batches of ASKL\_UN lignin powder and each batch were run two times, averaged and then the mean of the five averages were taken. This ensured consistency within each batch and repeatability between batches of the same powder. The 5 cycle process involved the following temperature scans; cycle 1: Ramp up (initial anneal) 10 °C/min to 105 °C and isothermally condition for 30 minutes; cycle 2: Ramp down (cool) 10 °C/min to -50 °C; cycle 3: Ramp up (heat 1) 10 °C/min to 180 °C for ASKL and UNF powders and 200 °C for AIKL powders; cycle 4: Ramp down (cool) 10 °C/min to -50 °C; cycle 5: Ramp up (heat 2) 10 °C/min to 200 °C for ASKL and UNF powders and 220 °C for AIKL powders. Standard deviations are plus or minus the five averaged samples and are presented in Table 13 of *section 4.1.2.1*. The coefficient of variation for the  $T_g$  analysis ranged from 0.3-9.5% showing good reproducibility.

### **3.10.2 Lignin-Ecoflex™ thermoplastic blends**

Approximately 5-6 mg of each dried thermoplastic blend was cut using a clean razor blade and the sample was sealed in a 40  $\mu$ L aluminum crucible taking special care to ensure full contact with the bottom of the pan. A 3-cycle process to determine the melting temperature ( $T_m$ ), crystallization temperature ( $T_c$ ),  $T_g$ , onset crystallization temperature ( $T_{os}$ ), the crystallization

enthalpy ( $\Delta H_c$ ), enthalpy of fusion ( $\Delta H_m$ ), and degree of crystallinity ( $X_c$ ) was developed and measured in triplicate for neat Ecoflex<sup>TM</sup>, and each plastic at each wt% lignin powder loading. The initial annealing temperature is approximately 20 °C above the Ecoflex<sup>TM</sup> melting temperature. The 3-cycle process involved the following temperature scans; cycle 1: Ramp up (initial anneal) 10 °C/min to 180 °C and isothermally condition for 10 minutes; cycle 2: Ramp down (cool) 10 °C/min to -60 °C and isothermally condition for 5 minutes; cycle 3: Ramp up (heat) 10 °C/min to 200-220 °C. The  $T_m$ ,  $T_g$ , and  $\Delta H_m$  were reported from the second heating cycle and the  $T_c$  and  $\Delta H_c$  were reported from the cooling cycle. The presented quantitative data in *section 4.2* Tables 18-20 and Table 22 are averages of three samples and the error bars in Figures 62, 64, 67, 68 and 69 represent plus or minus the standard deviation of the three individual samples. By running three tests per sample the coefficient of variation for reported values ranged from 1.1-8.8% showing good reproducibility and confirming that specimens were subjected to identical processing conditions.

### 3.10.2.1 Degree of crystallinity

Degree of crystallinity ( $X_c$ ) or percent crystallinity  $X_c$  % were calculated as follows:

$$X_c(\%) = \frac{\Delta H_m}{W_p * \Delta H_{fo}} * 100$$

where  $\Delta H_m$  is the experimental melting heat of fusion (J/g) obtained by horizontal integration of the melting curve recorded from DSC testing,  $W_p$  is the weight fraction of Ecoflex in the thermoplastic blend, and  $\Delta H_{fo}$  is the heat of fusion of 100% crystalline Ecoflex (114 J/g).<sup>197–199</sup>

### 3.11 Thermal gravimetric analysis (TGA)

The temperature at 5% weight loss ( $T_{5\%}$ ), the maximum degradation temperature ( $T_{\max}$ ), and the char yield for lignin powders and lignin-Ecoflex<sup>TM</sup> thermoplastic blends were determined using a TA Q500 thermogravimetric analyzer from TA Instruments, USA. All data was recorded and processed using TA instruments Universal Analysis 2000 software and Microsoft Excel. To ensure all moisture was removed prior to testing, all samples were kept in a 40°C model 280A Isotemp vacuum oven for 24 hours. All samples were analyzed under a 60 mL/min nitrogen flow and all powders were run in quintuplets while lignin-Ecoflex<sup>TM</sup> thermoplastic blends were run in triplicate. Approximately 15 mg of each dried sample was loaded onto a platinum pan and heated to 105 °C, isothermally held for 10 minutes to remove residual moisture and then heated to 600 °C at 10 °C/min. Due to the initial annealing and isothermal hold, 100 wt% was offset at 105 °C and 5 wt% loss was then determined. For the lignin powders, the presented data in *section 4.1* Table 13 are averages of five samples and the error bars in Figures 26, 34 and 40 represent plus or minus the standard deviation of the five individual samples. The coefficient of variation for the lignin powder TGA analysis ranged from 0.12-7.2% showing good reproducibility. For the lignin-Ecoflex<sup>TM</sup> thermoplastic blends, the presented data in *section 4.2.4.2* Table 21 are averages of 3 samples and the coefficient of variation for analysis ranged from 0.56 -2.4% showing good reproducibility.

### 3.12 Fourier – transform infrared spectroscopy (FT-IR)

The IR spectra were collected and the functional groups of lignin powders and lignin-Ecoflex thermoplastic blends were analyzed using an Infrared Spectrum One Spectrometer and accompanying software from Perkin Elmer, USA. To ensure all moisture was removed prior to testing, all samples were kept in a 40°C model 280A Isotemp vacuum oven for 24 hours.

Diamond lens attenuated total reflectance (ATR) was used and powders were compressed, and plastics were shaved into appropriately thick squares because ATR relies on intimate contact between sample surface and crystal. The resolution was  $4\text{ cm}^{-1}$  with 32 scans and a frequency region from 600 to  $4000\text{ cm}^{-1}$ . Baseline corrections were made, and all lignin powders were normalized with respect to the peak height at  $1510\text{ cm}^{-1}$ , while Ecoflex<sup>TM</sup>-lignin blend spectra were normalized with respect to the peak height at  $873\text{ cm}^{-1}$  which correspond to aryl ring stretching (former) and out of plane bending vibrations of the phenylene ring (latter).<sup>200,201</sup>

### **3.13 Gel permeation chromatography (GPC) analysis**

#### **3.13.1 Sample preparation**

All lignin powder samples were kept in a  $40^{\circ}\text{C}$  model 280A Isotemp vacuum oven for 24 hours to ensure all moisture was removed prior to testing. 10 mg of each powder were dissolved in 1 mL DMSO/LiBr (0.5% wt.) solvent at room temperature for 48 hours. The lignin solution was transferred to vials and filtered through  $0.45\text{ }\mu\text{m}$  polytetrafluoroethylene (PTFE) syringe filters.

#### **3.13.2 Sample analysis**

The absolute molar mass of the lignin powders were then determined using a GPC system (Agilent 1260 ISO pump, US) combined with multiple detectors. Specifically,  $100\text{ }\mu\text{L}$  of lignin solution was injected into the system and separated by two columns including PolarGel M (1-500 kDa) and PolarGel L (0.1-60 kDa) with eluting solvent DMSO/LiBr at  $0.5\text{ mL/min}$  flow rate and  $35^{\circ}\text{C}$ . The fractionated samples were analyzed by a multi-angle light scattering detector (MALS, DAWN HELEOS-II, Wyatt, US) and a refractive index detector ( $785\text{ nm}$ , dRI, Optilab T-rex, Wyatt, US). The MALS detector was preinstalled with  $10\text{ nm}$  bandwidth on the even numbered detectors to remove the fluorescence signal of lignin. The wavelength of these detectors was  $784$

nm. Specific refractive index increment ( $dn/dc$ ) for different lignin powders were determined using the on-line method based on RI traces.<sup>167,202,203</sup> The Astra 6.1 were used to collect the signal and analyze the molar mass data. Light scattering applied in absolute molecular weight characterization has an advantage in remedying potential errors resulting from calibration which typically uses poly(styrene sulfonate) (PSS) or polystyrene (PS). There is no size exclusion chromatography standard available for lignin, so PS or PSS is often used leading to a significant underestimation of lignin molar mass values because the structures are so different. Based on experimental methods molecular weight from light scattering analysis are generally degrees of order higher than conventional GPC calibration results but are far more accurate.<sup>202,203</sup> In the case of the acetone insoluble fraction, only the soluble portions could be analyzed.

### **3.14 Scanning electron microscopy (SEM)**

The surface morphologies of some cross-sectional areas of the lignin-Ecoflex<sup>TM</sup> thermoplastic blends were obtained using a Hitachi S4700 field-emission scanning electron microscope at an accelerating voltage of 5 kV. The lignin-Ecoflex<sup>TM</sup> blends were frozen in liquid nitrogen for 10 minutes and fractured with a clean razor blade. The fractured samples of post-tensile test dog bone samples were mounted on SEM stub vertically and attached onto sample holders with carbon tape and sputter coated with gold (Au) prior to imaging.

## **Chapter 4: Results and discussion**

### **4.1 Characterization of technical lignin powders for thermoplastic blends**

#### **4.1.1 Background**

The objective of this research is to understand the role that fractionation and modification of softwood kraft Lignoforce<sup>TM</sup> lignin plays in thermoplastic blends with the bio-compostable polymer Ecoflex<sup>TM</sup>. Ecoflex<sup>TM</sup> has similar mechanical properties to LDPE but is structurally different being a mixed polyester that may be miscible with an esterified lignin. Through detailed characterization and analysis, conclusions will be drawn about the impact of functional group distribution, chemical structure, molecular weight distribution, and thermal properties of the various technical lignin powders and how they affect the material and mechanical properties of the subsequent lignin-Ecoflex<sup>TM</sup> thermoplastic blends. Extensive research, as reviewed in *Section 2.3 and 2.4*, has shown that producing lignin powders of uniform functionality will improve miscibility in a blend system but a simple and efficient green chemistry process to carry out the task has yet to be established. The current work uses a green and potentially scalable approach to address this issue.

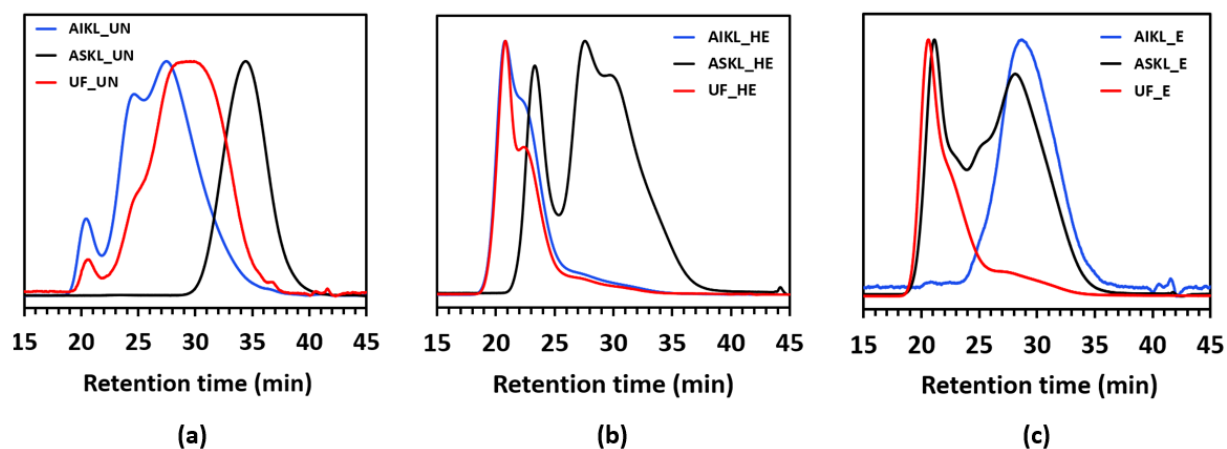
#### **4.1.2 Acetone fractionation of grade A Lignoforce<sup>TM</sup> softwood kraft lignin**

During the delignification process native ether linkages are cleaved resulting in technical kraft lignins that are heterogenous thus making renewably sourced lignin uncompetitive with non-renewable petroleum-based counterparts in commodity and engineering materials. One way to overcome the issue of heterogeneity is by performing a simple acetone fractionation which separates soluble (ASKL) from acetone insoluble (AIKL) portions of lignin. As Jiang et al demonstrated, a single step fractionation process will reduce operating and capital cost in a scale-



up event avoiding complex solvent recovery equipment thus making biorefinery conversion a viable option.<sup>109</sup>

After washing and drying the as received Lignoforce™ grade A softwood kraft lignin a single step acetone fractionation was performed. In this process, acetone insoluble lignin was separated across a filter. The AIKL fraction formed a solid filter cake with no tacky or syrup like substance which was the first indication of a successful liquid/solid separation. The yield for the acetone fractionation was 61% ASKL/39% AIKL and this distribution is a result of how the wood was processed during the delignification stage and the intensity of the cooking conditions. For the former, gel permeation chromatography was utilized to determine the molecular weight distribution of the unfractionated (UF), ASKL, and AIKL portions of lignin (Figure 24).



**Figure 24 GPC traces of unfractionated (UF), acetone soluble (ASKL), and acetone insoluble (AIKL) lignin fractions for unmodified (UN) (a), hydroxyethyl ether (HE) (b), and esterified (E) (c) lignin powders**

The unfractionated portion contains multiple peaks which indicated a mixture of lignin with differing molar masses. Further, both the UF and AIKL present a clear indication of bimodal or trimodal distributions, a result of potentially various sized lignins or previously reported self-aggregation due to strong intermolecular bonding. At high retention times, all the lignin types contained multiple small shoulders as well. The ASKL trace in Figure 24a presents a narrower distribution and shift to the right indicating a lower PDI and molecular weight while the AIKL trace widens and shifts to the left. The significant difference between the two fractions and their deviation from the unfractionated trace is a good indication the acetone fractionation was successful. The GPC traces in Figure 24 were quantified and presented in Table 13. The ASKL samples show decreased  $M_w$ ,  $M_n$ , and PDI values relative to the unfractionated samples. The AIKL samples show increased  $M_w$ ,  $M_n$ , and PDI values which likely still contain some low molecular weight (LMW) fragments as seen in Figure 24. One likely explanation for AIKL having a higher  $M_w$  than UF was that the high molecular weight samples were concentrated in this fraction, but lignin aggregation in solvents may also cause an overestimation of weight and larger polymers.

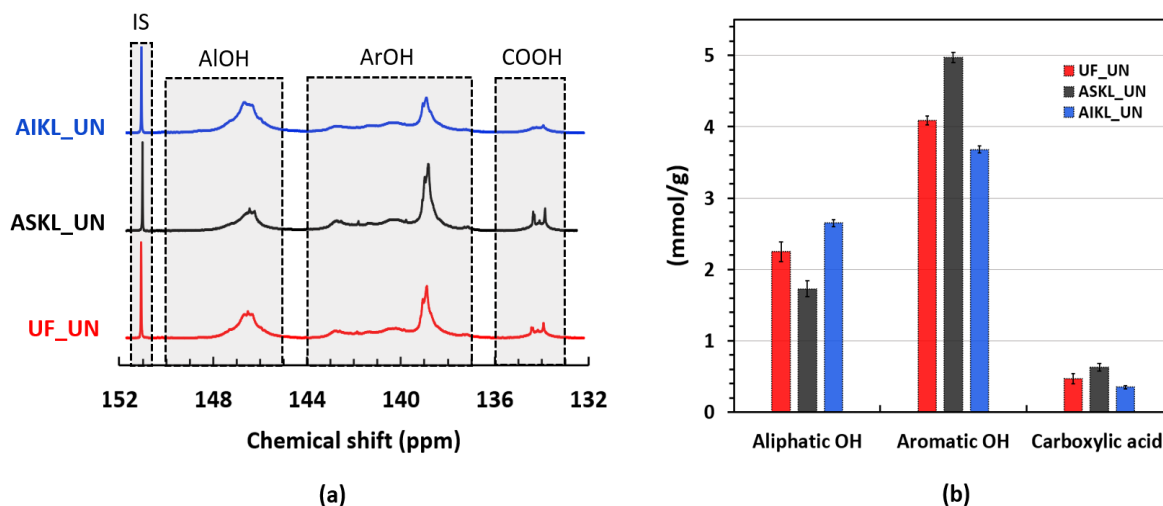
Table 13 is the quantitative account of the chemical and thermal properties for all of the lignin powders. The  $M_w$ ,  $M_n$ , and PDI were analyzed and calculated using absolute GPC techniques, while quantitative  $^{31}\text{P}$  NMR spectroscopy was used to analyze functional groups. Thermal properties such as  $T_g$ , temperature at 5 wt% weight loss ( $T_{D5\%}$ ), derivative weight peak temperature ( $T_{\text{max}}$ ) and residual wt% at 600 °C (char yield) were determined using DSC and TGA.

**Table 13 Molecular weight (GPC), functional group content (<sup>31</sup>P NMR), and thermal properties (DSC and TGA) for unfractionated (UF), acetone soluble (ASKL), acetone insoluble (AIKL), unmodified (UN), hydroxyethyl ether (HE), and esterified (E), lignin powders**

Lignin	Mw (kDa)	Mn (kDa)	PDI	ArOH (mmol/g)	AlOH (mmol/g)	ArOH/ AlOH	COOH (mmol/g)	T <sub>g</sub> (°C)	T <sub>D5%</sub> (°C)	T <sub>max</sub> (°C)	wt% at 600 °C
UF_UN <sup>b</sup>	18	4.9	3.7	4.09	2.25	1.8	0.46	162.33 ± 0.59	244	382	41.5
ASKL_UN <sup>b</sup>	2.1	0.91	2.3	4.97	1.73	2.9	0.63	125.06 ± 2.7	242	390	39.6
AIKL_UN <sup>a</sup>	68	48	1.4	3.68	2.65	1.4	0.35	206.74 ± 1.8	252	381	43.3
UF_HE <sup>b</sup>	497	26	19	trace	4.17	\	trace	121.10 ± 2.5	247	374	38.4
ASKL_HE <sup>b</sup>	50	6.9	7.2	trace	4.12	\	trace	104.53 ± 2.9	245	384	36.5
AIKL_HE <sup>a</sup>	934	190	4.9	0.45	3.50	\	0.02	169.39 ± 9.6	258	368	40.9
UF_E <sup>b</sup>	730	55	13	0.03	0.01	\	0.05	58.7 ± 3.1	280	395	33.4
ASKL_E <sup>b</sup>	130	33	3.9	0.01	0.02	\	0.01	48.4 ± 2.7	275	393	32.6
AIKL_E <sup>a</sup>	273	184	1.5	0.09	0.08	\	0.03	105.97 ± 10.2	285	385	36.2

Concerning M<sub>w</sub>, M<sub>n</sub>, and PDI: <sup>a</sup> only soluble parts were analyzed (1/3 parts dissolved) <sup>b</sup> greater than 2/3 parts dissolved

A yield with a higher amount of soluble fragmented LMW moieties could mean there was more degradation of native lignin bonds in this fraction as the formation of new phenolic hydroxyl groups occurs during the kraft pulping process. A detailed quantitative  $^{31}\text{P}$  NMR analysis was performed using the well-established protocol put forth by Argyropoulos et al. and results were on par with literature.<sup>194,204,205</sup> Figure 25 shows the  $^{31}\text{P}$  NMR spectra and the functional group content for the unmodified lignin samples.



**Figure 25**  $^{31}\text{P}$  NMR spectra for unfractionated, acetone soluble, and acetone insoluble unmodified (UF\_UN, ASKL\_UN, AIKL\_UN) lignin powders (a) and accompanying quantitative functional group content (b)

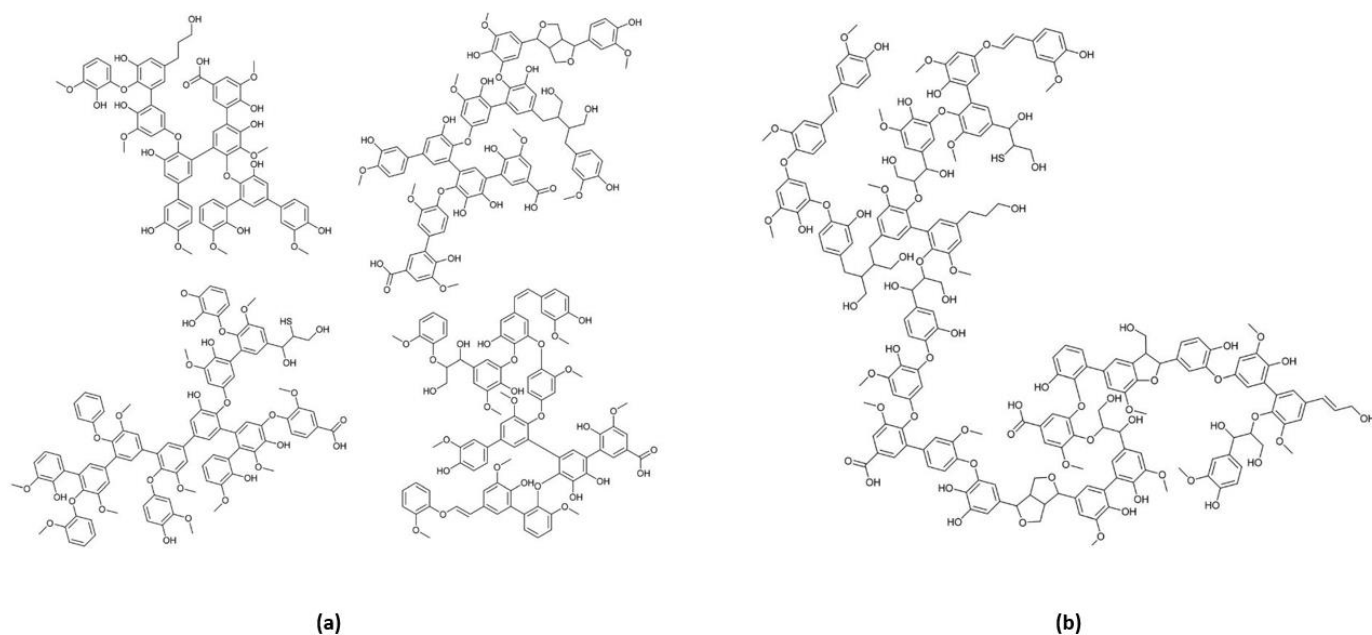
ASKL had more total aromatic hydroxyl groups (4.97 mmol/g) and carboxylic acid groups (0.63 mmol/g) and less aliphatic hydroxyl groups (1.73 mmol/g) than AIKL which had a total aromatic hydroxyl content of 3.68 mmol/g, a carboxylic acid content of 0.35 mmol/g, and an aliphatic hydroxyl content of 2.65 mmol/g. The unfractionated portion had values fall between the two for the phenolic, carboxylic acid, and aliphatic hydroxyl groups content, (4.09/0.47/2.25 mmol/g). It is important to note that ASKL has the greatest amount of C5-condensed aromatic hydroxyl groups (2.58 mmol/g) which are calculated using the chemical

shift from 140-145 ppm compared to AIKL (1.59 mmol/g) and UF (2.04 mmol/g). A higher amount of ArOH and COOH groups and a lower amount of AIOH groups is characteristic of ASKL which yielded in higher amounts. The opposite is true for AIKL which has a lower free phenolic content and a higher AIOH content compared to the acetone soluble and unfractionated samples. These results agree with literature that describes the acetone soluble fraction with a lack of native side chains, comprised of low molecular weight condensed polyphenols generated by fragmentation during pulping. The acetone insoluble fraction has more aryl-alkyl ether linkages with some typical native side chains intact and is comprised of medium to high molecular weight polymeric traces.<sup>203,204,206</sup>

For example, lignin prepared by Crestini et al. from softwood chips pulped using the kraft process was fractionated using acetone.<sup>206</sup> The acetone fractionation produced a yield of 70% acetone soluble and 30% acetone insoluble softwood kraft lignin.<sup>206</sup> <sup>31</sup>P NMR analysis revealed their ASKL sample contained 5.2 mmol/g total aromatic hydroxyl groups, 0.6 mmol/g carboxylic acid groups, and 2.4 mmol/g aliphatic hydroxyl groups while their AIKL sample contained 3.5 mmol/g total aromatic hydroxyl groups, 0.5 mmol/g carboxylic acid groups, and 3.0 mmol/g aliphatic hydroxyl groups.<sup>206</sup> Sadeghifar et al. performed an acetone fractionation on Lignoboost<sup>TM</sup> softwood kraft lignin and found similar results.<sup>189</sup> The acetone fractionation produced a yield of 65% acetone soluble and 35% acetone insoluble softwood kraft lignin.<sup>189</sup> <sup>31</sup>P NMR analysis revealed their ASKL sample contained 5.7 mmol/g total aromatic hydroxyl groups, 0.57 mmol/g carboxylic acid groups, and 1.63 mmol/g aliphatic hydroxyl groups while their AIKL sample contained 3.56 mmol/g total aromatic hydroxyl groups, 0.35 mmol/g carboxylic acid groups, and 2.74 mmol/g aliphatic hydroxyl groups.<sup>189</sup> Jiang et al. performed an acetone fractionation on Biochoice softwood kraft lignin and found similar results confirming the

conclusions drawn above.<sup>109</sup> <sup>31</sup>P NMR analysis revealed their ASKL sample contained 4.83 mmol/g total aromatic hydroxyl groups, 0.74 mmol/g carboxylic acid groups, and 1.51 mmol/g aliphatic hydroxyl groups while their AIKL sample contained 3.86 mmol/g total aromatic hydroxyl groups, 0.48 mmol/g carboxylic acid groups, and 2.83 mmol/g aliphatic hydroxyl groups

Further, detailed <sup>13</sup>C-<sup>1</sup>H heterosingle quantum coherence NMR data was collected and analyzed within our lab by Karaaslan et al. for a similar Lignoforce<sup>TM</sup> SWKL from BC research, Inc. and it showed that ASKL possessed more  $\beta$ -1 and  $\beta$ -5 stilbene structures that form in alkali solution due to condensation reactions during kraft pulping.<sup>205</sup> This helps justify the presented data (Table 13), confirms the structural schematics in Figure 26, and explains why ASKL is more condensed than AIKL which contains more methoxy groups at the C<sub>3</sub> and C<sub>5</sub> positions and more intact aliphatic side chains with native links like  $\beta$ -O-4 and  $\beta$ - $\beta$ . These are important findings because the glass transition temperature is a relevant processing parameter for amorphous polymers and is a function of both molecular weight and hydroxyl group content which both greatly impact chain mobility.

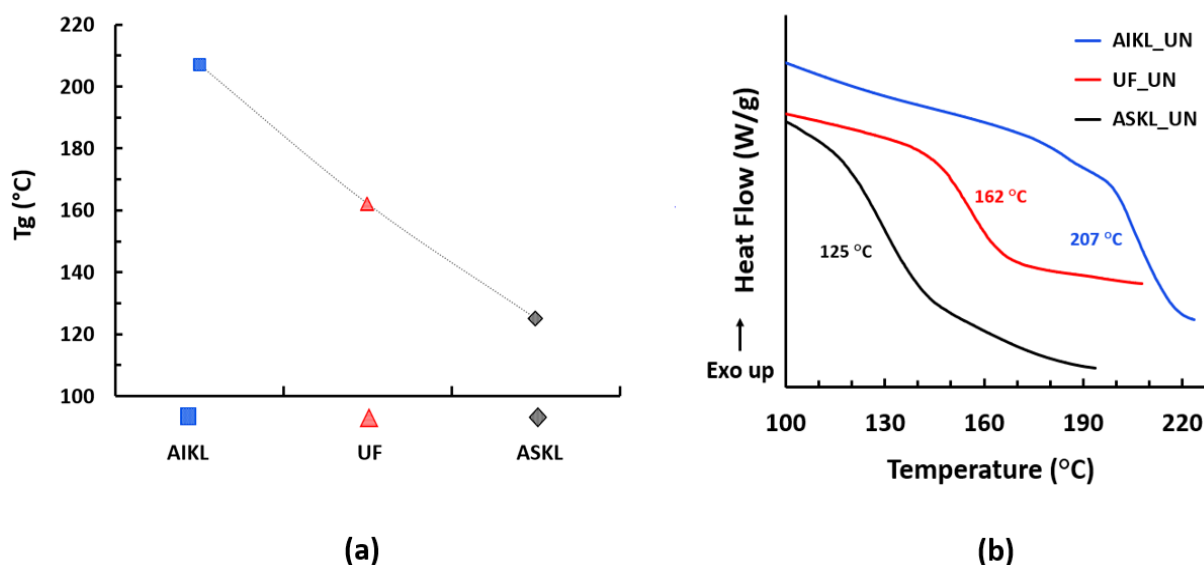


**Figure 26** A schematic of the chemical structure of acetone soluble softwood kraft lignin (a) and acetone insoluble softwood kraft lignin (b) shows a difference in fragmented portions of pulped moieties, hydroxyl content and molecular weight Reprinted with permission from ref<sup>205</sup> Copyright 2017 Royal Society of Chemistry

#### 4.1.2.1 $T_g$ of lignin as a function of molecular weight and chemical functionality

The glass transition temperature can be manipulated through fractionation and modification which is helpful in developing lignin building blocks that are stable in melt. Figure 27 plots the  $T_g$  values for the unmodified fractionated and unfractionated lignin powders. The dashed line presented is to guide the reader's eye. Standard deviations are presented in Table 13 and were less than 3 °C. The  $T_g$  for the unfractionated lignin is 162 °C, increased to 207 °C for AIKL and decreased to 125 °C for ASKL. There was a 82 °C temperature difference between the two fractions. The ASKL fraction had more condensed C<sub>5</sub> aromatics which can crosslink and restrict chain movement, which should raise the  $T_g$ . However, because the lignin is more fragmented there is less intermolecular hydrogen bonding with reduced aliphatic hydroxyl groups and the shorter chain lengths have greater mobility at lower temperatures which

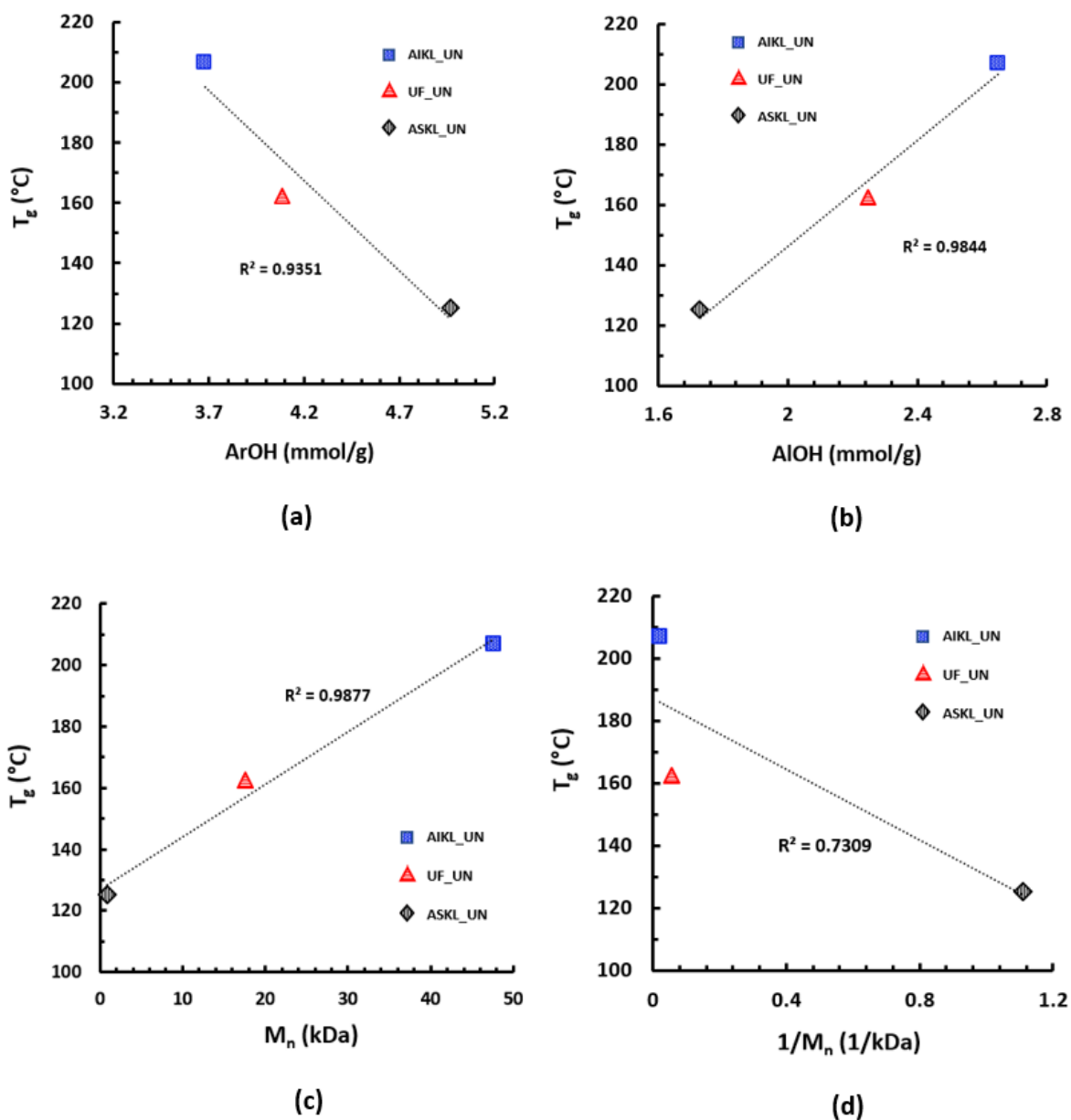
significantly decreased the glass transition temperature. The same thought process would assume that AIKL with its more flexible  $\beta$ -O-4 linkages and greater methoxy group content would increase free volume thus decreasing the  $T_g$ . However, the long chains create more entanglement and the aliphatic hydroxyl groups create strong intermolecular hydrogen bonding which ultimately reduces chain mobility and raises the glass transition temperature of the fraction. The Flory-Stockmayer polymer view states that larger chains need a smaller number of cross-linking events to create a network structure which helps justify why the AIKL fraction has the highest  $T_g$ .



**Figure 27** The glass transition temperatures for unmodified (UN) acetone insoluble (AIKL), unmodified unfractionated (UF), and unmodified acetone soluble (ASKL) lignin powders (a) and the correlating DSC curves (b)



The Flory-Fox relationship relates number average molecular weight to the glass transition temperature stating that as  $M_n$  increases so does  $T_g$ . This is an important concept as it proves that  $T_g$  shifts are a result of  $M_n$  differences which depend on the chemical structure. Concerning lignin, this relates to the functional group content of the lignin fraction. Figure 28a and Figure 28b show a linear correlation between aromatic and aliphatic hydroxyl group content and the glass transition temperature of the unmodified fractionated and unfractionated portions of the lignin. There was a strong linear relationship with a  $R^2$  value above 0.9 showing a decrease in  $T_g$  with an increase in ArOH functional groups (ASKL). This result may be more telling of the generation of phenolic groups in the lignin from chain scission related to a change in  $M_w$ , more than the impact of a specific chemical group. Moreover, there was a strong linear regression with a  $R^2$  value above 0.95 showing an increase in  $T_g$  with an increase in AlOH function groups (AIKL). Primary aliphatic groups can undergo strong hydrogen bonding and are not sterically hindered by methoxy groups on the lignin, when compared to phenolics. This result agrees with a previous investigation where model lignin compounds were used to study hydrogen bonding in Westvaco Corp. softwood kraft lignin.<sup>207</sup> Figure 28c shows  $T_g$  increasing as a function of  $M_n$  with a good linear correlation  $R^2$  value above 0.8 and Figure 28d is the classic Flory-Fox relationship which further justifies the relationship between molar mass distribution and  $T_g$  values. Figure 28 confirms glass transition temperatures are a function of both molecular weight and the hydrogen bonding effects exerted by hydroxyl functional groups.



**Figure 28** Linear relationships between aromatic hydroxyl functional groups ArOH and glass transition temperature  $T_g$  (a) aliphatic hydroxyl functional groups AlOH and  $T_g$  (b) number average molecular weight  $M_n$  and  $T_g$  (c) and the classic Flory-Fox relationship (d) for unfractionated unmodified (UF\_UN), acetone soluble unmodified (ASKL\_UN), and acetone insoluble unmodified (AIKL\_UN) lignin powders

#### 4.1.2.2 Thermal degradation of fractionated moieties

Thermogravimetric analysis was used to analyze the 5 wt% degradation temperature ( $T_{D5\%}$ ) of the lignin powders (offset to 105 °C), the maximum derivative temperature ( $T_{max}$ ) and the char yield or remaining wt% lignin powder at 600 °C. This information was tabulated in Table 13 and displayed in Figure 29 which highlights the percent weight loss data, the derivative weight loss as a function of temperature, and the graphical reporting of these average values for the different lignin samples. In Figure 29c and Figure 29e, the decomposition temperature at 5% weight loss and the char yield were higher for AIKL, but also had a smaller peak degradation rate profile as compared to ASKL and UF. These suggest a small difference in thermal stability for AIKL, but as evident in Figure 29a there is not significant differences based on fractionation. The acetone soluble portion, which has more free phenolic groups that are known to have a lower thermal stability than aliphatic counterparts had the lowest  $T_{D5\%}$  and char yield which agrees with literature.<sup>121,205</sup> The  $\alpha$  and  $\beta$  aryl-alkyl ether linkages are cleaved between 150-300 °C which do not create significant volatile products as shown by the TGA curves in Figure 29a. In Figure 29b the shoulders between 250-300 °C represent degradation of free ArOH groups and aliphatic side chains start cleaving off the aromatic rings at ~ 300 °C.<sup>205,208</sup> Overall, the thermal decomposition behavior of lignin was generally governed by various oxygen based functional groups with differing thermal stabilities that break down over a broad range of temperatures.

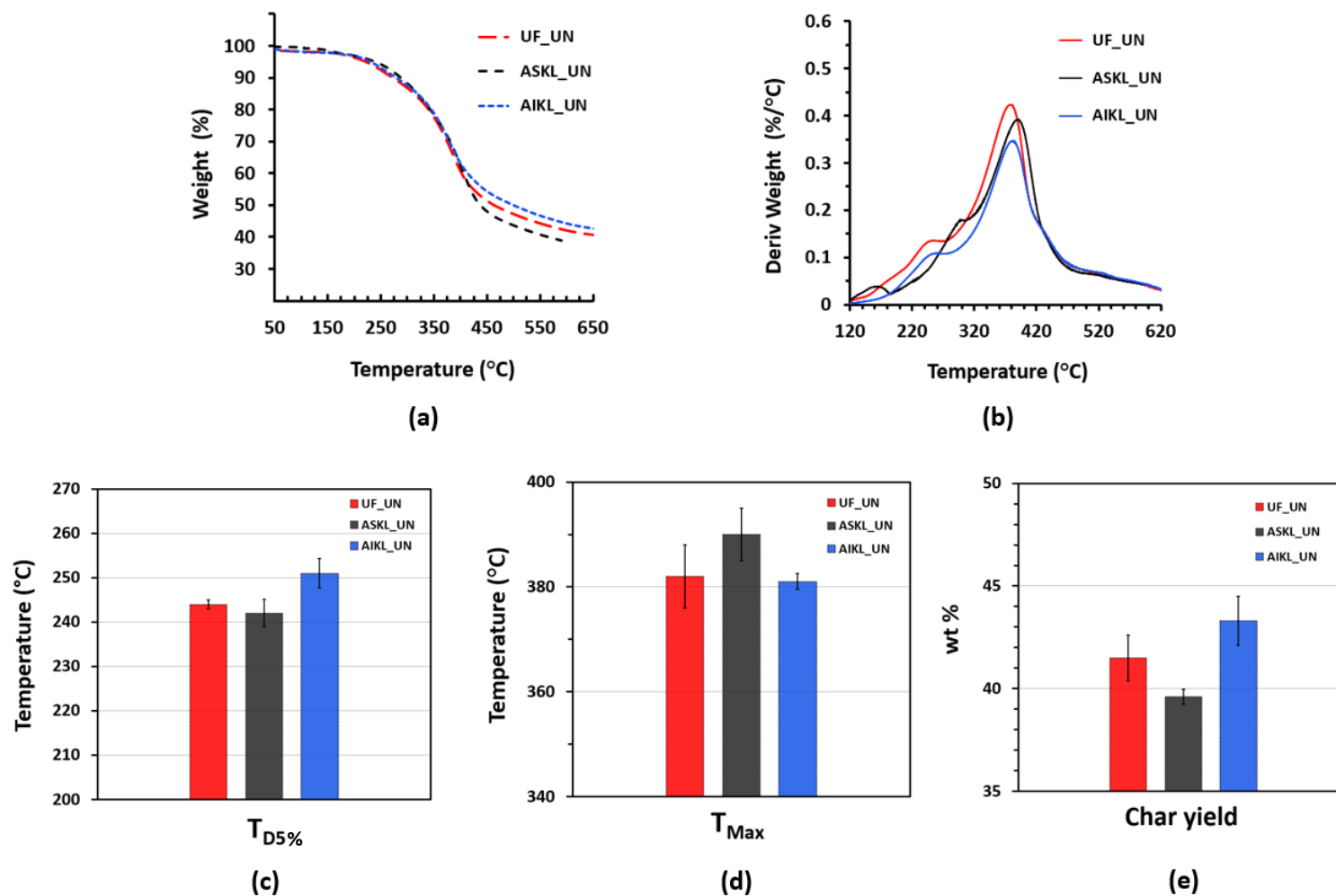
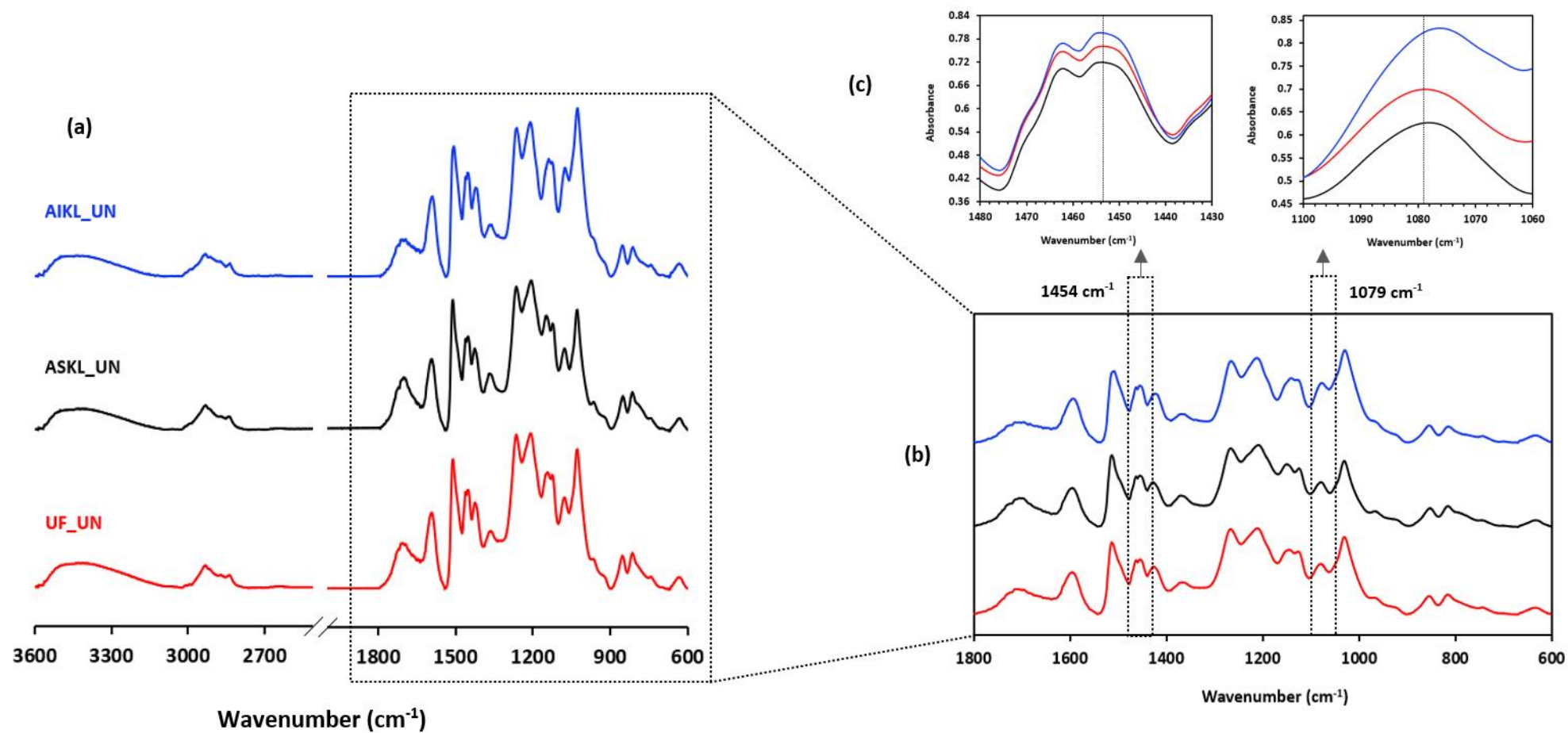


Figure 29 TGA analysis for unfractionated unmodified (UF\_UN), acetone soluble unmodified (ASKL\_UN), and acetone insoluble unmodified (AIKL\_UN) lignin powders weight % loss curves (a) maximum derivative weight % as a function of temperature curves (b) average values with standard deviation error bars for  $T_{D5\%}$  (c)  $T_{max}$  (d) and char yield (e)

#### 4.1.2.3 FT-IR analysis of fractionated and unfractionated lignin powders

Chemical structure was further investigated using FT-IR spectroscopy. At first glance the unmodified UF, ASKL and AIKL spectra look similar as seen in Figure 30. As reported in literature, signature peaks of the full lignin spectra contain signals at approximately 1260 and 1220  $\text{cm}^{-1}$  representing typical softwood G monomer units and C = O stretching between 1700-1800  $\text{cm}^{-1}$ .<sup>182,201,209</sup> The broad peak at 3400  $\text{cm}^{-1}$  is representative of the -OH stretching of aliphatic and aromatic functional groups alongside H-bonding.<sup>182,201,209</sup> The region does not reveal changes in the aliphatic and aromatic hydroxyl content as found in the NMR spectra. The peaks at 2933 and 2839  $\text{cm}^{-1}$  are typical of the C-H stretching seen in methyl and methylene groups.<sup>182,201,209</sup> The signals around 1600, 1510 and 1425  $\text{cm}^{-1}$  are related to skeletal vibrations of the aromatic rings and the spectra are normalized to 1510  $\text{cm}^{-1}$  so absorbance intensities can be compared.<sup>182,201,209</sup> Figure 30b highlights the lignin fingerprint region and a closer analysis reveals some differences in structure. Figure 30c shows a signal at 1454  $\text{cm}^{-1}$  for methoxy groups (-OCH<sub>3</sub>) where AIKL shows a higher intensity than UF and ASKL. As well, the signal at 1079  $\text{cm}^{-1}$  represents the C-O deformation of secondary alcohol and aliphatic ether groups in which AIKL shows the highest intensity. This agrees with the previous determination that AIKL contains more of these functional groups.



**Figure 30** FT-IR spectrum for unmodified unfractionated (UF\_UN), acetone soluble (ASKL\_UN), and acetone insoluble (AIKL\_UN) softwood kraft lignins (a) the lignin fingerprint region (b) and zoomed in signals at 1454  $\text{cm}^{-1}$  and 1079  $\text{cm}^{-1}$  with absorbance readings (c)

### 4.1.3 Hydroxyethyl ether modification of fractionated and unfractionated lignins

#### 4.1.3.1 Background

Carrying out an acetone fractionation is a quick, simple, and relatively inexpensive way to separate lignin by molar mass which immediately alters chemical and thermal processing parameters. However, free phenolics are polar, reactive, and known to induce thermal crosslinking within under conditions for melt processing polymers like Ecoflex<sup>TM</sup>. Because of thermal instabilities such blends are dynamic and typically incompatible so lignin must be further modified. A large portion of *Section 2.3* was dedicated to the many ways technical lignins can be modified for valorization in renewable materials. Sadeghifar et al performed a successful methylation with dimethyl carbonate to mask the aromatic hydroxyl groups in acetone fractionated lignin and blended with LDPE.<sup>189</sup> The group reported the methylation was selective for aromatic hydroxyl groups only which leaves reactive carboxylic acid groups behind and closes the door for further modification. Glasser et al. successfully blended oxypropylated lignin with Ecoflex<sup>TM</sup> and commercialized the product into carrier bags and other moldable plastics but used propylene oxide a known carcinogenic to synthesize the reaction.<sup>157</sup>

In this research ethylene carbonate (EC), a safer alternative was used to hydroxyalkylate the aromatic hydroxyl and carboxylic acid functional groups in the unfractionated, acetone soluble, and acetone insoluble lignin powders. In our lab Liu et al. studied the ethylene carbonate/lignin reaction in detail and optimized the reaction temperature to 120 °C with EC acting as both solvent and reagent and used sodium carbonate (Na<sub>2</sub>CO<sub>3</sub>) as the basic catalyst to deprotonate the OH groups.<sup>167</sup> This project aims to study how etherified lignin powders compare to esterified and unmodified lignin powders in a thermoplastic blend and so it was decided to carry out the HE reaction, wash the product with distilled water until a neutral pH was reached,

freeze dry, vacuum oven dry, and characterize with DSC, TGA and  $^{31}\text{P}$ NMR before performing the esterification with propionic acid.

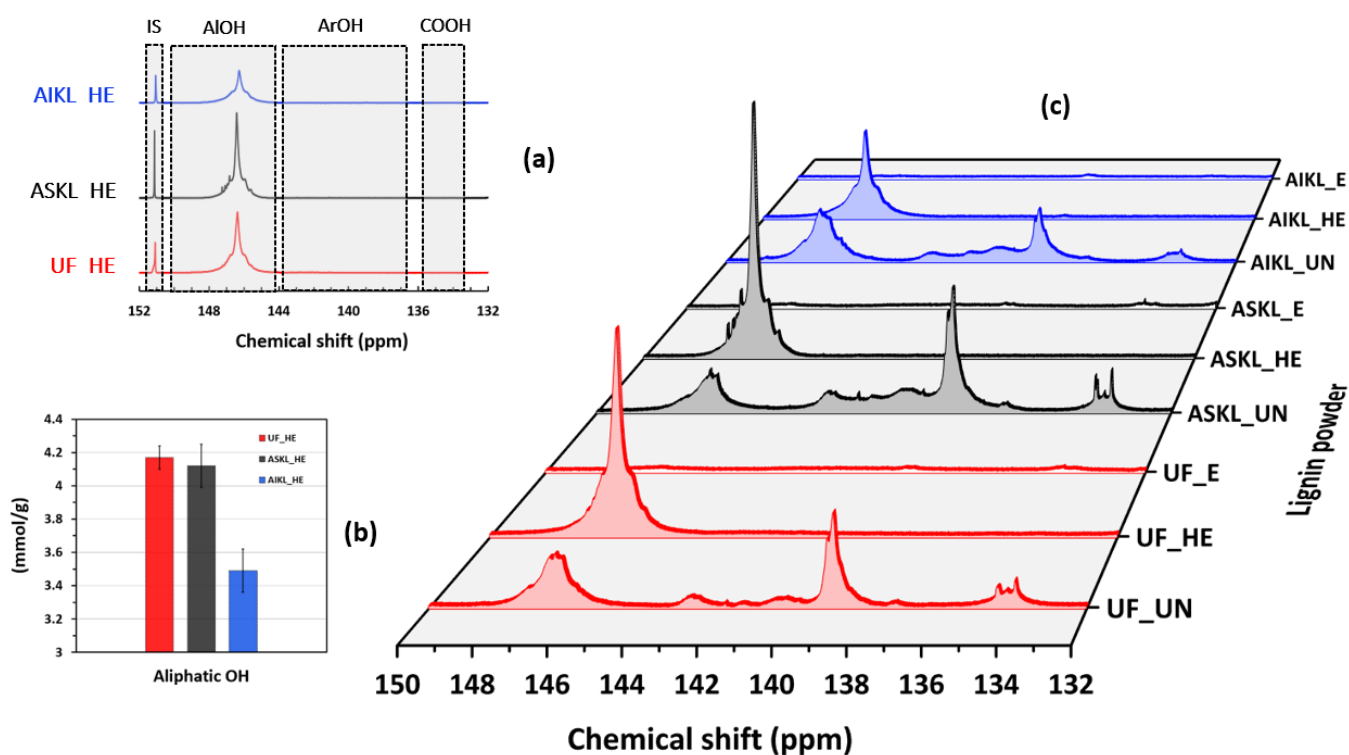
#### **4.1.3.2 Molecular weight and chemical functionality of HE lignin fractions**

As listed in Table 13, the reaction with ethylene carbonate raised the  $M_w$ ,  $M_n$ , and PDI for UF, ASKL, and AIKL powders in comparison to their unmodified counterpart. Figure 24b shows the molecular weight traces for the etherified lignin fractions (UF\_HE, ASKL\_HE, and AIKL\_HE). According to the quantitative data the acetone soluble portion had lower  $M_w$  and  $M_n$  values compared to UF\_HE and AIKL\_HE. However, it is AIKL\_HE which presented with the lowest PDI which is likely due to only the soluble portions being analyzed. Duval et al. reported similar crosslinking during ethylene carbonate modification of lignin at longer reaction times which resulted in skewed size exclusion chromatography results.<sup>166</sup> Liu et al. who analyzed a similar acetone soluble hydroxyethyl ether Indulin AT softwood kraft lignin (ASKL\_HE) used GPC data analysis relative to the PSS standard and found a 1,177% increase in  $M_w$ , an 85% increase in  $M_n$ , and a 558% increase in PDI after completing the HE reaction.<sup>167</sup> The quantitative values in Table 13 after the HE reaction of Lignoforce<sup>TM</sup> ASKL in this research indicated a 2,281% increase in  $M_w$ , a 658% increase in  $M_n$ , and a 213% increase in PDI. This increase in  $M_n$  corroborates with the GPC trace in Figure 24b for ASKL\_HE which showed a bimodal distribution after the reaction with ethylene carbonate.

Liu's work established that at a lower reaction temperature (100 °C) there are less side reactions and a narrower PDI is obtained but this led to an incomplete conversion of aromatic hydroxyl groups to primary alcohols.<sup>167</sup> At the experimental reaction temperature of 120 °C there will be structural changes and a decrease in overall OH content but an acceptable conversion (90-94%) of ArOH and COOH to AlOH.<sup>167</sup>



Figure 31 contains a detailed plot of  $^{31}\text{P}$  NMR spectra for the HE lignin samples. It revealed that the hydroxyalkylation reaction was successful as the signals for ArOH (144.0-137.6 ppm) and for COOH (136.0-133.6 ppm) have dissipated after the etherification. Figure 31b shows that UF and ASKL, which had a greater starting free phenolic count contain more aliphatic hydroxyl groups in g/mmol than AIKL after the HE reaction. With AIKL having more native linkages there are also less chain ends for modification, hence the AIKL will also have a lower total content of hydroxyl groups.



**Figure 31**  $^{31}\text{P}$  NMR spectra for hydroxyethyl ether unfractionated UF\_HE, acetone soluble ASKL\_HE and acetone insoluble AIKL\_HE lignin powders (a) the amount (mmol/g) of aliphatic hydroxyl groups (AIOH) present in each fraction (b) and the spectra plot for all nine lignin powders (c)

There are several explanations as to why the substitution of ALOH decreases the total OH count while increasing the molecular weight of the now modified technical lignins. The aliphatic hydroxyl groups can react with the ethylene carbonate by transesterification or polymerization thus creating carbonate linkages. As well, the basic catalyst creates an alkali environment to which free radical reactions can take place between lignin segments. The reader should refer to Figure 19 to view the many reaction mechanisms that can occur during the HE synthesis. Ultimately, the degree of condensation after modification is the main reason for an increased molecular weight and this relates to the structure of softwood lignins which have an open G-unit C<sub>5</sub> position. To develop a more complete understanding of the HE lignin structure/function relationship we utilized FT-IR analysis.

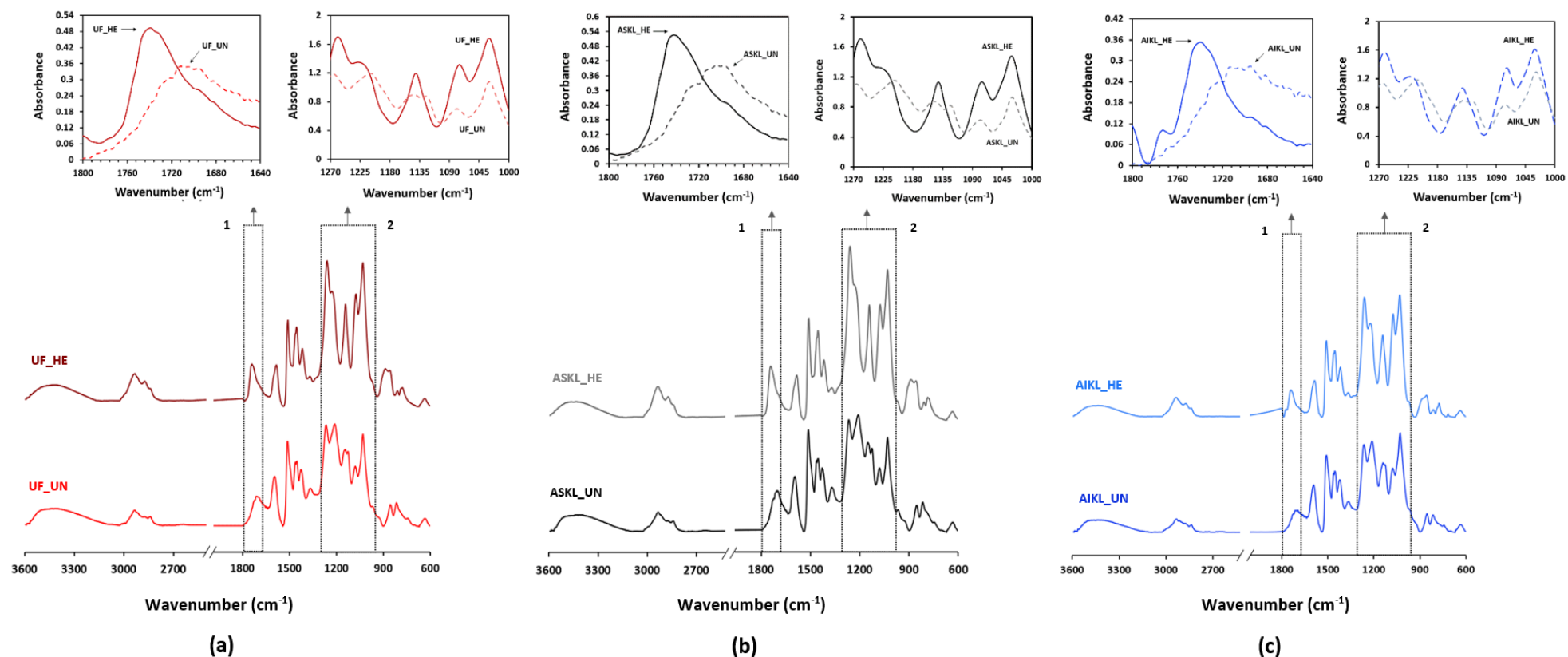
#### **4.1.3.3 FT-IR structural analysis of HE lignin powders**

The modified lignin was analyzed utilizing FT-IR in an ATR set-up and the spectra are plotted in Figure 32. For both unmodified and derivatized samples, the signal between 1720-1800 cm<sup>-1</sup> on the spectrum is the C=O stretch of ester groups, carboxyl groups, or unconjugated ketones (Figure 32). An increase in absorbance around 1740 cm<sup>-1</sup> is indicative of linear carbonate linkages which form during side reactions between either deprotonated lignin or modified HE lignin which attacked the carbonyl group of ethylene carbonate. Analysis showed such an increase for UF, ASKL and AIKL. The insets labeled 1 in Figure 32 a, b, and c show this absorbance increase is slightly greater for UF and ASKL and for all fractions the signal shifts to the left and sharpens. The AIKL sample showed a small peak at 1775 cm<sup>-1</sup> that ASKL\_UN and UF\_UN did not. Duval et al. reported this could possibly be a side reaction that led to the formation of cyclic carbonate groups as the neat ethylene carbonate FT-IR spectra presents a

peak at  $1774\text{ cm}^{-1}$ .<sup>166,210</sup> Using  $^{13}\text{C}$  NMR, Liu et al. previously reported minor carbonate linkages when compared to the hydroxyethyl content of the lignin, suggesting that most lignin samples were derivatized without a significant amount of polymerization of ethylene carbonate.<sup>191</sup> A cluster of peaks from  $1250\text{--}1270\text{ cm}^{-1}$  are assigned to aryl C-O stretching and from  $1020\text{--}1170\text{ cm}^{-1}$  to alkyl C-O stretching. A change of stretching in these regions is indicative of aryl-alkyl ether formation and is confirmation of a successful hydroxyethyl ether reaction. The insets labeled 2 in Figure 32 a, b, and c show this type of stretching for UF, ASKL, and AIKL. Lastly, the reduction in the signal for phenolic C-O around  $1200\text{ cm}^{-1}$  is further confirmation of substitution of the phenolics in the HE lignin powder.

Comparing the FT-IR data with the molar mass data confirms there were some unwanted side reactions. The ASKL\_UN distribution (Figure 24a) was narrow and unimodal while the ASKL\_HE distribution (Figure 24b) was bimodal indicating potentially different molecular weight lignin fractions were likely created during a side reaction event with ethylene carbonate. Overall, there were some unwanted side reactions but the synthesis of HE lignin was successful in creating uniform lignin derivatives consisting of nearly all primary OH groups in comparison to the starting material, which was a multi-functional network of ArOH, COOH, and aliphatic alcohols. This reaction consumed only ethylene carbonate and sodium carbonate in amounts calculated from the hydroxyl group content collected during  $^{31}\text{P}$ NMR analysis for each fraction and batch. The reaction time was controlled by  $\text{CO}_2$  off gassing in a novel real time process developed in house and no harsh acid was used to wash the product upon completion. This step meets the requirements for green chemistry and the HE lignin consisting of uniform aliphatic hydroxyl functional groups is more soluble in propionic acid and can easily be esterified. As

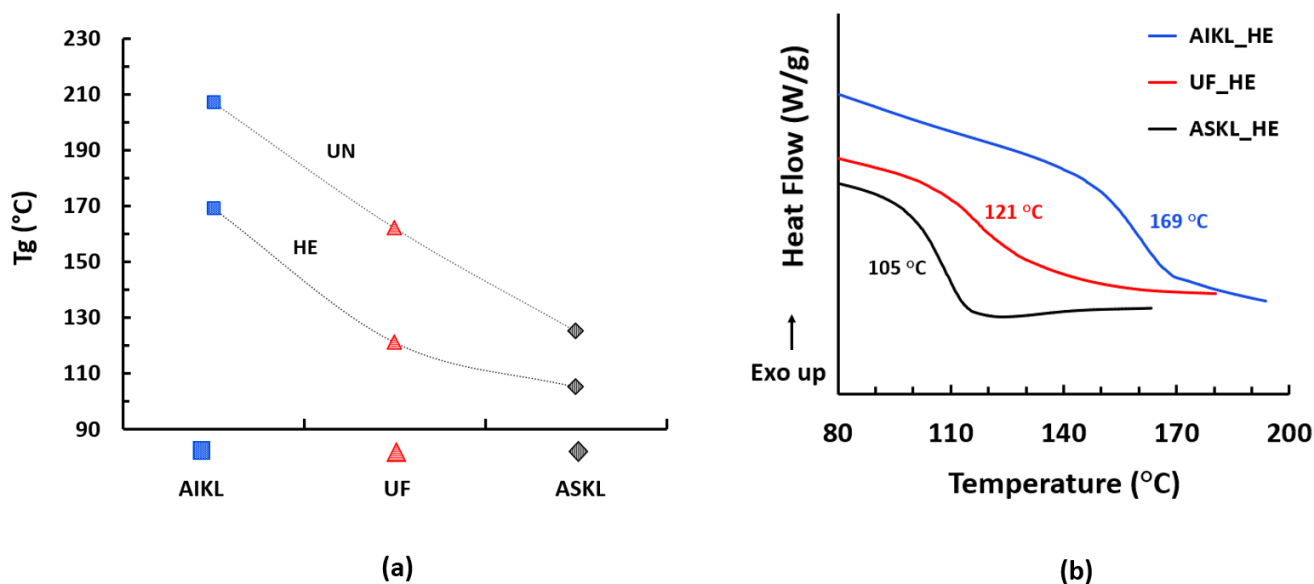
well, the unmodified lignin powders experienced some thermal property and degradation changes after the HE reaction.



**Figure 32** FT-IR spectra for unfractonated unmodified (UF\_UN) and unfractonated hydroxyethyl ether (UF\_HE) (a) acetone soluble unmodified (ASKL\_UN) and acetone soluble hydroxyethyl ether (ASKL\_HE) (b) acetone insoluble (AIKL\_UN) and acetone insoluble hydroxyethyl ether (AIKL\_HE) (c) and the carbonate linkages at 1740  $\text{cm}^{-1}$  (1) and aryl-alkyl ether formation at 1000-1270  $\text{cm}^{-1}$  (2)

#### 4.1.3.4 $T_g$ for HE lignin derivatives

The glass transition temperature for UF, ASKL, and AIKL were reduced by 41 °C, 20 °C, and 38 °C after the HE reaction (Table 13). In each case, the HE modified lignin was lower than the starting material. A combination of factors would cause the decrease in glass transition temperature due to an increase in alkyl content, an interruption of non-covalent aromatic interactions, and bulking from the ethylene groups. Figure 33a plots the  $T_g$  values for the unmodified fractionated and unfractionated lignin powders as compared to the HE fractionated and unfractionated lignin powders and Figure 33b is the accompanying HE DSC curves. The dashed lines in Figure 33a were presented only to guide the reader's eye.

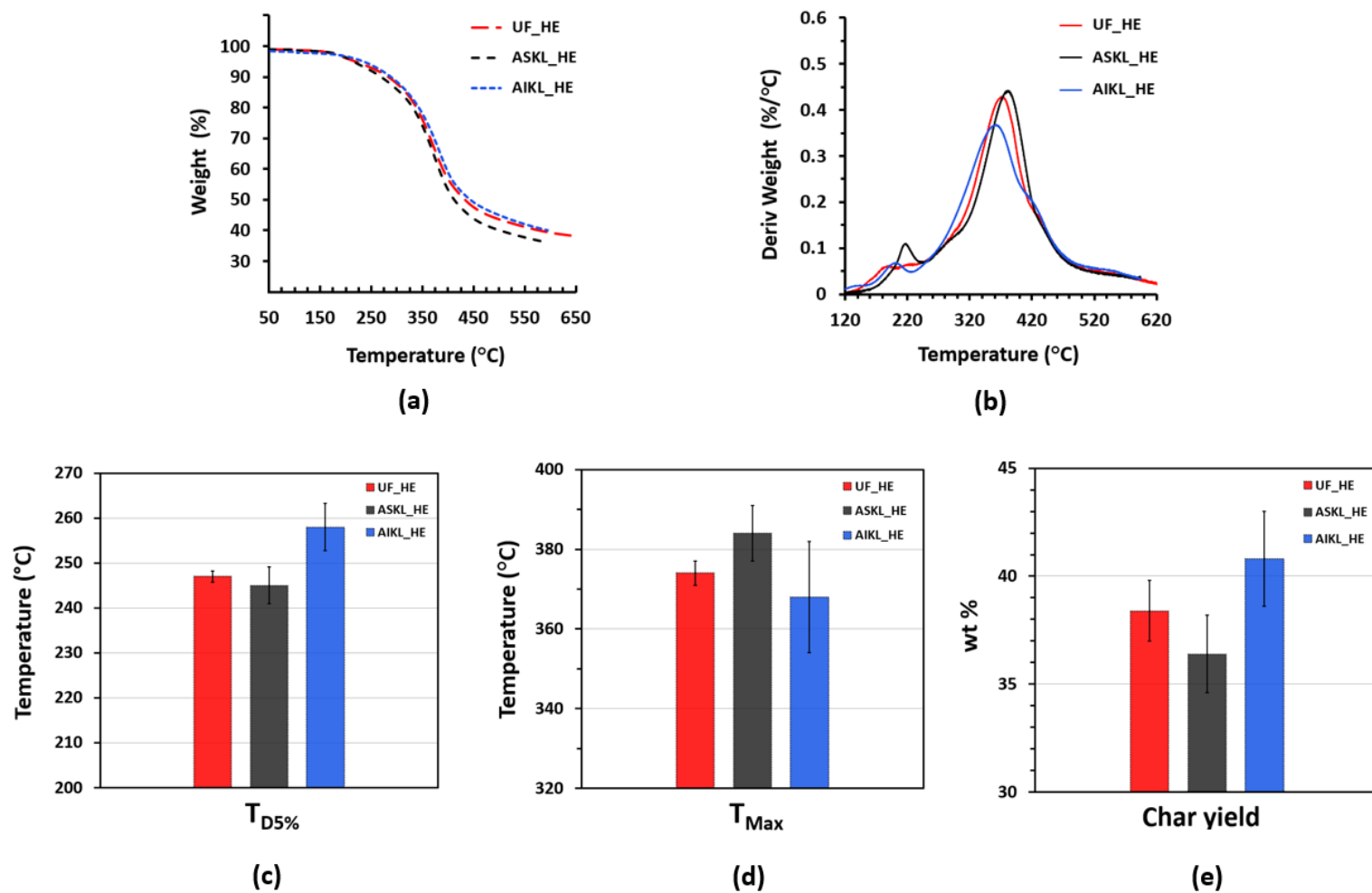


**Figure 33** The glass transition temperatures for unmodified (UN) and hydroxyethyl ether (HE), acetone insoluble (AIKL), unfractionated (UF), and acetone soluble (ASKL) lignin powders (a) and the correlating DSC curves (b)

A shift of 20 °C is greater than previously reported by Liu et al. for HE acetone soluble kraft lignin (Indulin AT) when measured by DSC, but similar using dynamic mechanical analysis in a compression torsion set-up.<sup>167</sup> For the AIKL, a 40 °C shift clearly illustrates that the hydroxyethylation impacts the packing and intermolecular interactions of this fraction.

#### **4.1.3.5 Thermal degradation for HE lignin derivatives**

Samples were tested for their thermal stabilities in a nitrogen atmosphere. There were some mild changes in thermal degradation profiles that occurred after the HE reaction (Figure 34) and all averaged values are listed in Table 13. When compared to unmodified samples, the 5% weight loss temperature increased slightly after modification for UF, ASKL, and AIKL with the latter having the highest temperature and the greatest increase in temperature after modification. The maximum derivative temperature of all samples were similar to the unmodified sample, but AIKL showed the slowest degradation rate profile (Figure 34b). Also, the shoulder related to degradation of free phenolic compounds at 275 °C was reduced as indicated in the derivative profile (Figure 34b).<sup>211</sup> AIKL had the highest char yield with 41 wt% remaining at 600 °C. Overall, the char yield for each HE lignin powder slightly decreased in comparison to its unmodified counterpart which may be the result of a compositional change and the molecular packing of the material.



**Figure 34** TGA analysis for unfractionated hydroxyethyl ether (UF\_HE), acetone soluble hydroxyethyl ether (ASKL\_HE), and acetone insoluble hydroxyethyl ether (AIKL\_HE) lignin powders weight % loss curves (a) maximum derivative weight % as a function of temperature curves (b) average values with standard deviation error bars for  $T_{D5\%}$  (c)  $T_{max}$  (d) and char yield (e)



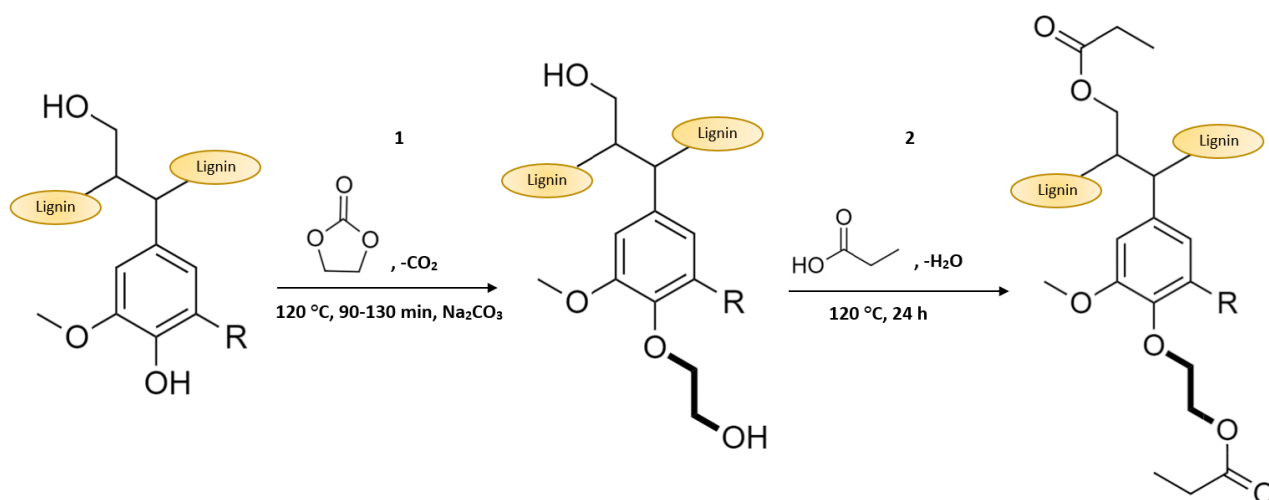
#### **4.1.4 Esterification of hydroxyethyl ether lignin powders**

##### **4.1.4.1 Background**

Modifications to lignin by esterification are anticipated to decrease lignins brittleness and increase miscibility and processability in a polymer matrix. As observed in chapter two, most esterification reactions are carried out using acyl chloride, anhydrides, and added catalyst. These chemicals are successful at modifying both aliphatic and aromatic hydroxyl groups, but they are toxic chemistries, wasteful in atom economy, and often cause separation issues in recovery which makes industrial scale-up difficult. Propionic acid was chosen for its low volatility, solubility in water, and for its ability to dissolve HE lignin. As such, propionic acid acted as both the solvent and catalyst in the reaction when used in an excess ratio of one part lignin to ten parts acid (1:10). Under these conditions, no catalyst was needed so it becomes easy to remove excess reagent upon completion. However, propionic acid is selective for aliphatic hydroxyl groups because of a difference in reactivity between aromatic and aliphatic hydroxyl groups which is why the HE reaction was necessary prior to esterification. Phenolates have a lower pKa value, meaning they are a weaker base, so it is more difficult to form the ester bond compared to aliphatic hydroxyl groups. In addition, converting the aromatic hydroxyl groups prevents condensed structures that form through quinone methide intermediates in an acidic environment.

Liu et al. showed the highest degree of substitution for esterified lignin powders were optimized at reaction conditions of 24 hours at 120 °C.<sup>153</sup> The 120 °C reaction temperature was ideal because it improved the acidity of propionic acid which subsequently offered up more free hydrogen ions to protonate the carbonyl groups. The boiling point of water is 100 °C, while the boiling point of propionic acid is 141 °C and so the reaction temperature chosen was within this temperature range. This makes it so the side product water which evaporates will move the

reaction equilibrium to the desired direction. Figure 35 shows the two part chemical reaction where step one is the etherification which makes the HE lignin powders and step two is the esterification which makes the E lignin powders for UF, ASKL, and AIKL. The esterification is likely carried out through an  $S_N2$  reaction where the aliphatic oxygen acts as a nucleophile that attacks the carbonyl carbon of the propionic acid forming a tetrahedral intermediate under acidic conditions.<sup>153</sup> After the tautomerism and a loss of water the aliphatic esters were formed.



**Figure 35** The complete chemical reaction with conditions, where step one is the etherification of lignin fractions using ethylene carbonate and step two is the esterification of the synthesized HE lignin powders using propionic acid

#### 4.1.4.2 Molecular weight and chemical functionality of esterified lignin fractions

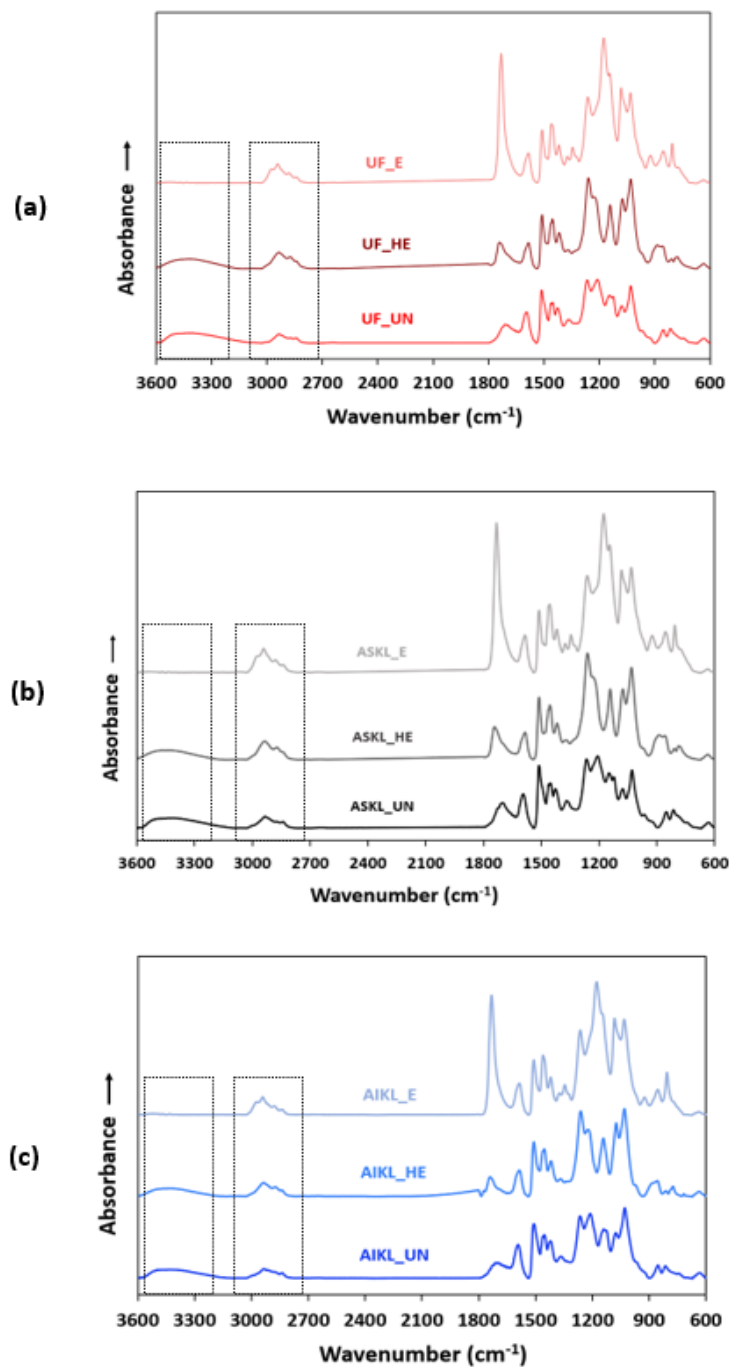
The molecular weight ( $M_w$ ) and number average molecular weight ( $M_n$ ) of both UF\_E and ASKL\_E increased in comparison to their HE and unmodified counterparts, while the PDI decreased in comparison to their HE counterparts (Table 13). This is likely because after esterification the lignin became more soluble and as a result the lignin could be better analyzed whereas the unmodified and HE lignins did not fully dissolve, and such excluded the highest molecular weight portion of the lignin from analysis. Liu et al. who also used propionic acid to

esterify unfractionated and acetone soluble HE lignin found a similar increase (2 to 50 times larger than unmodified lignin) in molecular weight for lignins modified with organic carbonates.<sup>153,191</sup> AIKL\_E showed a decrease in  $M_w$ ,  $M_n$  and PDI which is the result of only the soluble portions being analyzed (Table 13). The GPC trace in Figure 24c showed a narrower unimodal distribution for AIKL\_E compared to AIKL\_UN and AIKL\_E which again, is likely the result of only the soluble portions being analyzed.

$^{31}\text{P}$  NMR analysis was conducted to determine if the esterification was successful. The  $^{31}\text{P}$  NMR data presented in Figure 31c shows the complete spectra of all nine lignin powders. It can be observed that the UF\_E, ASKL\_E, and AIKL\_E spectra do not show signals for ArOH, ALOH, or COOH functional groups which highlights that the esterification was successful. Table 13 shows only trace amounts of ArOH, ALOH, and COOH functional groups detected in UF\_E, ASKL\_E, and AIKL\_E. While nearly complete esterification occurred for all three samples the AIKL had the highest residual functional group content of 0.20 mmol/g (Table 13).

#### **4.1.4.3 FT-IR structural analysis of esterified HE lignin powders**

The FT-IR analysis alongside the  $^{31}\text{P}$  NMR analysis provided a more detailed look into the structural changes that occur after the HE lignin powders were esterified. Figure 36 contains the complete spectra for the samples. The broad peak around  $3400\text{ cm}^{-1}$  seen for both unmodified and HE samples, flattens and disappears in Figure 36a, b and c for all esterified lignin samples. The signal was representative of the O-H stretching of aliphatic and phenolic functional groups alongside H-bonding. The reduction of this peak means the HE etherification followed up by the esterification with propionic acid was successful in removing free hydroxyl groups and thus reducing the capacity for hydrogen bonding. The signals at  $2920$  and  $2850\text{ cm}^{-1}$  increased as seen in Figure 36a, b, and c for the esterified lignin spectra which is the result of increased



**Figure 36 Complete FT-IR spectra for unfractionated (UF) (a) acetone soluble (ASKL) (b) and acetone insoluble (AIKL) (c) unmodified (UN), hydroxyethyl ether (HE), and esterified (E) lignin powders**

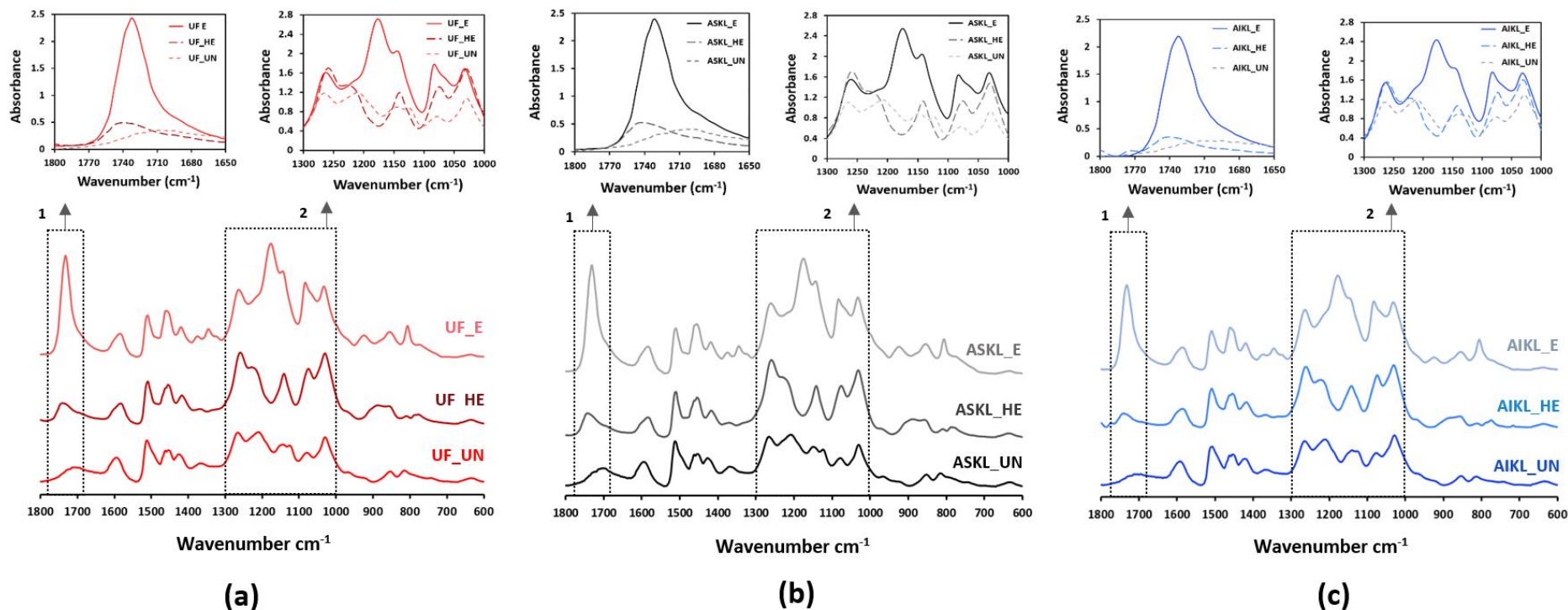
aliphatic carbon chains from the propionate ester. These results agree with work done by Liu et al. and Gordobil et al.<sup>150,153</sup> In addition, there are no peak signals for propionic acid characteristic bands at (3540, 2986, 2946, 2562, 1715, 1240, and 935) cm<sup>-1</sup> which indicates there are no traces of unreacted propionic acid.

The fingerprint region showed a large increase in signal absorbance for esterified UF, ASKL, and AIKL around 1735 cm<sup>-1</sup> (inset 1) which is the key C=O ester bond (Figure 37). It should be noted that only one signal is present at 1735 cm<sup>-1</sup> and there was no signal at 1760 cm<sup>-1</sup>. A signal stretch at 1735 cm<sup>-1</sup> represented aliphatic ester bonds while a signal at 1760 cm<sup>-1</sup> would have indicated the presence of aromatic ester bonds. Because the ArOH were converted to AIOH during the HE reaction this result was the expected outcome. The spectra in Figure 37 also showed a large signal increase between 1000 and 1300 cm<sup>-1</sup> for esterified UF, ASKL, and AIKL, which is indicative of C-O bond expansion of the ester groups (inset 2).

Using the FT-IR absorbance intensities at the 3435 cm<sup>-1</sup> signal the conversion of ArOH and AIOH functional groups to aliphatic esters was calculated to determine the degree of esterification. The method to establish conversion was set by Gordobil et al. and used the following equation<sup>182</sup>:

$$\alpha = 1 - \left[ \frac{\frac{H_{OH}(t=E)}{H_{ref}}}{\frac{H_{OH}(t=HE)}{H_{ref}}} \right] * 100$$

Where H<sub>ref</sub> is the normalized signal at 1510 cm<sup>-1</sup> and equals one and H<sub>OH</sub> equals the absorbance at 3435 cm<sup>-1</sup> for either the HE or E reactions. Using the data and this equation the conversion for UF\_E was 92.7%, ASKL\_E was 92.6%, and AIKL\_E was 91.1%. Liu et al. reported an 88%

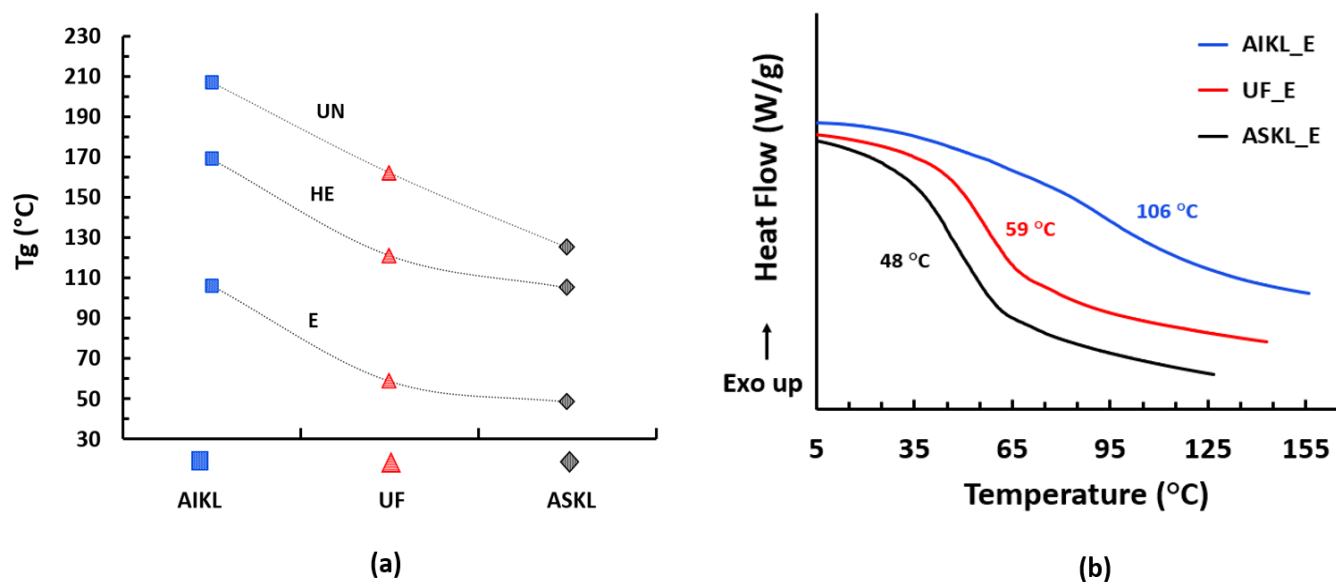


**Figure 37** FT-IR spectra for unfractionated unmodified (UF\_UN), unfractionated hydroxyethyl ether (UF\_HE) and unfractionated esterified (UF\_E) (a) acetone soluble unmodified (ASKL\_UN), acetone soluble hydroxyethyl ether (ASKL\_HE) and acetone soluble esterified (ASKL\_E) (b) acetone insoluble (AIKL\_UN), acetone insoluble hydroxyethyl ether (AIKL\_HE) and acetone insoluble esterified (AIKL\_E) (c) and the ester bond signal increase at 1740 cm<sup>-1</sup> (1) and C-O expansion in ester groups at 1000-1300 cm<sup>-1</sup> (2)

conversion of ArOH to AlOH groups for HE Biochoice softwood kraft lignin.<sup>153</sup> Following the esterification reaction with propionic acid performed on the HE lignin, the research group reported an 80% degree of conversion to aliphatic esters.<sup>153</sup> Liu et al. improved upon this after developing a real time control process for the HE reaction and reported a 91% conversion of ArOH to AlOH groups which would likely improve upon the conversion from AlOH to aliphatic esters during the esterification with propionic acid.<sup>191</sup> The esterification reaction with propionic acid was successful and these structural changes led to important changes in thermal properties.

#### **4.1.4.4 T<sub>g</sub> reduction for esterified HE lignin powders**

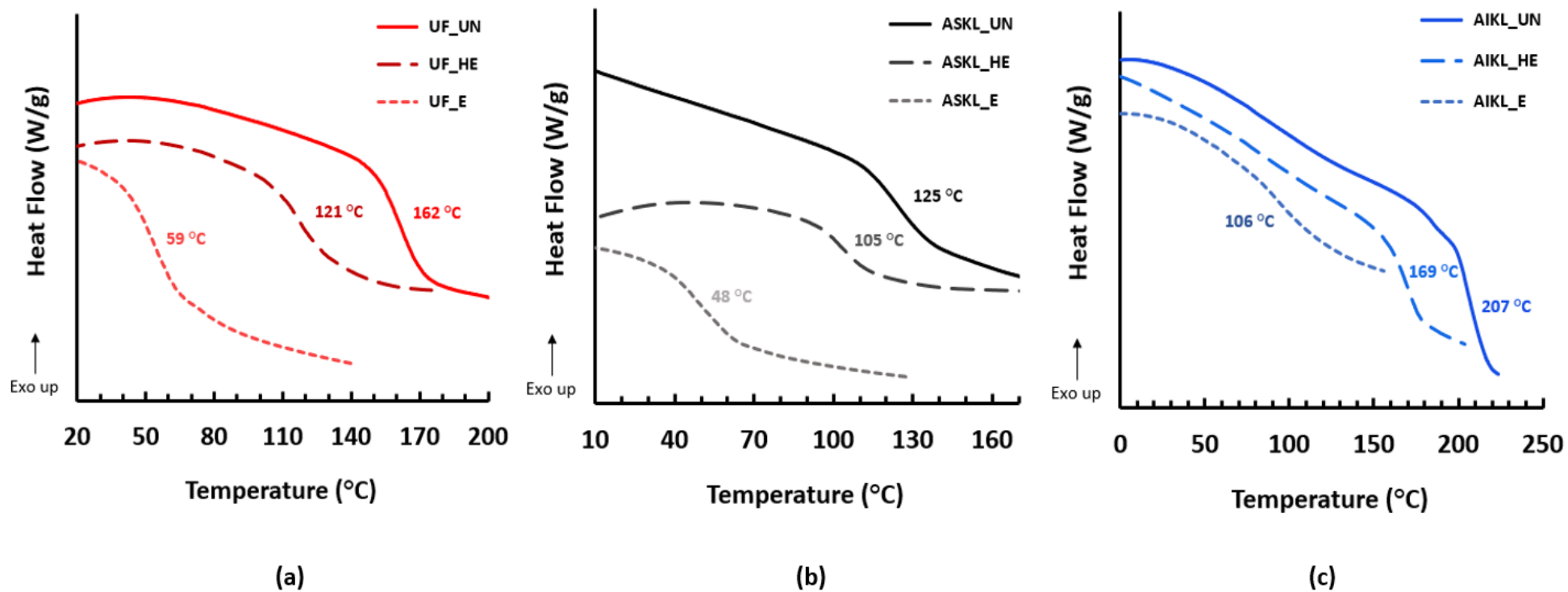
Figure 38a contains the T<sub>g</sub> values for the unmodified lignin powders as compared to the HE and esterified samples and Figure 38b is the accompanying DSC curves for the esterified samples. The dashed lines (Figure 38a) serve no functional purpose and are presented to guide the reader's eye. There was a major reduction in the glass transition temperature after the HE lignin powders were esterified. UF\_E decreased from 121.4 °C to 58.7 °C, ASKL\_E from 104.5 °C to 48.4 °C, and AIKL\_E from 169.4 °C to 105.9 °C (Table 13). These changes in glass transition temperature from the unmodified lignin powders to the esterified lignin powders decreased according to the following percentages: 64% for UF\_E, 61% for ASKL\_E, and 49% for AIKL\_E. The T<sub>g</sub> reduction is in part due to a decrease in aliphatic hydroxyl groups that removed the ability for inter and intra hydrogen bonds. Because of an increase in the carbon chain length after esterification there is an increase in molecular weight for ASKL\_E and UF\_E.



**Figure 38** The glass transition temperatures for unmodified (UN), hydroxyethyl ether (HE), and esterified (E) acetone insoluble (AIKL), unfractionated (UF), and acetone soluble (ASKL) lignin powders (a) and the correlating DSC curves (b)

It should be noted that the esterified DSC curves for all three fractions are sharper and more defined in comparison to their unmodified and HE counterparts as the result of the functional uniformity introduced by the esterification process (Figure 39a, b, and c). This result was further evidence that the HE reaction followed by the esterification was successful in creating highly uniform lignin powders ready for melt blending. The acetone soluble and insoluble lignin fractions show very different thermal properties with ASKL\_E having the lowest  $T_g$ . However, the AIKL\_E sample has a  $T_g$  that is near the melting temperature of thermoplastics such as polyethylene.

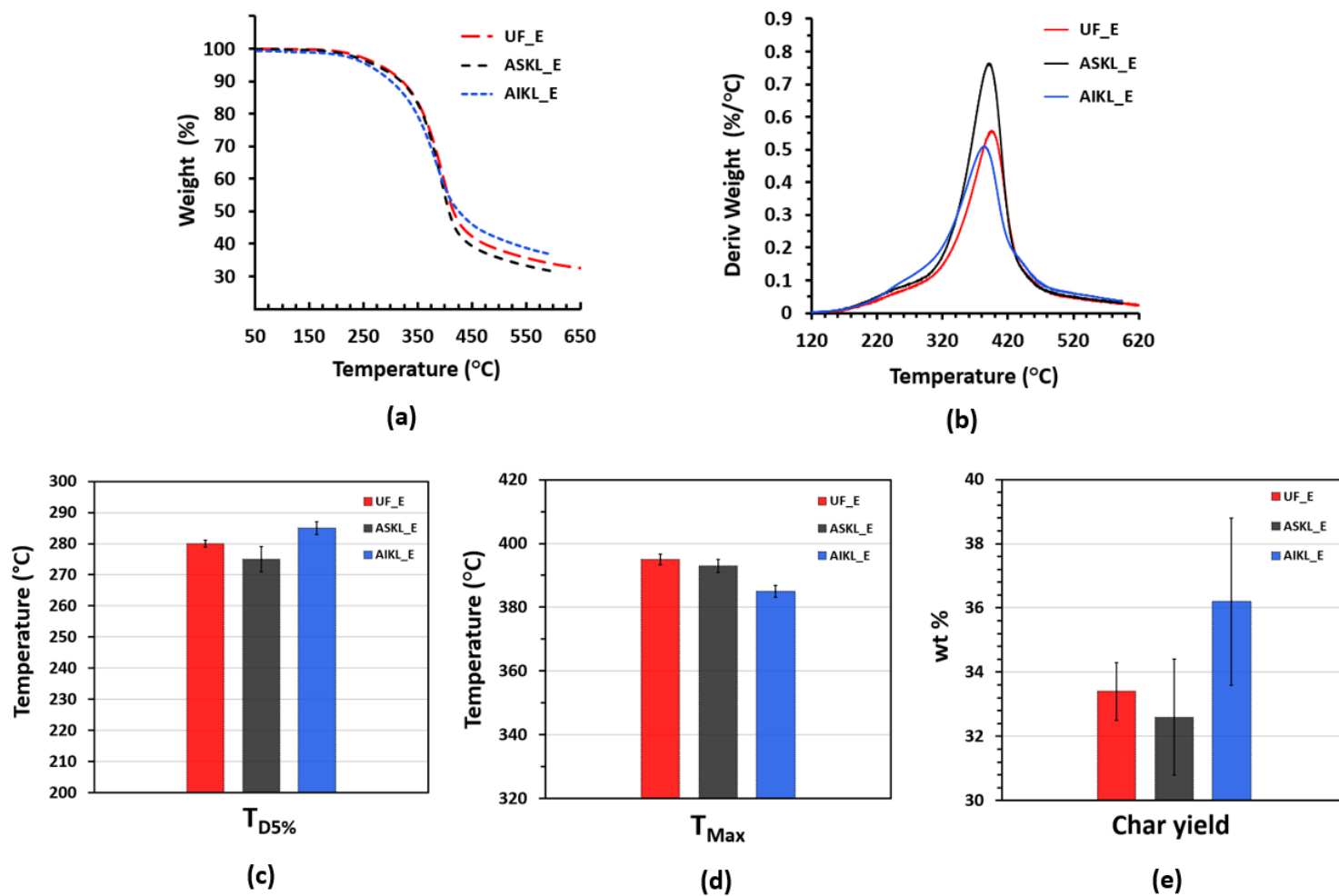




**Figure 39** DSC curves for unfractionated (UF) (a) acetone soluble (ASKL) (b) and acetone insoluble (AIKL) (c) unmodified (UN), hydroxyethyl ether (HE) modified, and esterified (E) modified lignin powders

#### **4.1.4.5 Thermal degradation for esterified lignin powders**

There were several important observations made in the analysis of the TGA data for the lignin ester fractions. All values are listed in Table 13, but Figure 40 shows the percent weight loss curves and the derivative weight loss as a function of temperature curves for both esterified fractionated portions in comparison to their unfractionated counterpart. The 5% weight loss temperature increased overall after the HE lignin was esterified for all samples with AIKL\_E having the highest temperature stability and increase in temperature relative to the HE samples (Figure 40c). The maximum derivative temperature of all samples were similar but AIKL\_E showed the slowest degradation rate profile (Figure 40b and c) similar to the other AIKL samples. AIKL had the highest char yield with 36 wt% remaining at 600 °C (Figure 40e). Overall, the char yield for all esterified lignin samples slightly decreased in comparison to their unmodified and HE counterparts which may be the result of a more functionally uniform material.



**Figure 40** TGA analysis for unfractionated esterified (UF\_E), acetone soluble esterified (ASKL\_E), and acetone insoluble esterified (AIKL\_E) lignin powders weight % loss curves (a) maximum derivative weight % as a function of temperature curves (b) average values with standard deviation error bars for T<sub>D5%</sub> (c) T<sub>max</sub> (d) and char yield (e)

Figure 41 shows a side by side view of the percent weight loss curves and the derivative weight loss as a function of temperature curves for individual fractions UF, ASKL, and AIKL at each modification (HE and E) compared to their unmodified counterpart. Concerning the percent weight loss curve a clear pattern emerged for UF, ASKL, and AIKL where the char yield at 600 °C slightly decreased from unmodified to esterified lignin powders. In addition, the curves for UF\_E, ASKL\_E and AIKL\_E are sharper and more pronounced than their unmodified and HE counterparts. When analyzing the derivative weight loss as a function of temperature, it can be observed that there is a sharp increase and a smoothing out of the UF\_E, ASKL\_E, and AIKL\_E curves when compared to their unmodified and HE counterparts. Most notably, the shoulders between 200-300 °C have vanished which indicated that the ArOH and AlOH functional groups are no longer present and the esterification was successful. The outcomes were the result of uniform lignin powders with more consistent and reliable thermal properties for melt blending with thermoplastics such as Ecoflex™. Each fraction has unique thermal characteristics which will be evaluated in blend with Ecoflex™ in the upcoming sections.

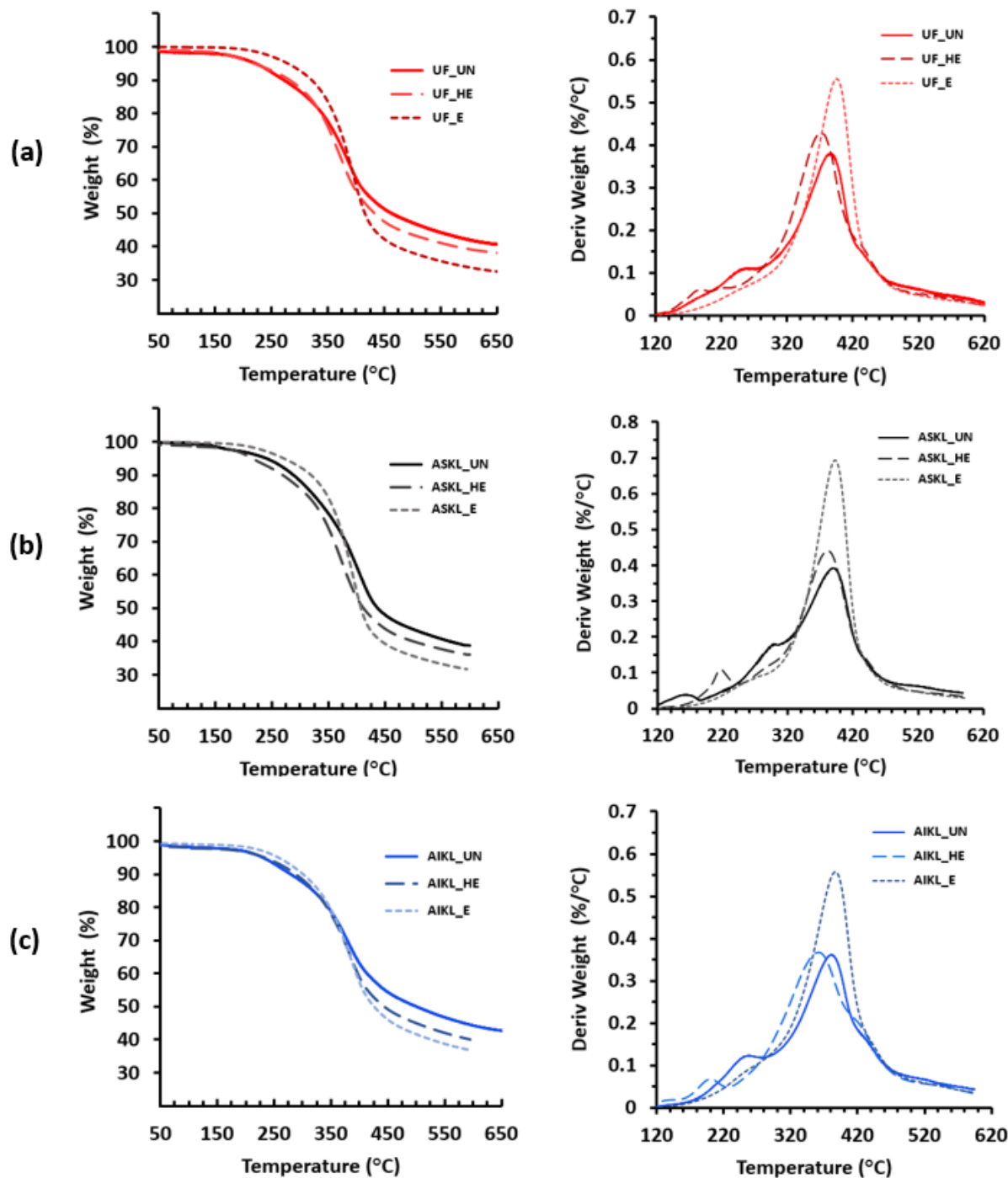


Figure 41 TGA weight % loss curves and maximum derivative weight % as a function of temperature curves for unfractionated (UF) (a) acetone soluble (ASKL) (b) and acetone insoluble (AIKL) (c) unmodified (UN), hydroxyethyl ether (HE) modified, and esterified (E) modified lignin powders

#### 4.1.5 Concluding remarks

(1) The acetone fractionation of softwood grade A Lignoforce<sup>TM</sup> lignin, followed by the etherification with ethylene carbonate, and the esterification with propionic acid was successful in creating nine technical lignin powders (UF\_UN, UF\_HE, UF\_E, ASKL\_UN, ASKL\_HE, ASKL\_E, and AIKL\_UN, AIKL\_HE, AIKL\_E) ready for melt blending with Ecoflex<sup>TM</sup>.

(2) The fractionation followed by the modifications created lignin powders with different molecular weights, molecular weight distributions, chemical functionality, and thermal stability which will be compared through mechanical and thermal property testing after melt blending with Ecoflex<sup>TM</sup>.

(3) The processes developed, and the chemical reactions carried out to complete the fractionation and modifications of technical lignin powders were driven by green chemistry principles and the ability for easy scale-up potential which feeds into a circular bioeconomy.

## **4.2 Characterization of lignin-Ecoflex™ thermoplastic blends**

### **4.2.1 Background**

Lignin based thermoplastic blends have the potential to be an alternative to petroleum based thermoplastics that offer both renewable and biodegradable components. The difficulties that polar lignin presents in melt with a hydrophobic polyester like Ecoflex™ have been extensively discussed and subsequently addressed through the fractionation and modification processes carried out on softwood kraft lignin and the detailed analysis which followed in the previous section. Ultimately, component molecular interactions will determine the structure and properties of the lignin-Ecoflex™ blend. There are several ways to discuss interaction compatibility or homogeneity/miscibility of the melt blend. Kun et al. raised an excellent point in their 2017 review of polymer/lignin blends and their interactions, properties, and applications when they indicated, “full homogeneity is impossible to reach and even more impossible to prove.”<sup>212</sup> Kun and co-workers claimed that too many research groups look at one aspect of miscibility and state they have developed a fully homogenous blend, but much of the data was inconclusive without proper evidence. The same paper indicated that many research groups fail to compare their modified lignins in blend with the unmodified counterpart and that makes drawing definitive conclusions difficult. This study intends on using mechanical property analysis, DSC, and FT-IR data for unfractionated and fractionated, unmodified, and modified technical lignin powders in blend with Ecoflex™ at varying weight percentages to develop a complete understanding about the interaction compatibility of the developed biobased material.

## **4.2.2 Tensile properties of lignin-Ecoflex™ thermoplastic blends**

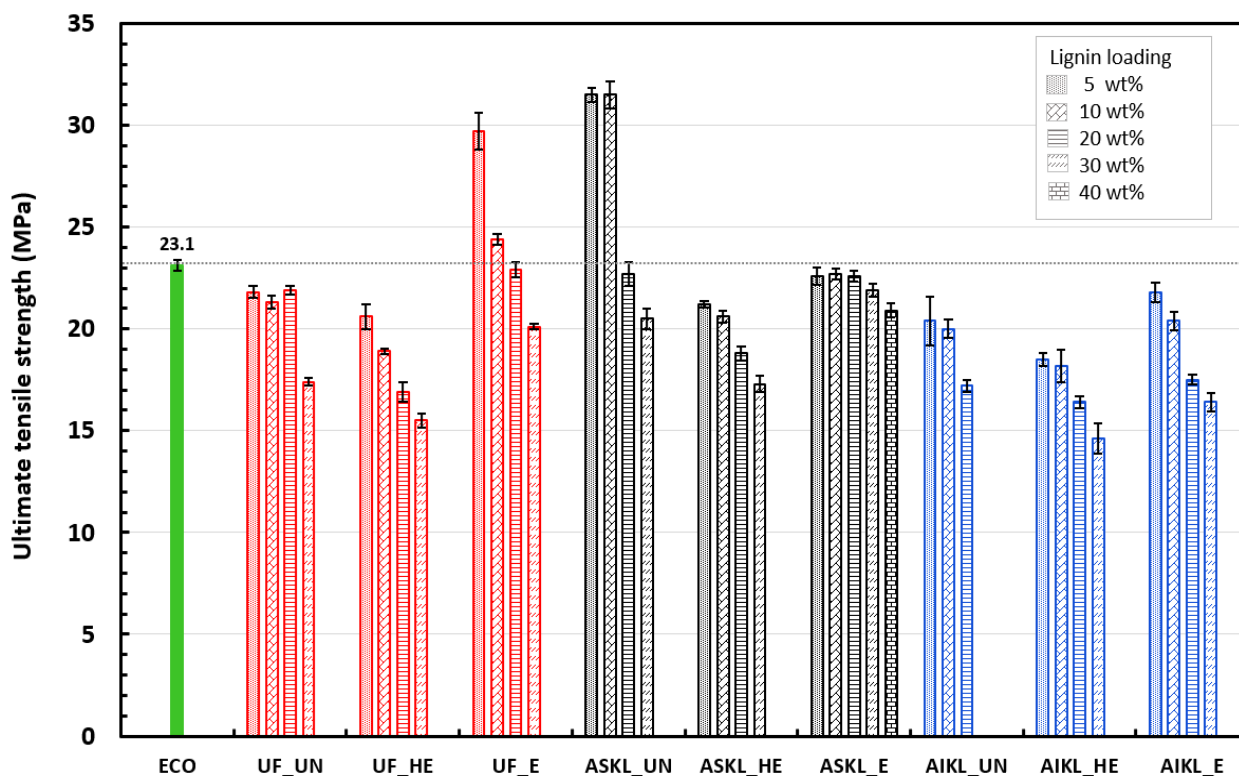
Tensile properties like ultimate tensile strength (UTS), Young's modulus (E), and percent total elongation at break can be determined from the uniaxial tension applied during tensile testing. Toughness, the measure of energy required to fracture the material can be determined by analyzing the area under the engineering stress/strain curve. For these tests, the key is to have uniform samples without defects arising from processing. To overcome this issue, all materials were melt blended (at 180 °C) and mould injected into standard dumbbell type V test specimens. The samples were then tested at a strain rate of 50 mm/min using the ASTM D638 standard and the strict protocol described in *section 3.9* of this work. Neat Ecoflex™ was melt blended at 100 wt% ECO or 0 wt% lignin, extruded, and tested as the control for all comparison to added lignin blends; hence all samples underwent similar processing. All lignin loading was carried out on a weight percentage basis ranging from 5-40% depending on fraction and modification. The tensile properties of the polymers were analyzed using processed engineering stress/strain curves and are important for the design of plastic materials and the prediction of their performance under stress. The tensile properties were also necessary to compare one lignin powder to another which provided insight into the lignin-Ecoflex™ interactions and miscibility based on lignin functionality.

### **4.2.2.1 Ultimate tensile strength (UTS)**

The ultimate tensile strength or tensile strength is an important material parameter which determines mechanical performance and a polymers ability to resist deformation under tension. The nine lignin powders; unfractionated unmodified (UF\_UN), unfractionated hydroxyethyl ether (UF\_HE), unfractionated esterified (UF\_E), acetone soluble unmodified (ASKL\_UN), acetone soluble hydroxyethyl ether (ASKL\_HE), acetone soluble esterified (ASKL\_E), acetone



insoluble unmodified (AIKL\_UN), acetone insoluble hydroxyethyl ether (AIKL\_HE), and acetone insoluble esterified (AIKL\_E) were loaded with Ecoflex™ at a weigh percent of 5, 10, 20, and 30. Additionally, ASKL\_E was loaded at 40 wt% and AIKL\_UN could not be properly extruded at 30 wt% because the blend resulted in poor samples (brittleness) that did not allow testing. Figure 42 shows the UTS (MPa) for all nine lignin powders at 5, 10, 20, and 30 wt% loading, with ASKL\_E being loaded at 40 wt%. The UTS of the neat Ecoflex™ control was measured 23.1 MPa for the dog bone sample which is less than the tensile strength of 36-44 MPa



**Figure 42** Ultimate tensile strength for neat Ecoflex™ (ECO), unfractionated unmodified (UF\_UN), unfractionated hydroxyethyl ether (UF\_HE), unfractionated esterified (UF\_E), acetone soluble unmodified (ASKL\_UN), acetone soluble hydroxyethyl ether (ASKL\_HE), acetone soluble esterified (ASKL\_E), acetone insoluble unmodified (AIKL\_UN), acetone insoluble hydroxyethyl ether (AIKL\_HE), and acetone insoluble esterified (AIKL\_E) at a lignin loading of 5, 10, 20, and 30 wt% with ASKL\_E blended to 40 wt%

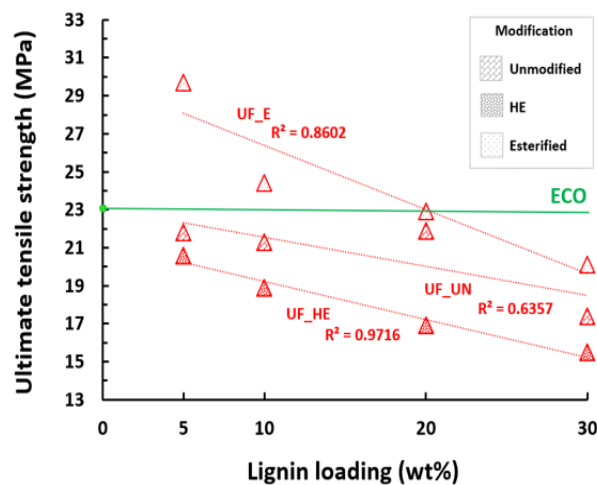
reported in the specification sheet for Ecoflex<sup>TM</sup> films (Table 6).<sup>94</sup> However, Chen et al who followed the ASTM D638 standard and developed similar dog bone samples via melt processing reported 21.7 MPa for neat Ecoflex<sup>TM</sup>.<sup>213</sup> In addition, Wang et al., Xiong et al., and Kargarzadeh et al. whom all worked with lignin-Ecoflex<sup>TM</sup> blended films reported neat Ecoflex<sup>TM</sup> films as 23.0 MPa, 23.7 MPa, and 19.6 MPa.<sup>190,192,214</sup>

There was an increase in tensile strength for UF\_E and ASKL\_UN blended at 5 and 10 wt%. In comparison to the Ecoflex<sup>TM</sup> control (23.1 MPa) the tensile strength of 5 wt% UF\_E increased by 29% to 29.7 MPa, 10 wt% UF\_E increased by 6% to 24.4, and both 5 and 10 wt% ASKL\_UN increased by 36% to 31.5 MPa. Previous research indicated that when lignin was added into thermoplastic blends, the strength decreased.<sup>144,157,189,190,192,213,214,215</sup> There are some instances where lignin has increased the tensile strength but these are in blend with, soy meal, PLA or nitrile rubber.<sup>216-218</sup> The 30 wt% ASKL\_E powder showed a minimal decrease in tensile strength of only 5.2% to 21.9 MPa when compared to neat Ecoflex<sup>TM</sup> (23.1 MPa). This prompted the 40 wt% loading of ASKL\_E which showed a decrease in tensile strength of 9.5% to 20.9 MPa.

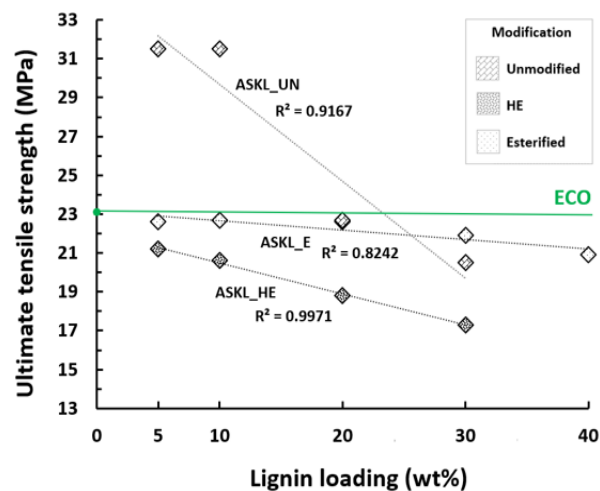
The hydroxyethyl ether modified lignin powders, UF\_HE, ASKL\_HE, and AIKL\_HE all showed a systematic deterioration in tensile strength with increased lignin loading with a 32%, 25%, and 37% decrease at 30 wt% loading for each of these hydroxyethylated samples. A significant decrease in strength suggests that the hydroxyethyl lignin derivatives serve to create defects in the Ecoflex<sup>TM</sup> matrix that would serve as stress concentrators. Further, the AIKL\_UN lignin powder was the most physically difficult to blend with Ecoflex<sup>TM</sup> and samples could not be produced beyond 20 wt% loading; the torque on the mixer was significant during the 20 wt% loading and too great for processing at a higher loading level. The esterification of AIKL did

noticeably improve blending during processing but at 30 wt% the tensile strength had decreased by 29% to 16.4 MPa.

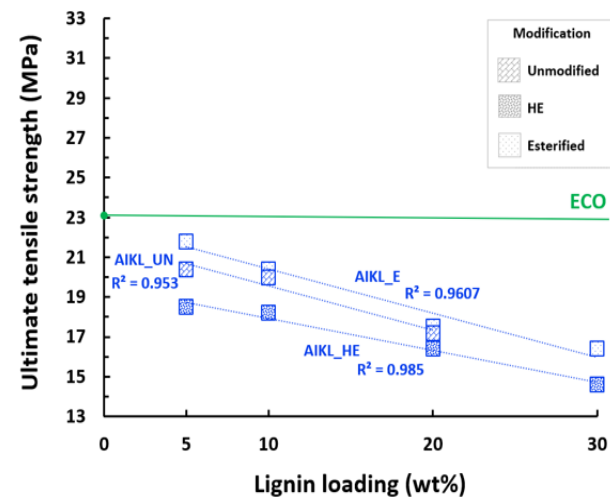
Figure 43 shows tensile strength as a function of wt% lignin loading for the two lignin fractions (ASKL and AIKL) and their unfractionated (UF) counterpart with modifications hydroxyethyl ether (HE) and esterified (E). All nine lignin powders indicated a negative trending linear regression: with an added weight percentage of lignin to Ecoflex™, the tensile strength decreased. In Figure 43a (UF), the esterified modification resulted in an increase in tensile strength at 5 and 10 wt% loading. All other loading levels of unmodified unfractionated lignin there was an observed decrease in tensile strength. In Figure 43b (ASKL), the addition of unmodified acetone soluble lignin to Ecoflex™ resulted in a large increase in tensile strength at 5 and 10 wt% loading providing a synergistic response for this sample at the loading level. There is overlap of the 20 wt% ASKL\_UN and ASKL\_E tensile strengths. Further, it should be noted that the esterified lignin blended samples showed nearly an independent response to the loading up to 40 wt% when compared with neat Ecoflex™. For the highest loading of acetone soluble esterified lignin there was a decrease of 9.5% for the tensile strength. In Figure 43c (AIKL), there were strong correlations for the different modifications signified with a goodness of fit values,  $R^2$  values ranging from 0.953-0.985. For AIKL, the trend was negative for all samples and as lignin loading increased, tensile strength decreased. Surprisingly, it should be noted at the 20 wt% loading level of AIKL, the level of modification did not create a significant differing response. From this standpoint the chemical functionality of the lignin did not seem to result in a change in the blend mechanical response. This response is unusual considering the difference in functionality of the sample.



(a)



(b)



(c)

**Figure 43** Ultimate tensile strength as a function of wt% lignin loading for unfractionated unmodified, hydroxyethyl ether, and esterified samples (UF\_UN, UF\_HE, UF\_E) (a) acetone soluble unmodified, hydroxyethyl ether, and esterified samples (ASKL\_UN, ASKL\_HE, ASKL\_E) (b) and acetone insoluble unmodified, hydroxyethyl ether, and esterified samples (AIKL\_UN, AIKL\_HE, AIKL\_E) (c) with the neat Ecoflex™ (ECO) control at 23.1 MPa

Tensile strength as a function of wt% lignin loading was plotted in Figure 44 for all nine lignin powders allowing a side by side comparison in performance. It is clear to see that AIKL\_UN, AIKL\_HE, and AIKL\_E demonstrated the lowest tensile strengths at all loadings, while ASKL\_E showed a minimum decline in tensile strength with added lignin. Tensile strength deteriorated with a strong linear regression for all HE powders as lignin was added up to 30 wt%. All fractions showed some improvement with esterification, but most fell below the neat Ecoflex™ performance. The most notable outcome was the increase in tensile strength for UF\_E and ASKL\_UN at 5 and 10 wt% lignin.

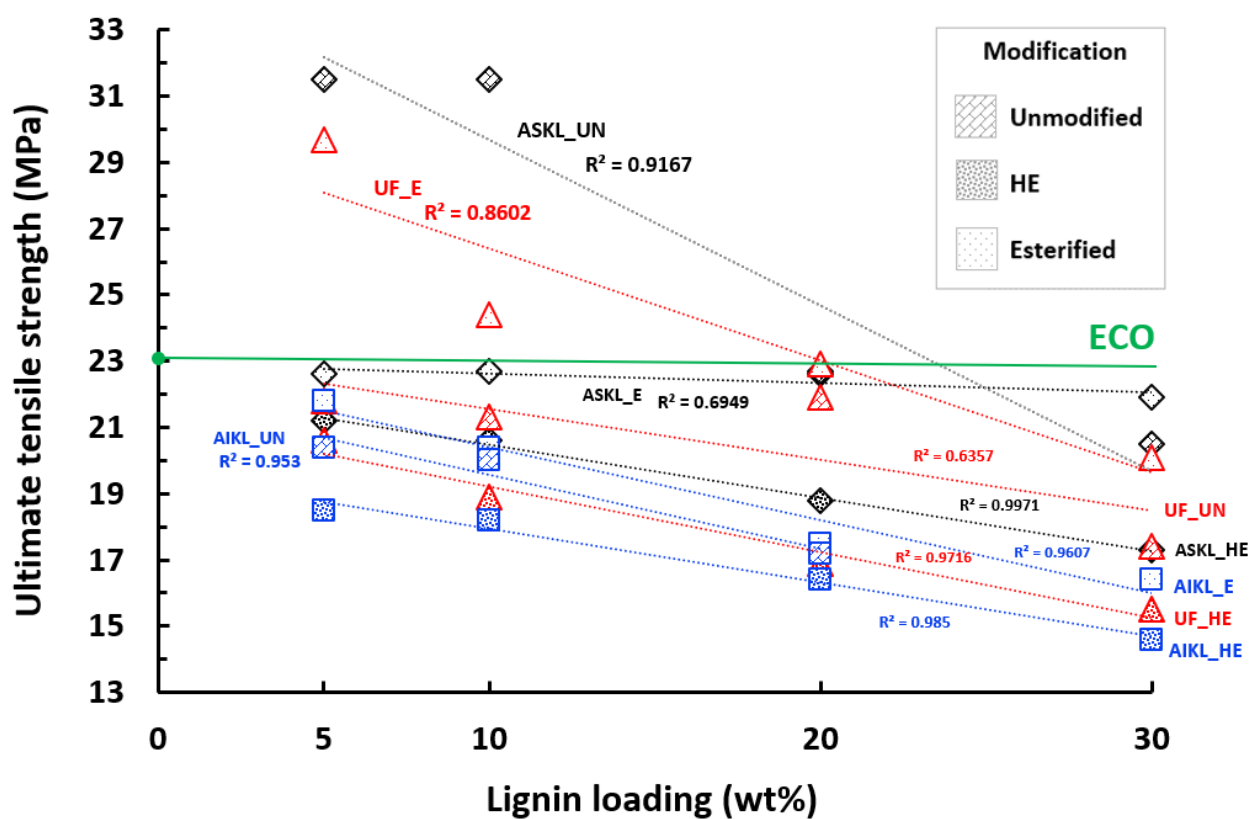


Figure 44 Ultimate tensile strength as a function of wt% lignin loading for unfractionated, acetone soluble, and acetone insoluble, unmodified, hydroxyethyl ether, and esterified (UF\_UN, UF\_HE, UF\_E, ASKL\_UN, ASKL\_HE, ASKL\_E, AIKL\_UN, AIKL\_HE, and AIKL\_E) samples with the neat Ecoflex™ (ECO) control at 23.1 MPa

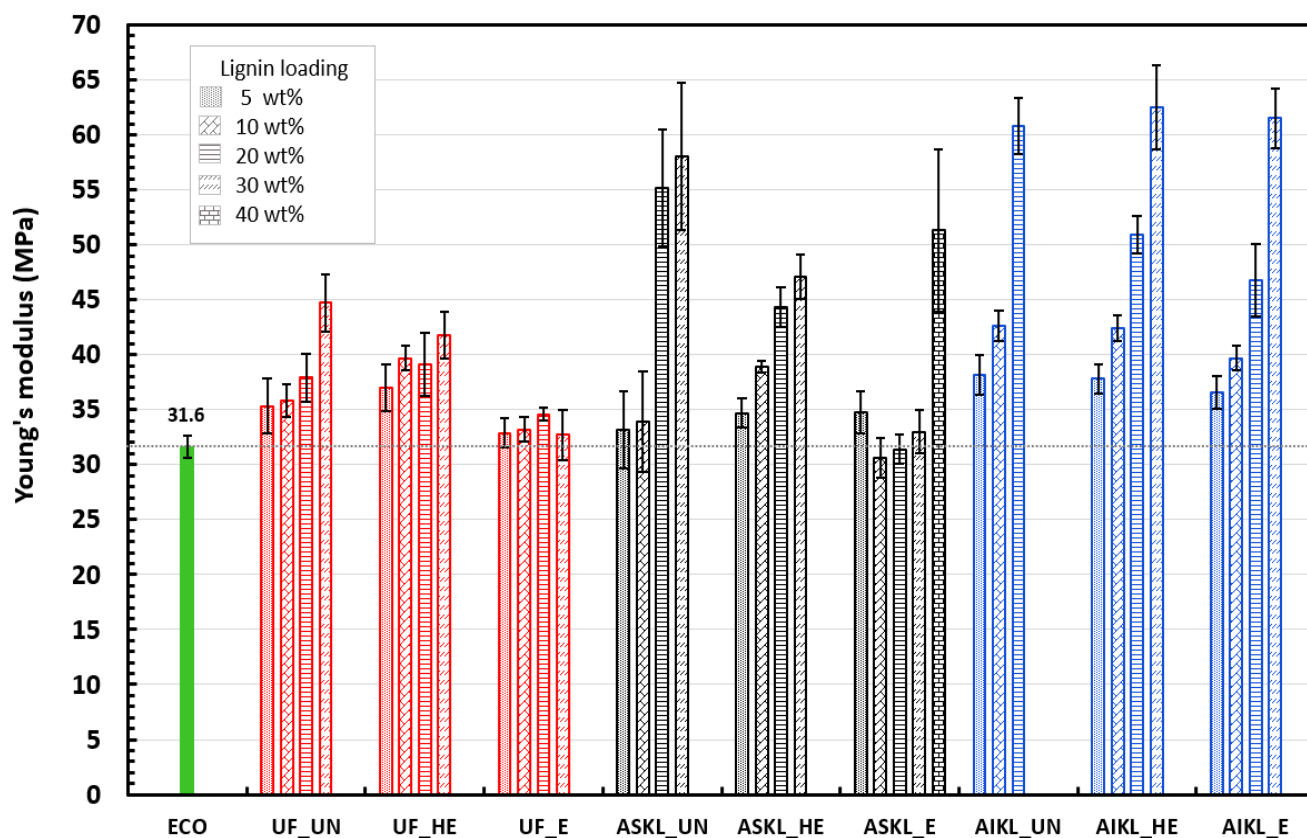
Another curious observation was that at 20 wt% lignin loading, ASKL unmodified or esterified, along with unfractionated esterified samples had similar UTS values. The chemical differences between ASKL\_UN and ASKL\_E is significant, yet it had almost no impact on performance for these samples at this loading level. With a strong decrease in the performance of the acetone insoluble lignin samples at this loading level, it appears a more hydrophilic material with greater hydrogen bonding characteristics that does not get evenly distributed in the Ecoflex™ matrix. Additionally, the AIKL\_E may have too large a molecular weight to overcome the aggregation induced interactions at this loading level.

#### **4.2.2.2 Young's modulus (E)**

The modulus of elasticity or Young's modulus for tensile specimens is the initial slope of the engineering stress/strain curve and is an index of the stiffness of a material under an applied uniaxial force. Polymers deform elastically at low strain and that deformation is homogenous so if the sample is removed it will return to its original shape and size. Beyond the elastic limit the material will yield, begin necking, and by definition deformation will no longer be recoverable. Neat Ecoflex™ was evaluated and reflected a relatively soft polymer with a Young's modulus of 31.6 MPa.

Figure 45 shows the modulus of elasticity (MPa) for all nine lignin powders at 5, 10, 20, and 30 wt% loading, with ASKL\_E being loaded to 40 wt%. There is an increase in modulus for all lignin powders at all weight percentage loadings except ASKL\_E 10 and 20 wt% which were around the same stiffness as neat Ecoflex™ (31.6 MPa). In comparison to the Ecoflex™ control, the Young's modulus of 5 and 10 wt% UF\_E and ASKL\_UN only increased by 4-7% to a max of 33.9 MPa. At a loading of 5 and 10 wt% both UF\_E and ASKL\_UN showed an increase in tensile strength but only a slight increase in stiffness which demonstrated a stronger material that

retains similar stiffness. The insoluble lignin fraction showed the greatest increase in stiffness at 30 wt% loading where AIKL\_UN increased by 92% to 60.8 MPa, AIKL\_HE increased by 98% to 62.5 MPa, and AIKL\_E increased by 95% to 61.5 MPa.



**Figure 45** Young's modulus for neat Ecoflex (ECO), unfractionated unmodified (UF\_UN), unfractionated hydroxyethyl ether (UF\_HE), unfractionated esterified (UF\_E), acetone soluble unmodified (ASKL\_UN), acetone soluble hydroxyethyl ether (ASKL\_HE), acetone soluble esterified (ASKL\_E), acetone insoluble unmodified (AIKL\_UN), acetone insoluble hydroxyethyl ether (AIKL\_HE), and acetone insoluble esterified (AIKL\_E) at a lignin loading of 5, 10, 20, and 30 wt% with ASKL\_E blended to 40 wt%

Young's modulus as a function of wt% loading for all nine lignin types were reported in Figure 46, allowing a side by side comparison in performance. The addition of most lignin powders created a stiffer material in comparison to neat Ecoflex™. AIKL\_UN, AIKL\_HE, and AIKL\_E

demonstrated the highest Young's modulus at all loadings, while UF\_E and ASKL\_E showed similar stiffness to neat Ecoflex™ with increased lignin loading resulting in low  $R^2$  values. For other samples, there was a strong linear correlation between an increase in wt% loading of lignin powder resulting in an increase in stiffness of blended material as can be seen with  $R^2$  values ranging from 0.75 to 0.99. In general, as lignin powder was increased in blend with Ecoflex™, the resultant material showed an increased Young's modulus or an increasing stiffness.

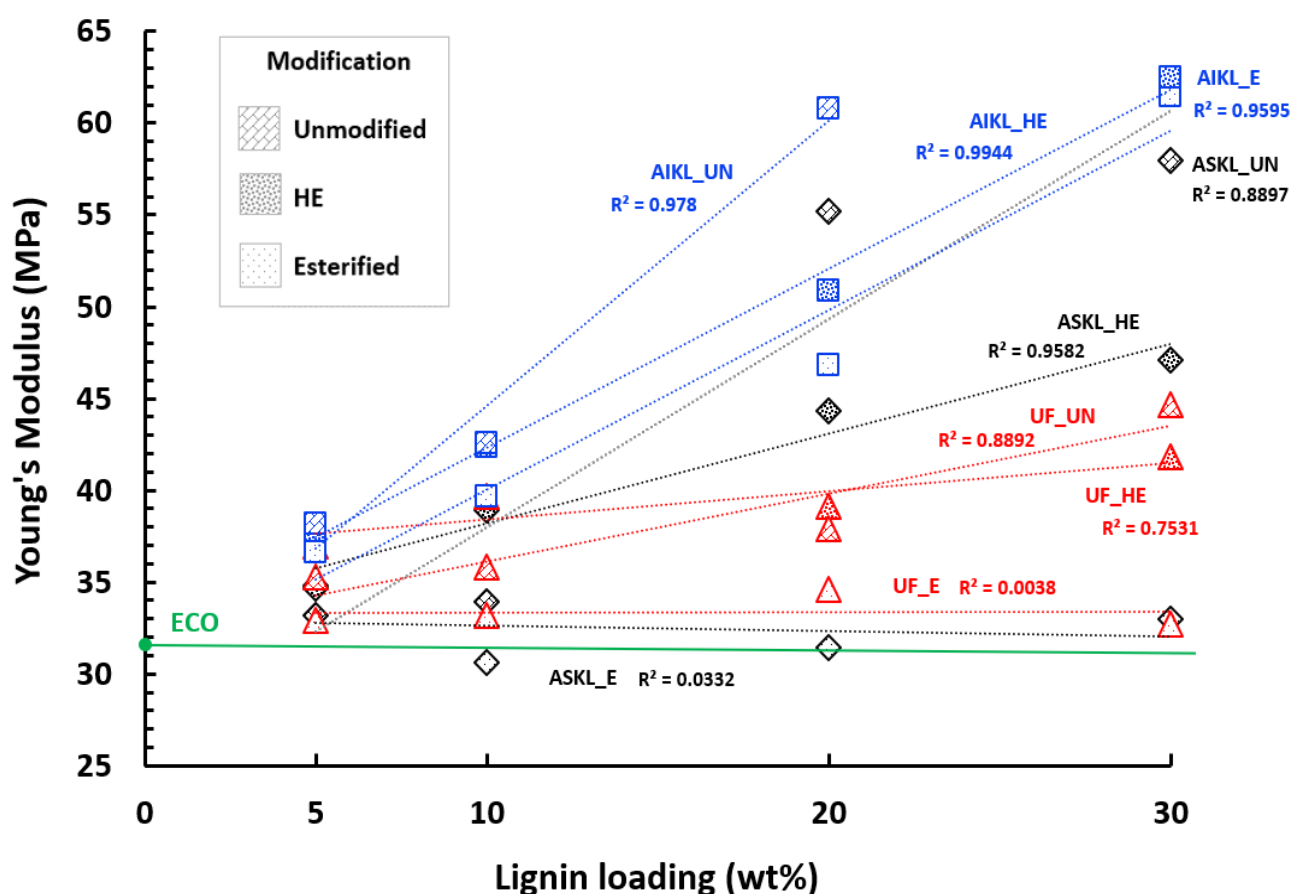
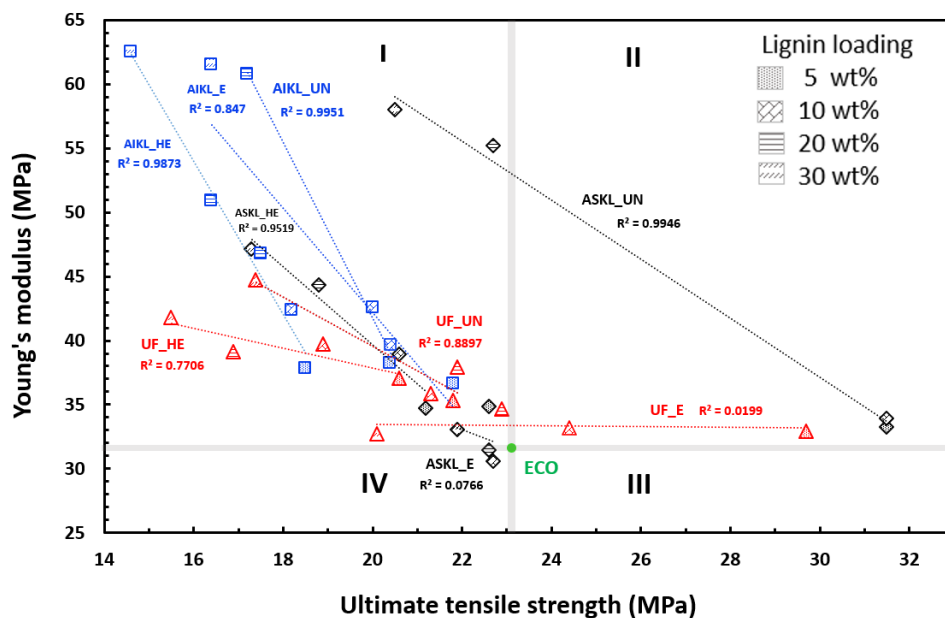


Figure 46 Young's modulus as a function of wt% lignin loading for unfractionated, acetone soluble, and acetone insoluble, unmodified, hydroxyethyl ether, and esterified (UF\_UN, UF\_HE, UF\_E, ASKL\_UN, ASKL\_HE, ASKL\_E, AIKL\_UN, AIKL\_HE, and AIKL\_E) samples with the neat Ecoflex™ (ECO) control at 31.6 MPa



The relationship between Young's modulus and UTS can be seen in Figure 47 which is broken into four quadrants. Quadrant one, where most of the data points lie is indicative of a lower tensile strength and higher stiffness in comparison to neat Ecoflex™. Quadrant two, where 5 and 10 wt% UF\_E and ASKL\_UN data points lie was indicative of a higher tensile strength and a higher stiffness in comparison to neat Ecoflex™ revealing a synergistic combination. There was no data that falls in quadrant three which would be a higher tensile strength and lower stiffness in comparison to neat Ecoflex and only 10 and 20 wt% ASKL\_E fall in quadrant four which is indicative of a lower tensile strength and a lower stiffness in comparison to neat Ecoflex. It should be noted that with the standard deviation 10 and 20 wt% ASKL\_E barely fall into quadrant four but there is a slight softening of the material and loss of strength at this lignin loading which may be worth future investigation for impact on other properties.

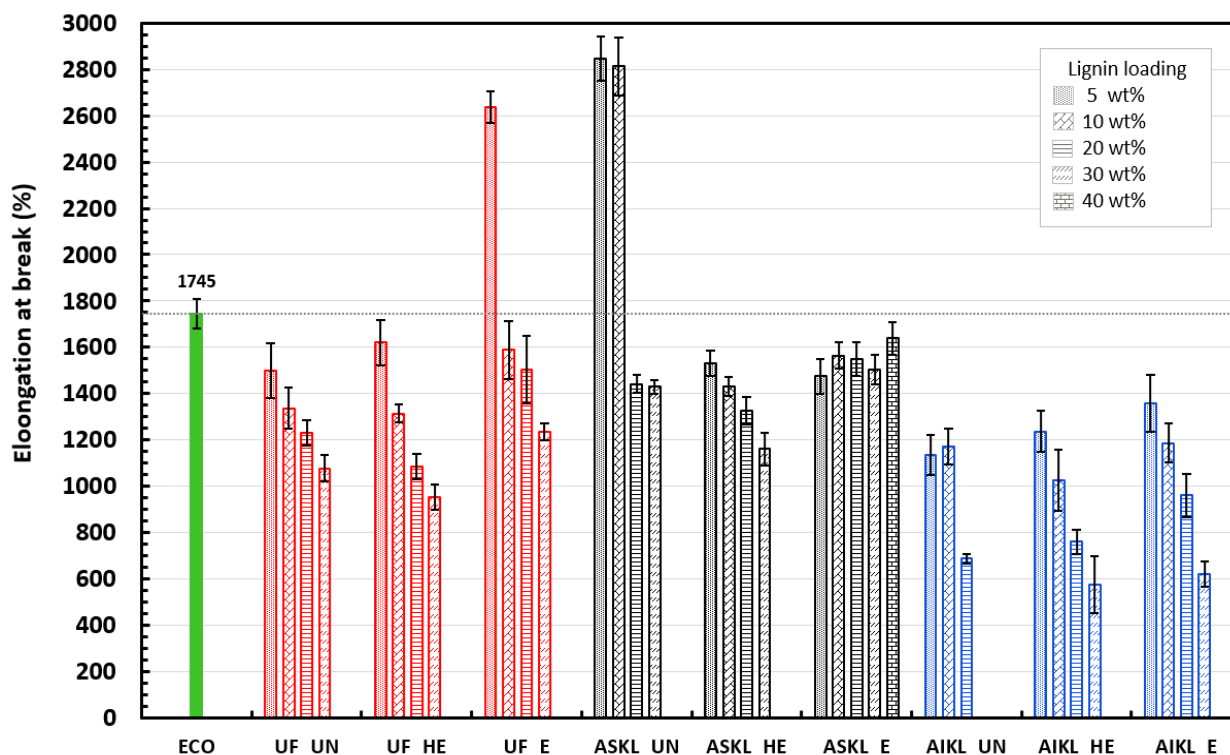


**Figure 47** Young's modulus as a function of ultimate tensile strength for unfractionated, acetone soluble, and acetone insoluble, unmodified, hydroxyethyl ether, and esterified (UF\_UN, UF\_HE, UF\_E, ASKL\_UN, ASKL\_HE, ASKL\_E, AIKL\_UN, AIKL\_HE, AIKL\_E) samples with the neat Ecoflex™ (ECO) control at 23.1, 31.6 MPa

#### 4.2.2.3 Elongation at break

Elongation at break or fracture strain is calculated as the ratio between change of length and initial length and it is reported as a percentage. Elongation at break relates to the ability of a specimen in plastic deformation to resist a change of shape without cracking. Elongation at break values are an indication of ductility of a polymer and are directly correlated to the toughness of a material.

The elongation at break (%) was plotted in Figure 48 for all nine lignin powders at 5, 10, 20, and 30 wt% loading, with ASKL\_E being loaded to a level of 40 wt%. There was a decrease in elongation at break for all lignin powders at all weight percentage loadings except for three samples (Figure 48). UF\_E 5 wt%, ASKL\_UN 5 wt%, and ASKL\_UN 10 wt% all showed an increase in elongation compared to neat Ecoflex<sup>TM</sup> (1745%). In comparison to the Ecoflex<sup>TM</sup> control, the elongation at break for 5 wt% UF\_E increased by 51% to 2638% and increased for ASKL\_UN 5 and 10 wt% by 63% and 61% to 2847% and 2814%. The ASKL\_E lignin powder loaded between 5 and 40 wt% showed only a slight decrease by 6.1% to 1638%. Although slight, the ASKL\_E powder demonstrated a reduced percent elongation at break with an increased weight percentage of lignin loaded which was similar to previous studies with the inclusion of esterified lignin into PBAT and esterified lignin into HDPE.<sup>144,214</sup> The AIKL powders showed the greatest reduction in fracture strain with AIKL\_HE at 30 wt% showing the greatest reduction of 67% to 576%.



**Figure 48 Elongation at break for neat Ecoflex™ (ECO), unfractionated unmodified (UF\_UN), unfractionated hydroxyethyl ether (UF\_HE), unfractionated esterified (UF\_E), acetone soluble unmodified (ASKL\_UN), acetone soluble hydroxyethyl ether (ASKL\_HE), acetone soluble esterified (ASKL\_E), acetone insoluble unmodified (AIKL\_UN), acetone insoluble hydroxyethyl ether (AIKL\_HE), and acetone insoluble esterified (AIKL\_E) at a lignin loading of 5, 10, 20, and 30 wt% with ASKL\_E blended to 40 wt%**

Percent elongation at break as a function of wt% loading for all nine lignin powders was displayed in Figure 49, allowing a side by side comparison in performance. The addition of most lignin powders reduced the plastic deformation in comparison to neat Ecoflex™. AIKL\_UN, AIKL\_HE, and AIKL\_E demonstrated the greatest reduction in percent elongation at all loadings, while UF\_E and ASKL\_UN at lower lignin loadings showed significant increase in percent elongation at break when compared to neat Ecoflex™. There was a strong linear correlation between an increase in wt% loading of lignin powder and a decrease of fracture strain for blended material as can be seen with  $R^2$  values ranging from 0.69 to 0.98. The relationship for ASKL\_E showed a low  $R^2$  values because with the increased percentage of lignin, the

response of the material was invariant with lignin loading. In general, there was a strong linear correlation, as lignin powder increased in blend the resultant material decreased in strain at break.

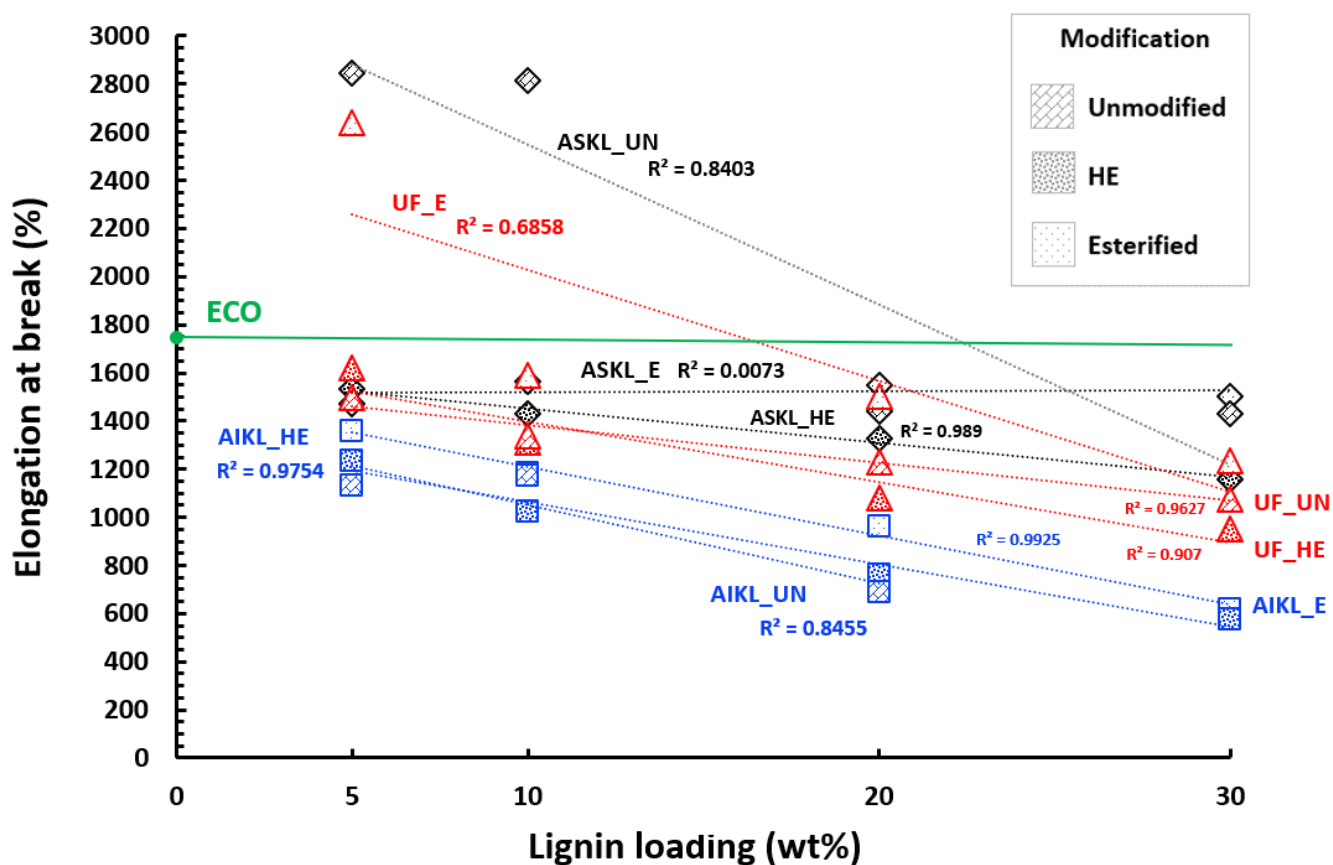
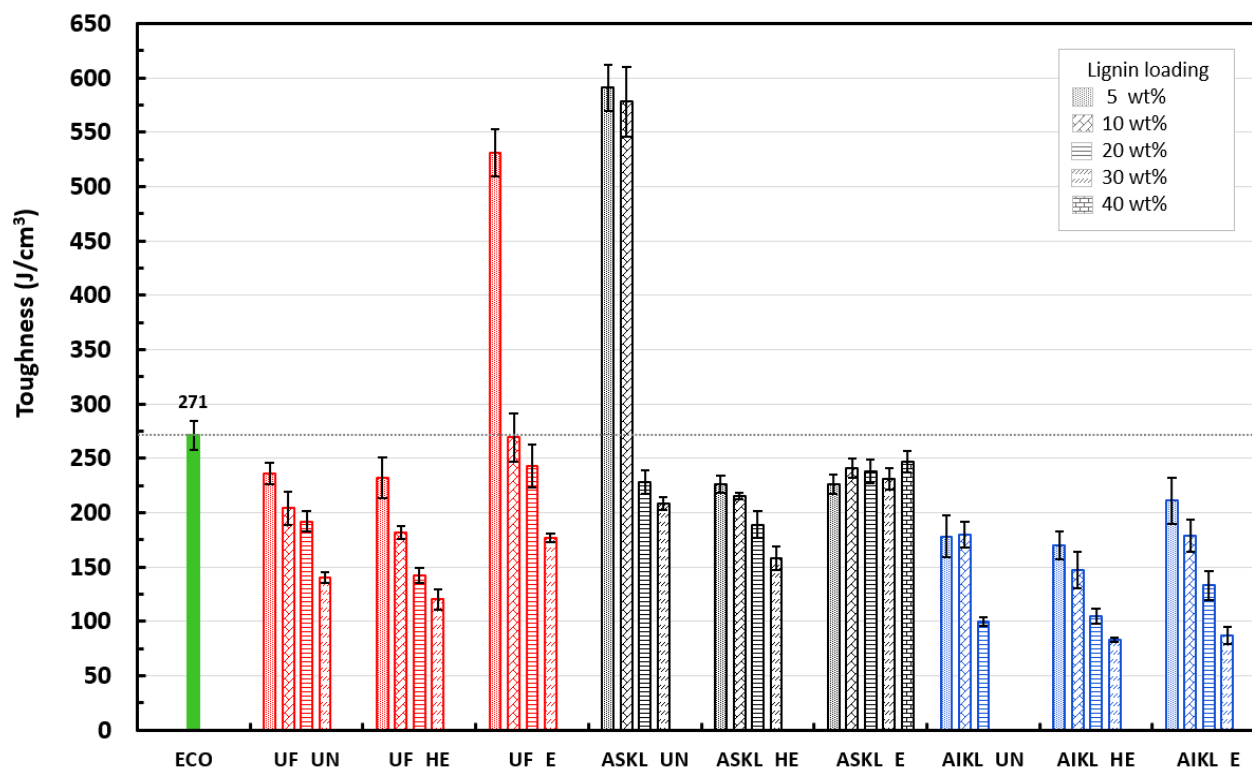


Figure 49 Percent elongation at break as a function of wt% lignin loading for unfractionated, acetone soluble, and acetone insoluble, unmodified, hydroxyethyl ether, and esterified (UF\_UN, UF\_HE, UF\_E, ASKL\_UN, ASKL\_HE, ASKL\_E, AIKL\_UN, AIKL\_HE, and AIKL\_E) samples with the neat Ecoflex™ (ECO) control at 1745%

#### 4.2.2.4 Toughness

Toughness is an important material property which requires a balance of strength and ductility. Toughness is a materials ability to absorb energy and plastically deform without fracturing and it was calculated using the area under the engineering stress/strain curve of the five averaged samples from each lot. The combination of high ultimate tensile strength and high elongation at break leads to a material with a high toughness.

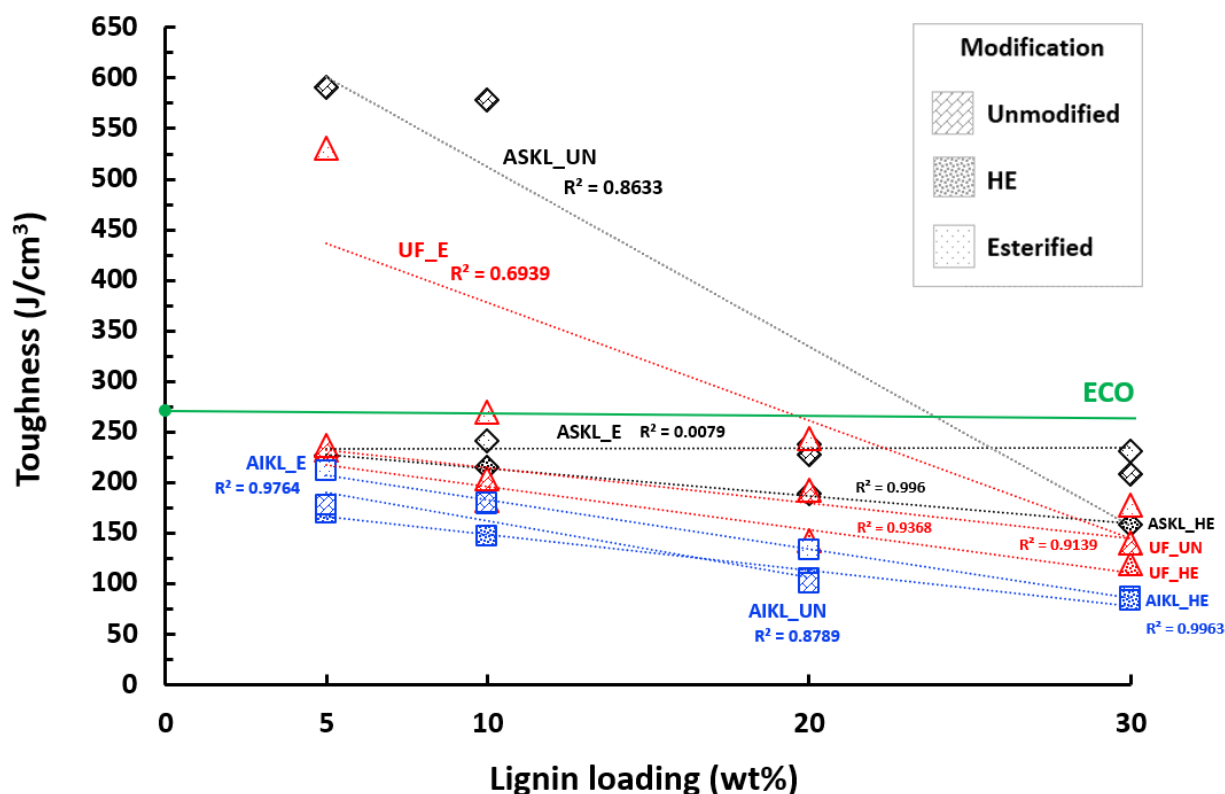
The toughness ( $\text{J}/\text{cm}^3$ ) was reported in Figure 50 for all nine lignin powders at 5, 10, 20, and 30 wt% loading, with ASKL\_E loaded to 40 wt%. There was a decrease in toughness for all lignin powders at all weight percentage loadings except for UF\_E 5 wt%, ASKL\_UN 5 wt% and 10 wt% which showed an increase in toughness compared to neat Ecoflex<sup>TM</sup> ( $271 \text{ J}/\text{cm}^3$ ). In comparison to the Ecoflex<sup>TM</sup> control, the toughness for 5 wt% UF\_E increased by 96% to  $531 \text{ J}/\text{cm}^3$  and increased for ASKL\_UN 5 and 10 wt% by 118% and 113% to  $591 \text{ J}/\text{cm}^3$  and  $578 \text{ J}/\text{cm}^3$ . The ASKL\_E lignin powder loaded between 5 and 40 wt% showed only a slight decrease in toughness by 8.9% to  $247 \text{ J}/\text{cm}^3$ . The AIKL powders showed the greatest reduction in fracture strain with AIKL\_HE at 30 wt% showing the greatest reduction of 69% to  $83 \text{ J}/\text{cm}^3$ . For comparison the tensile toughness reported by other research groups for different materials is as follows: Galeja et al. tested 3D printed acrylonitrile butadiene styrene (ABS) natural white (2W) samples at an optimal  $55^\circ$  winding angle and reported  $98 \pm 14 \text{ J}/\text{cm}^3$ , Maphutha et al. tested carbon nanotubes in a polymer composite solution at 7.5 wt% and reported  $0.31 \text{ J}/\text{cm}^3$ , Hilburg et al. blended softwood kraft lignin with polystyrene and reported  $0.014 \text{ MJ}/\text{m}^3$ , Sun et al. blended 2% functionalized lignin with epoxy and reported  $1.7 \text{ MJ}/\text{m}^3$ , and Lou et al. reported  $3.5 \text{ J}/\text{cm}^3$  for a dry-wet cycle emulsion-cement composite.<sup>219–223</sup>



**Figure 50 Toughness for neat Ecoflex (ECO), unfractionated unmodified (UF\_UN), unfractionated hydroxyethyl ether (UF\_HE), unfractionated esterified (UF\_E), acetone soluble unmodified (ASKL\_UN), acetone soluble hydroxyethyl ether (ASKL\_HE), acetone soluble esterified (ASKL\_E), acetone insoluble unmodified (AIKL\_UN), acetone insoluble hydroxyethyl ether (AIKL\_HE), and acetone insoluble esterified (AIKL\_E) at a lignin loading of 5, 10, 20, and 30 wt% with ASKL\_E blended to 40 wt%**

Figure 51 showed the toughness as a function of wt% loading for all nine lignin powders allowing a side by side comparison in performance. The addition of most lignin powders into the plastic decreased the toughness in comparison to neat Ecoflex<sup>TM</sup>. AIKL\_UN, AIKL\_HE, and AIKL\_E demonstrated the greatest reduction in toughness at all loadings, while UF\_E and ASKL\_UN at lower lignin loadings showed a remarkable increase in toughness when compared to neat Ecoflex<sup>TM</sup>. There is a strong linear correlation between an increase in wt% loading of lignin powder and a decrease in toughness of blended material as can be seen with  $R^2$  values ranging from 0.69 to 0.99. The line for ASKL\_E showed a low  $R^2$  value because with increasing

wt% lignin the material does not show much change in toughness as noted in the other properties. In general, there was a strong linear correlation, as lignin powder increased in the blend there was a resultant decrease in toughness.



**Figure 51** Toughness as a function of wt% lignin loading for unfractionated, acetone soluble, and acetone insoluble, unmodified, hydroxyethyl ether, and esterified (UF\_UN, UF\_HE, UF\_E, ASKL\_UN, ASKL\_HE, ASKL\_E, AIKL\_UN, AIKL\_HE, and AIKL\_E) samples with the neat Ecoflex™ (ECO) control at 271 J/cm<sup>3</sup>

The relationship between total elongation at break and toughness can be seen in Figure 52a (UF\_UN, ASKL\_UN, AIKL\_UN), 52b (UF\_HE, ASKL\_HE, AIKL\_HE) and 52c (UF\_E, ASKL\_E, AIKL\_E) which is broken into four quadrants. There were no data points that lie in quadrant one or quadrant three, which indicated that in comparison to neat Ecoflex™ the materials under investigation, 1) did not decrease in toughness while increasing in percent

elongation at break or, 2) increase in toughness while decreasing in percent elongation at break. Most of the data points lie in quadrant four which is indicative of a decrease in percent elongation and a reduction in toughness in comparison to neat Ecoflex<sup>TM</sup>. Quadrant two, where 5 wt% UF\_E and 5 and 10 wt% ASKL\_UN data points lie is indicative of an increase in total percent elongation at break and a greater toughness value in comparison to neat Ecoflex<sup>TM</sup>. As displayed in Figure 52b, the hydroxyethyl ether modified lignin fractions showed a strong linear regression behavior with  $R^2$  values equaling 0.99. This result indicated that as hydroxylated lignin is increasingly loaded into blend, the material properties consistently deteriorate. The same behavior was portrayed in Figure 52a and 52c however, the ASKL\_E lignin powder at all wt% loading hovered close to the neat Ecoflex<sup>TM</sup> values.

There are several things to consider moving forward, like why the acetone soluble fraction of the softwood kraft lignin both modified and unmodified seemed to retain or improve mechanical properties while the insoluble fraction showed a consistent decline in mechanical properties with added lignin to blend. Unexpectedly, the unfractionated esterified lignin powder showed an increase in mechanical properties at lower lignin loadings while the acetone soluble esterified lignin powder remained nearly unchanged even at higher lignin loadings when compared to neat Ecoflex<sup>TM</sup>. As expected, the lignin modifications (HE and E) performed quite different in melt compared to one another and their unmodified counterpart, namely the increase in UTS and toughness for 5 and 10 wt% ASKL\_UN. The next section will analyze these results and offer some explanation.



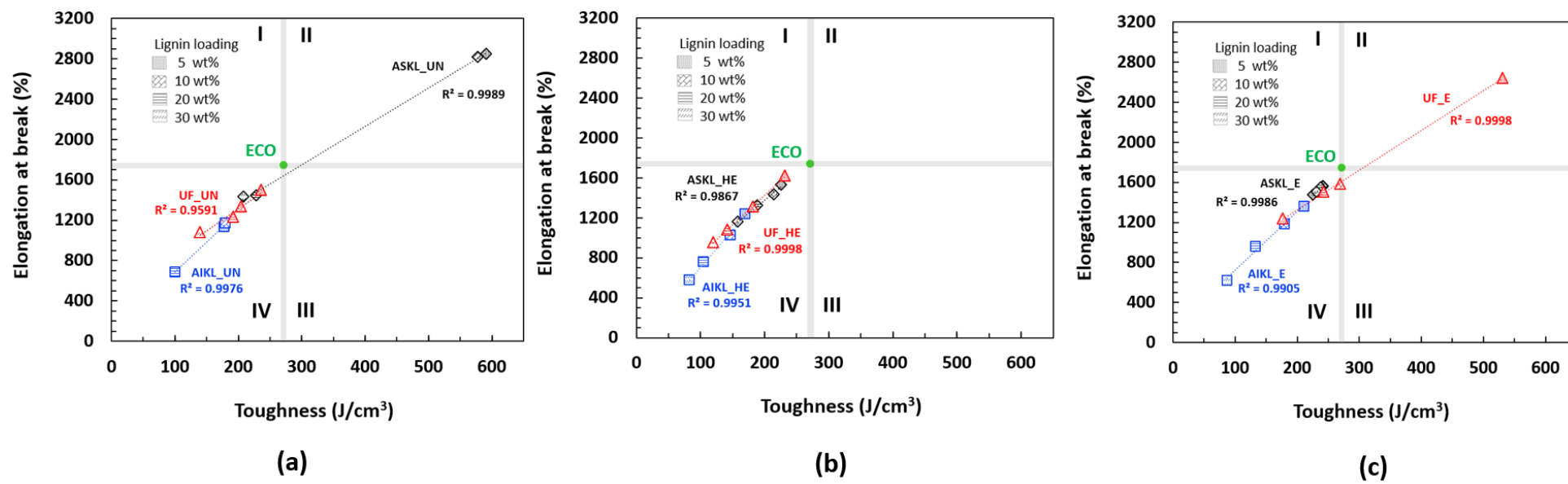


Figure 52 Total elongation at break as a function of toughness for unfractionated, acetone soluble, and acetone insoluble, unmodified, hydroxyethyl ether, and esterified (UF\_UN, UF\_HE, UF\_E, ASKL\_UN, ASKL\_HE, ASKL\_E, AIKL\_UN, AIKL\_HE, AIKL\_E) samples with the neat Ecoflex™ (ECO) control at  $271 \text{ J}/\text{cm}^3$ , 1745%

### 4.2.3 Analysis of tensile properties of lignin-Ecoflex™ thermoplastic blends

A summary of the mechanical properties of the lignin-Ecoflex™ blends is presented in Tables 14-17, (UTS, Young's modulus, total percent elongation at break, and toughness) which provides an increase (+) or a decrease (-) for the given mechanical property by percentage as related to the Ecoflex™ control at the relevant wt% loaded lignin powder.

**Table 14 The ultimate tensile strength of neat Ecoflex™ (ECO) and the percent increase (+) or decrease (-) of the nine lignin powders loaded in melt (5-40 wt%) in comparison to the Ecoflex™ control**

Lignin loading	ECO	UF_UN	UF_HE	UF_E	ASKL_UN	ASKL_HE	ASKL_E	AIKL_UN	AIKL_HE	AIKL_E
0 wt%	23.1 MPa	23.1 MPa	23.1 MPa	23.1 MPa	23.1 MPa	23.1 MPa	23.1 MPa	23.1 MPa	23.1 MPa	23.1 MPa
5 wt%	/	-5.6%	-11%	+29%	+36%	-8.2%	-2.2%	-12%	-20%	-5.6%
10 wt%	/	-7.8%	-18%	+6%	+36%	-11%	-1.7%	-13%	-21%	-12%
20 wt%	/	-5.2%	-27%	-0.88%	-1.7%	-19%	-2.2%	-26%	-29%	-24%
30 wt%	/	-25%	-32%	-13%	-11%	-25%	-5.2%	/	-37%	-29%
40 wt%	/	/	/	/	/	/	-9.5%	/	/	/

**Table 15 The Young's modulus of neat Ecoflex™ (ECO) and the percent increase (+) or decrease (-) of the nine lignin powders loaded in melt (5-40 wt%) in comparison to the Ecoflex™ control**

Lignin loading	ECO	UF_UN	UF_HE	UF_E	ASKL_UN	ASKL_HE	ASKL_E	AIKL_UN	AIKL_HE	AIKL_E
0 wt%	31.6 MPa	31.6 MPa	31.6 MPa	31.6 MPa	31.6 MPa	31.6 MPa	31.6 MPa	31.6 MPa	31.6 MPa	31.6 MPa
5 wt%	/	+12%	+26%	+4.2%	+5.4%	+9.8%	+10%	+21%	+20%	+16%
10 wt%	/	+13%	+24%	+5.7%	+7.4%	+23%	-3.1%	+35%	+34%	+26%
20 wt%	/	+20%	+32%	+9.4%	+75%	+40%	-0.63%	+92%	+61%	+48%
30 wt%	/	+41%	+32%	+3.5%	+84%	+49%	+4.4%	/	+98%	+95%
40 wt%	/	/	/	/	/	/	+62%	/	/	/

**Table 16 The total percent elongation at break of neat Ecoflex™ (ECO) and the percent increase (+) or decrease (-) of the nine lignin powders loaded in melt (5-40 wt%) in comparison to the Ecoflex™ control**

Lignin loading	ECO	UF_UN	UF_HE	UF_E	ASKL_UN	ASKL_HE	ASKL_E	AIKL_UN	AIKL_HE	AIKL_E
0 wt%	1745 %	1745%	1745%	1745%	1745%	1745%	1745%	1745%	1745%	1745%
5 wt%	/	-14%	-7.2%	+51%	+63%	-12%	-16%	-35%	-29%	-22%
10 wt%	/	-23%	-25%	-9.1%	+61%	-18%	-10%	-33%	-41%	-32%
20 wt%	/	-30%	-38%	-14%	-17%	-24%	-11%	-61%	-56%	-45%
30 wt%	/	-38%	-45%	-29%	-18%	-34%	-14%	/	-67%	-65%
40 wt%	/	/	/	/	/	/	-6.1%	/	/	/

**Table 17 The toughness of neat Ecoflex™ (ECO) and the percent increase (+) or decrease (-) of the nine lignin powders loaded in melt (5-40 wt%) in comparison to the Ecoflex™ control**

Lignin loading	ECO	UF_UN	UF_HE	UF_E	ASKL_UN	ASKL_HE	ASKL_E	AIKL_UN	AIKL_HE	AIKL_E
0 wt%	271 J/cm <sup>3</sup>	271 J/cm <sup>3</sup>	271 J/cm <sup>3</sup>	271 J/cm <sup>3</sup>	271 J/cm <sup>3</sup>	271 J/cm <sup>3</sup>	271 J/cm <sup>3</sup>	271 J/cm <sup>3</sup>	271 J/cm <sup>3</sup>	271 J/cm <sup>3</sup>
5 wt%	/	-13%	-14%	+96%	+118%	-17%	-17%	-34%	-37%	-22%
10 wt%	/	-25%	-33%	-0.74%	+113%	-21%	-11%	-34%	-46%	-34%
20 wt%	/	-29%	-48%	-10%	-17%	-30%	-12%	-63%	-61%	-51%
30 wt%	/	-48%	-56%	-35%	-23%	-42%	-15%	/	-69%	-68%
40 wt%	/	/	/	/	/	/	-8.9%	/	/	/

To generalize the above tables, as lignin loading increased to 30 wt% for all nine lignin powders, tensile strength, total elongation at break, and toughness decreased while stiffness increased. Ecoflex™ is an outstanding alternative for competitive polyolefins like LDPE or PP because of its ability to biodegrade without persisting in the natural environment but it is relatively expensive, so adding lignin without a major loss of mechanical properties is the objective.<sup>214</sup> Ecoflex™ contains aromatic rings within its structure which allow strong  $\pi$  stacking interactions with lignin and therefore potentially better compatibility than blending with most

polyolefins. Several research groups found that maintaining or improving the tensile properties of lignin/PE or PP blends was difficult without lignin modification plus the assistance of a plasticizer or compatibilizer and still, blending beyond a 20-25 wt% lignin loading the tensile properties completely deteriorated.<sup>144,189,224</sup>

Ecoflex<sup>TM</sup> is a semi-crystalline polymer and the deformation behavior is complex because of the chain entangled amorphous regions and the crystals found in the crystalline region. During tensile testing both the amorphous and crystalline phases become oriented and mechanisms like crazing, shear bonding, and cavitation affect the mechanical properties of the final material.<sup>225</sup> Cavitation is common in semicrystalline polymers like Ecoflex<sup>TM</sup> when deformation occurs above the glass transition temperature (-27.9 °C) and the crystals act as stress concentrators forming cavities in the amorphous region.<sup>144,192,225</sup> Free volume pores also exist in the amorphous region and grow bigger during cold drawing of the polymer during tensile testing.<sup>192</sup> When a complex filler polymer like lignin is added to a hydrophobic semicrystalline polyester like Ecoflex<sup>TM</sup> other possible mechanisms like debonding can occur.<sup>192</sup> Debonding of the matrix (Ecoflex<sup>TM</sup>) – particle (lignin) interface shifts the load transfer during tensile testing and lignin absorbs energy during deformation which can result in enhanced mechanical properties of the resultant blend.<sup>192</sup> However, deformation is far more complex and the tensile strength of a heterogenous material depends on the strength of interfacial adhesion which is determined by contact surface of the phases, strength of interactions, and lignin particle size.<sup>188,225</sup> Debonding stress tends to increase with decreasing particle size and less voids are formed leading to fracture at higher strains.<sup>188,225</sup>

#### 4.2.3.1 Unmodified lignin-Ecoflex™ thermoplastic blends

With the addition of unfractionated unmodified (UF\_UN) and acetone insoluble unmodified (AIKL\_UN) lignin powder to Ecoflex™ in melt, the resultant blend showed a decrease in tensile strength, fracture strain, and toughness and an increase in stiffness. The unfractionated lignin powder did not show a drastic decrease in strength until 30 wt% while the insoluble fraction could not be blended at 30 wt%. Because of the larger particle sizes arising from aggregation of the lignin, the high molecular weight fraction (AIKL) has less specific surface area which disturbs stress transfer between lignin and the continuous Ecoflex™ matrix. The melt processing temperature for all blends was 180 °C and the glass transition temperature for AIKL\_UN is 208 °C meaning AIKL\_UN remained in its glass state during thermal processing. During melt mixing the AIKL\_UN fraction acted like solid particles which led to poor blending with discrete particles. In addition, with no modification to mask the aliphatic and aromatic hydroxyl groups the lignin molecule was polar and hydrogen bonding led to lignin agglomeration and potential crosslinking at the processing temperature. If lignin agglomerates and is unevenly distributed, stress cannot transfer homogeneously through the matrix. Sadeghifar et al. reported a major deterioration in tensile properties for AIKL-PE blends at 20 wt% lignin citing the larger the polymer the more likely lignin was to crosslink; lignin-lignin interactions are notoriously brittle which results in a lower strength and toughness of the final material.<sup>189</sup>

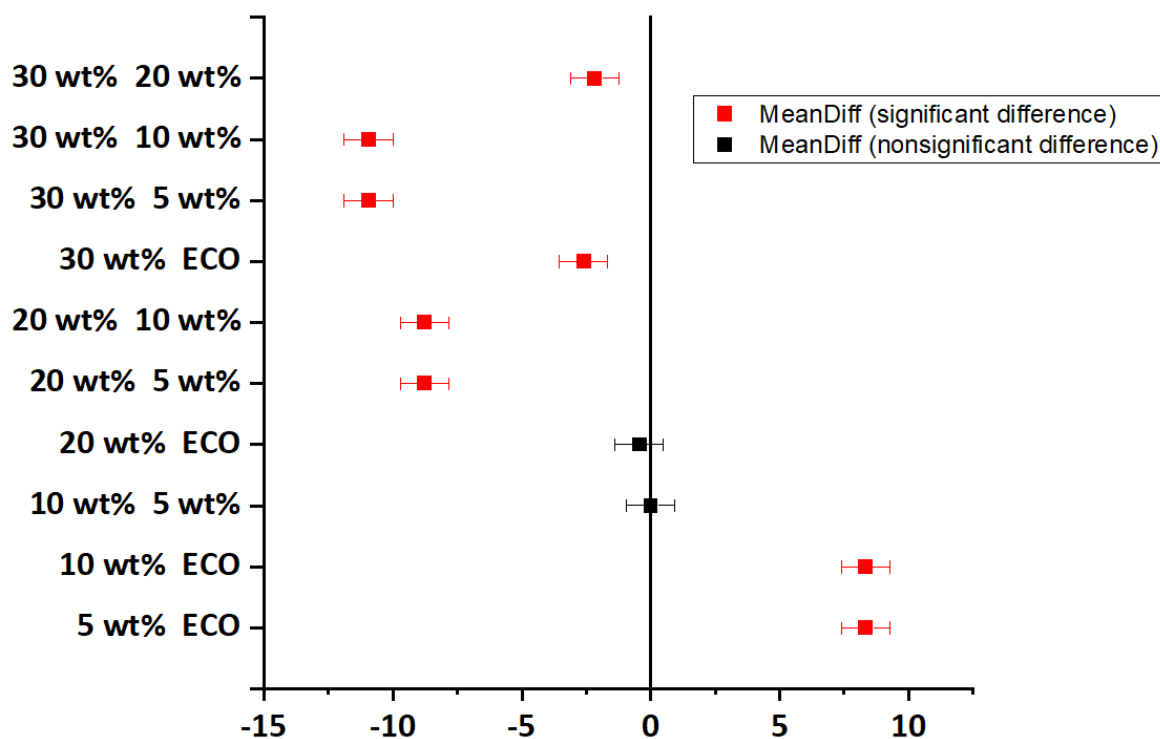
The unfractionated parent lignin in the current study showed better blendability with Ecoflex™ with the greatest loss of strength at 30 wt% loading. This result was likely due to the glass transition temperature being 162 °C which puts the lignin polymer in its rubbery state during thermal processing. Kargarzadeh et al recently reported unfractionated and unmodified kraft lignin particles blended with Ecoflex™ at a thermal processing temperature of 180 °C into

1mm thin films and showed an increase in strength, strain at break and Young's modulus at very low lignin loadings (0.5 wt%) followed by a decrease at 6 wt% loading.<sup>192</sup> At higher amounts of lignin powder in blend, the stress concentration zones which surround the lignin particles merge and this can lead to premature fracture of tensile tested material.

The acetone soluble unmodified lignin powder (ASKL\_UN) showed the greatest increase in mechanical properties at 5 wt% and 10 wt% lignin loading. This result was an unexpected outcome and led to a repeat in the experiment with another five samples for each of the loadings which produced similar results. At a lignin loading up to 10 wt% ASKL\_UN showed up to a 36% increase in strength, an 118% increase in toughness and a 7.4% increase in stiffness when compared to the neat Ecoflex<sup>TM</sup> control. These numbers are significant for enhancing the properties of materials with an additive or blend component. This study asked the question, what is the least amount of lignin modification chemistry needed to make the best lignin-Ecoflex<sup>TM</sup> blend? Unexpectedly, the unmodified low molecular weight fraction (ASKL\_UN) significantly improved the mechanical properties of Ecoflex<sup>TM</sup>.

A one-way analysis of variance (ANOVA) is an important tool which allows researchers to determine whether the mean difference between groups of data are statistically significant. Before developing an understanding as to why ASKL\_UN showed the greatest increase in tensile properties, it was first necessary to see if the observed differences were statistically significant. In this scenario the continuous dependent variable is ultimate tensile strength (UTS) and the categorical independent variable is 0, 5, 10, 20, and 30 wt% ASKL\_UN lignin loading, where 0 wt% lignin is the neat Ecoflex<sup>TM</sup> control (ECO). The standard hypotheses for one-way ANOVA tests are null, all group means are equal, and alternative, not all group means are equal. If the p-value is less than the significance level of 0.05 the null hypothesis was rejected. In the ANOVA

for the UTS of ASKL\_UN powders at different lignin loadings the p value was equal to 3.7 E-20 which is less than 0.05 so the null hypothesis was rejected. This meant at least one sample lot is different from another sample lot, but the ANOVA alone does not indicate which sample. To determine which sample lots are statistically different a post hoc Tukey test was performed. Tukey's method covers all combinations of groups and individually adjusts p-values for each comparison. A hypothesis test with a significance level of 0.05 corresponds to 95% confidence intervals and a 5% experiment-wise error rate. Figure 53 illustrated a simple visual assessment of statistical significance between specific groups and allowed further conclusions to be drawn aside from the overall p-value alone.



**Figure 53** Tukey simultaneous 95% confidence intervals (CIs) difference of means for ultimate tensile strength (UTS) of acetone soluble unmodified softwood kraft lignin powders (ASKL\_UN) at different lignin loadings (0, 5, 10, 20, 30 wt%) where 0 wt% ASKL\_UN is the neat Ecoflex™ control (ECO)

In Figure 53, when a group mean on the y-axis had an interval that contained zero there was no statistical significance between the groups and when a confidence interval did not contain zero, there was statistical significance between the groups. The y-axis shows which two groups were being compared, for instance 10 wt% ECO is defined as 10 wt% ASKL\_UN in blend with 90 wt% Ecoflex<sup>TM</sup> being compared to neat Ecoflex<sup>TM</sup> (ECO) which is 0 wt% ASKL\_UN. The x-axis represents the mean differences that were found between those pairs. In the case of 10 wt% ECO there is a statistical significance between means. The 10 wt% ASKL\_UN blend indicated a mean increase of approximately 8.5 when compared to neat Ecoflex<sup>TM</sup>. There was no statistical significance between 5 and 10 wt% ASKL\_UN in blend and furthermore the 20 wt% ASKL\_UN lignin blend does not significantly change the mean strength of neat Ecoflex<sup>TM</sup> (Figure 53). The conclusion that can be drawn from this statistical analysis is that ASKL\_UN lignin powder can be blended up to 10 wt% for an increase in tensile properties and up to 20 wt% to maintain the original properties of neat Ecoflex<sup>TM</sup>. In addition, the narrow width of the confidence intervals is indicative of the precision of this estimate.

Tensile strength depends on stress transfer between lignin and Ecoflex<sup>TM</sup> which is affected by particle size, particle distribution, and particle/matrix interfacial strength. A stable and strong bond between filler and matrix is necessary for a blended material to have improved mechanical properties in filled systems. The acetone soluble unmodified lignin powder still contained reactive polar aromatic and aliphatic hydroxyl groups, but the low molecular weight and low PDI established a lignin consisting of small molecules. During tensile stretching filler particles can localize shear and stress zones because of the different mechanical properties of each component. In a polymer blend (analogous to a metal alloy) the second component could be fully dispersed at the molecular level. These zones most likely located in polar regions can cause

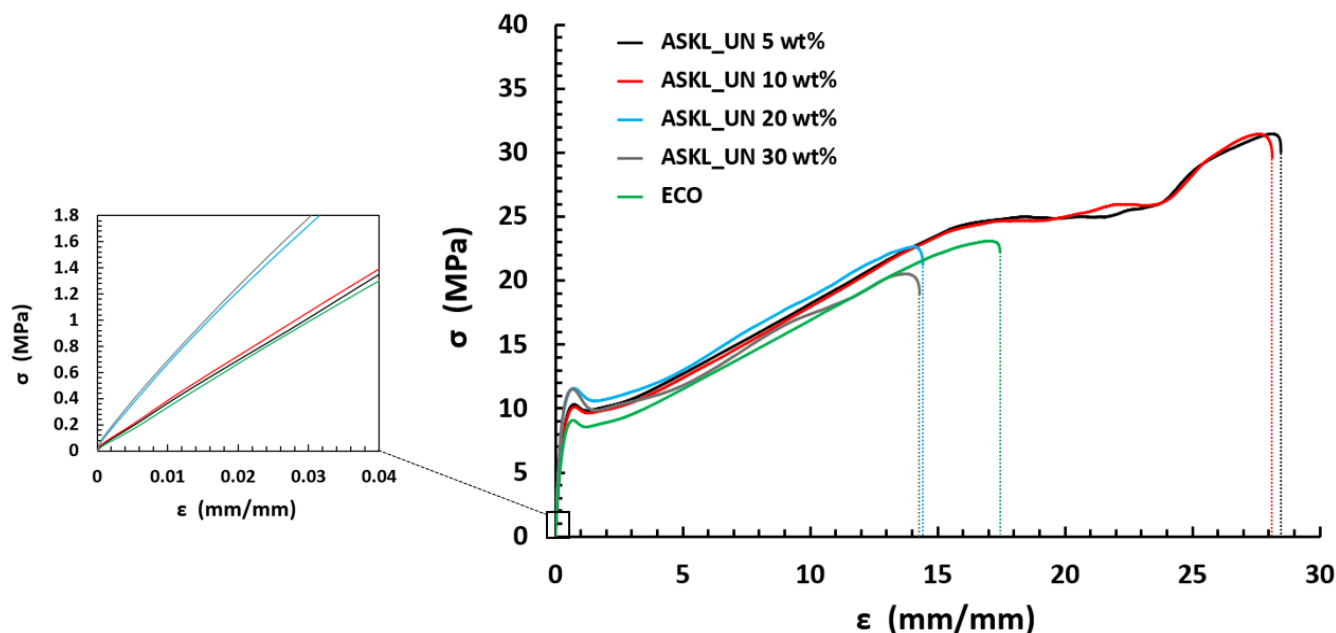


debonding in the matrix-lignin interface and form micro-voids which no longer transmit stress. After the formation of micro-voids, the matrix deforms plastically through the bulk of the material in the direction of stretch and visible whitening was noted with alignment of polymer chains. Whether the tensile properties increase, or decrease depends upon interfacial adhesion. Because the tensile properties for the Ecoflex<sup>TM</sup> - ASKL\_UN blend increased at a 10 wt% lignin loading it is assumed there was good interfacial adhesion between the lignin polymer and the Ecoflex<sup>TM</sup> polymer matrix. The presence of the lignin at this loading level did not overwhelm the matrix material but instead it served as a stress transfer agent in the semi-crystalline polymer. This is a novel finding as there are no other research groups that have increased mechanical properties to this extent for an unmodified lignin fraction.

Figure 54 showed the engineering stress/strain curves (average of five samples) with the Young's modulus inset for ASKL\_UN at all loadings compared to neat Ecoflex<sup>TM</sup>. For ASKL\_UN 5 and 10 wt% there was a second yielding event which drastically increased tensile strength, fracture strain, and therefore toughness while only slightly increasing the materials stiffness. For ASKL\_UN 20 wt% tensile strength was retained while fracture strain and toughness decreased but stiffness increased.

Wang et al. who blended hardwood esterified lignin with a coupling reagent and Ecoflex<sup>TM</sup> studied the interaction energy of the developed films. The group found that the higher the non-covalent bond energy, van der Waals interactions and electrostatic potential energy are between the polymers, the better the compatibility. They reported the highest interaction energies for their films were associated with a particular melt temperature speculating a correlation between melt temperature, lignin-Ecoflex<sup>TM</sup> compatibility and therefore mechanical properties. The glass transition temperature for ASKL\_UN was 125 °C so the 180 °C melt temperature

could be the ideal temperature to optimize interaction energy and potentially allow some transesterification between the polymers. Molecular dynamic simulation should be done to calculate the interaction energy at the blend interface and confirm speculation.



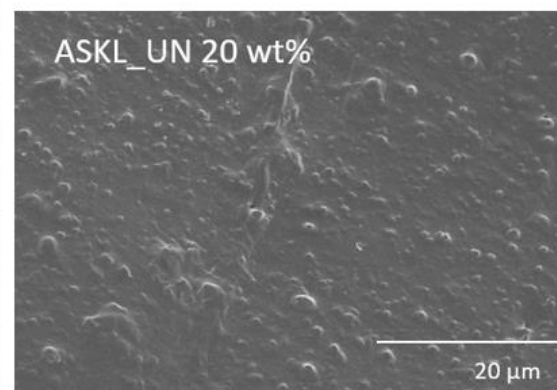
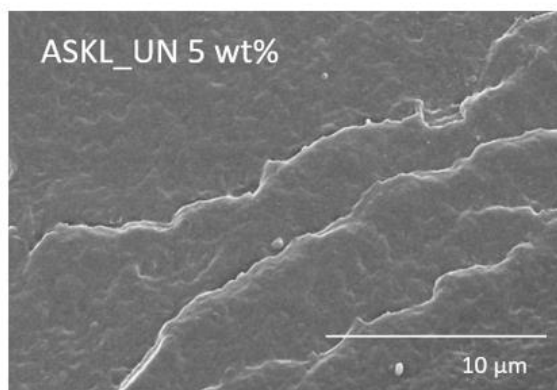
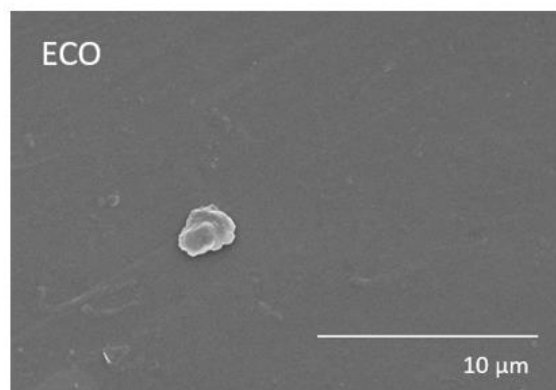
**Figure 54 Engineering stress strain curves (average of five samples) with inset Young's modulus (average of five samples) for acetone soluble unmodified samples (ASKL\_UN) at 5, 10, 20, 30 wt% lignin loading as compared to neat Ecoflex™ (ECO)**

The SEM images of the ASKL\_UN-Ecoflex™ thermoplastic blends at 5 and 20 wt% lignin loading can be seen in Figure 55a which represented the cryo-fractured samples and Figure 55b which represented a cross section of the fractured surface after tensile testing was carried out with the Instron load frame. Figure 55a showed only a slight 'puffing' or expansion of the surface at 5 wt% ASKL\_UN loading but the interface between the ASKL lignin component and the Ecoflex™ matrix is indistinguishable. However, at 20 wt% ASKL\_UN, small lignin particles with preserved spherical shapes were observed in the Ecoflex™ matrix.

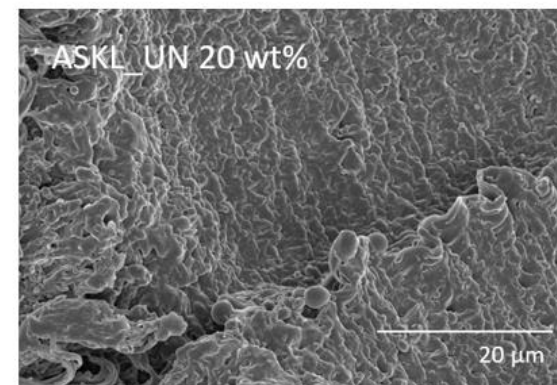
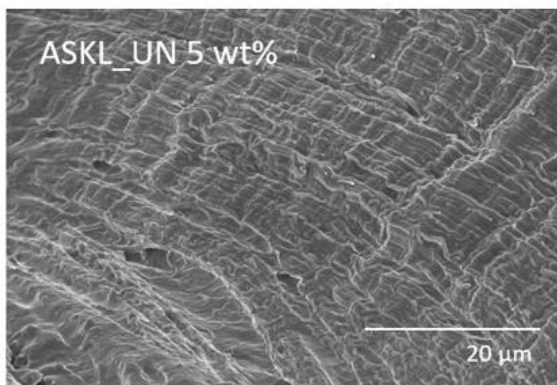
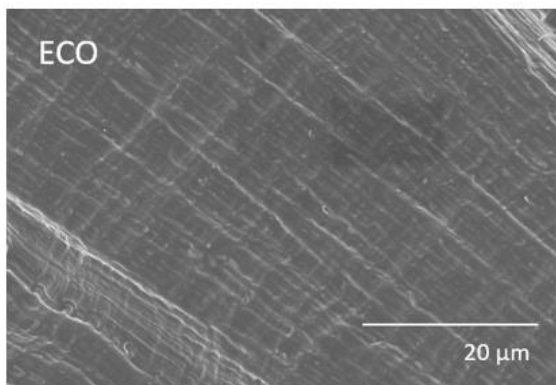
These observed spheres were very small in size and have a large surface area. As previously discussed, the small lignin particles dispersed in the Ecoflex<sup>TM</sup> matrix can help to transfer stress evenly thus improving mechanical properties. Figure 55b which examined the fracture site showed a comparably rougher surface at 20 wt% ASKL\_UN. However, at both 5 and 20 wt% ASKL\_UN loading it appeared the lignin had evenly dispersed throughout the Ecoflex<sup>TM</sup> matrix.

Chen et al. reported large 50  $\mu\text{m}$  lignin agglomerates in their lignin-Ecoflex thermoplastic blends, citing the formation of intermolecular lignin-lignin bonds.<sup>213</sup> The formation of these large particles would reduce surface area for stress between the Ecoflex<sup>TM</sup> matrix and the lignin.<sup>213</sup> The lignin spheres observed in Figure 55a and 55b are much smaller, on the scale of single digit microns, and no evidence of pull out or separated particles is present. This observation indicates interfacial interactions between the low molecular weight ASKL\_UN powder and the Ecoflex<sup>TM</sup> matrix and confirms prior speculation that the smaller lignin filler particles act as stress transfer agents that likely strengthen the blend.

(a)



(b)



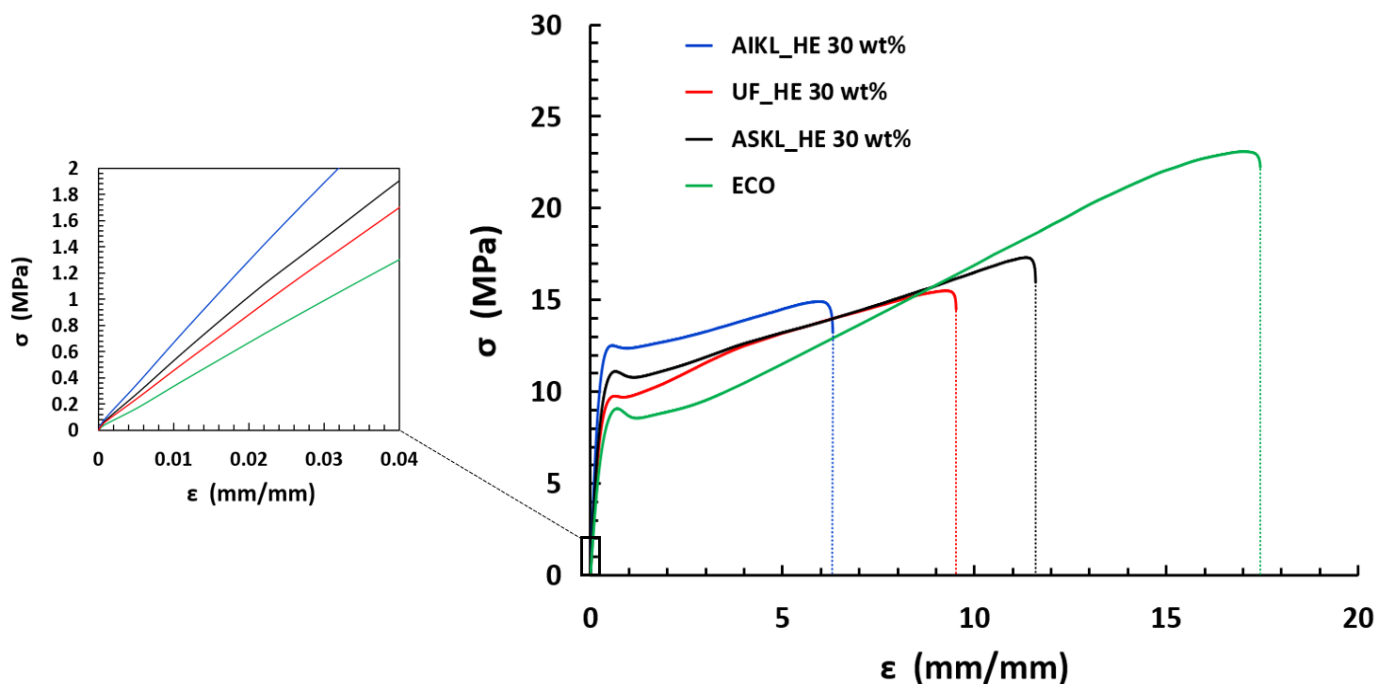
**Figure 55 SEM images of neat Ecoflex (ECO) blended with 5 and 20 wt% acetone soluble unmodified lignin powders (ASKL\_UN) frozen and fractured (a) and a cross section of the fractured surface after tensile testing is carried out (b)**

#### 4.2.3.2 Hydroxyethyl ether lignin-Ecoflex<sup>TM</sup> thermoplastic blends

With the addition of unfractionated, acetone soluble and acetone insoluble etherified lignin powder to Ecoflex<sup>TM</sup> in melt, the resultant blends showed a systematic decrease in tensile strength, fracture strain, and toughness and an increase in stiffness with increasing amounts of lignin. For all three fractions, as lignin loading increased towards 30 wt% there was a sharply negative linear regression in UTS, Young's modulus and toughness and a positive linear increase in stiffness of the material. As discussed in *section 4.1.3.2* there were some side reactions during the HE process which resulted in unwanted crosslinking between lignin from ethylene carbonate giving rise to larger lignin molecules. Overall, there was an increase in molecular weight for all HE fractions of lignin with AIKL reporting only the molar mass values for its soluble portion. The inability of AIKL\_HE to fully solubilize indicated potential crosslinking between AIKL lignins. ASKL\_HE showed a distinct bimodal distribution. All three fractions had polar primary alcohol groups available for hydrogen bonding in melt with Ecoflex<sup>TM</sup> and with other lignin molecules.

Ecoflex<sup>TM</sup> undergoes stress induced crystallization which increases the force required to fracture the material but added HE lignin served as defects and prevented the polymer chains from slipping and thus creating a stiffer blend. With potentially reduced chain entanglement and a lowered degree of stress induced crystallinity for Ecoflex<sup>TM</sup>, ultimate tensile strength, total elongation at break and toughness will all decrease for the produced blend. In addition, there could be a lack of strong interfacial interactions due to lignin agglomeration which caused an uneven distribution of stress transfer throughout the Ecoflex<sup>TM</sup> - lignin matrix.

The engineering stress/strain curves was illustrated in Figure 56 with the Young's modulus inset for UF\_HE, ASKL\_HE, and AIKL\_HE at a 30 wt% lignin loading compared to neat Ecoflex<sup>TM</sup>. The acetone soluble fraction (ASKL\_HE) shows the highest tensile strength and toughness at 30 wt% while the acetone insoluble portion (AIKL\_HE) shows the greatest stiffness. There is potential application for the hydroxyethyl ether modified lignins in a material that requires a high stiffness. The HE lignins do improve the modulus of Ecoflex<sup>TM</sup> which is relatively low on its own however, there was associated loss in tensile strength.



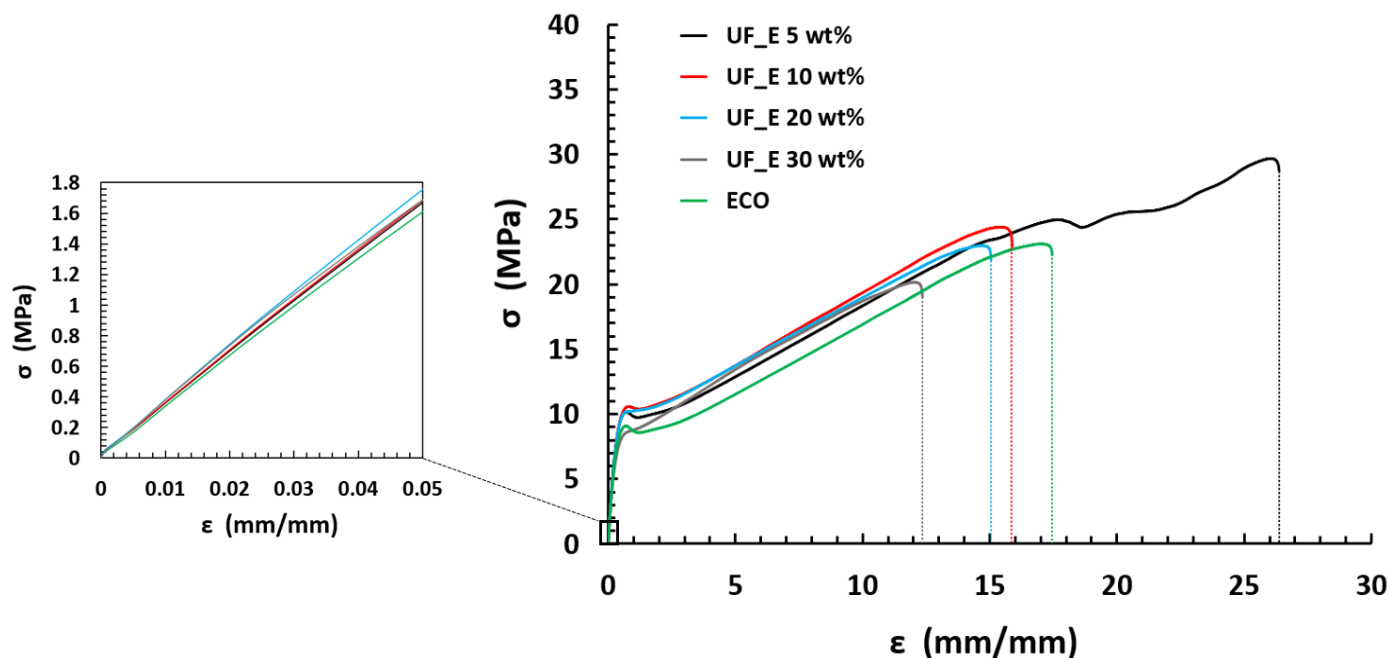
**Figure 56** Engineering stress strain curves (average of five samples) with inset Young's modulus (average of five samples) for UF\_HE, ASKL\_HE, and AIKL\_HE at 30 wt% lignin loading as compared to neat Ecoflex<sup>TM</sup> (ECO)

#### 4.2.3.3 Esterified lignin-Ecoflex<sup>TM</sup> thermoplastic blends

With the addition of unfractionated, acetone soluble and acetone insoluble esterified lignin powder to Ecoflex<sup>TM</sup> in melt, the resultant blends showed differing mechanical behavior based on fraction. The UF\_E lignin powder loaded at 5 wt% demonstrated an increase in tensile strength, toughness, and stiffness. The ASKL\_E lignin powder was the most stable in melt and the resultant blend up to 30 wt% lignin loading showed a minor loss in tensile strength and toughness when compared to neat Ecoflex<sup>TM</sup>. This prompted the blending of ASKL\_E at 40 wt% which increased the stiffness of the material while still maintaining strength and toughness. The AIKL\_E still showed a systematic decrease in tensile strength and toughness and an increase in stiffness with the addition of lignin powder at all loading levels. However, the acetone insoluble esterified lignin powder did show improved performance as compared to its unmodified and hydroxyethyl ether counterparts.

All fractions of the esterified lignin powders had very polar hydroxyl groups replaced by less polar ester groups during the modification with propionic acid. This esterification was responsible for better dispersion of the lignin into the Ecoflex<sup>TM</sup> matrix because there were weaker interactions among lignin molecules as noted with a reduced  $T_g$ . While the tensile strength for all fractions decreased by 30 wt% added lignin, the extent of the decrease was smaller for the esterified lignins compared to the unmodified and HE lignins. Additionally, it was physically easier to process, blend and extrude all esterified samples from the micro compounder. To keep samples uncontaminated, no waxes or lubricants were used in the dumbbell specimen mould and esterified specimens were the easiest to remove.

The unfractionated esterified lignin powder loaded at a 5 wt% lignin loading with Ecoflex<sup>TM</sup> showed a 29% increase in tensile strength, a 96% increase in toughness, and a 4.2% increase in stiffness compared to neat Ecoflex<sup>TM</sup>. By 10 wt% there was a 6% increase in tensile strength, a 1% decrease in toughness, and a 5.7% increase in stiffness compared to neat Ecoflex<sup>TM</sup>. The engineering stress/strain curves for the unmodified esterified samples were displayed in Figure 57 with the Young's modulus inset for UF\_E at all loadings compared to neat Ecoflex<sup>TM</sup>. At 5 wt% loading the UF\_E lignin sample tests revealed the same second yielding phenomena that ASKL\_UN showed at 5 and 10 wt% loading. It can be observed that UF\_E loaded up to 20 wt% showed good strength and toughness compared to neat Ecoflex<sup>TM</sup> and UF\_E loaded up to 30 wt% did not show a substantial change in stiffness of the blend when compared to neat Ecoflex<sup>TM</sup>.



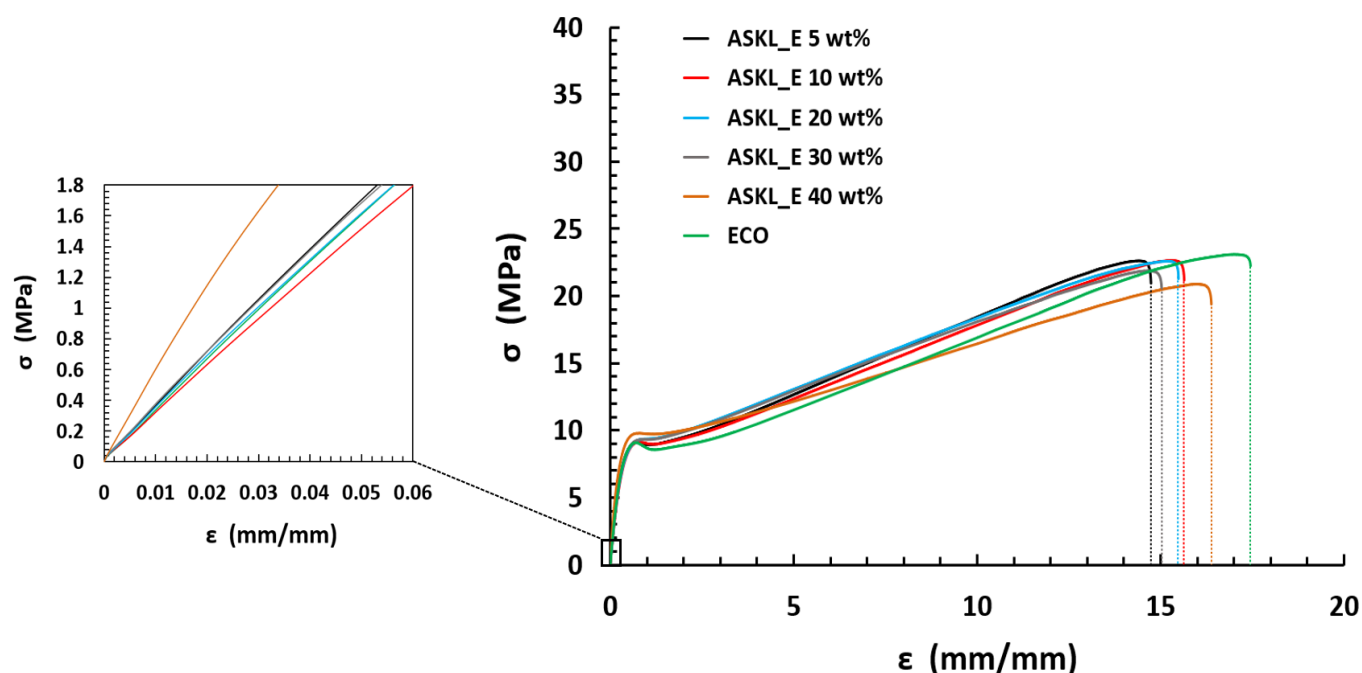
**Figure 57** Engineering stress strain curves (average of five samples) with inset Young's modulus (average of five samples) for UF\_E at 5, 10, 20, 30 wt% lignin loading as compared to neat Ecoflex<sup>TM</sup> (ECO)



This was an important observation as the tensile strength of the 30 wt% UF\_E blend has only decreased by 13% while the stiffness has increased by 3.5%. This finding challenges the phenomenon that generally the fractionated lignin portions perform best in melt with polymers like Ecoflex<sup>TM</sup> and PE.<sup>188,189,213</sup>

The acetone soluble esterified lignin powder was blended up to 40 wt% with a good retention of mechanical properties when compared to neat Ecoflex<sup>TM</sup>. ASKL\_E at a 40 wt% lignin loading had a higher tensile strength than all the AIKL powders at all loadings except for 5 wt% AIKL\_E. This outcome highlighted the real difference in fractional performance, where the bulkier high molecular weight AIKL consistently showed the greatest loss in strength and toughness, even when modified. At 40 wt% ASKL\_E tensile strength, total elongation at fracture, and toughness had decreases by a mere 9.5%, 6.1%, and 8.9% while the blend showed an increase in stiffness of 65% compared to neat Ecoflex<sup>TM</sup>. This was in stark contrast to 30 wt% AIKL\_E which showed a decrease of 29% for tensile strength, 65% for total elongation at fracture, and 68% for toughness. Based on the performance of the AIKL\_E samples, although there are propionate ester groups, the samples still cannot be effectively blended in the matrix and the lignin phase seemed to serve as a stress concentrator.

The engineering stress/strain curves for the acetone soluble esterified samples were displayed in Figure 58 with the Young's modulus inset for ASKL\_E at all loadings compared to neat Ecoflex<sup>TM</sup>. A good consistency in shape was seen for each ASKL\_E lignin - Ecoflex<sup>TM</sup> blend engineering stress/strain curve as compared to the neat Ecoflex<sup>TM</sup> curve meaning enhanced miscibility and a more even distribution of lignin molecules in the matrix resulted from the esterification. A reduction in molecular size of the low molecular weight fraction and an increase in length of the carbon chain due to the esterification leads to a more homogenous blend of

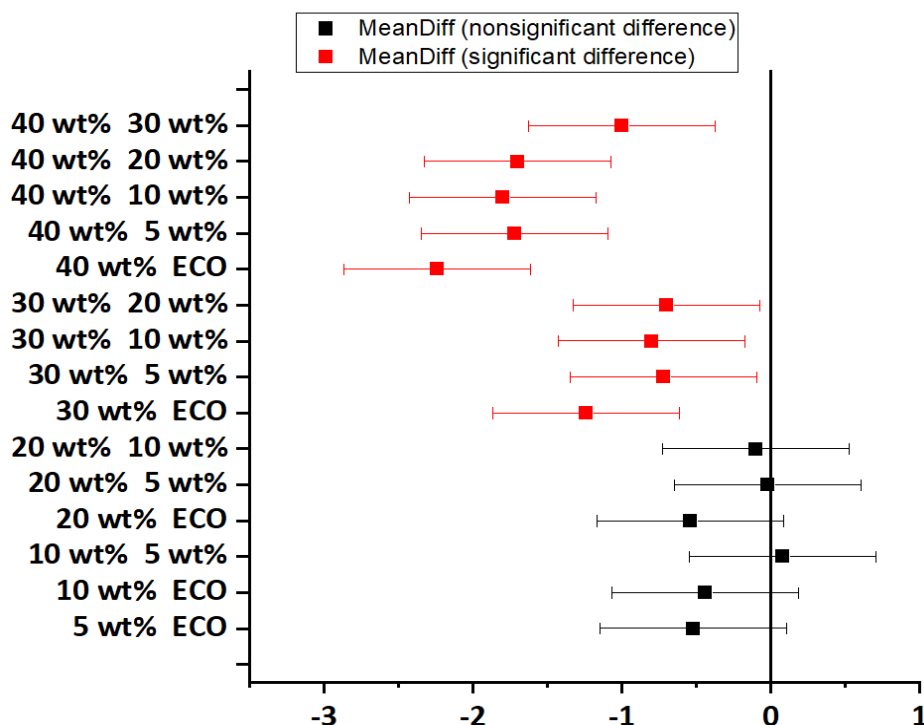


**Figure 58** Engineering stress strain curves (average of five samples) with inset Young's modulus (average of five samples) for ASKL\_E at 5, 10, 20, 30, 40 wt% lignin loading as compared to neat Ecoflex™ (ECO)

ASKL\_E throughout the matrix. Dehne et al. blended unfractionated butyrate hardwood kraft lignin with polyethylene and found that overall tensile strength decreased as lignin was added but tensile strength was retained to some degree up to 40 wt% lignin.<sup>188</sup> Dehne also conducted a grain size analysis to show that smaller lignin particles do incorporate more readily into the PE matrix.<sup>188</sup> One possible suggestion for the preservation of tensile properties with esterified lignins was transesterification in the melt with PE which is even more likely with a polymer like Ecoflex.<sup>188</sup>

In the ANOVA for UTS of the ASKL\_E samples at different lignin loadings the p value was equal to 1.1 E-9 which is less than 0.05 so the null hypothesis is rejected. A post hoc Tukey test was performed and illustrated in Figure 59; when a group mean on the y-axis had an interval that contained zero there was no statistical significance between the groups. For example, in the

case of 5 wt% ECO the interval contains zero so, there is no statistical significance. The y-axis showed which two groups are being compared, for instance 5 wt% ECO is defined as 5 wt% ASKL\_E in blend with 95 wt% Ecoflex<sup>TM</sup> being compared to neat Ecoflex<sup>TM</sup> which is 0 wt% ASKL\_E. The x-axis represents the mean differences that were found between those pairs.



**Figure 59** Tukey simultaneous 95% confidence intervals (CIs) difference of means for ultimate tensile strength (UTS) of acetone soluble esterified softwood kraft lignin powders (ASKL\_E) at different lignin loadings (0, 5, 10, 20, 30, 40 wt%) where 0 wt% ASKL\_E is the neat Ecoflex<sup>TM</sup> control (ECO)

Figure 59 showed that all blends up to 20 wt% ASKL\_E show no statistical significance which equates to only a minor change in UTS as compared to neat Ecoflex<sup>TM</sup>. Once ASKL\_E is increased to 30 and 40 wt% in blend a statistical significance between means arises. For example, the confidence interval for the difference between 40 wt% (ASKL\_UN) and ECO (neat Ecoflex<sup>TM</sup>) extends from -1.6 to -2.8 which does not contain zero. In comparison to the ultimate tensile strength ASKL\_UN Tukey test (Figure 53), the difference of means range for ASKL\_E in

Figure 59 is more narrow, 10 to -15 (former) as compared to 1 to -3 (latter). This showed the range for mean differences of UTS for ASKL\_UN are broad in comparison to ASKL\_E which confirms a retention in tensile strength for the esterified modification as compared to neat Ecoflex<sup>TM</sup>. This result was likely because ASKL\_E and Ecoflex<sup>TM</sup> have similar chemistries as well as good compatibility and a homogenous distribution of the esterified sample in Ecoflex<sup>TM</sup>. The smaller molecules of the low molecular weight fraction have more surface area which equates to more interfacial contact area and improved stress transfer.

On the other hand, lignin can agglomerate causing a lack of strong interfacial interactions and a reduction in the continuous region of Ecoflex<sup>TM</sup>, thus lowering tensile properties. The esterified lignins performed the best in the melt with Ecoflex<sup>TM</sup> as most likely the strong lignin-lignin interactions between lignin macromolecules were weakened by the modification. A reduction in lignin agglomeration improved the mobility of lignin segments by disrupting strong hydrogen bonds. This observation was also supported by the lack of good mechanical properties when additional hydrogen bonding components were introduced into the lignin through hydroxyethylation. The soft segments (hydrocarbon side chains) of the esterified lignins were more effective at intermolecular bonding and exhibit better compatibility and distribution within the Ecoflex<sup>TM</sup> matrix as compared to unmodified or etherified hydroxyethyl lignins. ASKL\_E showcased the most promising ability to act in a polymer blend with Ecoflex<sup>TM</sup>.

To further understand why some mechanical properties were improved or deteriorated with added lignin, it was necessary to take a close look at the thermal properties and crystallinity data of the lignin-Ecoflex<sup>TM</sup> blends.

#### 4.2.4 Thermal properties of lignin-Ecoflex™ blends

Differential scanning calorimetry (DSC) is one of the tools used to determine miscibility of polymeric blends. To study the basic thermal properties and crystallization behavior of lignin-Ecoflex™ blends the onset crystallization temperature ( $T_{os}$ ), crystallization peak temperature ( $T_c$ ), and the crystallization enthalpy ( $\Delta H_c$ ) from the exothermal peak were obtained from the cooling scan. The melting temperature ( $T_m$ ), glass transition temperature ( $T_g$ ), and enthalpy of fusion ( $\Delta H_m$ ) from the endothermic peak were obtained from the second heating scan. Subtraction of ( $T_{os} - T_c$ ) reveals a change in crystallization rate. Degree of crystallinity reported in a percentage  $X_c$  (%) was calculated according to *section 3.10.2.1*. Tables 18 through 20 report these averaged values for all lignin powders blended with Ecoflex™ at different weight percentages where 0 wt% was neat Ecoflex™ without additives.

**Table 18 DSC results of neat Ecoflex™ (ECO) and unfractionated (UF) unmodified (UN), hydroxyethyl ether (HE), and esterified (E) lignin-Ecoflex™ blends at different lignin loadings (wt %)**

Samples	$T_g$ (°C)	$T_m$ (°C)	$T_c$ (°C)	$T_{os}$ (°C)	$T_{os}-T_c$ (°C)	$\Delta H_m$ (J/g)	$\Delta H_c$ (J/g)	$X_c$ (%)
ECO 0 wt%	-27.8	126.8	69.9	79.1	9.1	6.2	11.3	5.5
UF_UN 5 wt%	-26.1	127.1	78.4	87.9	9.6	5.1	9.7	4.6
UF_UN 10 wt%	-24.8	127.1	78.8	88.5	9.7	4.3	9.1	4.2
UF_UN 20 wt%	-21.2	126.3	79.7	90.1	10.4	3.8	8.6	4.2
UF_UN 30 wt%	-19.2	127.2	81.9	91.8	9.9	2.8	6.8	3.6
UF_HE 5 wt%	-27.3	127.4	77.9	86.8	8.9	4.6	9.3	4.3
UF_HE 10 wt%	-26.9	127.4	79.2	88.5	9.3	4.2	8.7	4.1
UF_HE 20 wt%	-26.5	127.6	80.8	90.4	9.6	3.5	7.1	3.9
UF_HE 30 wt%	-25.3	127.1	81.1	90.4	9.3	3.1	5.5	3.8
UF_E 5 wt%	-26.1	127.9	80.4	89.3	9.0	5.2	8.9	4.8
UF_E 10 wt%	-26.3	127.8	79.8	88.1	8.2	4.2	8.2	4.1
UF_E 20 wt%	-24.1	127.2	79.2	87.4	7.3	3.7	7.3	3.9
UF_E 30 wt%	-22.3	126.6	77.9	86.6	6.4	3.1	6.4	3.8

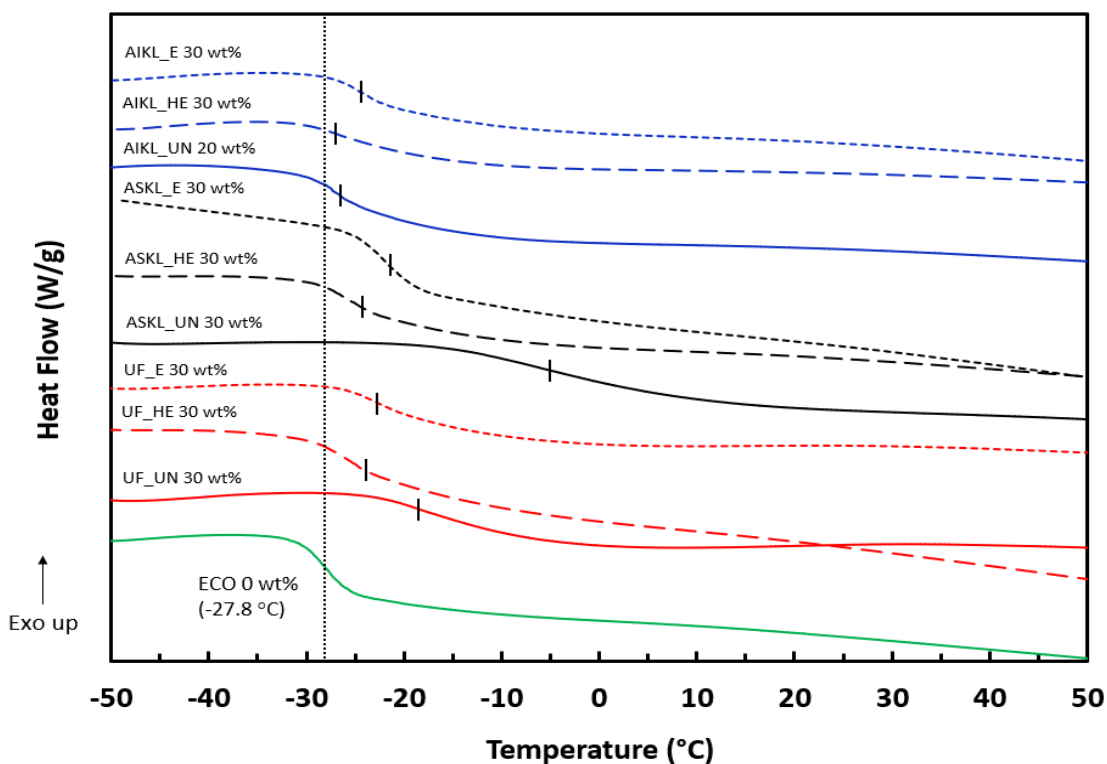
**Table 19 DSC results of neat Ecoflex™ (ECO) and acetone soluble (ASKL) unmodified (UN), hydroxyethyl ether (HE), and esterified (E) lignin-Ecoflex™ blends at different lignin loadings (wt %)**

Samples	T <sub>g</sub> (°C)	T <sub>m</sub> (°C)	T <sub>c</sub> (°C)	T <sub>os</sub> (°C)	T <sub>os</sub> -T <sub>c</sub> (°C)	ΔH <sub>m</sub> (J/g)	ΔH <sub>c</sub> (J/g)	X <sub>c</sub> (%)
ECO 0 wt%	-27.8	126.8	69.9	79.1	9.1	6.2	11.3	5.5
ASKL_UN 5 wt%	-24.1	126.7	76.1	84.1	8.1	5.4	10.5	5.0
ASKL_UN 10 wt%	-19.7	125.6	74.9	83.4	8.5	4.7	9.8	4.5
ASKL_UN 20 wt%	-11.9	124.3	52.1	62.9	10.8	4.1	8.6	4.4
ASKL_UN 30 wt%	-6.9	123.9	63.5	73.6	10.1	3.3	7.7	4.3
ASKL_HE 5 wt%	-26.9	127.1	79.2	88.3	9.2	4.5	9.3	4.2
ASKL_HE 10 wt%	-26.8	127.3	79.8	88.9	9.1	4.0	8.5	3.9
ASKL_HE 20 wt%	-25.5	126.3	77.0	86.5	9.5	3.5	8.3	3.9
ASKL_HE 30 wt%	-25.8	126.3	79.5	89.1	9.5	3.1	7.4	3.9
ASKL_E 5 wt%	-26.9	127.6	79.3	88.3	9.0	4.1	8.9	3.8
ASKL_E 10 wt%	-25.9	127.2	78.8	87.8	9.0	3.8	8.7	3.7
ASKL_E 20 wt%	-23.5	126.4	78.1	87.2	9.0	3.3	7.5	3.6
ASKL_E 30 wt%	-24.2	125.6	77.1	86.0	8.9	2.9	7.3	3.6
ASKL_E 40 wt%	-21.1	123.3	73.2	81.4	8.2	2.4	5.8	3.6

**Table 20 DSC results of neat Ecoflex™ (ECO) and acetone insoluble (AIKL) unmodified (UN), hydroxyethyl ether (HE), and esterified (E) lignin-Ecoflex™ blends at different lignin loadings (wt %)**

Samples	T <sub>g</sub> (°C)	T <sub>m</sub> (°C)	T <sub>c</sub> (°C)	T <sub>os</sub> (°C)	T <sub>os</sub> -T <sub>c</sub> (°C)	ΔH <sub>m</sub> (J/g)	ΔH <sub>c</sub> (J/g)	X <sub>c</sub> (%)
ECO 0 wt%	-27.8	126.8	69.9	79.1	9.1	6.2	11.3	5.5
AIKL_UN 5 wt%	-19.9	125.8	73.4	81.5	8.2	5.2	9.3	4.9
AIKL_UN 10 wt%	-28.1	127.6	80.3	89.8	9.5	4.7	9.3	4.6
AIKL_UN 20 wt%	-27.1	127.6	82.5	92.4	9.9	3.1	8.8	3.4
AIKL_UN 30 wt%	/	/	/	/	/	/	/	/
AIKL_HE 5 wt%	-27.7	127.7	78.0	87.2	9.3	5.2	10.3	4.8
AIKL_HE 10 wt%	-27.7	128.2	81.2	90.8	9.6	4.7	9.3	4.6
AIKL_HE 20 wt%	-28.1	128.2	82.3	92.2	9.8	4.1	8.1	4.5
AIKL_HE 30 wt%	-27.3	128.9	85.3	96.2	10.9	3.3	7.5	4.1
AIKL_E 5 wt%	-26.8	127.3	78.5	87.5	9.0	4.2	8.7	3.7
AIKL_E 10 wt%	-26.4	127.7	80.6	89.3	8.7	3.8	7.6	3.7
AIKL_E 20 wt%	-25.6	127.9	81.0	89.3	9.3	3.3	7.3	3.6
AIKL_E 30 wt%	-24.7	128.0	83.7	93.2	9.5	2.8	5.8	3.5

DSC scans for all lignin powders at all weight percentages of lignin loaded in blend with Ecoflex™ showed one  $T_g$  value which confirmed some compatibility between lignin and Ecoflex™. However, while one  $T_g$  can indicate miscibility within the blend the change in heat flow from the  $T_g$  of the lignin powder may be too subtle to observe. Figure 60 showed the glass transition curve at 30 wt% loading for each lignin powder except for AIKL\_UN which could not undergo blending at 30 wt%, and therefore 20 wt% was presented. All lignin - Ecoflex™  $T_g$  curves were compared to neat Ecoflex™ (0 wt% lignin loading) and show a shift to the right or to a higher temperature. An increased glass transition temperature indicated some interactions between lignin and Ecoflex™ at the molecular level.



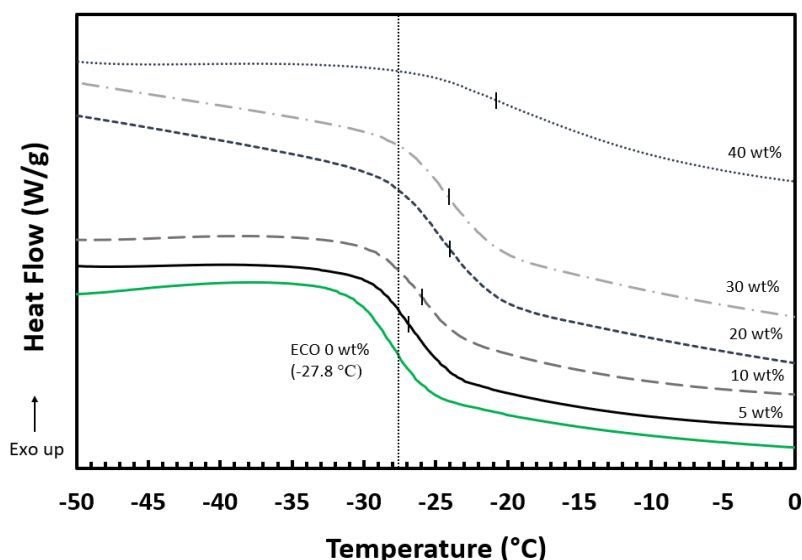
**Figure 60** DSC scans for second heating cycle showing the glass transition temperatures for neat Ecoflex™ at 0 wt% lignin loading and all lignin powders at 30 wt% loading in lignin-Ecoflex™ blend with AIKL\_UN reported at 20 wt% loading because of inability to blend at 30 wt%

Several observations can be made from Figure 60; the acetone insoluble lignin fractions despite modification showed the smallest increase in glass transition temperature while the unfractionated unmodified (UF\_UN) and acetone soluble unmodified (ASKL\_UN) at 30 wt% loading in the lignin-Ecoflex<sup>TM</sup> blend showed the greatest increase in glass transition temperature. Looking back on the overall decrease in tensile strength of the acetone insoluble fraction of lignin powders in blend regardless of modification it follows that the glass transition temperature was mostly unchanged. This means AIKL powders demonstrated less compatibility in blend with Ecoflex<sup>TM</sup> at a processing temperature of 180 °C which can also be traced back to the  $T_g$  values of the AIKL powders in *section 4.1*.

Smita et al. blended Ecoflex<sup>TM</sup> with silica nano clay and their DSC thermograms revealed a similar increase in  $T_g$  values.<sup>197</sup> The research group hypothesized that an enhancement in  $T_g$  could be due to intermolecular interactions between the nano clay and the Ecoflex<sup>TM</sup>.<sup>197</sup> This could hold true for ASKL\_UN and UF\_UN lignin powders in blend with Ecoflex<sup>TM</sup>. The ASKL\_UN lignin powder was low molecular weight and had hydroxyl groups available to react with the ester groups in Ecoflex<sup>TM</sup>. In addition, hydrogen bonds can form resulting in immobilization of the polymer chains and an increased  $T_g$ . Chen et al. performed a methanol fractionation on softwood kraft lignin and then blended the different fractions up to 30 wt% with Ecoflex<sup>TM</sup>.<sup>213</sup> This research group found the methanol insoluble portion could not be blended without a compatibilizer and the greatest increase in  $T_g$  values of subsequent blends came from the methanol soluble and unfractionated lignin portions.<sup>213</sup> The group hypothesized that the shift in unfractionated lignin was due to its soluble portion and the lignin fractions (soluble and insoluble) formed intermolecular bonds typical of a miscible two polymer system.<sup>213</sup>

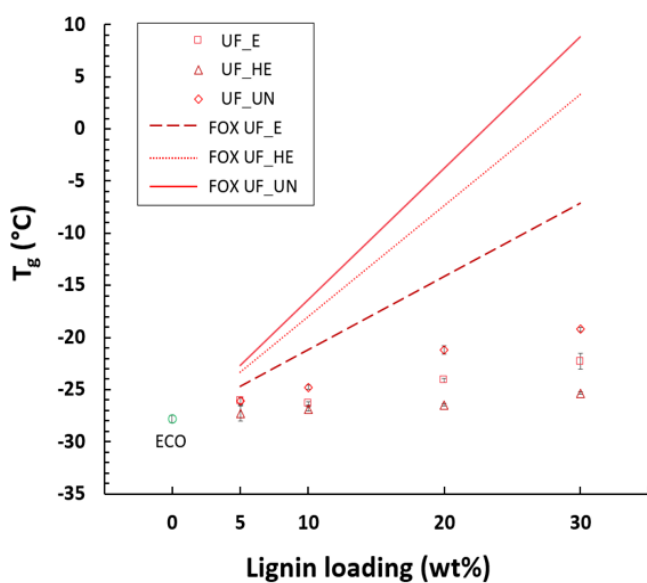


Overall, intermolecular bonds will affect lignins ability to disperse and the methods of interactions within the Ecoflex<sup>TM</sup> polymer matrix during melt processing. The unmodified acetone soluble fraction and its modified counterparts showed the lowest molecular weights, lowest  $T_g$  powder values, and the greatest consistency or improvement in tensile properties in blend with lignin up to 40 wt%. The ASKL\_E – Ecoflex<sup>TM</sup> blend up to 40 wt% showed a 6.3 °C increase in  $T_g$  compared to neat Ecoflex<sup>TM</sup> which indicated some form of interaction and miscibility. The DSC thermogram for the  $T_g$  curves were illustrated in Figure 61 for neat Ecoflex<sup>TM</sup> and ASKL\_E at lignin loadings 5-40 wt%. An increase in  $T_g$  can be observed with lignin addition.

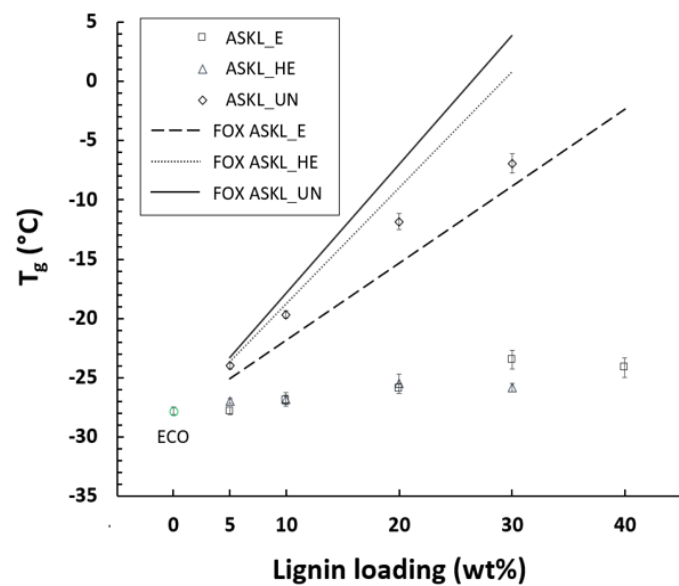


**Figure 61 DSC scans for second heating cycle showing the glass transition temperatures for neat Ecoflex<sup>TM</sup> at 0 wt% lignin loading and acetone soluble esterified (ASKL\_E) lignin powder at 5-40 wt% loading in lignin-Ecoflex<sup>TM</sup> blend**

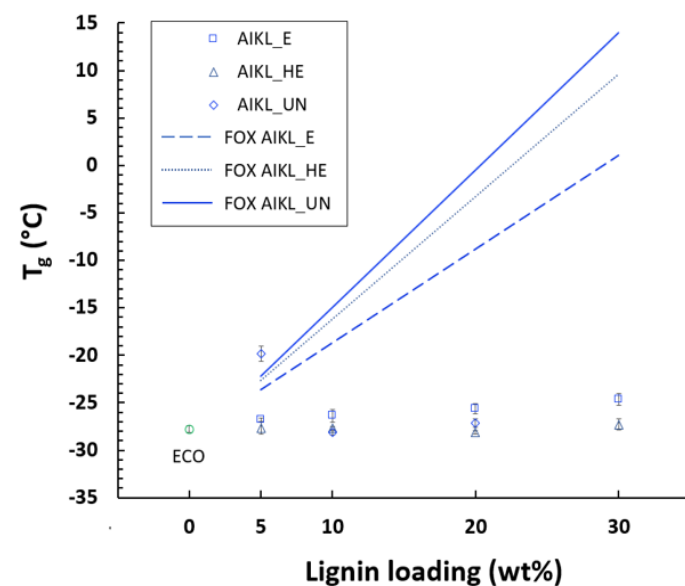
In Figure 62 the  $T_g$  values for all samples as a function of lignin loadings in blend revealed a shift in the  $T_g$  of Ecoflex<sup>TM</sup>. The presented data were averages of three samples and error bars represent plus or minus the standard deviation of three individual samples.



(a)



(b)



(c)

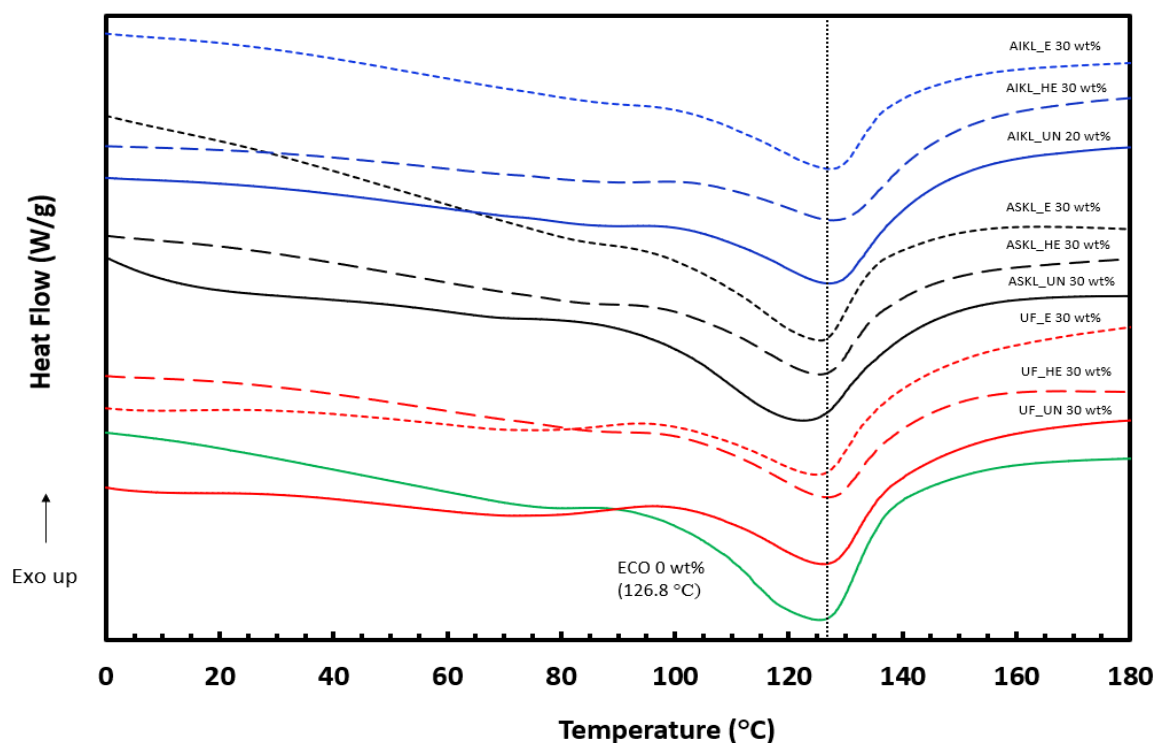
**Figure 62** Glass transition temperature ( $T_g$ ) as a function of lignin loading (wt %) for unmodified (UN), hydroxyethyl ether (HE) and esterified (E) unfractionated lignin powders (UF) (a) acetone soluble lignin powders (ASKL) (b) and acetone insoluble lignin powders (AIKL) (c) as compared to neat Ecoflex™ (ECO) with theoretical Fox equation (FOX) linear fit

For all fractions the addition of the higher  $T_g$  lignin powder caused the  $T_g$  value of the Ecoflex<sup>TM</sup> to shift. The insoluble portion (AIKL) and the etherification (HE) modification had a modest increase in  $T_g$ . The Fox equation was used to estimate the glass transition temperature of the mixture using the properties of the pure components:

$$\frac{1}{T_{g,mix}} \approx \frac{\omega_A}{T_{gA}} + \frac{\omega_B}{T_{gB}}$$

Where  $\omega_A$  is the mass fraction component and  $T_{gA}$  is the glass transition temperature of the 100% lignin powder samples,  $\omega_B$  is the mass fraction component and  $T_{gB}$  is the glass transition temperature of neat Ecoflex<sup>TM</sup>, and  $T_{g,mix}$  is the glass transition of the mixture.<sup>226</sup> If the relationship was extrapolated towards 100% lignin, it was clear that the impact of the lignin did not reflect a single  $T_g$  and rule of mixtures of the lignin via the Fox equation. This result could be due to the rigid phenolic structures and possible bonding between lignin molecules which leads to agglomeration and non-homogenous mixing. Clearly the acetone soluble unmodified lignin had better mixing per the relationship seen in the Fox rule of mixtures equation that was nearly obeyed (Figure 62b).

The melting temperatures ( $T_m$ ) of the lignin blends highlighted that the different lignin loading levels did not greatly impact the peak melting temperature of the neat Ecoflex<sup>TM</sup> sample. As an example, Figure 63 plotted the melting endotherm peaks at 30 wt% loading for each lignin powder except for AIKL\_UN which could not undergo blending at 30 wt%, and therefore 20 wt% was presented. All lignin-Ecoflex<sup>TM</sup> melt curves are compared to neat Ecoflex (0 wt% lignin loading) and show subtle variation in behavior. While Ecoflex<sup>TM</sup> is a semicrystalline polymer, Table 18-20 highlights that the crystalline content is relatively low for this material.

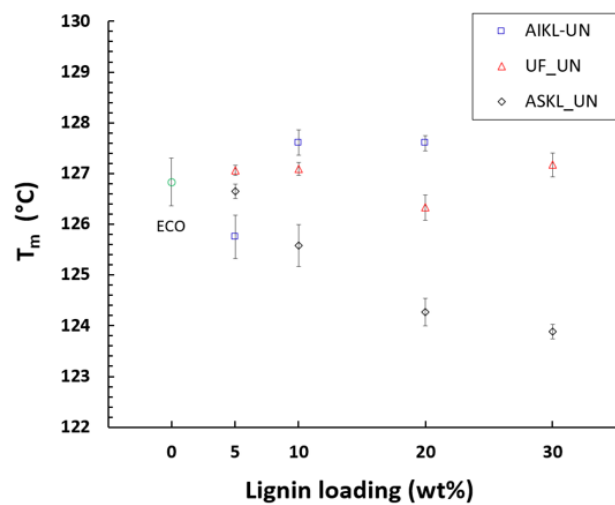


**Figure 63** DSC scans for second heating cycle showing the melting endotherm peaks for neat Ecoflex™ (ECO) at 0 wt% lignin loading and all lignin powder samples loaded at 30 wt% in lignin-Ecoflex™ blend with AIKL\_UN reported at 20 wt% loading because of an inability to blend at 30 wt%

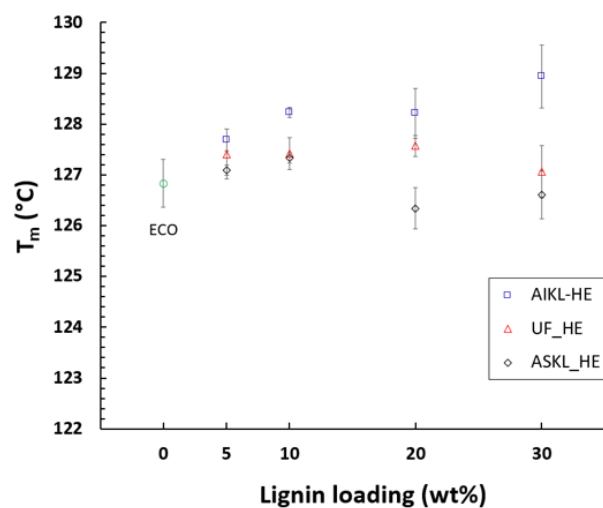
Luo et al. blended esterified Indulin AT SWKL with PP and found a decrease in enthalpy of fusion ( $\Delta H_m$ ) with an addition of lignin to the Ecoflex™ matrix. In addition, the group found two melting temperatures related to homogenous and heterogenous nucleation.<sup>145</sup> Wang et al. blended esterified hydrothermal lignin with Ecoflex™ into films and found a single melting temperature which decreased with increasing lignin.<sup>214</sup> The group hypothesized this was a result of grafting soft fatty chains onto the lignin and then blending with Ecoflex™.<sup>214</sup> Kargarzadeh et al. blended kraft lignin particles with Ecoflex™ and found the melting temperatures increased with increasing amounts of lignin.<sup>192</sup> The group measured crystal thickness and reported a larger polymer crystal thickness with increasing lignin up to 6 wt%.<sup>192</sup>

In this research as lignin powders ASKL\_UN, ASKL\_HE, and ASKL\_E were blended with Ecoflex<sup>TM</sup> up to 30 wt%, a slight decrease in  $T_m$  was observed with ASKL\_E showing the largest decrease of 3.5 °C. These findings agree with Luo's work but could be a result of an anti-nucleating effect on the Ecoflex<sup>TM</sup> which retards the crystallization process.<sup>145,227</sup> The rest of the lignin powders reported a slight increase in  $T_m$  as lignin reached 30 wt% in blend and AIKL\_HE showed the largest increase of 2.1 °C. These findings are comparable to Kargarzadeh's research group who worked with only as received unmodified unfractionated kraft lignin particles. There was a slight correlation between molar mass and an increase or decrease in  $T_m$ . In blend, the lower molecular weight fraction despite modification decreased the melting temperature of neat Ecoflex<sup>TM</sup> while the higher molecular weight fractions increased the melting temperature. The change in  $T_m$  values was reported in Figure 64 for all lignin powders containing samples at all wt% loadings in blend.

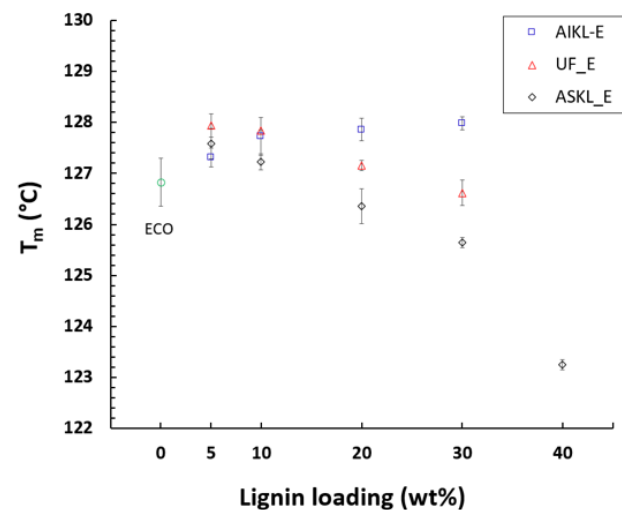
Melting is an endothermic process which requires the absorption of heat and while the amorphous regions of the polymer will undergo a secondary transition at lower temperatures, the crystalline regions undergo melting. Subtle changes in a polymers structure can result in significant changes in the glass transition temperature but only minor changes in the melting temperature as seen above. As well, additives that do not impact polymer structure can serve as physical nucleating sites increasing the number of crystals. Examining the crystallization behavior of neat Ecoflex<sup>TM</sup> and the lignin-Ecoflex<sup>TM</sup> blends is necessary for further characterization.



(a)



(b)



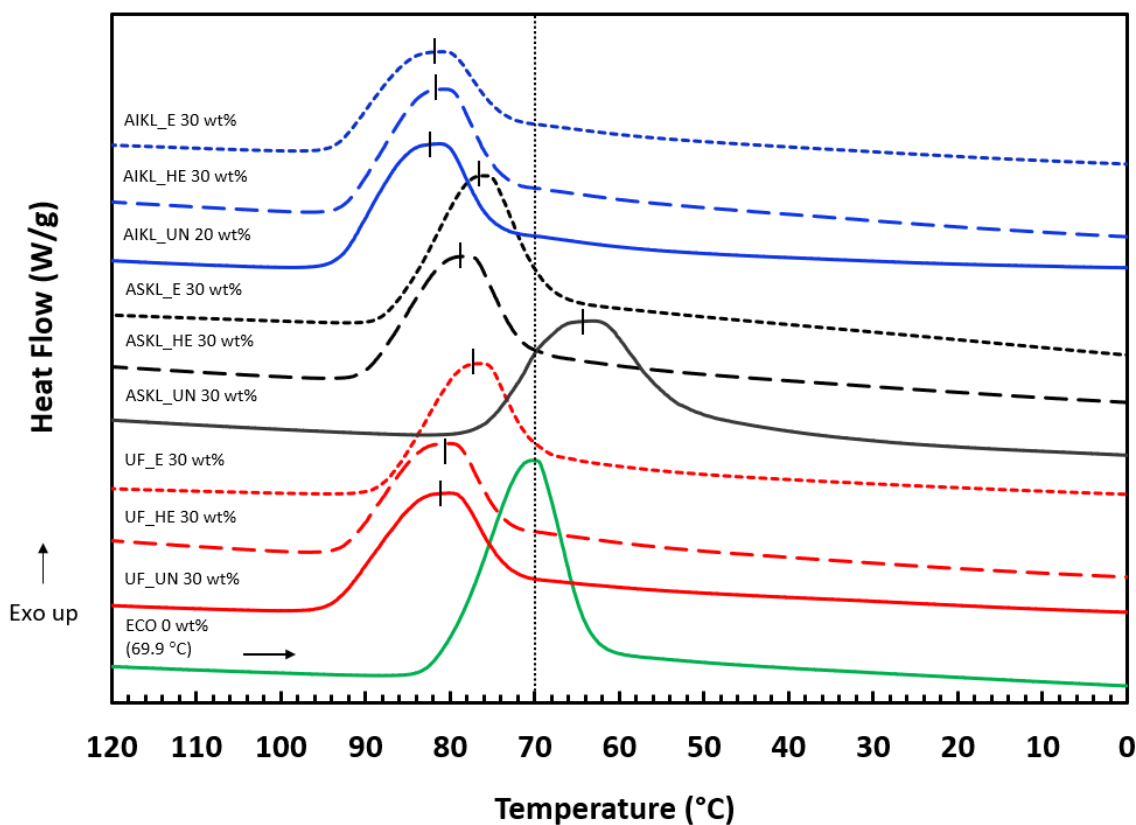
(c)

**Figure 64** Melting temperature ( $T_m$ ) as a function of lignin loading (wt %) for unfractionated (UF), acetone soluble (ASKL), and acetone insoluble (AIKL), unmodified (UN) lignin powders (a), hydroxyethyl ether lignin powders (HE) (b) and esterified (E) lignin powders (c) as compared to neat Ecoflex™ (ECO)

Crystallization affects the mechanical, thermal, and chemical properties of polymer blends and so it is important to study the non-isothermal crystallization DSC scans from the cooling cycle. Molecules like lignin that have aromatic chemical structures can act through  $\pi$ - $\pi$  interactions as nucleating agents for semicrystalline polymers containing an aromatic ring in their backbone like Ecoflex<sup>TM</sup>. The previous thermal history of the polymer affects the measured degree of crystallinity and must be considered when analyzing data.

The crystallization peak on the DSC cooling scan was used to confirm that crystallization occurred and to find the crystallization temperature ( $T_c$ ) or the highest point of the peak. The onset temperature of crystallization ( $T_{os}$ ) is important in reference to the  $T_c$  and the crystallization enthalpy is the area under the crystallization peak. Figure 65 showed the crystallization curves at 30 wt% loading for each lignin powder except for AIKL\_UN which could not undergo blending at 30 wt%, and therefore 20 wt% is presented. All lignin-Ecoflex<sup>TM</sup> melt curves were compared to neat Ecoflex (0 wt% lignin loading) and showed some variation in behavior. The temperature is descending to illustrate the cooling cycle of the DSC scan.

It can be immediately observed that the crystallization curves for all the lignin-Ecoflex<sup>TM</sup> thermoplastic blends shifted to the left of neat Ecoflex<sup>TM</sup> or to a higher  $T_{os}$  and  $T_c$  temperature except for ASKL\_UN. The AIKL blends despite modification showed the greatest shift to higher temperatures, while ASKL\_E and UF\_E showed the smallest shift. The ASKL\_UN lignin powder showed a different behavior with  $T_c$  first increasing to 76.1 and 74.9 °C at a 5 and 10 wt% lignin loading and then decreasing to 52.1 °C at 20 wt% loading and 63.5 °C at 30 wt% loading (Table 19). All lignin powders loaded at 30 wt% with Ecoflex<sup>TM</sup> showed a decrease in  $\Delta H_c$  and a broadening of the  $T_c$  peak.



**Figure 65** DSC scans for cooling cycle showing the crystallization exothermic curves for neat Ecoflex™ (ECO) at 0 wt% lignin loading and all lignin powder samples loaded at 30 wt% in lignin-Ecoflex™ blend with AIKL\_UN reported at 20 wt% loading because of inability to blend at 30 wt%

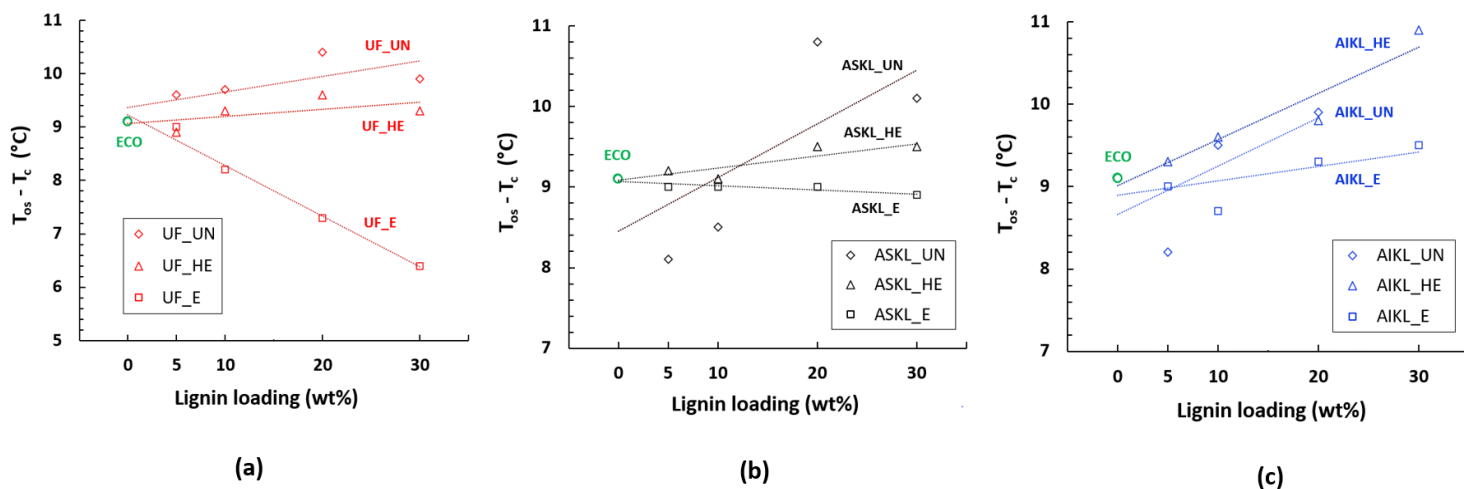
An increase in  $T_c$  and therefore an increase in  $T_{os}$  with a decrease in  $\Delta H_c$  and a broadening of the  $T_c$  peak was widely reported in literature when blending lignin or other fillers with semicrystalline polymers like Ecoflex™.<sup>192,197,224</sup> Several research groups reported the increase in  $T_c$  was likely due to the presence of lignin in the Ecoflex™ matrix which means lignin modifies the way that Ecoflex™ nucleates.<sup>192,197,224</sup> Smita et al. discussed the potential for a heterogenous nucleation effect that comes from introducing filler into the Ecoflex™ matrix.<sup>197</sup> The increase in crystallization temperature for most of the lignin-Ecoflex™ blends was likely due to the presence of lignin increasing the nucleation sites in the Ecoflex™ matrix. The widening of the crystallization peak and the decrease in crystallization enthalpy with an



increased lignin loading observed in all blends indicated to some extent that lignin was an efficient nucleating agent (Table 18-20).

These results confirm that the regular mode of Ecoflex<sup>TM</sup> crystallization was interfered with as weight percentage of lignin powders increased. Sousa et al. who performed a detailed kinetics study on coconut fibre blended with Ecoflex<sup>TM</sup> found a correlation between  $T_{os} - T_c$  and rate of crystallization.<sup>198,228</sup> While the difference between the onset temperature of crystallization and the peak crystallization temperature was no substitute for a reliable kinetics analysis it can be used to index a slower or faster crystallization rate when comparing lignin-Ecoflex<sup>TM</sup> blends to one another and to neat Ecoflex<sup>TM</sup>.<sup>198,228</sup> As such, the temperature difference between the onset crystallization temperature and the peak crystallization temperature as a function of lignin loading in blend as compared to neat Ecoflex<sup>TM</sup> was presented in Figure 66. A larger temperature difference is indicative of a slower crystallization rate while a smaller temperature difference was indicative of a faster crystallization rate. The dashed lines served no functional purpose and are presented only to guide the reader's eye.

The UF\_E, ASKL\_E, and to a lesser extent AIKL\_E showed a smaller temperature difference as lignin loading increased which refers to a faster crystallization process in comparison to their etherified or unmodified counterparts (Figure 66). Both ASKL and AIKL unmodified lignin powders showed a faster crystallization process at 5 and 10 wt% loading and a slow down with increased addition of lignin at 20 and 30 wt%. UF\_HE and ASKL\_HE do not show a significant change in temperature difference as compared to neat Ecoflex<sup>TM</sup>. On the other hand, AIKL\_HE showed an increase in temperature difference or a slower crystallization process.

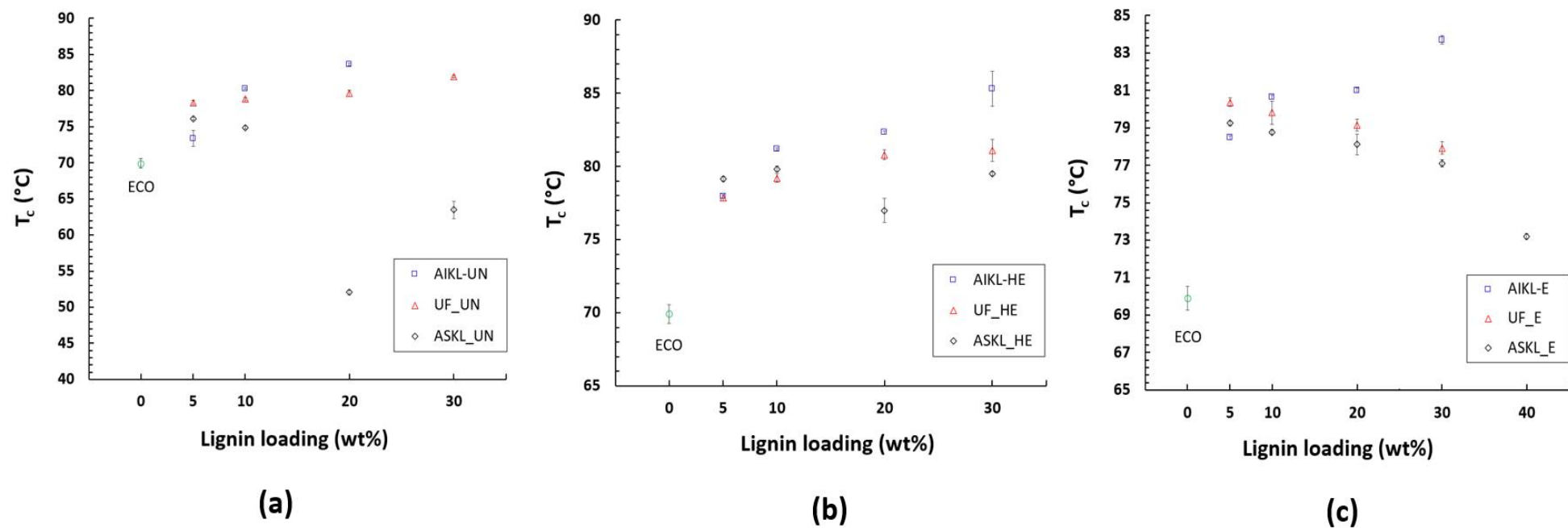


**Figure 66** The temperature difference between the onset crystallization temperature  $T_c$  and the peak crystallization temperature  $T_{os}$  as a function of lignin loading (wt %) for unmodified (UN), hydroxyethyl ether (HE) and esterified (E) unfractionated lignin powders (UF) (a) acetone soluble lignin powders (ASKL) (b) and acetone insoluble lignin powders (AIKL) (c) as compared to neat Ecoflex<sup>TM</sup> (ECO)

Kargarzadeh et al. performed detailed isothermal crystallization DSC testing and found that increased kraft lignin particles in blend with Ecoflex<sup>TM</sup> increased the crystallization rate of Ecoflex<sup>TM</sup> because of the nucleating effect that lignin has on the Ecoflex matrix.<sup>192</sup> As such, it is curious how the different lignin samples, at different lignin loadings can either accelerate or slow down the crystallization process as evaluated by the quasi-rate index. In the future, subjecting these lignin-Ecoflex<sup>TM</sup> blends to different thermal treatments in DSC prior to crystallization analysis could help to develop optimal processing conditions for a scale-up procedure. As well, in depth rheological testing would investigate the filler properties and dispersion quality of the developed lignin powders in blend with Ecoflex<sup>TM</sup>.

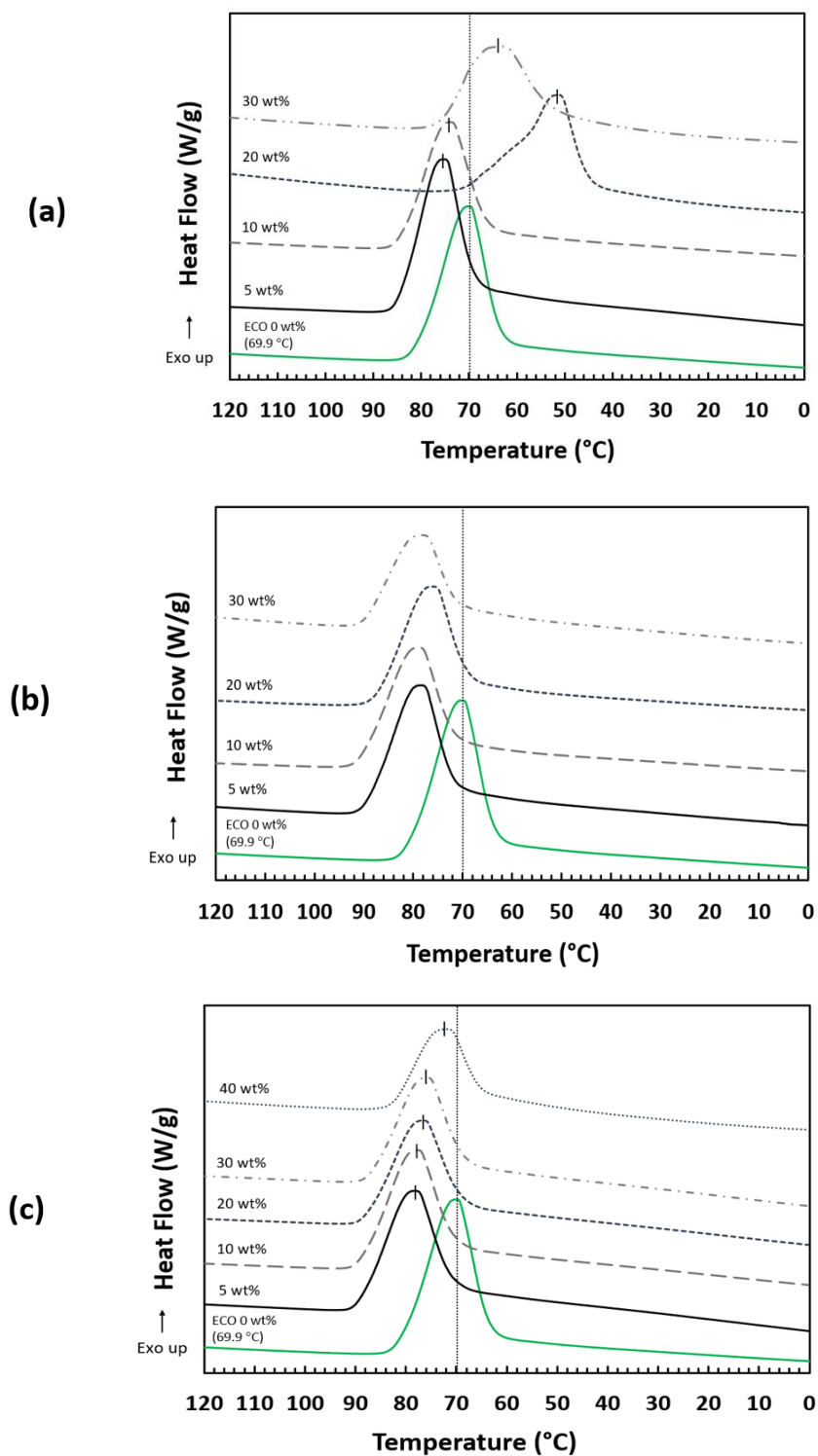
Figure 67 showed the change in  $T_c$  values for all lignin powders at all wt% loadings in blend with Ecoflex<sup>TM</sup>. At a 20 and 30 wt% ASKL\_UN loading the  $T_c$  decreased substantially when compared to neat Ecoflex<sup>TM</sup> and the other lignin powders in blend. While ASKL\_E and

UF\_E powders show an overall increase in  $T_c$  for all weight percent loadings, as lignin loading increased, the  $T_c$  first increased and then slightly decreased at the maximum lignin loading level. Luo et al. found a decrease in  $T_c$  with the addition of 30 wt% Indulin AT softwood kraft lignin that suggested the lignin hindered the crystallization process of Ecoflex<sup>TM</sup>.<sup>145</sup> The increase and then decrease in  $T_c$  for the lignin esters might suggest that as weight percentage of lignin powder is added to Ecoflex<sup>TM</sup> the lignin restricts motion of the Ecoflex<sup>TM</sup> chains due to intermolecular interactions either lignin-Ecoflex<sup>TM</sup> or lignin-lignin.



**Figure 67 Crystallization peak temperature ( $T_c$ ) as a function of lignin loading (wt %) for unfractionated (UF), acetone soluble (ASKL), and acetone insoluble (AIKL), unmodified (UN) lignin powders (a), hydroxyethyl ether lignin powders (HE) (b) and esterified (E) lignin powders (c) as compared to neat Ecoflex™ (ECO)**

The ASKL\_UN lignin powders in blend with Ecoflex<sup>TM</sup> showed the most variation in both tensile properties and in thermal properties. The side by side comparison of the peak crystallization temperature in Figure 68 for the acetone soluble fraction of the lignin with the various modification levels was plotted for each lignin fraction. It can be seen that ASKL\_UN loaded at 5 and 10 wt% showed a slight increase in  $T_c$  with minimal peak width broadening but at 20 and 30 wt% loading the  $T_c$  decreased and the peak substantially broadened further. The ASKL\_HE powders show a steady increase in  $T_c$  and peak broadening with increasing lignin powder in blend while the ASKL\_E powders show an initial increase in  $T_c$  and then a gradual decrease with increased lignin powder in blend. Although subtle, the difference in thermal behavior for these three lignin powders can be attributed to the structural and chemical differences between modifications and be somewhat related to the reported tensile properties. From *section 4.2.2* in comparison to neat Ecoflex<sup>TM</sup>, the tensile strength of ASKL\_E was the most consistent with added lignin while the tensile strength for ASKL\_HE showed a steady decline with increased lignin. The tensile strength and subsequently the toughness and total elongation at break all increased for 5 and 10 wt% loaded ASKL\_UN and then showed a minor decrease with an increased stiffness as lignin was added.



**Figure 68** DSC scans for cooling cycle showing the crystallization exothermic curves for unmodified (UN) (a), hydroxyethyl ether (HE) (b), and esterified (E) (c) acetone soluble lignin powders (ASKL) at lignin loading 5-40 wt% as compared to neat Ecoflex™ (ECO)

#### 4.2.4.1 Degree of crystallinity

Crystallinity of a polymer helps describe order within the material and will affect properties i.e. the more regularly aligned the chains or increasing degree of crystallinity the more hard or dense the polymeric material properties. In this research the lignin blends are compared to neat Ecoflex<sup>TM</sup> which was melt processed and extruded into dog bone specimens at 180 °C and the samples were cooled in the mould at room temperature before removal. Semicrystalline polymers like Ecoflex<sup>TM</sup> undergo cold crystallization above their  $T_g$  which makes it difficult to report the degree of crystallinity. Cold crystallization is an exothermic process which can be observed by heating a sample that has previously been cooled. The cooling DSC scan falls far below the glass transition temperature of neat Ecoflex<sup>TM</sup> and all of the lignin-Ecoflex<sup>TM</sup> blends giving sufficient time for crystallization to occur. As discussed in detail in the previous section, the crystallization peak for neat Ecoflex<sup>TM</sup> and all lignin-Ecoflex<sup>TM</sup> blends is clearly visible in the cooling cycle and this leads into the second heating cycle which is where the enthalpy of fusion ( $\Delta H_m$ ) data was collected to calculate the  $X_c$ . Despite following protocols developed in literature and DSC manuals, thermal history and cooling rates will affect degree of crystallization.<sup>229,230</sup> For the purpose of consistency in this study all samples in melt and mould were handled identically and all samples were run through the DSC at a heating rate of 10 °C/min so they could be compared to one another for correlation purposes, but if the thermal history or heat/cool rate was changed the degree of crystallinity would also change.

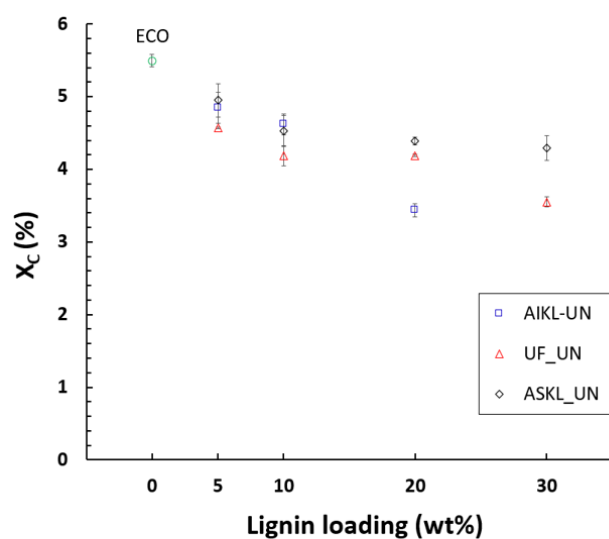
All lignin-Ecoflex<sup>TM</sup> blends despite fraction or modification showed a small decrease in degree of crystallinity as compared to neat Ecoflex<sup>TM</sup> (Tables 18-20). Lignin is an amorphous polymer with no melting temperature and melt processing it with Ecoflex<sup>TM</sup> created a less crystalline polymer blend. In this research following the protocol in *section 3.10.2*, the degree of

crystallinity for neat Ecoflex<sup>TM</sup> melt processed and extruded at 180 °C was 5.5%. Zhou et al. reported neat Ecoflex<sup>TM</sup> at 5.3%, Sousa et al. at 11.5%, Smita et al. at 3.5%, Bastarrachea at 10%, and Kargarzadeh at 23.3% which were all contingent on the heating and cooling rates used during DSC analysis.<sup>192,197–199,217</sup>

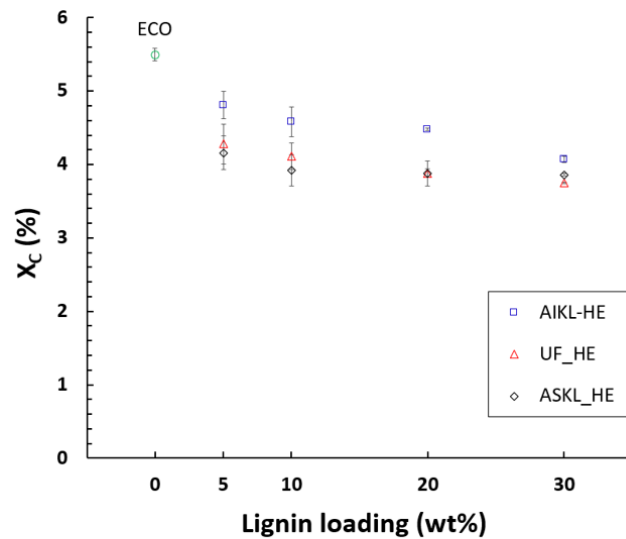
The esterified lignin modification in blend with Ecoflex<sup>TM</sup> showed the largest decrease in degree of crystallinity with UF\_E decreasing by 1.7%, ASKL\_E decreasing by 1.9% and AIKL\_E decreasing by 2.0% of the absolute crystallinity of 5.5% (Figure 69). ASKL\_UN lignin powder with Ecoflex<sup>TM</sup> showed the smallest impact (1.2% decrease) in degree of crystallinity of the Ecoflex<sup>TM</sup>. The etherified lignins decreased within the same range, UF\_HE by 1.7%, ASKL\_HE by 1.6% and AIKL\_HE by 1.4%.

Kargarzadeh et al. reported a 2.6% decrease in degree of crystallinity for their kraft lignin – Ecoflex<sup>TM</sup> blends as lignin was increased to 6 wt%.<sup>192</sup> This group attributed the slight decrease to cold crystallization which caused incomplete crystallization during cooling.<sup>192</sup> However, the group reported only a slight decrease (0.1 J/g) in their enthalpy of fusion ( $\Delta H_m$ ) data with added lignin while this study reported a larger decrease in  $\Delta H_m$  with added lignin (up to 3.8 J/g). In addition, Kargarzadeh's group blended only 6 wt% lignin with Ecoflex<sup>TM</sup> while this study blended up to 40 wt%. Bastarrachea et al. reported a similar decrease (4.7%) in degree of crystallinity as nisin was increasingly blended with Ecoflex.<sup>199</sup> The group speculated that the introduction of foreign molecules into the Ecoflex<sup>TM</sup> matrix lessened the space available for crystal growth and this obstructed crystal formation thus reducing crystallinity.<sup>199</sup> Zhou et al. who blended soy meal with Ecoflex<sup>TM</sup> found that the degree of crystallinity did not change or slightly increased.<sup>217</sup> In this case, the group reported that the soy meal did not act as a nucleating

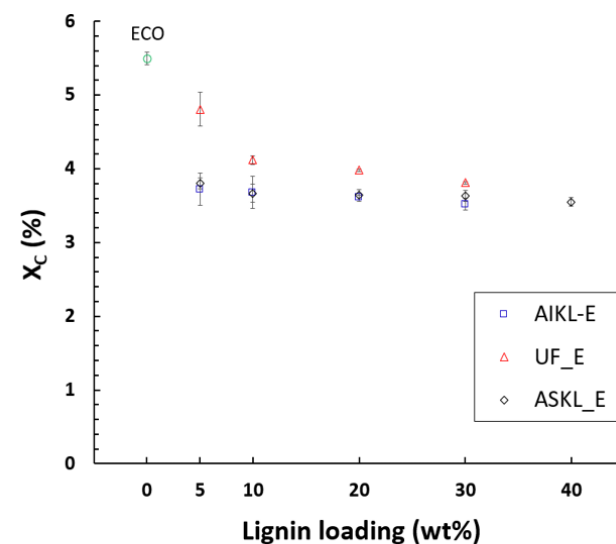




(a)



(b)

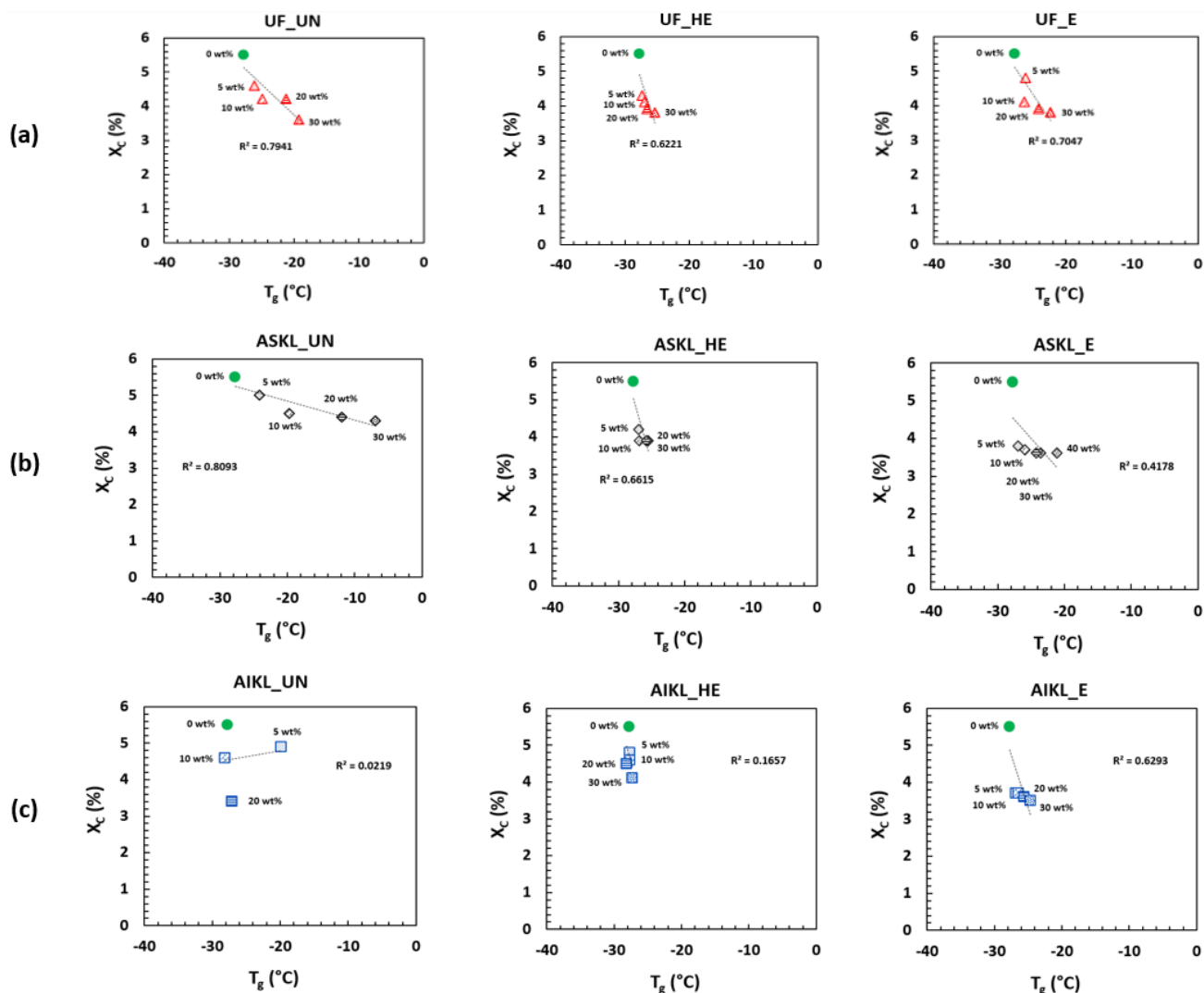


(c)

**Figure 69 Degree of crystallinity ( $X_c$ ) as a function of lignin loading (wt %) for unfractionated (UF), acetone soluble (ASKL), and acetone insoluble (AIKL), unmodified (UN) lignin powders (a), hydroxyethyl ether lignin powders (HE) (b) and esterified (E) lignin powders (c) as compared to neat Ecoflex<sup>TM</sup> (ECO)**

agent and so the crystallinity of Ecoflex<sup>TM</sup> did not change.<sup>217</sup> Maldhure et al. blended esterified industrial waste lignin with PP and found a decrease (19.3%) in degree of crystallinity.<sup>224</sup> The group hypothesized that the decrease supported some kind of interaction between the lignin and the polypropylene.<sup>224</sup>

The glass transition temperatures were compared with the degree of crystallinity of the lignin-Ecoflex<sup>TM</sup> blends (Figure 70). There were almost no linear relationship for the AIKL\_HE lignin powder in blend with Ecoflex<sup>TM</sup> as the glass transition temperature does not show a substantial increase and the  $X_c$  showed only a small decrease with added lignin. The AIKL\_UN lignin powder shows erratic behavior with a drastic increase in glass transition temperature at 5 wt% lignin loading followed by a decrease in  $T_g$ , while  $X_c$  steadily decreased. AIKL\_UN could not be blended above 20 wt% lignin loading because of torque overload on the twin screw extruder. The AIKL\_E lignin powder showed somewhat of a linear regression as  $T_g$  slightly increased,  $X_c$  decreased. The degree of crystallinity drops immediately upon lignin addition and remains nearly unchanged as lignin is added. A similar pattern is seen with ASKL\_E although the  $T_g$  increased more substantially. The unfractionated portion of the lignin powder despite different modification reported  $R^2$  values over 0.6 and consistently showed as lignin loading had increased in the blend,  $T_g$  increased and  $X_c$  decreased. ASKL\_UN presented the highest  $R^2$  value of 0.81 and also showed the greatest improvement in tensile strength, toughness, and total elongation at break as compared to neat Ecoflex<sup>TM</sup>. As such, the lignin powders which significantly maintained the tensile properties or improved the tensile properties of Ecoflex<sup>TM</sup> also demonstrated the most substantial increase in glass transition temperatures and decreased in degree of crystallinity with added lignin loading. These types of changes were signs of enhanced interaction between the lignin and the Ecoflex<sup>TM</sup> matrix.



**Figure 70** Glass transition temperature ( $T_g$ ) of lignin-Ecoflex<sup>TM</sup> blends at weight percentage lignin loading (wt%) where 0 wt% is neat Ecoflex<sup>TM</sup> (ECO), as a function of degree of crystallinity (%) for unmodified (UN), hydroxyethyl ether (HE) and esterified (E) lignin modification for unfractonated (UF) (a), acetone soluble (ASKL) (b), and acetone insoluble (AIKL) (c) lignin fractions

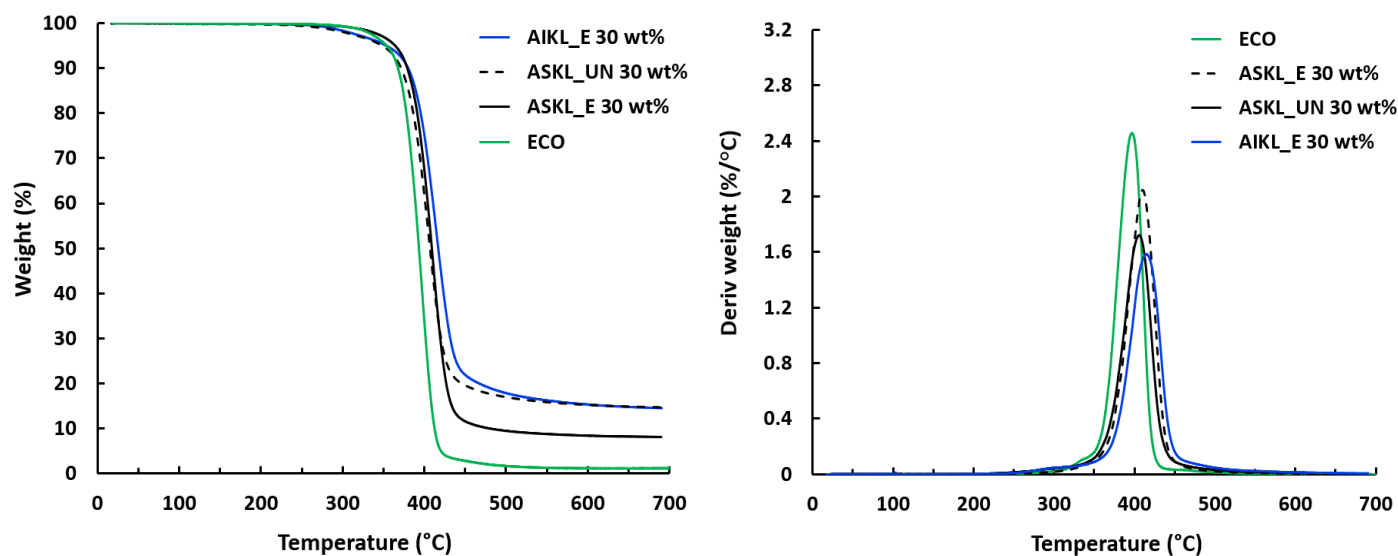
#### 4.2.4.2 Thermogravimetric analysis of lignin-Ecoflex™ blends

To study the thermal decomposition of ASKL\_UN, ASKL\_E and AIKL\_E lignin-Ecoflex™ thermoplastic blends TGA and differential thermogravimetric (DTG) curves for 30 wt% lignin loading were analyzed. Table 21 shows the 10 wt% degradation temperature ( $T_{D10\%}$ ) of the lignin powders (offset to 105 °C), the maximum derivative temperature ( $T_{max}$ ) and the char yield or remaining wt% lignin powder at 600 °C for neat Ecoflex™ (0 wt% lignin), and 30 wt% blends with ASKL\_UN, ASKL\_E and AIKL\_E. A 10 wt% degradation temperature was reported because of no discernible difference between temperatures at 5 wt% degradation.

**Table 21 TGA data for acetone soluble unmodified and esterified lignin powders (ASKL\_UN and ASKL\_E) and acetone insoluble esterified lignin powder (AIKL\_E) at a 30 wt% lignin loading in comparison to neat Ecoflex™ (ECO)**

	$T_{D10\%}$ (°C)	$T_{max}$ (°C)	wt% at 600 °C
Ecoflex (neat)	368	399	1.11
ASKL_UN 30 wt%	372	407	15.2
ASKL_E 30 wt%	379	411	8.35
AIKL_E 30 wt%	380	419	15.3

An expected increase in maximum derivative temperature and char yield occurred for all three lignin fractions at 30 wt% loading in blend with Ecoflex™; AIKL\_E and ASKL\_UN had a greater yield of remaining ash residue at 600 °C than ASKL\_E. An important finding was the increase in 10 wt% degradation temperature of the lignin-Ecoflex™ blends compared to neat Ecoflex™ for all three lignin powders at 30 wt% loading. Figure 71 illustrated the percent weight loss curves and the derivative weight loss as a function of temperature curves for neat Ecoflex™ and ASKL\_UN, ASKL\_E, and AIKL\_E in blend at 30 wt% loading.



**Figure 71 TGA weight % loss curves and maximum derivative weight % as a function of temperature curves (DTG) for esterified acetone soluble, esterified acetone insoluble, and unmodified acetone soluble (ASKL\_E, AIKL\_E, ASKL\_UN) samples in blend with Ecoflex™ as compared to neat Ecoflex™ (ECO).**

There was only one peak in the DTG curve which indicated the samples degraded in a one-step process with the main loss or degradation occurring between 270-450 °C. Kargarzadeh et al. who blended kraft lignin particles up to 6 wt% with Ecoflex™ reported weight loss beginning at 100 °C and mainly occurring between 150-450 °C. It is well reported in literature that lignin tends to decrease the onset degradation temperature when in blend with semicrystalline polymers.<sup>185,190,192,214</sup> Xiong et al. reported a 10-19 °C decrease in  $T_{D10\%}$  with increasing lignin in blend with Ecoflex™. Dias et al. who blended bio-content polypropylene with different industrial lignins found up to a 30 °C decrease in  $T_{D5\%}$  with added lignin and hypothesized a lack of interactions between the PP matrix and the lignin particles.<sup>185</sup>

In this research ASKL\_UN, ASKL\_E and AIKL\_E showed an increase for the onset degradation temperature up to 12 °C. Liao et al. who blended lignin with polypropylene found a similar increase in  $T_{D10\%}$  and reported good interactions within the lignin-PP matrix which

resulted in better heat resistance and thermal stability of the blended material. The acetone insoluble fraction showed the greatest increase in TD<sub>10%</sub>, char yield and T<sub>max</sub> in comparison to neat Ecoflex<sup>TM</sup> which is likely due to its higher molecular weight.

Overall, the thermal properties, degree of crystallinity and thermal degradation results indicate that there was compatibility between certain lignin powders and the Ecoflex<sup>TM</sup> matrix. The esterified modifications, especially for lower molecular weight ASKL reported thermal stability and reliable tensile properties likely due to the hydrocarbon side chains which formed effective intermolecular bonds between lignin molecules and the Ecoflex<sup>TM</sup> matrix. The results suggest that molecular mixing between esterified lignins and Ecoflex<sup>TM</sup> was possible which gives good mechanical properties even with additional lignin. However, it is the unmodified acetone soluble lignin fraction that showed the most interesting results with a drastic increase in tensile strength and toughness, while enhancing the thermal stability. With the aid of Fourier transform infrared spectroscopy it is necessary to take a closer look at the interactions within the Ecoflex<sup>TM</sup> matrix that govern the mechanical and thermal property results.

#### **4.2.5 Fourier transform infrared spectroscopy for thermoplastic blends**

FT-IR spectroscopy was used to further examine the chemical structures of the lignin-Ecoflex<sup>TM</sup> blends. The full spectrum for ASKL\_UN lignin-Ecoflex<sup>TM</sup> blends at a 0-30 wt% lignin loading with 0 wt% being neat Ecoflex<sup>TM</sup> can be seen in Figure 72a. It is important to examine the unmodified lower molecular weight lignin fraction because it showed an increase in tensile strength, toughness, and total elongation at break at 5 and 10 wt% loading with Ecoflex<sup>TM</sup>. The peaks at 729, 1100, and 1170 cm<sup>-1</sup> were characteristic Ecoflex<sup>TM</sup> peaks and the blend spectra were normalized to 873 cm<sup>-1</sup> in accordance with literature.<sup>200,231</sup> The broad peak for the ASKL\_UN lignin powder (prior to blending) at 3400-3600 cm<sup>-1</sup> represented the O-H

stretching of aliphatic and phenolic functional groups alongside H-bonding. There were no reported peaks in this range for neat Ecoflex™ but after 5-30 wt% ASKL\_UN was melt-processed and blended with Ecoflex™ the broad shoulder signal appeared on the spectra from 3400-3600 cm<sup>-1</sup>.<sup>231,200</sup> The ASKL\_UN lignin powder peaks prior to blending at 2933 and 2839 cm<sup>-1</sup> were typical of the C-H stretching seen in methyl and methylene groups. The neat Ecoflex™ peaks at 2952 and 2873 cm<sup>-1</sup> are the asymmetric and symmetric stretching vibrations of CH<sub>2</sub> groups.<sup>200,231</sup> After blending 5-30 wt% ASKL\_UN lignin powder with Ecoflex™ there are no signals for the ASKL\_UN lignin powder peaks and the Ecoflex™ peaks have shifted to 2954 and 2874 cm<sup>-1</sup>. Figure 72b enlarged the lignin-Ecoflex™ fingerprint region and a closer analysis revealed some potential inferences about interactions between ASKL\_UN and the Ecoflex™ matrix. Figure 72c contained a signal for neat Ecoflex™ at 1709 cm<sup>-1</sup> which is representative of C=O group stretching.<sup>200,231</sup> The unmodified acetone soluble lignin powder does not report this signal before blending because there are no ester bonds in this sample. After blending 5-30 wt% ASKL\_UN lignin powder with Ecoflex™ the signal shifts to 1714 cm<sup>-1</sup>. Figure 72c also shows a signal for neat Ecoflex™ at 1269 cm<sup>-1</sup> which is representative of C-O stretching.<sup>200,231</sup> After blending 5-30 wt% ASKL\_UN lignin powder with Ecoflex™ the signal shifts to 1265 cm<sup>-1</sup>.

It is well documented in literature that shifts in the FT-IR spectrum can indicate interactions and therefore miscibility between polymer systems.<sup>213,231-233</sup> Chen et al. who blended methanol soluble lignin powder with Ecoflex™ reported similar results with a shift in carbonyl stretching at the 1712 cm<sup>-1</sup> peak and the appearance of the broad shoulder around 3400-3600 cm<sup>-1</sup> after blending with lignin.<sup>213</sup> This group also reported a shift of peak 1593 to 1597 cm<sup>-1</sup> for the methanol soluble lignin powder's first aromatic skeletal vibration peak and a shift of

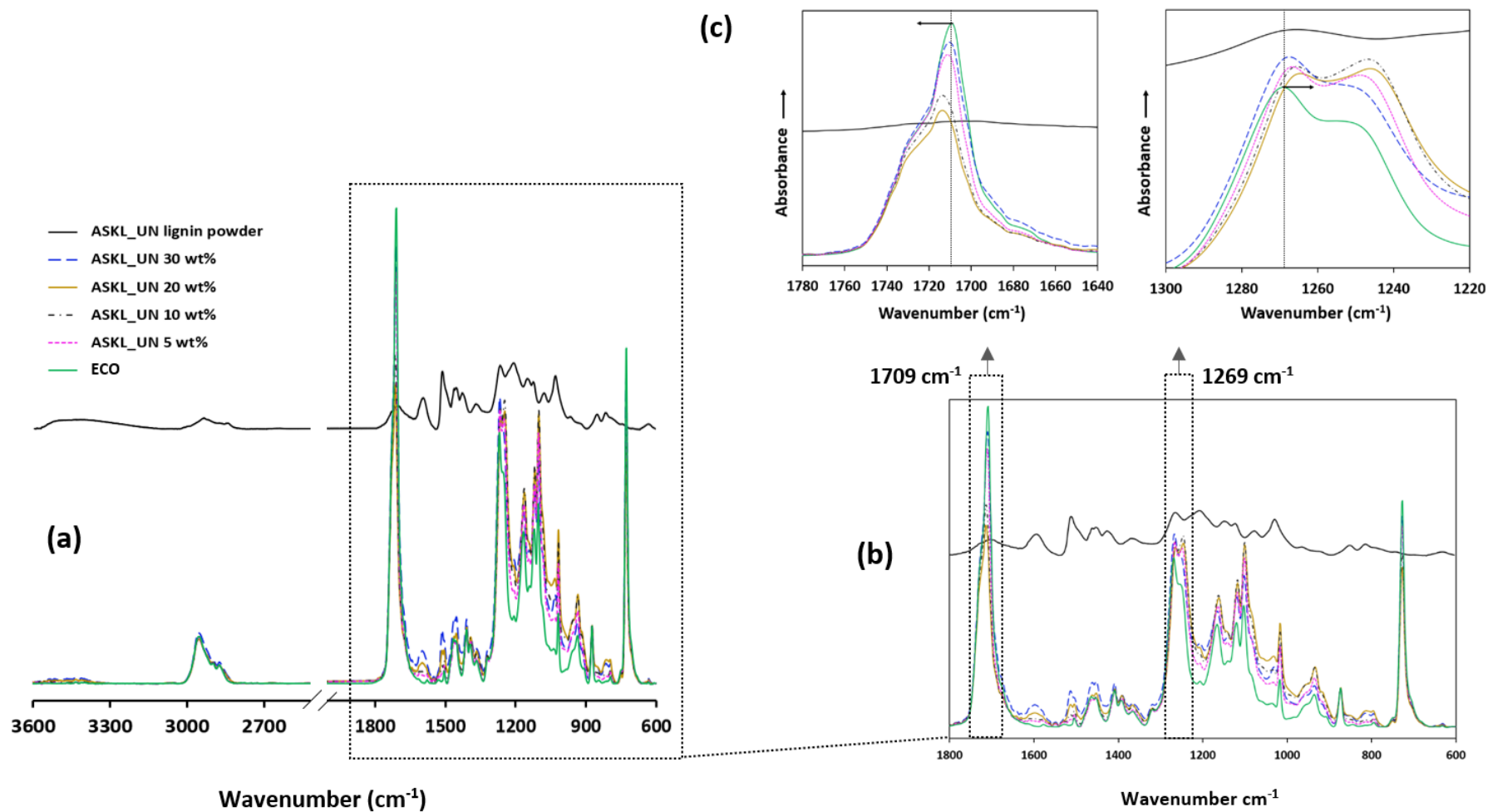
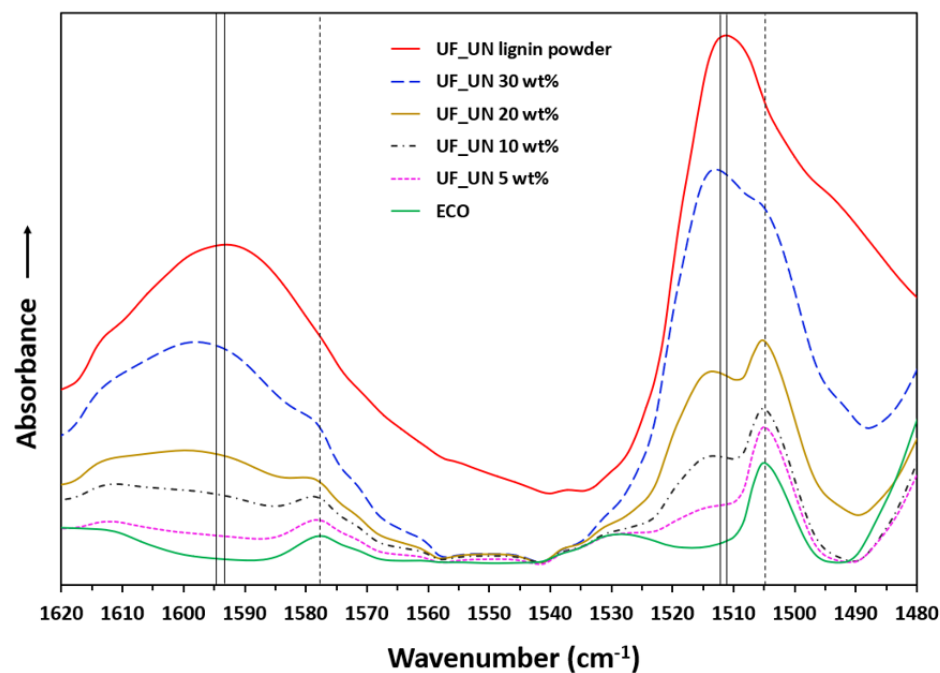


Figure 72 FT-IR spectrum for unmodified acetone soluble (ASKL\_UN) powder, neat Ecoflex™ (ECO), and 5-30 wt% ASKL\_UN – Ecoflex™ blends (a) the fingerprint region (b) and enlarged signals at 1709 and 1269  $\text{cm}^{-1}$  (c)

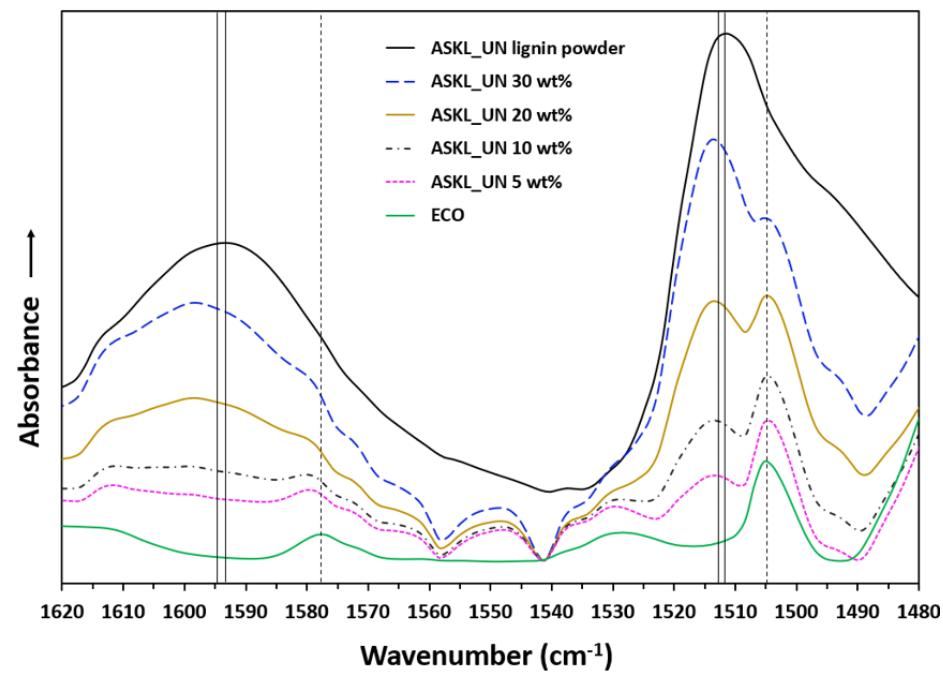


peak 1511 to 1514  $\text{cm}^{-1}$  for the second aromatic skeletal vibration peak after blending with Ecoflex<sup>TM</sup>. A side by side comparison of unfractionated unmodified lignin powder (UF\_UN) blended with Ecoflex<sup>TM</sup> and ASKL\_UN blended with Ecoflex<sup>TM</sup> in the enlarged region of the aforementioned signals can be seen in Figure 73.

The signals for UF\_UN powder before blend are 1511 and 1594  $\text{cm}^{-1}$  and shift to 1513 and 1598  $\text{cm}^{-1}$  after the lignin powder is blended with Ecoflex<sup>TM</sup>. The signals for ASKL\_UN powder before blend are 1511 and 1594  $\text{cm}^{-1}$  and shift to 1514 and 1598  $\text{cm}^{-1}$  after the lignin powder is blended with Ecoflex<sup>TM</sup>. The signals at 1504 and 1578  $\text{cm}^{-1}$  were skeleton vibrations of the benzene rings in neat Ecoflex<sup>TM</sup>. The 1511 and 1594  $\text{cm}^{-1}$  spectral peak shifts are likely attributed to interactions between lignin and the polyester Ecoflex<sup>TM</sup> where hydrogen bonding can occur between the hydroxyl groups in the unmodified lignin powders and the carbonyl groups in the Ecoflex<sup>TM</sup> matrix. Further confirmation comes from the carbonyl stretching shift of the 1709  $\text{cm}^{-1}$  Ecoflex<sup>TM</sup> peak with added lignin powder (Figure 72c).



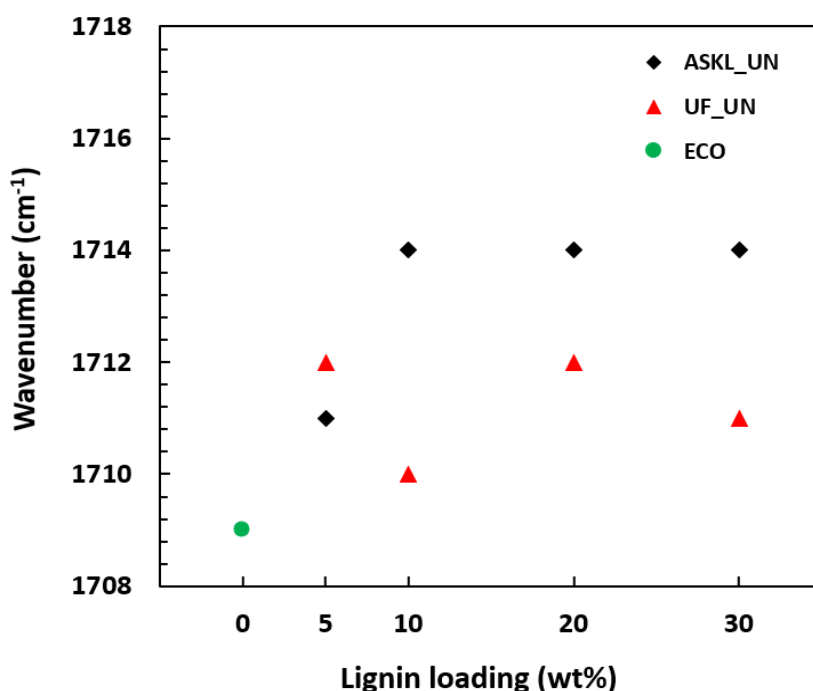
(a)



(b)

Figure 73 FT-IR spectrum for unfractionated unmodified lignin powder (UF\_UN) (a) and acetone soluble unmodified lignin powder (ASKL\_UN) (b) melt processed with neat Ecoflex™ (ECO) in blend with 5-30 wt% with signals 1512 and 1594  $\text{cm}^{-1}$  belonging to aromatic skeletal vibrations in lignin and signals 1504 and 1577  $\text{cm}^{-1}$  belonging to skeletal vibrations of the benzene ring in Ecoflex™

Figure 74 illustrated increasing lignin loading as a function of wavenumber for the neat Ecoflex™ peak at 1709 cm<sup>-1</sup> and both UF\_UN and ASKL\_UN in blend with Ecoflex™ at different wt% loading. It was observed that the ASKL\_UN sample in blend with Ecoflex™ showed a larger peak shift than the UF\_UN sample in blend with Ecoflex™ which contained both high and low molecular weight fractions. However, for both the unfractionated and acetone soluble portions the aromatic ring of Ecoflex™ offers  $\pi$ -hydrogen bonding between the OH lignin groups and the aromatic Ecoflex™ ring.<sup>234</sup>



**Figure 74 Lignin loading (wt%) as a function of wavenumber (cm<sup>-1</sup>) for the neat Ecoflex™ (ECO) peak at 1709 cm<sup>-1</sup> and the subsequent peak shift for unfractionated unmodified (UF\_UN) and acetone soluble unmodified (ASKL\_UN) samples in blend with Ecoflex™**

Overall, the discussed peak shifts were more noticeable in the ASKL\_UN powders in blend with Ecoflex™ which means the lower molecular weight fraction showed more H-bonding and  $\pi$ - $\pi$  interactions than its unfractionated counterpart.

The acetone soluble esterified lignin powder (ASKL\_E) in blend with Ecoflex<sup>TM</sup> showed an excellent consistency in mechanical properties and thermal stability in melt. ASKL\_E was the only lignin powder that was blended over 30 wt% and at a 40 wt% loading there was no issue with processing or a significant decline in mechanical properties.

The full spectra for ASKL\_E – Ecoflex<sup>TM</sup> blends at a 0-40 wt% lignin loading with 0 wt% being neat Ecoflex<sup>TM</sup> were reported in Figure 75. Because the acetone soluble lignin powder was esterified there is no longer a signal for the broad shoulder from 3400-3600 cm<sup>-1</sup>. The ASKL\_E powder showed a signal for ester bonds at 1731 cm<sup>-1</sup> and neat Ecoflex<sup>TM</sup> showed a signal for its ester bonds at 1709 cm<sup>-1</sup>. The resultant blends show a shift in the neat Ecoflex<sup>TM</sup> signal from 1709 to 1714 cm<sup>-1</sup> and no signal reported at 1731 cm<sup>-1</sup> for the lignin related ester peak. This could imply that transesterification between ASKL\_E and Ecoflex<sup>TM</sup> occurred in the melt. Additionally, the signal for neat Ecoflex<sup>TM</sup> at 1269 cm<sup>-1</sup> which is representative of C-O stretching shifted to 1265 cm<sup>-1</sup> after blending with ASKL\_E.

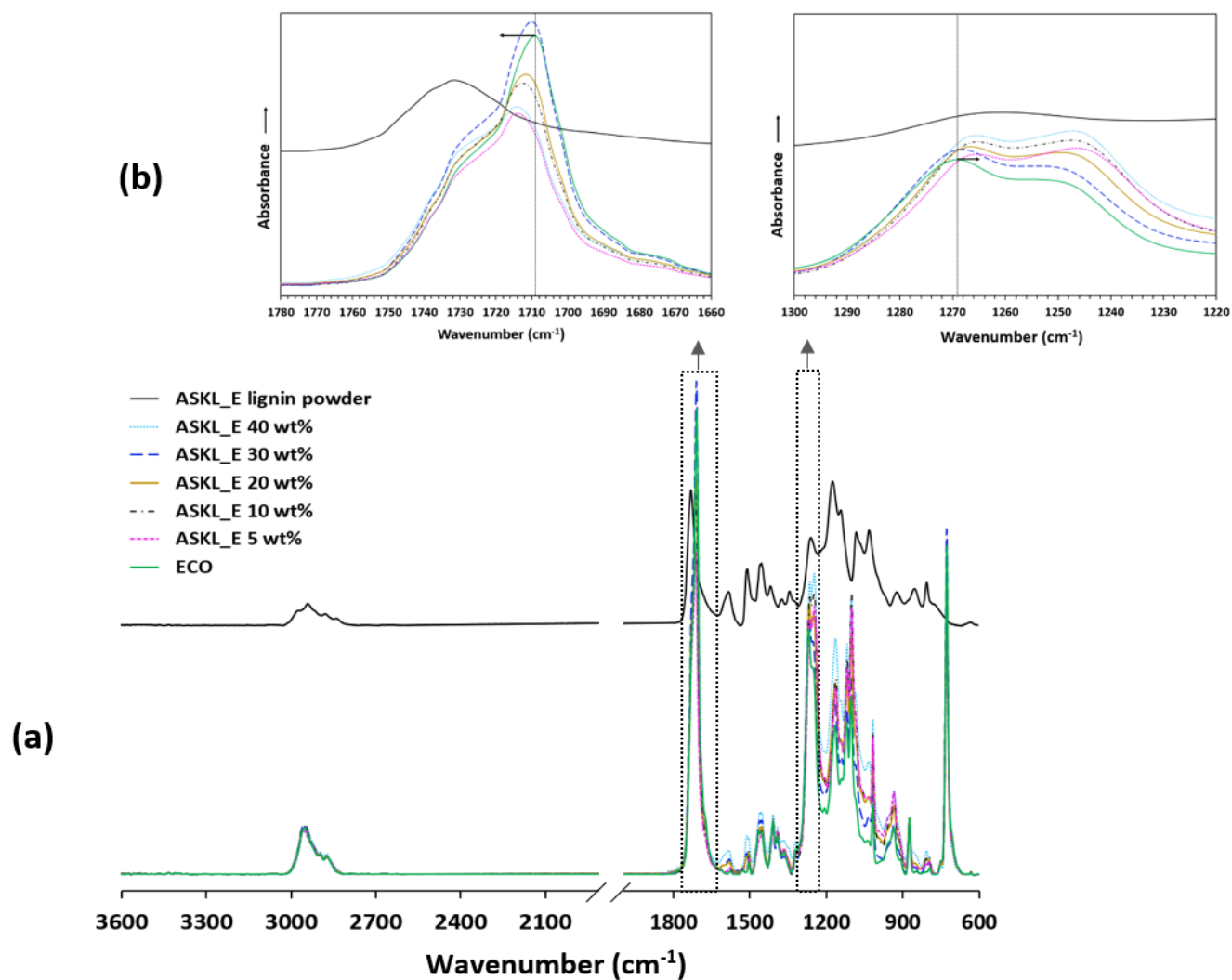
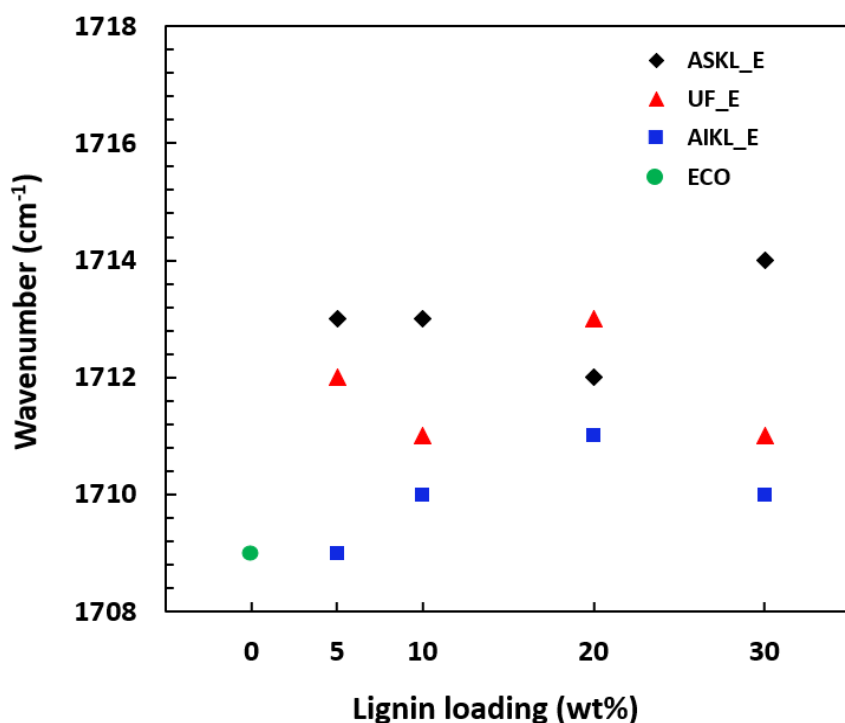


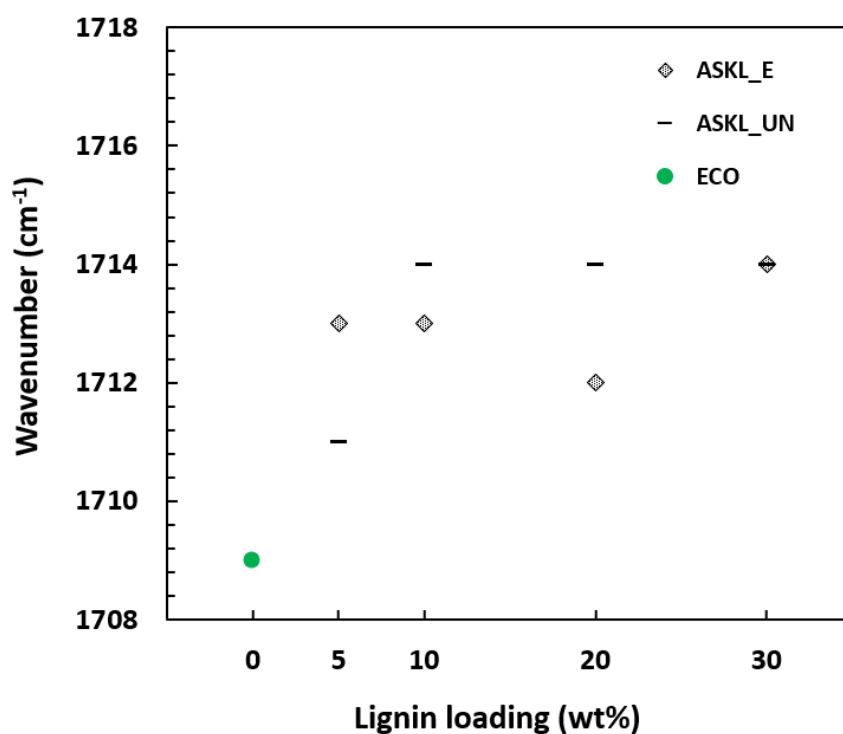
Figure 75 FT-IR spectrum for esterified acetone soluble (ASKL\_E) powder, neat Ecoflex™ (ECO), and 5-40 wt% ASKL\_E – Ecoflex™ blends (a) and enlarged signals from 1660-1780 and 1220-1300  $\text{cm}^{-1}$  (c)

In Figure 76, a shift can be viewed related to increased lignin loading for the neat Ecoflex<sup>TM</sup> peak at 1709 cm<sup>-1</sup> and UF\_E and ASKL\_E, and AIKL\_E. It was observed for the spectra that the ASKL\_E fraction and the UF\_E portion contained a larger peak shift than the AIKL\_E fraction which has a substantially higher molecular weight. These shifts in signal show that the lignin-Ecoflex<sup>TM</sup> blends are compatible with relatively strong and stable intermolecular interactions. The AIKL\_E powder in blend with Ecoflex<sup>TM</sup> showed a steady decrease in tensile strength and toughness as loading was increased, however, it performed better than its unmodified or HE counterparts in mechanical testing. The shifts in the spectra suggest that AIKL\_E had some interaction with Ecoflex<sup>TM</sup> but not as much as ASKL\_E and UF\_E which both showed better mechanical performance in the blend.



**Figure 76 Lignin loading (wt%) as a function of wavenumber (cm<sup>-1</sup>) for neat Ecoflex (ECO) peak 1709 cm<sup>-1</sup> and the subsequent peak shift for unfractionated esterified (UF\_E), acetone soluble esterified (ASKL\_E), and acetone insoluble esterified (AIKL\_E) lignin powders in blend with Ecoflex<sup>TM</sup>**

Figure 77 has the plot of increasing lignin load as a function of wavenumber for the neat Ecoflex<sup>TM</sup> peak at 1709 cm<sup>-1</sup> and ASKL\_UN as compared to ASKL\_E. The unmodified low molecular weight fraction of lignin showed the greatest increase in tensile properties at 5 and 10 wt% loading while the esterified low molecular weight fraction showed tensile properties similar to neat Ecoflex<sup>TM</sup> at a loading up to 40 wt%. It can be observed that both powders in blend showed an increased shift in signal as lignin was added to the blend however, it was likely for different reasons. The reactive hydroxyl groups in the unmodified lignin may have interacted with the aromatic groups in the Ecoflex<sup>TM</sup> matrix which grafted the polymers while the ester groups in both the esterified lignins chemical structure and the Ecoflex<sup>TM</sup> chemical structure led to transesterification in melt as indicated by the loss of the propionate ester peak.



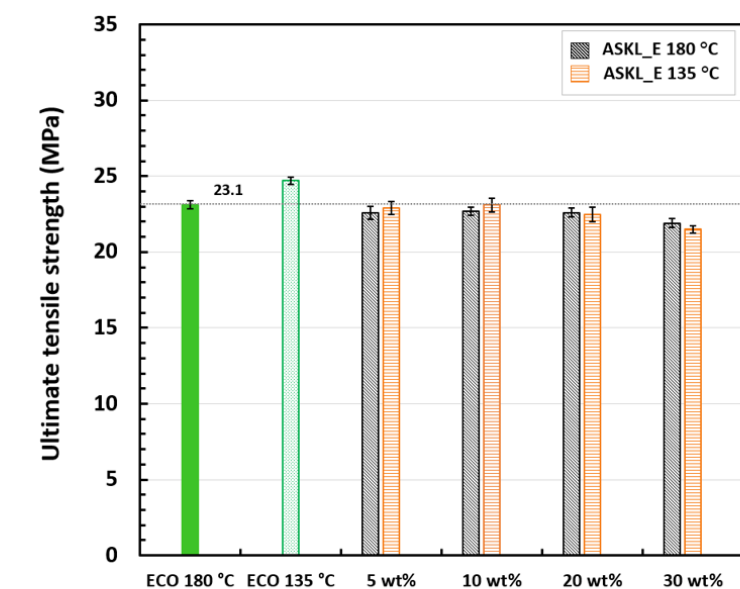
**Figure 77** Lignin loading (wt%) as a function of wavenumber (cm<sup>-1</sup>) for neat Ecoflex<sup>TM</sup> (ECO) peak 1709 cm<sup>-1</sup> and the subsequent peak shift for acetone soluble unmodified (ASKL\_UN) and acetone soluble esterified (ASKL\_E) lignin powders in blend with Ecoflex<sup>TM</sup>

#### **4.2.6 Melt processing temperature comparison for ASKL\_E – Ecoflex™ blends**

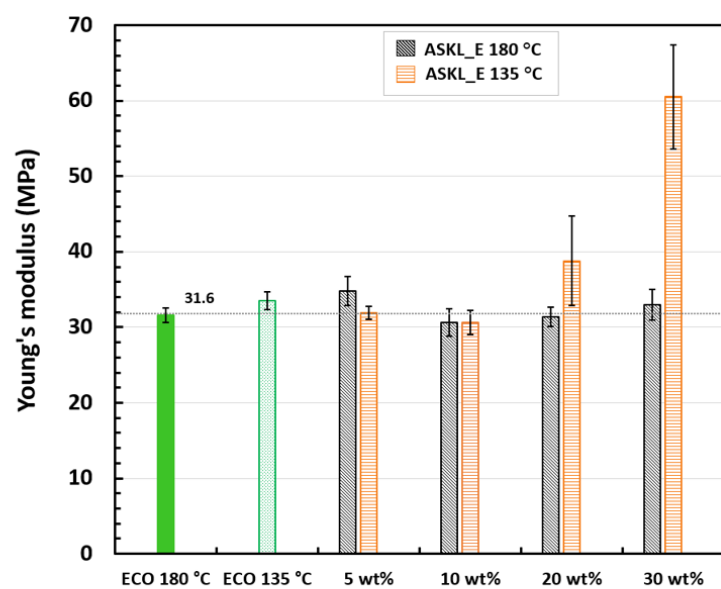
All lignin – Ecoflex™ blends were melt processed at 180 °C in order to properly compare the lignin powders mechanical, thermal, and structural property performances. Because the ASKL\_E powder showed great stability and had a substantially lower  $T_g$  there was potential for utilization at a melt processing temperature of 135 °C. This lower processing temperature was attempted to determine if changing this processing condition would drastically change the mechanical or thermal properties. In the following section ASKL\_E blended with Ecoflex at 180 °C will briefly be compared to ASKL\_E blended with Ecoflex at 135 °C. The mechanical property analysis and comparison for the different melt processing temperatures is presented in Figure 78.

Overall, the ASKL\_E powder performed better when processed with Ecoflex™ at 180 °C in comparison to 135 °C for elongation at break and toughness. The impact of processing temperature for ultimate tensile strength was subtle. The decrease in elongation at break and toughness for the 135 °C processed ASKL\_E sample indicated the higher melt processing temperature was ideal, although further rheological experiments could be developed to find the optimal processing temperature.

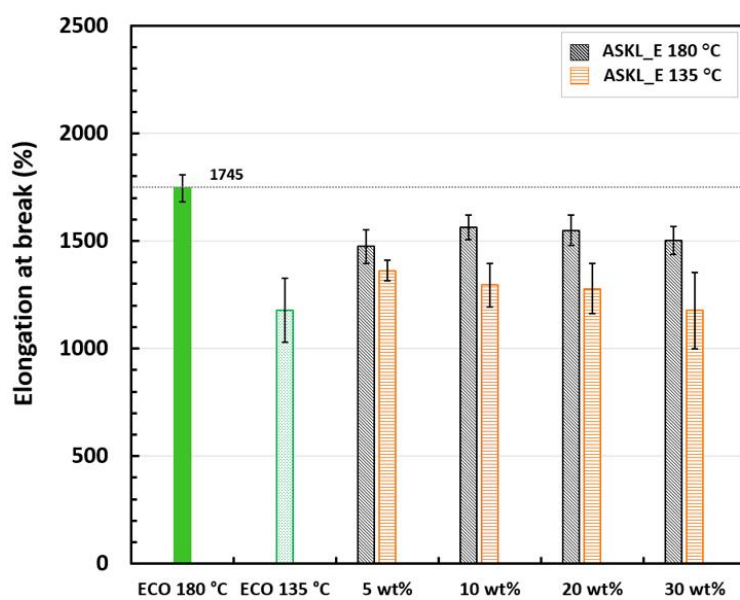




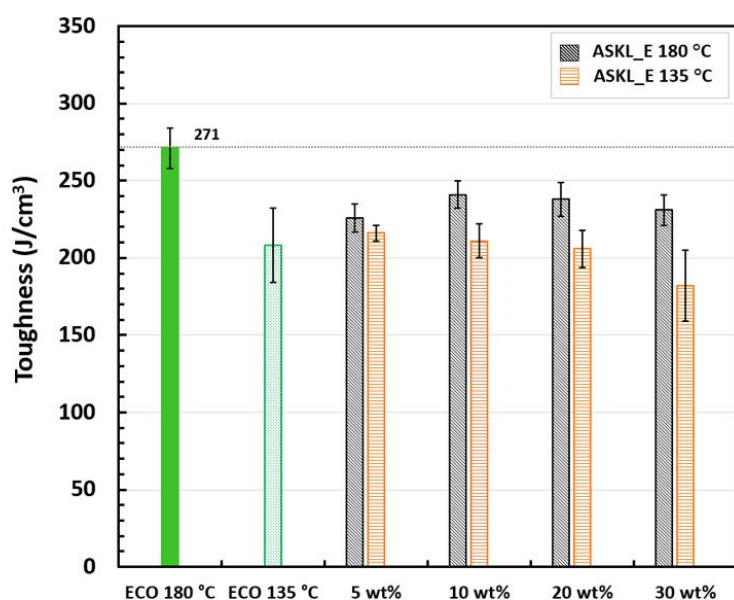
(a)



(b)



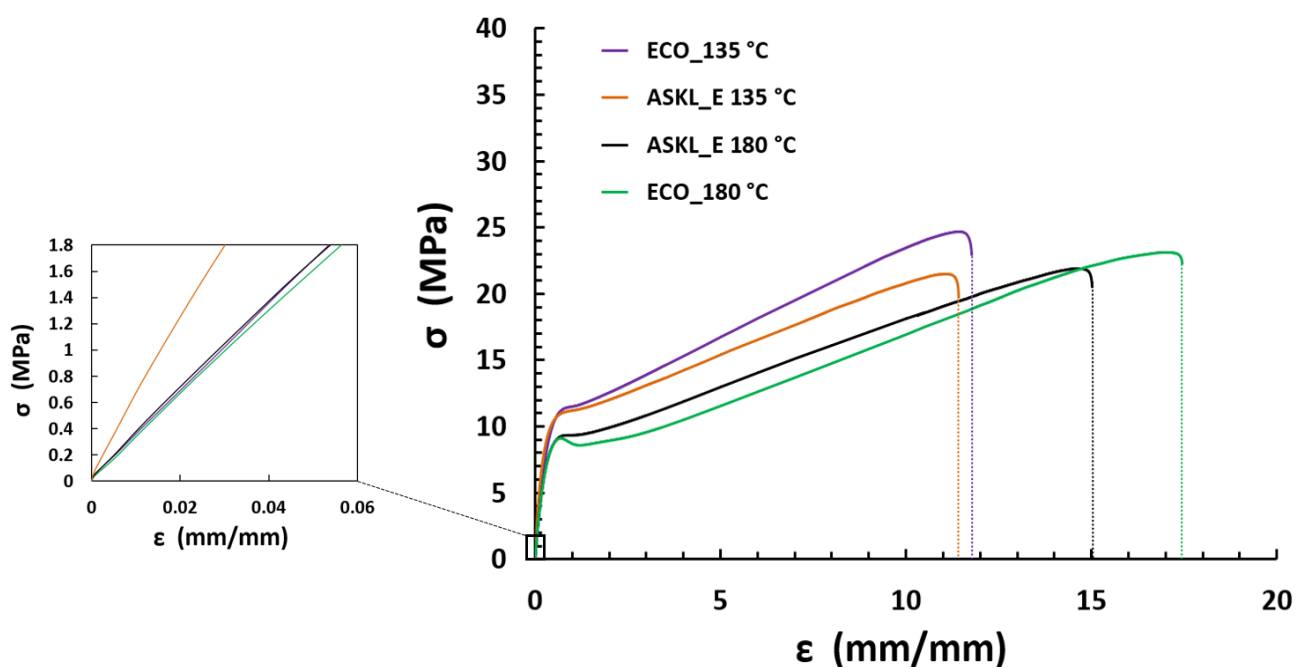
(c)



(d)

**Figure 78** Ultimate tensile strength (a) Young's modulus (b) percent elongation at break (c) and toughness (d) for neat Ecoflex™ (ECO) at a 180 °C and 135 °C melt processing temperature blended with acetone soluble esterified (ASKL\_E) at a lignin loading of 5, 10, 20, and 30 wt%

The accompanying engineering stress strain curves for neat Ecoflex™ blended with ASKL\_E at 30 wt% loading for both processing temperatures was reported in Figure 79. Yielding was more clearly defined in the neat Ecoflex™ and 30 wt% ASKL\_E – Ecoflex™ blend processed at 180 °C. The stress falls after yield before constantly increasing as the neck extends along the sample in a process known as cold drawing. During cold drawing, both the amorphous and crystalline regions of the polymer align with the direction of pull and the material in the neck can support a higher stress.<sup>235</sup> This process was clearly defined despite the difference in processing temperature processing temperature and no brittle fracture was observed. The Young's modulus showed a large increase for the 30 wt% ASKL\_E processed at 135 °C but only a minor increase for ASKL\_E processed at 180 °C. This response is curious and warrants future investigation.



**Figure 79** Engineering stress strain curves with inset Young's modulus for ASKL\_E at 30 wt% lignin loading as compared to neat Ecoflex™ (ECO) at processing temperatures 135 °C and 180 °C

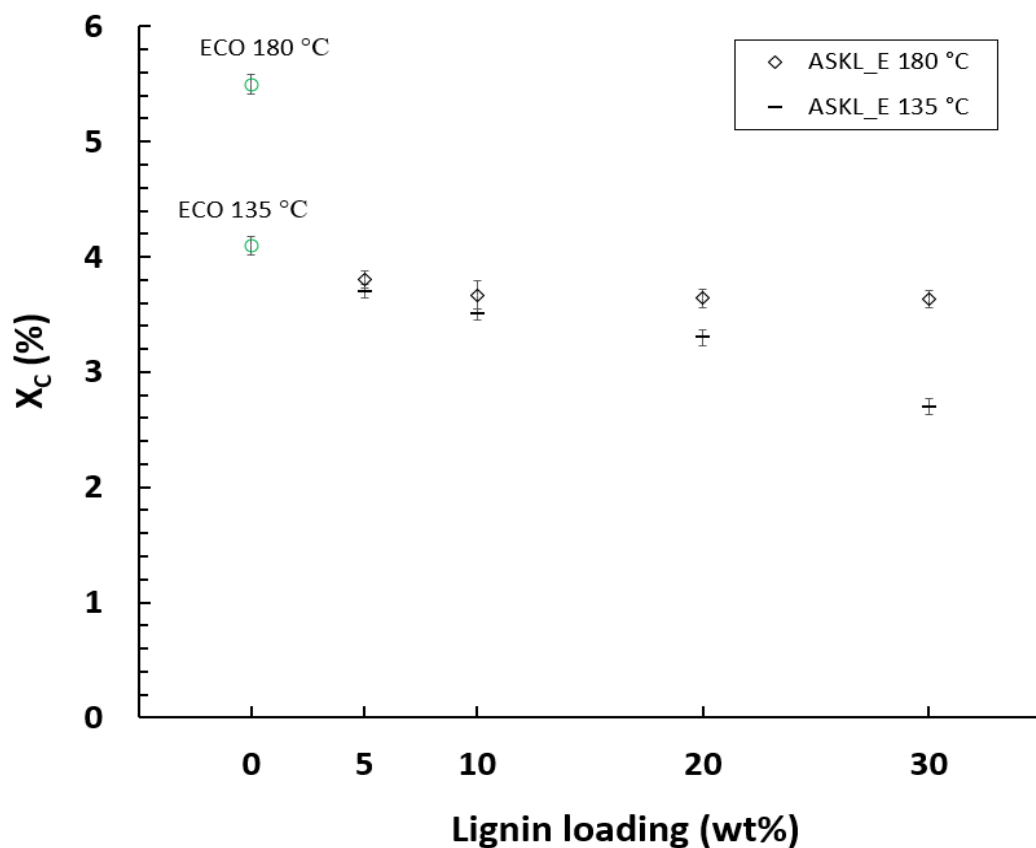
The thermal properties and degree of crystallinity comparison between ASKL\_E melt processed at 135 °C and 180 °C with Ecoflex™ can be observed at all wt% loadings with 0 wt% being neat Ecoflex™ in Table 22. There was not a statistically significant difference between the  $T_g$ , or  $T_m$  values presented by the ASKL\_E blended at the two processing temperatures. The  $T_c$  and  $T_{os}$  for ASKL\_E blended at both processing temperatures showed a similar increase which was discussed in detail in *section 4.2.4.2*. The melting and crystallization enthalpy are lower for the 135 °C processing temperature in comparison to the 180 °C which leads to a lower degree of crystallinity as lignin loading increases.

**Table 22 DSC results for neat Ecoflex™ (ECO) and acetone soluble esterified lignin (ASKL\_E) blended from 5-30 wt% lignin loading at 135 °C and 180 °C melt processing temperatures**

Samples	Melt processing temperature	$T_g$ (°C)	$T_m$ (°C)	$T_c$ (°C)	$T_{os}$ (°C)	$T_{os}-T_c$ (°C)	$\Delta H_m$ (J/g)	$\Delta H_c$ (J/g)	$X_c$ (%)
ECO 0 wt%	180 °C	-27.8	126.8	69.9	79.1	9.1	6.2	11.3	5.5
ECO 0 wt%	135 °C	-27.8	126.4	71.9	81.2	9.3	4.7	10.6	4.1
ASKL_E 5 wt%	180 °C	-26.9	127.6	79.3	88.3	9.0	4.1	8.9	3.8
ASKL_E 5 wt%	135 °C	-26.1	127.2	78.3	86.7	8.4	3.8	8.7	3.7
ASKL_E 10 wt%	180 °C	-25.9	127.2	78.8	87.8	9.0	3.8	8.7	3.7
ASKL_E 10 wt%	135 °C	-26.1	126.6	77.8	86.6	8.9	3.5	8.2	3.5
ASKL_E 20 wt%	180 °C	-23.5	126.4	78.1	87.2	9.0	3.3	7.5	3.6
ASKL_E 20 wt%	135 °C	-23.9	126.1	77.8	86.9	9.1	3.1	7.5	3.3
ASKL_E 30 wt%	180 °C	-24.2	125.6	77.1	86.0	8.9	2.9	7.3	3.6
ASKL_E 30 wt%	135 °C	-23.3	125.1	79.2	89.7	9.4	2.1	6.6	2.7

The change in degree of crystallinity for neat Ecoflex™ and ASKL\_E blended at 5-30 wt% lignin loading for both the 135 °C and 180 °C processing temperatures was illustrated in Figure 80. At 30 wt% the ASKL\_E blend processed at 135 °C has an  $X_c$  value 0.9% lower than the ASKL\_E blended at 180 °C. It was mentioned in literature that when blending a two polymer

system the processing temperature selected should be 20 °C higher than that of the melting temperature of the highest component.<sup>92,189</sup> Since lignin does not have a melting temperature, Ecoflex<sup>TM</sup> would be the component with the highest  $T_m$  and should be melt processed at approximately 150 °C.<sup>92,189</sup>



**Figure 80** Degree of crystallinity ( $X_c$ ) as a function of lignin loading (wt %) for acetone soluble esterified lignin (ASKL\_E) powders, and neat Ecoflex<sup>TM</sup> (ECO) at a 135 °C and 180 °C processing temperatures

#### 4.2.7 Mechanical property comparison of lignin thermoplastic blends

A literature comparison of the reported ultimate tensile strength in this study as compared to other research group lignins in blend with Ecoflex<sup>TM</sup> and other polymers like polyethylene, polypropylene, and PLA is presented in Table 23. Aside from this work, all of the modifications done to the lignin in Table 23 used the harsh chemicals discussed in *section 2.3*. The UTS comparison showed that the ASKL\_UN (10 wt%) and ASKL\_E (40 wt%) from this work are competitive with other lignin-polymer blends described in literature. Additionally, tensile strength was compared to Young's modulus or the stiffness of resultant lignin thermoplastic blends for this work and that of other research groups in Figure 81. Hence, based on the different modification levels and performances, this research has created several potential pathways to either increase lignin loading and maintain mechanical properties, or have enhanced mechanical performance without toxic chemicals.

**Table 23 Literature comparison of the Ultimate tensile strength (UTS) of lignin-Polymer blends**

Lignin type	Fractionation	Modification	wt% lignin	Polymer	Additive	Specimen	UTS (MPa) before lignin	UTS (MPa) after lignin	Ref.
SWKL	Acetone	None	10	Ecoflex™	None	Dog bone ASTM D638	23.1	31.5	This work
SWKL	Acetone	Esterification	40	Ecoflex™	None	Dog bone ASTM D638	23.1	20.9	This work
SWKL	Methanol	None	30	Ecoflex™	None	Dog bone ASTM D638	21.7	14.6	212
SWKL	None	None	30	Ecoflex™	None	Dog bone ASTM D638	21.7	13.0	212
SWKL	None	None	6	Ecoflex™	None	Films	19.6	17.0	214
Eucalypt Hydrothermal	None	Esterification	40	Ecoflex™	MAH <sup>a</sup>	Films	23.0	13.2	213
Eucalypt Hydrothermal	None	Methylation	40	Ecoflex™	None	Films	23.7	19.5	190
SWKL	None	None	10	Polypropylene	MAH <sup>a</sup>	Dog bone ASTM D638	24.9	20.3	185
SWKL	None	Esterification	30	Polypropylene	None	Dog bone ASTM D1708	32.6	27.4	145
HWKL	None	Esterification	40	Polyethylene (high density)	Paraffin wax	Dog bone DIN norms	23.0	21.0	144
SWKL	Acetone	Methylation	25	Polyethylene	None	Dog bone ASTM D638	23.6	20.4	189
SWKL	None	Acetylation	20	PLA	None	Films	48.7	32.1	182

<sup>a</sup> Maleic anhydride is an additive used to improve adhesion between lignin and the polymer matrix

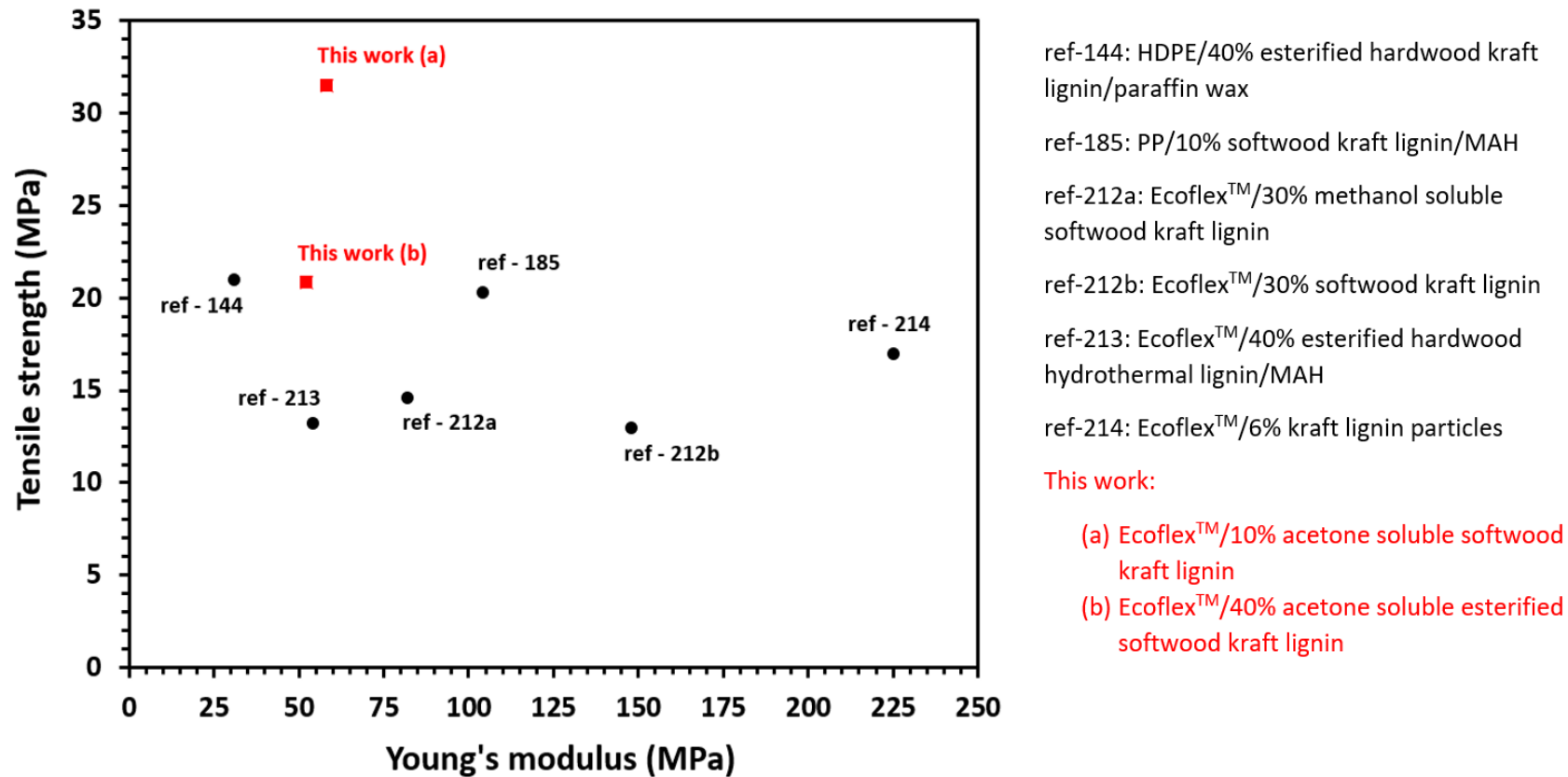


Figure 81 Comparison of the tensile strength and Young's modulus (stiffness) for lignin based thermoplastic blends

#### 4.2.8 Concluding highlights

- (1) Independent of fractionation or modification, all lignin powders were melt-processable at 180 °C with Ecoflex<sup>TM</sup> up to 20 wt%
- (2) All mechanical and thermal testing showed high consistency and good repeatability which is critical in lignin research
- (3) The acetone soluble unmodified lignin powder at 5 and 10 wt% loading showed an increase in ultimate tensile strength, total elongation at break, and toughness compared to neat Ecoflex<sup>TM</sup>
- (4) The unfractionated esterified lignin powder at 5 wt% loading showed an increase in ultimate tensile strength, total elongation at break, and toughness compared to neat Ecoflex<sup>TM</sup>
- (5) The acetone soluble esterified lignin powder was blended with Ecoflex<sup>TM</sup> up to 40 wt% without a major loss in mechanical properties and showed promise at these higher lignin loadings
- (6) The acetone insoluble esterified lignin powder reported an overall decrease in most mechanical properties but showed a large increase in Young's modulus and performed the best of the insoluble samples in blend with Ecoflex<sup>TM</sup>
- (7) Fractionation of the lignin powder does affect the mechanical properties of lignin in blend with Ecoflex<sup>TM</sup>
- (8) Glass transition temperature governed by modification of the lignin powder does affect the mechanical properties of lignin in blend with Ecoflex<sup>TM</sup> in most cases
- (9) Following green chemistry principles lignin powders were successfully blended with Ecoflex<sup>TM</sup> which are competitive with other lignin thermoplastic blends in literature



## Chapter 5: Conclusions and future work

### 5.1 Conclusions

The overall goal of this research was to investigate how modified low and high molecular weight fractions of lignin behave in melt with the biodegradable polyester Ecoflex<sup>TM</sup> in comparison to unmodified unfractionated as received Lignoforce<sup>TM</sup> softwood kraft lignin through extensive mechanical and thermal behavioral testing and analysis. With a high-paced societal dependency on non-renewably sourced petroleum based plastics and an increasing awareness at the health risks they pose to ecosystems and humans alike, the demand for alternative materials are increasing. Lignin, a renewable byproduct of the paper and pulping industry and an excellent source of naturally occurring aromatics known for their structure-function relationship has the potential to be part of the global plastic crisis solution. However, lignin is a multi-functional complex polymer that requires modification to become processable in a two-system polymeric blend. Fractionated modified lignins blended with polymers like Ecoflex<sup>TM</sup>, polypropylene and polyethylene are documented in literature but there are very few studies that focus on green chemistry processes. Harsh malignant chemicals and plasticizers are often used to change lignins structure defeating the purpose of developing an environmentally safer material. Despite ongoing advancements in lignin valorization there is a gap in attaining its full utilization. The key point of this work was to fill that gap and show the potential of a novel lignin based green thermoplastic blend so kraft pulping mills can potentially evolve into biorefineries that use lignin not only as an energy source but as a profitable commodity building block for highly demanded materials.

In section 4.1, the as received lignin was washed and fractionated into low and high molecular weight portions in a simple one-step process using readily available acetone that was

easily recovered. The fractions then underwent etherification using ethylene carbonate a safer alternative to propylene oxide. Using a real-time control procedure developed within our laboratory, ethylene carbonate successfully transformed lignin's aromatic hydroxyl groups into aliphatic hydroxyl groups creating a more uniform thermally stable polymer. The hydroxyethyl ether lignins were then esterified using only propionic acid a safer alternative to the anhydrides used in other studies. Modifications were proven successful through  $^{13}\text{P}$  NMR, DSC, TGA, GPC, and FT-IR analysis and nine lignin powders were developed for melt-processing and extrusion with Ecoflex<sup>TM</sup>.

In section 4.2 using the experimental procedures developed in this research, the nine lignin powders were blended at 5-40 wt% loading with Ecoflex<sup>TM</sup> using a twin screw microcompounder at a melt-processing temperature of 180 °C. The blend was injection moulded into standard type V dumbbell shaped test specimens. All samples went through extensive mechanical property testing strictly following ASTM D638 protocols. The acetone soluble lower molecular weight fraction without any modification (ASKL\_UN) showed an increase in tensile strength, total elongation at break and toughness with a minor increase in stiffness at 5 and 10 wt% lignin loading. As lignin loading increased to 30 wt% stiffness increased and tensile strength, total elongation at break, and toughness slightly decreased. The esterified acetone soluble lower molecular weight fraction (ASKL\_E) showed great promise as a filler in blend with Ecoflex<sup>TM</sup> up to 40 wt% and potentially beyond. Tensile strength, total elongation at break and toughness only slightly decreased as lignin loading increased, while stiffness only slightly increased. The esterified unfractionated lignin powder (UF\_E) showed an increase in tensile strength, total elongation at break, and toughness at 5 wt% loading. Additional DSC, TGA, and FT-IR analysis was used to confirm intermolecular interactions between the lignin powders and

the Ecoflex<sup>TM</sup> matrix. It was observed that the lower molecular weight fraction and the unfractionated as received lignin were more stable in melt with Ecoflex<sup>TM</sup> than the higher molecular weight acetone insoluble portion. The AIKL powders, especially the unmodified sample had a higher glass transition temperature than their unfractionated and acetone soluble counterparts. The lignin molecules in the AIKL powders tended to react with one another and agglomerate instead of bonding with the Ecoflex<sup>TM</sup> matrix. The lignin-lignin interaction is a brittle one which decreases strength and toughness while drastically increasing stiffness. This showed a correlation between mechanical property improvement and the molecular weight and thermal properties of the starting lignin powders. The powders that performed best in blend had lower starting  $T_g$  values and lower molecular weights. Overall, the green chemistry practices used which consider environmental impact and possible scale-up operations were successful in making lignin powders that are processible with Ecoflex<sup>TM</sup> and competitive with other studies presented in literature.

At the start of this thesis a question was proposed: which lignin powder makes a good thermoplastic blend? It was hypothesized that ASKL\_E would be the most stable in blend with Ecoflex<sup>TM</sup> and this was a good speculation as ASKL\_E could act as a filler in plastics. The unexpected performance of ASKL\_UN and UF\_E at lower lignin loadings showed good promise in enhancing mechanical properties such as strength and toughness of thermoplastic blends and this could have many material implications. These results show there is not one key feature that makes a “good lignin powder” but a plethora of conditions that will contribute. The ASKL\_UN powder contains reactive aromatic hydroxyl groups but its low molecular weight and low  $T_g$  in combination with the Ecoflex<sup>TM</sup> structure and the melt processing temperature led to an increase in important mechanical properties while its more uniform esterified counterpart showed

relatively unchanging mechanical properties similar to that of neat Ecoflex<sup>TM</sup>. This indicates there are complex intermolecular interactions going on within the lignin-Ecoflex matrix<sup>TM</sup>. Further investigation is needed to understand these interactions and develop a lignin-based material ready for utilization in a world that is demanding safer more environmentally conscious plastics.

## **5.2 Future work**

The scope of this research project was large as nine different lignin powders were blended at five different weight ratios in a melt-processed extrusion experiment with biodegradable Ecoflex<sup>TM</sup> and then analyzed and characterized using DSC, TGA, FT-IR, SEM, and tensile testing . This leaves several relevant and very important areas open to further research.

### **5.2.1 Acetone soluble unmodified and esterified lignin-Ecoflex<sup>TM</sup> films**

This research used mould injection techniques make dog bone specimens that determined mechanical properties which helped to make inferences between lignin powders. Films could be blown and studied using the lignin powders that showed improvements in or stability of tensile strength and toughness. Kargarzadeh et al. who developed 1 mm thick films with kraft lignin particles and Ecoflex<sup>TM</sup> used isothermal DSC techniques and the Thomson-Gibbs equation to measure the thickness of the crystal structure. More research in this area could reveal important micromechanical, structural, and interaction properties.

### **5.2.2 Small angle X-ray scattering of developed thermoplastic blends**

Further research that focuses on structural changes between the different lignin powders and the weight percentage of loading in blend with Ecoflex<sup>TM</sup> is necessary for material development. Small angle X-ray scattering along with atomic force microscopy and scanning

electron microscopy could help to determine the structural changes of the specimens during deformation and detect nanovoids or the onset of the formation of nanovoids.

### **5.2.3 Biodegradation testing**

The lignin-Ecoflex<sup>TM</sup> thermoplastic blends should undergo standardized testing for biodegradability. There are a series of standards that any new material must meet to be considered compostable and biodegradable under certain conditions. Ecoflex<sup>TM</sup> is certified through the ISO 17088 and the ISO 14855 composting test and the lignin-Ecoflex<sup>TM</sup> blends presented in this research should undergo the same testing and analysis for comparison.

### **5.2.4 Improving lignin powder chemistries**

The molar mass data showed a bi-modal wider molecular weight distribution for the acetone soluble fractionated hydroxyethyl ether and esterified lignin powders in comparison to the acetone fractionated unmodified lignin powder. This is likely due to side reaction that took place during the etherification however, both ASKL\_UN and ASKL\_E improved or upheld the tensile properties of Ecoflex<sup>TM</sup>. The potential for further improvement may be possible if the fractionation is done after the hydroxyethyl etherification and this should be investigated.

### **5.2.5 Techno-economic analysis**

When engineering any new material, it is crucial to analyze its economic feasibility. Jiang et al. prepared an excellent study that examined lignin fractionation and the utility for scale-up commercialization. A similar study could be done to test the economic potential for ASKL\_UN-Ecoflex<sup>TM</sup> thermoplastic blends.

### **5.2.6 Crystallization kinetics of lignin-Ecoflex<sup>TM</sup> thermoplastic blends**

The melt crystallization characteristics of a thermoplastic blend can be helpful in optimizing processability. Sousa et al. produced a thorough study on the crystallization kinetics

of Ecoflex<sup>TM</sup> and coconut fibre blends using extensive DSC testing. The study provided quantitative information about crystallization temperatures, rates, and development. Pseudo-Avrami and Mo models represented the data and were used to best optimize processing conditions which led to the most effective thermoplastic blend.

#### **5.2.7 Carbon spun fibres from acetone insoluble lignin fraction**

In this study, the high molecular weight acetone insoluble lignin powders showed a steady decline in tensile properties and a great increase in stiffness at a melt processing temperature of 180 °C with Ecoflex<sup>TM</sup>. The starting glass transition temperature for the AIKL powders is greater than its low molecular weight counterpart. In this study melt processing temperature was a controlled variable but it would be interesting to study how the AIKL powders performed at a higher melt-processing temperature. Dynamic mechanical thermal analysis could be utilized to determine how Ecoflex<sup>TM</sup> performs at higher melt-processing temperatures and then AIKL powders added with the potential for carbon spun fibres which require greater stiffness than the ASKL powders provide.

## Bibliography

- (1) Pelley, J. Plastic Contamination of the Environment: Sources, Fate, Effects, and Solutions. *Am. Chem. Soc.* **2018**, 2–31.
- (2) Allen, K. Captain Charles Moore <http://www.captain-charles-moore.org/>.
- (3) Baker, M. How to eliminate plastic waste and plastic pollution with science and engineering <https://interestingengineering.com/>.
- (4) Geyer, R.; Jambeck, J. R.; Law, K. L. Production, Use, and Fate of All Plastics Ever Made. *Sci. Adv.* **2017**, 3 (7), 25–29.
- (5) Boerjan, W.; Ralph, J.; Baucher, M. Lignin Biosynthesis. *Annu. Rev. Plant Biol.* **2003**, 54 (1), 519–546.
- (6) Upton, B. M.; Kasko, A. M. Strategies for the Conversion of Lignin to High-Value Polymeric Materials: Review and Perspective. *Chem. Rev.* **2016**, 116 (4), 2275–2306.
- (7) Zakzeski, J.; Bruijninx, P. C. A.; Jongerius, A. L.; Weckhuysen, B. M. The Catalytic Valorization of Lignin for the Production of Renewable Chemicals. *Chem. Rev.* **2010**, 110 (6), 3552–3599.
- (8) Sjöström, E. 4. Wood Chemistry Fundamentals and Applications: Lignin. *Wood Chem. Fundam. Appl.* **1993**, 1–36.
- (9) Henriksson, G. Lignin. In *Wood Chemistry and Wood Biotechnology*; Walter de Gruyter, 2009; pp 121–146.
- (10) Wang, C.; Kelley, S. S.; Venditti, R. A. Lignin-Based Thermoplastic Materials. *ChemSusChem* **2016**, 9 (8), 770–783.
- (11) Adler, E. Lignin Chemistry - Past, Present and Future. *Wood Sci. Technol.* **1977**, 8 (11), 169–218.

- (12) Whetten, R. W.; MacKay, J. J.; Sederoff, R. R. Recent Advances in Understanding Lignin Biosynthesis. *Annu. Rev. Plant Physiol. Plant Mol. Biol.* **1998**, *49* (1), 585–609.
- (13) McCarthy, J. L.; Islam, A. Lignin Chemistry, Technology, and Utilization: A Brief History. *American* **1999**, 2–99.
- (14) Humphreys, J. M.; Chapple, C. Rewriting the Lignin Roadmap. *Curr. Opin. Plant Biol.* **2002**, *5* (3), 224–229.
- (15) Buranov, A. U.; Mazza, G. Lignin in Straw of Herbaceous Crops. *Ind. Crops Prod.* **2008**, *28* (3), 237–259.
- (16) Lin, S.; Dence, C. *Methods in Lignin Chemistry*; Springer, 1992.
- (17) Faraji, M.; Fonseca, L. L.; Escamilla-Treviño, L.; Barros-Rios, J.; Engle, N.; Yang, Z. K.; Tschaplinski, T. J.; Dixon, R. A.; Voit, E. O. Mathematical Models of Lignin Biosynthesis Mike Himmel. *Biotechnol. Biofuels* **2018**, *11* (1), 1–17.
- (18) Baucher, M.; Monties, B.; Van Montagu, M.; Boerjan, W. Biosynthesis and Genetic Engineering of Lignin. *CRC. Crit. Rev. Plant Sci.* **1998**, *17* (2), 125–197.
- (19) Li, X.; Chapple, C. Understanding Lignification: Challenges beyond Monolignol Biosynthesis. *Plant Physiol.* **2010**, *154* (2), 449–452.
- (20) Campbell, M. M.; Sederoff, R. R.; Campbell, M. M.; Sederoff, R. R. Variation in Lignin Content and Composition : Mechanisms of Control and Implications for the Genetic Improvement of Plants. *Plant Physiol.* **2017**, *110* (1), 3–13.
- (21) Alejandro, S.; Lee, Y.; Tohge, T.; Sudre, D.; Osorio, S.; Park, J.; Bovet, L.; Lee, Y.; Geldner, N.; Fernie, A. R.; Martinoia, E. AtABCG29 Is a Monolignol Transporter Involved in Lignin Biosynthesis. *Curr. Biol.* **2012**, *22* (13), 1207–1212.
- (22) Miao, Y. C.; Liu, C. J. ATP-Binding Cassette-like Transporters Are Involved in the



- Transport of Lignin Precursors across Plasma and Vacuolar Membranes. *Proc. Natl. Acad. Sci. U. S. A.* **2010**, *107* (52), 22728–22733.
- (23) Freudenberg, K. Polysaccharides and Lignin. *Annu. Rev. Biochem.* **1960**, No. 4.
  - (24) Ghosh, I.; Jain, R. K.; Glasser, W. G. Blends of Biodegradable Thermoplastics with Lignin Esters. In *Lignin: Historical, biological, and materials perspectives*; American Chemical Society, 1999; pp 331–350.
  - (25) Douglas, C. J. Phenylpropanoid Metabolism and Lignin Biosynthesis: From Weeds to Trees. *Trends Plant Sci.* **1996**, *1* (6), 171–178.
  - (26) Boudet, A. M. A New View of Lignification. *Trends Plant Sci.* **1998**, *3* (2), 67–71.
  - (27) Glasser, W. G. About Making Lignin Great Again—Some Lessons From the Past. *Front. Chem.* **2019**, *7* (August), 1–17. <https://doi.org/10.3389/fchem.2019.00565>.
  - (28) Tarasov, D.; Leitch, M.; Fatehi, P. Lignin – Carbohydrate Complexes: Properties , Applications , Analyses , and Methods of Extraction : A Review. *Biotechnol. Biofuels* **2018**, *11* (269), 1–28.
  - (29) Atalla, R. H.; Agarwal, U. P. Raman Microprobe Evidence for Lignin Orientation in the Cell Walls of Native Woody Tissue. *Science* (80-. ). **1985**, *227* (4687), 636–638.
  - (30) Donaldson, L. A. Lignification and Lignin Topochemistry - An Ultrastructural View. *Phytochemistry* **2001**, *57* (6), 859–873.
  - (31) Wang, Y.; Chantreau, M.; Sibout, R.; Hawkins, S. Plant Cell Wall Lignification and Monolignol Metabolism. *Front. Plant Sci.* **2013**, *4* (JUL), 1–14.
  - (32) Gellerstedt, G. L. F.; Henriksson, E. G. Lignins: Major Sources, Structure and Properties. *Monomers, Polym. Compos. from Renew. Resour.* **2008**, 201–224.
  - (33) Björkman, A. Lignin and Lignin-Carbohydrate Complexes Extraction from Wood Meal

- with Neutral Solvents. *Ind. Eng. Chem.* **1957**, *49* (9), 1395–1398.
- (34) Gratzl, J. S.; Chen, Chen-Loung, W. G. Chemistry of Pulping: Lignin Reactions. In *Lignin: Historical, Biological, and Materials Perspective*; 1999; pp 392–421.
- (35) Schwanninger, M.; Hinterstoisser, B. Klason Lignin: Modifications to Improve the Precision of the Standardized Determination. *Holzforschung* **2002**, *56* (2), 161–166.
- (36) Beňo, E.; Góra, R.; Hutta, M. Characterization of Klason Lignin Samples Isolated from Beech and Aspen Using Microbore Column Size-Exclusion Chromatography. *J. Sep. Sci.* **2018**, *41* (16), 3195–3203.
- (37) Berlin, A.; Balakshin, M. *Industrial Lignins: Analysis, Properties, and Applications*; Elsevier, 2014.
- (38) Rinaldi, R.; Jastrzebski, R.; Clough, M. T.; Ralph, J.; Kennema, M.; Bruijninx, P. C. A.; Weckhuysen, B. M. Paving the Way for Lignin Valorisation: Recent Advances in Bioengineering, Biorefining and Catalysis. *Angew. Chem - Int. Ed.* **2016**, *55* (29), 8164–8215.
- (39) Holladay, J. E.; White, J. F.; Bozell, J. J.; Johnson, D. *Top Value-Added Chemicals from Biomass Volume II — Results of Screening for Potential Candidates from Biorefinery Lignin*; 2007.
- (40) Zhang, Z.; Harrison, M. D.; Rackemann, D. W.; Doherty, W. O. S.; O'Hara, I. M. Organosolv Pretreatment of Plant Biomass for Enhanced Enzymatic Saccharification. *Green Chem.* **2016**, *18* (2), 360–381. <https://doi.org/10.1039/c5gc02034d>.
- (41) Lora, J. H. Industrial Commercial Lignins: Sources, Properties and Applications. In *Monomers, Polymers and Composites from Renewable Resources*; 2008; pp 225–241.
- (42) Kanungo, D.; Francis, R. C.; Shin, N. H. Mechanistic Differences between Kraft and

- Soda/AQ Pulping. Part 2: Results from Lignin Model Compounds. *J. Wood Chem. Technol.* **2009**, 29 (3), 227–240.
- (43) Rueda, C.; Calvo, P. A.; Moncalián, G.; Ruiz, G.; Coz, A. Biorefinery Options to Valorize the Spent Liquor from Sulfite Pulping. *J. Chem. Technol. Biotechnol.* **2015**, 90 (12), 2218–2226.
- (44) Gellerstedt, G. Softwood Kraft Lignin: Raw Material for the Future. *Ind. Crops Prod.* **2015**, 77, 845–854.
- (45) Demuner, I. F.; Colodette, J. L.; Demuner, A. J.; Jardim, C. M. Biorefinery Review: Wide-Reaching Products through Kraft Lignin. *BioResources* **2019**, 14 (3), 7543–7581.
- (46) Bajwa, D. S.; Pourhashem, G.; Ullah, A. H.; Bajwa, S. G. A Concise Review of Current Lignin Production, Applications, Products and Their Environment Impact. *Ind. Crops Prod.* **2019**, 139 (October), 1–10.
- (47) Mandlekar, N.; Cayla, A.; Rault, F.; Giraud, S.; Salaün, F.; Malucelli, G.; Guan, J.-P. An Overview on the Use of Lignin and Its Derivatives in Fire Retardant Polymer Systems. *Lignin - Trends Appl.* **2018**.
- (48) Chakar, F. S.; Ragauskas, A. J. Review of Current and Future Softwood Kraft Lignin Process Chemistry. *Ind. Crops Prod.* **2004**, 20 (2), 131–141.
- (49) Gellerstedt, G.; Majtnerova, A.; Zhang, L. Towards a New Concept of Lignin Condensation in Kraft Pulping. Initial Results. *Comptes Rendus - Biol.* **2004**, 327 (9–10), 817–826.
- (50) Smook, G. *Handbook for Pulp & Paper Technologists*; 2016.
- (51) Gierer, J. Chemistry of Delignification. *Wood Sci. Technol.* **1986**, 20 (1), 1–33.
- (52) Gosselink, R. J. A.; De Jong, E.; Guran, B.; Abächerli, A. Co-Ordination Network for

- Lignin - Standardisation, Production and Applications Adapted to Market Requirements (EUROLIGNIN). *Ind. Crops Prod.* **2004**, *20* (2), 121–129.
- (53) Schorr, D.; Diouf, P. N.; Stevanovic, T. Evaluation of Industrial Lignins for Biocomposites Production. *Ind. Crops Prod.* **2014**, *52*, 65–73.
- (54) Balakshin, M. Y.; Capanema, E. A. Comprehensive Structural Analysis of Biorefinery Lignins with a Quantitative <sup>13</sup>C NMR Approach. *RSC Adv.* **2015**, *5* (106), 87187–87199.
- (55) Balakshin, M.; Capanema, E. On the Quantification of Lignin Hydroxyl Groups with <sup>31</sup>P and <sup>13</sup>C NMR Spectroscopy. *J. Wood Chem. Technol.* **2015**, *35* (3), 220–237.
- (56) Balakshin, M. Y.; Capanema, E. A.; Santos, R. B.; Chang, H. M.; Jameel, H. Structural Analysis of Hardwood Native Lignins by Quantitative <sup>13</sup>C NMR Spectroscopy. *Holzforschung* **2016**, *70* (2), 95–108.
- (57) Magina, S.; Marques, A. P.; Evtuguin, D. V. Study on the Residual Lignin in Eucalyptus Globulus Sulphite Pulp. *Holzforschung* **2015**, *69* (5), 513–522. <https://doi.org/10.1515/hf-2014-0218>.
- (58) Bahrpaima, K.; Fatehi, P. Synthesis and Characterization of Carboxyethylated Lignosulfonate. *ChemSusChem* **2018**, *11* (17), 2967–2980.
- (59) Hu, Z.; Du, X.; Liu, J.; Chang, H. M.; Jameel, H. Structural Characterization of Pine Kraft Lignin: BioChoice Lignin vs Indulin AT. *J. Wood Chem. Technol.* **2016**, *36* (6), 432–446.
- (60) Tomani, P. The Lignoboost Process. *Cellul. Chem. Technol.* **2010**, *44* (1–3), 53–58.
- (61) Liu, L. Toward Lignin-Based Polymeric Materials Using Greener Modification Methods, 2020.
- (62) Zhu, W.; Westman, G.; Theliander, H. Investigation and Characterization of Lignin Precipitation in the Lignoboost Process. *J. Wood Chem. Technol.* **2014**, *34* (2), 77–97.

- (63) Kouisni, L.; Paleologou, M.; Holt-Hindle, P.; Maki, K. The LignoForce System™ A New Process for the Production of High-Quality Lignin from Black Liquor. *Sci. Technol. For. Prod. Process.* **2012**, *2* (4), 306–308.
- (64) Kouisni, L.; Gagné, A.; Maki, K.; Holt-Hindle, P.; Paleologou, M. LignoForce System for the Recovery of Lignin from Black Liquor: Feedstock Options, Odor Profile, and Product Characterization. *ACS Sustain. Chem. Eng.* **2016**, *4* (10), 5152–5159.
- (65) Kai, D.; Tan, M. J.; Chee, P. L.; Chua, Y. K.; Yap, Y. L.; Loh, X. J. Towards Lignin-Based Functional Materials in a Sustainable World. *Green Chem.* **2016**, *18* (5), 1175–1200.
- (66) Dong, D.; Fricke, A. L. Intrinsic Viscosity and the Molecular Weight of Kraft Lignin. *Polymer (Guildf).* **1995**, *36* (10), 2075–2078.
- (67) Janshekar, H.; Haltmeier, T.; Brown, C. Fungal Degradation of Pine and Straw Alkali Lignins. *Eur. J. Appl. Microbiol. Biotechnol.* **1982**, *14* (3), 174–181.
- (68) Datta, R.; Kelkar, A.; Baraniya, D.; Molaei, A.; Moulick, A.; Meena, R. S.; Formanek, P. Enzymatic Degradation of Lignin in Soil: A Review. *Sustain.* **2017**, *9* (7), 1–18.
- (69) PennState. Engineering, Department of Energy and Mineral. In *Are we running out of oil?*; 2020.
- (70) Baheti, P. How Is Plastic Made? British Plastics Federation 2020.
- (71) Kuczenski, B.; Geyer, R. Material Flow Analysis of Polyethylene Terephthalate in the US, 1996-2007. *Resour. Conserv. Recycl.* **2010**, *54* (12), 1161–1169.
- (72) Hoornweg, D.; Bhada-Tata, P.; Kennedy, C. Waste Production Must Peak This Century. *Nature* **2013**, *502* (7473), 615–617.
- (73) Rochman, C. M. Plastics and Priority Pollutants: A Multiple Stressor in Aquatic Habitats.

- Environ. Sci. Technol.* **2013**, 47 (6), 2439–2440.
- (74) Jambeck, J.; Geyer, R.; Wilcox, C.; Siegler, T. R.; Perryman, M.; Andrady, A.; Narayan, R.; Law, K. L. Plastic Waste Inputs from Land into the Ocean. *Science* (80-. ). **2015**, 347 (6223), 768–770.
- (75) Rochman, C. M.; Cook, A. M.; Koelmans, A. A. Plastic Debris and Policy: Using Current Scientific Understanding to Invoke Positive Change. *Environ. Toxicol. Chem.* **2016**, 35 (7), 1617–1626.
- (76) Rochman, C. M.; Kurobe, T.; Flores, I.; Teh, S. J. Early Warning Signs of Endocrine Disruption in Adult Fish from the Ingestion of Polyethylene with and without Sorbed Chemical Pollutants from the Marine Environment. *Sci. Total Environ.* **2014**, 493, 656–661.
- (77) Rochman, C. M.; Hoh, E.; Hentschel, B. T.; Kaye, S. Long-Term Field Measurement of Sorption of Organic Contaminants to Five Types of Plastic Pellets: Implications for Plastic Marine Debris. *Environ. Sci. Technol.* **2013**, 47 (3), 1646–1654.
- (78) McDevitt, J. P.; Criddle, C. S.; Morse, M.; Hale, R. C.; Bott, C. B.; Rochman, C. M. Addressing the Issue of Microplastics in the Wake of the Microbead-Free Waters Act - A New Standard Can Facilitate Improved Policy. *Environ. Sci. Technol.* **2017**, 51 (12), 6611–6617.
- (79) Karapanagioti, H. K.; Takada, H. *Hazardous Chemicals Associated with Plastics in the Marine Environment*; 2019.
- (80) Barnes, D. K. A.; Galgani, F.; Thompson, R. C.; Barlaz, M. Accumulation and Fragmentation of Plastic Debris in Global Environments. *Philos. Trans. R. Soc. B Biol. Sci.* **2009**, 364 (1526), 1985–1998.

- (81) Waters, C. N.; Zalasiewicz, J.; Summerhayes, C.; Barnosky, A. D.; Poirier, C.; Gałuszka, A.; Cearreta, A.; Edgeworth, M.; Ellis, E. C.; Ellis, M.; Jeandel, C.; Leinfelder, R.; McNeill, J. R.; Richter, D. D. B.; Steffen, W.; Syvitski, J.; Vidas, D.; Wagreich, M.; Williams, M.; Zhisheng, A.; Grinevald, J.; Odada, E.; Oreskes, N.; Wolfe, A. P. The Anthropocene Is Functionally and Stratigraphically Distinct from the Holocene. *Science* (80-. ). **2016**, *351* (6269).
- (82) Dris, R.; Gasperi, J.; Mirande, C.; Mandin, C.; Guerrouache, M.; Langlois, V.; Tassin, B. A First Overview of Textile Fibers, Including Microplastics, in Indoor and Outdoor Environments. *Environ. Pollut.* **2017**, *221*, 453–458.
- (83) Worm, B.; Lotze, H. K.; Jubinville, I.; Wilcox, C.; Jambeck, J. Plastic as a Persistent Marine Pollutant. *Annu. Rev. Environ. Resour.* **2017**, *42*, 1–26.
- (84) Bakir, A.; Rowland, S. J.; Thompson, R. C. Enhanced Desorption of Persistent Organic Pollutants from Microplastics under Simulated Physiological Conditions. *Environ. Pollut.* **2014**, *185*, 16–23.
- (85) Rochman, C.; Browne, M. A. Classify Plastic Waste as Hazardous. *Nature* **2013**, 6–8.
- (86) Sussarellu, R.; Suquet, M.; Thomas, Y.; Lambert, C.; Fabioux, C.; Pernet, M. E. J.; Goïc, N. Le; Quillien, V.; Mingant, C.; Epelboin, Y.; Corporeau, C.; Guyomarch, J.; Robbens, J.; Paul-Pont, I.; Soudant, P.; Huvet, A. Oyster Reproduction Is Affected by Exposure to Polystyrene Microplastics. *Proc. Natl. Acad. Sci. U. S. A.* **2016**, *113* (9), 2430–2435.
- (87) Environment and Climate Change Canada; Health Canada. Draft Science Assessment of Plastic Pollution. **2020**, No. January, 1–153.
- (88) Ragusa, A.; Svelato, A.; Santacroce, C.; Catalano, P.; Notarstefano, V.; Carnevali, O.; Papa, F.; Rongioletti, M. C. A.; Baiocco, F.; Draghi, S.; D’Amore, E.; Rinaldo, D.; Matta,

- M.; Giorgini, E. Plasticenta: First Evidence of Microplastics in Human Placenta. *Environ. Int.* **2021**, *146*.
- (89) Skoog, E.; Shin, J. H.; Saez-Jimenez, V.; Mapelli, V.; Olsson, L. Biobased Adipic Acid – The Challenge of Developing the Production Host. *Biotechnol. Adv.* **2018**, *36* (8), 2248–2263.
- (90) Debuissy, T.; Pollet, E.; Avérous, L. Synthesis of Potentially Biobased Copolyesters Based on Adipic Acid and Butanediols: Kinetic Study between 1,4- and 2,3-Butanediol and Their Influence on Crystallization and Thermal Properties. *Polymer (Guildf)*. **2016**, *99*, 204–213.
- (91) Tachibana, Y.; Kimura, S.; Kasuya, K. I. Synthesis and Verification of Biobased Terephthalic Acid from Furfural. *Sci. Rep.* **2015**, *5*, 1–5.
- (92) Siegenthaler, K. O.; Kunkel, A.; Skupin, G.; Yamamoto, M. Ecoflex and Ecovio: Biodegradable, Performance-Enabling Plastics. In *Synthetic Biodegradable Polymers*; Springer-Verlag, 2012; Vol. 245, pp 91–136.
- (93) Kabasci, S. *Bio-Based Plastics Materials and Applications*; John Wiley & Sons, Ltd, 2014.
- (94) BASF. Product Information for Ecoflex ® F Blend C1200. **2013**, 1–3.
- (95) BASF. Safety Data Sheet Ecoflex ® F Blend C1200. **2012**, 1–7.
- (96) Petrochemicals, M. O. L. Technical Data Sheet LDPE for Film. 2–5.
- (97) Rennert, M.; Nase, M.; Lach, R.; Reincke, K.; Arndt, S.; Androsch, R.; Grellmann, W. Influence of Low-Density Polyethylene Blown Film Thickness on the Mechanical Properties and Fracture Toughness. *J. Plast. Film Sheeting* **2013**, *29* (4), 327–346.
- (98) [https://www.engineeringtoolbox.com/young-modulus-d\\_417.html](https://www.engineeringtoolbox.com/young-modulus-d_417.html). Young's Modulus -



- Tensile and Yield Strength for Common Materials. 2018.
- (99) ASTM D6400. Standart Specification for Compostable Plastics. *Am. Soc. Test. Mater.* **2004**, 1–3.
- (100) European Bioplastics. EN13432 Certified Bioplastics Performance in Industrial Composting. **2015**, 1–5.
- (101) Standards for Compostable GreenPla Products. **2012**, 1–4.
- (102) Greene, J. *Degradation and Biodegradation Standards for Starch-Based and Other Polymeric Materials*; Elsevier B.V., 2014.
- (103) Liebenstein, A.; Manz, W.; Pesch, R.; Schmidt, G.; Schröder, W.; Wahrendorf, D. S. Miniaturisierung Des Wachstumshemmtestes Mit Der Grünalge *Desmodesmus Subspicatus* Nach DIN 38412 Teil 30. *Umweltwissenschaften und Schadstoff-forsch.* **2009**, 21 (6), 504–515.
- (104) Gigli, M.; Crestini, C. Fractionation of Industrial Lignins: Opportunities and Challenges. *Green Chem.* **2020**, 22 (15), 4722–4746.
- (105) Teng, N. Y.; Dallmeyer, I.; Kadla, J. F. Effect of Softwood Kraft Lignin Fractionation on the Dispersion of Multiwalled Carbon Nanotubes. *Ind. Eng. Chem. Res.* **2013**, 52 (19), 6311–6317.
- (106) Baker, D.; Gallego, N. C. On the Characterization and Spinning of an Organic Purified Lignin Toward the Manufacture of Low-Cost Carbon Fiber. *J. Appl. Polym. Sci.* **2010**, 116 (5), 227–234.
- (107) Morck, R.; Yoshida, H.; Kringstad, K. P.; Hatakeyama, H. Fractionation of Kraft Lignin by Successive Extraction with Organic Solvents. *Holzforschung* **1986**, 40 (2), 51–60.
- (108) Cui, C.; Sun, R.; Argyropoulos, D. S. Fractional Precipitation of Softwood Kraft Lignin:

- Isolation of Narrow Fractions Common to a Variety of Lignins. *ACS Sustain. Chem. Eng.* **2014**, 2 (4), 959–968.
- (109) Jiang, X.; Abbati de Assis, C.; Kollman, M.; Sun, R.; Jameel, H.; Chang, H.; Gonzalez, R. Lignin Fractionation from Laboratory to Commercialization: Chemistry, Scalability and Techno-Economic Analysis. *Green Chem.* **2020**, 7448–7459.
- (110) Saito, T.; Perkins, J. H.; Vautard, F.; Meyer, H. M.; Messman, J. M.; Tolnai, B.; Naskar, A. K. Methanol Fractionation of Softwood Kraft Lignin: Impact on the Lignin Properties. *ChemSusChem* **2014**, 7 (1), 221–228.
- (111) Duval, A.; Vilaplana, F.; Crestini, C.; Lawoko, M. Solvent Screening for the Fractionation of Industrial Kraft Lignin. *Holzforschung* **2016**, 70 (1), 11–20.
- (112) Boeriu, C. G.; Fițigău, F. I.; Gosselink, R. J. A.; Frissen, A. E.; Stoutjesdijk, J.; Peter, F. Fractionation of Five Technical Lignins by Selective Extraction in Green Solvents and Characterisation of Isolated Fractions. *Ind. Crops Prod.* **2014**, 62, 481–490.
- (113) Ajao, O.; Jeaidi, J.; Benali, M.; Abdelaziz, O. Y.; Hultberg, C. P. Green Solvents-Based Fractionation Process for Kraft Lignin with Controlled Dispersity and Molecular Weight. *Bioresour. Technol.* **2019**, 291, 1–9.
- (114) Ropponen, J.; Ra, L.; Rovio, S.; Mikkonen, H. Solvent Extraction as a Means of Preparing Homogeneous Lignin Fractions. *Holzforschung* **2011**, 65, 543–549.
- (115) Domínguez-Robles, J.; Tamminen, T.; Liitiä, T.; Peresin, M. S.; Rodríguez, A.; Jääskeläinen, A. S. Aqueous Acetone Fractionation of Kraft, Organosolv and Soda Lignins. *Int. J. Biol. Macromol.* **2018**, 106, 979–987.
- (116) Jääskeläinen, A. S.; Willberg-Keyriläinen, P.; Liitiä, T.; Tamminen, T. Carbohydrate-Free and Highly Soluble Softwood Kraft Lignin Fractions by Aqueous Acetone Evaporation

- Fractionation. *Nord. Pulp Pap. Res. J.* **2017**, 32 (4), 485–492.
- (117) Majdar, R. E.; Ghasemian, A.; Resalati, H.; Saraeian, A.; Crestini, C.; Lange, H. Case Study in Kraft Lignin Fractionation: “Structurally Purified” Lignin Fractions - The Role of Solvent H-Bonding Affinity.” *ACS Sustain. Chem. Eng.* **2020**, 8, 16803–16813.
- (118) Burke, J. *Solubility Parameters : Theory and Application*; 1984; Vol. 3.
- (119) Boiling Points of Common Organic Solvents. In *Chem-Lists*; Mulzer University, 2012; Vol. 66, pp 37–38.
- (120) Joshi, D. R.; Adhikari, N. An Overview on Common Organic Solvents and Their Toxicity. *J. Pharm. Res. Int.* **2019**, 28 (3), 1–18.
- (121) Laurichesse, S.; Avérous, L. Chemical Modification of Lignins: Towards Biobased Polymers. *Prog. Polym. Sci.* **2014**, 39 (7), 1266–1290.
- (122) Calvo-Flores, F. G.; Dobado, J. A.; Isac-García, J.; Martín-Martínez, F. J. Applications of Modified and Unmodified Lignins. In *Lignin and Lignans as Renewable Raw Materials: Chemistry, Technology, and Applications*; 2015; pp 250–287.
- (123) Goheen, D. W. Hydrogenation of Lignin by the Noguchi Process. In *Chemicals From Lignin*; 1966; pp 205–255.
- (124) Ragauskas, A. J.; Beckham, G. T.; Biddy, M. J.; Chandra, R. Lignin Valorization : Improving Lignin Processing in the Biorefinery. In *Science*; 2014; Vol. 344, pp 709–721.
- (125) Sergeev, A. G.; Hartwig, J. F. Selective , Nickel-Catalyzed Hydrogenolysis of Aryl Ethers. In *Science*; 2011; Vol. 332, pp 439–443.
- (126) Sels, B. F.; Renders, T.; Navare, K.; Nicolai, T.; Aelst, K. Van; Maesen, M.; Matsushima, H.; Thevelein, J. M.; Acker, K. Van; Lagrain, B.; Verboekend, D. A Sustainable Wood Biorefinery for Low – Carbon Footprint Chemicals Production. *J. Sci.* **2020**, 1390

- (March), 1385–1390.
- (127) Tarabanko, V. E.; Chelbina, Y. V. Separation of Vanillin and Syringaldehyde Produced from Lignins. *Sep. Sci. Technol.* **2013**, *48*, 127–132.
- (128) Tarabanko, V. E.; Tarabanko, N. Catalytic Oxidation of Lignins into the Aromatic Aldehydes : General Process Trends and Development Prospects. *Int. J. Mol. Sci.* **2017**, *18*, 1–29.
- (129) Yu, G.; Li, B.; Wang, H.; Liu, C.; Mu, X. Preparation of Concrete Superplasticizer by Oxidation- Sulfomethylation of Sodium Lignosulfonate. *BioResources* **2013**, *8* (1), 1055–1063.
- (130) Eraghi Kazzaz, A.; Hosseinpour Feizi, Z.; Fatehi, P. Grafting Strategies for Hydroxy Groups of Lignin for Producing Materials. *Green Chem.* **2019**, *21*, 5714–5752.
- (131) Glasser, W. G.; Barnett, C. A.; Rials, T. G.; Saraf, V. P. Engineering Plastics from Lignin II. Characterization of Hydroxyalkyl Lignin Derivatives. *J. Appl. Polym. Sci.* **1984**, *29* (5), 1815–1830.
- (132) Peng, W.; Riedl, B. The Chemorheology of Phenol-Formaldehyde Thermoset Resin and Mixtures of the Resin with Lignin Fillers. *Polymer (Guildf)*. **1994**, *35* (6), 1280–1286.
- (133) Talabi, S. I.; Luz, A. P. da; Pandolfelli, V. C.; Lima, V. H. Graphitization of Lignin-Phenol-Formaldehyde Resins. *Mater. Res.* **2020**, *23* (2), 1–13.
- (134) Chen, Y.; Zhang, H.; Zhu, Z.; Fu, S. High-Value Utilization of Hydroxymethylated Lignin in Polyurethane Adhesives. *Int. J. Biol. Macromol.* **2020**, *152*, 775–785.
- (135) Bertella, S.; Luterbacher, J. S. Lignin Functionalization for the Production of Novel Materials. *Trends Chem.* **2020**, *2* (5), 440–453.
- (136) Zhang, L.; Huang, J. Effects of Nitrolignin on Mechanical Properties of Polyurethane-

- Nitrolignin Films. *J. Appl. Polym. Sci.* **2001**, *80* (8), 1213–1219.
- (137) Graglia, M.; Pampel, J.; Hantke, T.; Fellingner, T. P.; Esposito, D. Nitro Lignin-Derived Nitrogen-Doped Carbon as an Efficient and Sustainable Electrocatalyst for Oxygen Reduction. *ACS Nano* **2016**, *10* (4), 4364–4371.
- (138) Du, X.; Li, J.; Lindström, M. E. Modification of Industrial Softwood Kraft Lignin Using Mannich Reaction with and without Phenolation Pretreatment. *Ind. Crops Prod.* **2014**, *52*, 729–735.
- (139) Wu, H.; Chen, F.; Feng, Q.; Yue, X. Oxidation and Sulfomethylation of Alkali-Extracted Lignin from Corn Stalk. *BioResources* **2012**, *7* (3), 2742–2751.
- (140) Zhao, W.; Xiao, L. P.; Song, G.; Sun, R. C.; He, L.; Singh, S.; Simmons, B. A.; Cheng, G. From Lignin Subunits to Aggregates: Insights into Lignin Solubilization. *Green Chem.* **2017**, *19* (14), 3272–3281.
- (141) Liu, Y.; Li, K. Preparation and Characterization of Demethylated Lignin-Polyethylenimine Adhesives. *J. Adhes.* **2006**, *82* (6), 593–605.
- (142) Nahmany, M.; Melman, A. Chemoselectivity in Reactions of Esterification. *Org. Biomol. Chem.* **2004**, *2* (11), 1563–1572.
- (143) Thielemans, W.; Wool, R. P. Lignin Esters for Use in Unsaturated Thermosets: Lignin Modification and Solubility Modeling. *Biomacromolecules* **2005**, *6* (4), 1895–1905.
- (144) Dehne, L.; Vila Babarro, C.; Saake, B.; Schwarz, K. U. Influence of Lignin Source and Esterification on Properties of Lignin-Polyethylene Blends. *Ind. Crops Prod.* **2016**, *86*, 320–328.
- (145) Luo, S.; Cao, J.; McDonald, A. G. Esterification of Industrial Lignin and Its Effect on the Resulting Poly(3-Hydroxybutyrate-Co-3-Hydroxyvalerate) or Polypropylene Blends. *Ind.*

- Crops Prod.* **2017**, *97*, 281–291.
- (146) Chiappero, L. R.; Bartolomei, S. S.; Estenoz, D. A.; Moura, E. A. B.; Nicolau, V. V. Lignin-Based Polyethylene Films with Enhanced Thermal, Opacity and Biodegradability Properties for Agricultural Mulch Applications. *J. Polym. Environ.* **2020**, 1–10.
- (147) Dai, Z.; Ren, P. G.; He, W.; Hou, X.; Ren, F.; Zhang, Q.; Jin, Y. L. Boosting the Electrochemical Performance of Nitrogen-Oxygen Co-Doped Carbon Nanofibers Based Supercapacitors through Esterification of Lignin Precursor. *Renew. Energy* **2020**, *162*, 613–623.
- (148) Teramoto, Y.; Lee, S. H.; Endo, T. Phase Structure and Mechanical Property of Blends of Organosolv Lignin Alkyl Esters with Poly( $\epsilon$ -Caprolactone). *Polym. J.* **2009**, *41* (3), 219–227.
- (149) Hult, E. L.; Koivu, K.; Asikkala, J.; Ropponen, J.; Wrigstedt, P.; Sipilä, J.; Poppius-Levlin, K. Esterified Lignin Coating as Water Vapor and Oxygen Barrier for Fiber-Based Packaging. *Holzforschung* **2013**, *67* (8), 899–905.
- (150) Gordobil, O.; Robles, E.; Egüés, I.; Labidi, J. Lignin-Ester Derivatives as Novel Thermoplastic Materials. *RSC Adv.* **2016**, *6* (90), 86909–86917.
- (151) Laurichesse, S.; Huillet, C.; Avérous, L. Original Polyols Based on Organosolv Lignin and Fatty Acids: New Bio-Based Building Blocks for Segmented Polyurethane Synthesis. *Green Chem.* **2014**, *16* (8), 3958–3970.
- (152) An, L.; Si, C.; Wang, G.; Choi, C. S.; Yu, Y. H.; Bae, J. H.; Lee, S. M.; Kim, Y. S. Efficient and Green Approach for the Esterification of Lignin with Oleic Acid Using Surfactant-Combined Microreactors in Water. *BioResources* **2020**, *15* (1), 89–104.
- (153) Liu, L. Y.; Hua, Q.; Renneckar, S. A Simple Route to Synthesize Esterified Lignin

- Derivatives. *Green Chem.* **2019**, *21* (13), 3682–3692.
- (154) Wu, L. C. F.; Glasser, W. G. Engineering Plastics from Lignin. I. Synthesis of Hydroxypropyl Lignin. *J. Appl. Polym. Sci.* **1984**, *29* (4), 1111–1123.
- (155) Hofmann, K.; Glasser, W. G. Engineering Plastics from Lignin. Synthesis and Properties of Epoxidized Lignin- Poly (Propylene Oxide) Copolymers. *J. Wood Chem. Technol.* **1993**, *13* (1), 73–95.
- (156) de Oliveria, W.; Glasser, W. G. Multiphase Materials with Lignin. Starlike Copolymers with Caprolactone. *Macromolecules* **1994**, *27* (1), 5–11.
- (157) Glasser, W. G.; Loos, R.; Cox, B.; Cao, H. Melt-Blown Compostable Polyester Films with Lignin. *Tappi J.* **2017**, *16* (3), 111–121.
- (158) Wei, M.; Fan, L.; Huang, J.; Chen, Y. Role of Star-like Hydroxypropyl Lignin in Soy-Protein Plastics. *Macromol. Mater. Eng.* **2006**, *291* (5), 524–530.
- (159) Cateto, C. A.; Barreiro, M. F.; Rodrigues, A. E.; Belgacem, M. N. Optimization Study of Lignin Oxypropylation in View of the Preparation of Polyurethane Rigid Foams. *Ind. Eng. Chem. Res.* **2009**, *48* (5), 2583–2589.
- (160) Muthuraj, R.; Horrocks, A. R.; Kandola, B. K. Hydroxypropyl-Modified and Organosolv Lignin/Bio-Based Polyamide Blend Filaments as Carbon Fibre Precursors'. *J. Mater. Sci.* **2020**, *55* (16), 7066–7083.
- (161) Li, Y.; Ragauskas, A. J. Kraft Lignin-Based Rigid Polyurethane Foam. *J. Wood Chem. Technol.* **2012**, *32* (3), 210–224.
- (162) Sadeghifar, H.; Cui, C.; Argyropoulos, D. S. Toward Thermoplastic Lignin Polymers. Part 1. Selective Masking of Phenolic Hydroxyl Groups in Kraft Lignins via Methylation and Oxypropylation Chemistries. *Ind. Eng. Chem. Res.* **2012**, *51* (51), 16713–16720.

- (163) Lora, J. H.; Glasser, W. G. Recent Industrial Applications of Lignin: A Sustainable Alternative to Nonrenewable Materials. *J. Polym. Environ.* **2002**, *10* (1–2), 39–48.
- (164) Cui, C.; Sadeghifar, H.; Sen, S.; Argyropoulos, D. S. Toward Thermoplastic Lignin Polymers; Part II: Thermal & Polymer Characteristics of Kraft Lignin & Derivatives. *BioResources* **2013**, *8* (1), 864–886.
- (165) Clements, J. H. Reactive Applications of Cyclic Alkylene Carbonates. *Ind. Eng. Chem. Res.* **2003**, *42* (4), 663–674.
- (166) Duval, A.; Avérous, L. Cyclic Carbonates as Safe and Versatile Etherifying Reagents for the Functionalization of Lignins and Tannins. *ACS Sustain. Chem. Eng.* **2017**, *5* (8), 7334–7343.
- (167) Liu, L. Y.; Cho, M.; Sathitsuksanoh, N.; Chowdhury, S.; Renneckar, S. Uniform Chemical Functionality of Technical Lignin Using Ethylene Carbonate for Hydroxyethylation and Subsequent Greener Esterification. *ACS Sustain. Chem. Eng.* **2018**, *6* (9), 12251–12260.
- (168) Sen, S.; Patil, S.; Argyropoulos, D. S. Methylation of Softwood Kraft Lignin with Dimethyl Carbonate. *Green Chem.* **2015**, *17* (2), 1077–1087.
- (169) Li, Y.; Mlynar, J.; Sarkanen, S. The First 85% Kraft Lignin-Based Thermoplastics. *J. Polym. Sci. Part B Polym. Phys.* **1997**, *35* (12), 1899–1910.
- (170) Glasser, W. G. Alkylated Kraft Lignin-Based Polymeric Materials. In *Lignin: Historical, biological, and materials perspectives*; American Chemical Society, 1999; pp 360–365.
- (171) Alexy, P.; Kosikova, B.; Podstranska, G. The Effect of Blending Lignin with Polyethylene and Polypropylene on Physical Properties. *Polymer (Guildf)*. **2000**, *41* (13), 4901–4908.
- (172) Nitz, H.; Semke, H.; Mülhaupt, R. Influence of Lignin Type on the Mechanical Properties of Lignin Based Compounds. *Macromol. Mater. Eng.* **2001**, *286* (12), 737–743.



- (173) Li, Y.; Sarkanen, S. Alkylated Kraft Lignin-Based Thermoplastic Blends with Aliphatic Polyesters. *Macromolecules* **2002**, *35* (26), 9707–9715.
- (174) Nagele, H.; Pfitzer, J.; Nagele, E.; Inone, E. R.; Eisenreic, N.; Eckl, W.; Eyerer, P. ARBOFORM - A Thermoplastic, Processable Material, from Lignin and Natural Fibers. In *Chemical Modification, Properties, and Usage of Lignin*; 2002; pp 101–119.
- (175) Toriz, G.; Denes, F.; Young, R. A. Lignin-Polypropylene Composites. Part 1: Composites from Unmodified Lignin and Polypropylene. *Polym. Compos.* **2002**, *23* (5), 806–813.
- (176) Toriz, G.; Ramos, J.; Young, R. A. Lignin-Polypropylene Composites. II. Plasma Modification of Kraft Lignin and Particulate Polypropylene. *J. Appl. Polym. Sci.* **2004**, *91* (3), 1920–1926.
- (177) Li, Y.; Sarkanen, S. Miscible Blends of Kraft Lignin Derivatives with Low-T<sub>g</sub> Polymers. *Macromolecules* **2005**, *38* (6), 2296–2306.
- (178) Sailaja, R. R. N.; Deepthi, M. V. Mechanical and Thermal Properties of Compatibilized Composites of Polyethylene and Esterified Lignin. *Mater. Des.* **2010**, *31* (9), 4369–4379.
- (179) Aradoaei, S.; Darie, R.; Constantinescu, G.; Olariu, M.; Ciobanu, R. Modified Lignin Effectiveness as Compatibilizer for PET/LDPE Blends Containing Secondary Materials. *J. Non. Cryst. Solids* **2010**, *356* (11–17), 768–771.
- (180) Feng, C.; Honghu, D.; Xiaoli, D.; Jintao, Y.; Mingquiang, Z. Physical Properties of Lignin-Based Polypropylene Blends. *Polym. Polym. Compos.* **2011**, *16* (2), 1019–1025.
- (181) Yue, X.; Chen, F.; Zhou, X.; He, G. Preparation and Characterization of Poly (Vinyl Chloride) Polyblends with Fractionated Lignin. *Int. J. Polym. Mater. Polym. Biomater.* **2012**, *61* (3), 214–228.
- (182) Gordobil, O.; Delucis, R.; Egüés, I.; Labidi, J. Kraft Lignin as Filler in PLA to Improve

- Ductility and Thermal Properties. *Ind. Crops Prod.* **2015**, 72, 46–53.
- (183) Tran, C. D.; Chen, J.; Keum, J. K.; Naskar, A. K. A New Class of Renewable Thermoplastics with Extraordinary Performance from Nanostructured Lignin-Elastomers. *Adv. Funct. Mater.* **2016**, 26 (16), 2677–2685.
- (184) Bova, T.; Tran, C. D.; Balakshin, M. Y.; Chen, J.; Capanema, E. A.; Naskar, A. K. An Approach towards Tailoring Interfacial Structures and Properties of Multiphase Renewable Thermoplastics from Lignin-Nitrile Rubber. *Green Chem.* **2016**, 18 (20), 5423–5437.
- (185) Dias, O. A. T.; Sain, M.; Cesarino, I.; Leão, A. L. Development of High Bio-Content Polypropylene Composites with Different Industrial Lignins. *Polym. Adv. Technol.* **2019**, 30 (1), 70–78.
- (186) Beaucamp, A.; Wang, Y.; Culebras, M.; Collins, M. N. Carbon Fibres from Renewable Resources: The Role of the Lignin Molecular Structure in Its Blendability with Biobased Poly(Ethylene Terephthalate). *Green Chem.* **2019**, 21 (18), 5063–5072.
- (187) Ge, X.; Chang, M.; Jiang, W.; Zhang, B.; Xing, R.; Bulin, C. Investigation on Two Modification Strategies for the Reinforcement of Biodegradable Lignin/Poly(Lactic Acid) Blends. *J. Appl. Polym. Sci.* **2020**, 137 (44), 1–13.
- (188) Dehne, L.; Vila, C.; Saake, B.; Schwarz, K. U. Esterification of Kraft Lignin as a Method to Improve Structural and Mechanical Properties of Lignin-Polyethylene Blends. *J. Appl. Polym. Sci.* **2017**, 134 (11), 1–8.
- (189) Sadeghifar, H.; Argyropoulos, D. S. Macroscopic Behavior of Kraft Lignin Fractions: Melt Stability Considerations for Lignin-Polyethylene Blends. *ACS Sustain. Chem. Eng.* **2016**, 4 (10), 5160–5166.

- (190) Xiong, S. J.; Pang, B.; Zhou, S. J.; Li, M. K.; Yang, S.; Wang, Y. Y.; Shi, Q.; Wang, S. F.; Yuan, T. Q.; Sun, R. C. Economically Competitive Biodegradable PBAT/Lignin Composites: Effect of Lignin Methylation and Compatibilizer. *ACS Sustain. Chem. Eng.* **2020**, 8 (13), 5338–5346.
- (191) Liu, L. Y.; Bessler, K.; Chen, S.; Cho, M.; Hua, Q.; Rennecker, S. In-Situ Real-Time Monitoring of Hydroxyethyl Modification in Obtaining Uniform Lignin Derivatives. *Eur. Polym. J.* **2020**, No. July.
- (192) Kargarzadeh, H.; Galeski, A.; Pawlak, A. PBAT Green Composites: Effects of Kraft Lignin Particles on the Morphological, Thermal, Crystalline, Macro and Micromechanical Properties. *Polymer (Guildf)*. **2020**, 203 (April), 1–11.
- (193) Lagerquist, L.; Rahkila, J.; Eklund, P. Utilization of <sup>31</sup>P PULCON for Quantitative Hydroxyl Group Determination in Lignin by NMR Spectroscopy. *ACS Sustain. Chem. Eng.* **2019**, 7 (9), 9002–9006.
- (194) Meng, X.; Crestini, C.; Ben, H.; Hao, N.; Pu, Y.; Ragauskas, A. J.; Argyropoulos, D. S. Determination of Hydroxyl Groups in Biorefinery Resources via Quantitative <sup>31</sup>P NMR Spectroscopy. *Nat. Protoc.* **2019**, 14 (9), 2627–2647.
- (195) Pu, Y.; Ragauskas, A. J.; Cao, S. Environmental Science Application of Quantitative <sup>31</sup>P NMR in Biomass Lignin and Biofuel Precursors Characterization. *Energy Environ. Sci.* **2011**, 4, 3154–3166.
- (196) Standard Test Method of Tensile Properties of Plastics Designation: D638-14. In *ASTM International*; 2015; Vol. 82, pp 1–17.
- (197) Smita, M.; Sanjay, N. Aromatic-Aliphatic Poly(Butylene Adipate-Co- Terephthalate) Bionanocomposite: Influence of Organic Modification on Structure and Properties. *Polym.*

- Polym. Compos.* **2009**, *16* (2), 1194–1204.
- (198) Sousa, J. C.; Arruda, S. A.; Lima, J. C.; Wellen, R. M. R.; Canedo, E. L.; De Almeida, Y. M. B. Crystallization Kinetics of Poly (Butylene Adipate Terephthalate) in Biocomposite with Coconut Fiber. *Rev. Mater.* **2019**, *24* (3), 1–17.
- (199) Bastarrachea, L.; Dhawan, S.; Sablani, S. S.; Mah, J. H.; Kang, D. H.; Zhang, J.; Tang, J. Biodegradable Poly(Butylene Adipate-Co-Terephthalate) Films Incorporated with Nisin: Characterization and Effectiveness against *Listeria Innocua*. *J. Food Sci.* **2010**, *75* (4), 215–224.
- (200) Cai, Y.; Lv, J.; Feng, J. Spectral Characterization of Four Kinds of Biodegradable Plastics: Poly (Lactic Acid), Poly (Butylenes Adipate-Co-Terephthalate), Poly (Hydroxybutyrate-Co-Hydroxyvalerate) and Poly (Butylenes Succinate) with FTIR and Raman Spectroscopy. *J. Polym. Environ.* **2013**, *21* (1), 108–114.
- (201) Stark, N. M.; Yelle, D. J.; Agarwal, U. P. Techniques for Characterizing Lignin. *Lignin Polym. Compos.* **2016**, 49–66.
- (202) Zinovyev, G.; Sulaeva, I.; Podzimek, S.; Rössner, D.; Kilpeläinen, I.; Summerskii, I.; Rosenau, T.; Potthast, A. Getting Closer to Absolute Molar Masses of Technical Lignins. *ChemSusChem* **2018**, *11* (18), 3259–3268.
- (203) Ji, L. Characterization of Lignin Molar Mass and Molecular Conformation by Multi-Angle Light Scattering, 2019.
- (204) Sadeghifar, H.; Ragauskas, A. Perspective on Technical Lignin Fractionation. *ACS Sustain. Chem. Eng.* **2020**, *8* (22), 8086–8101.
- (205) Karaaslan, M. A.; Cho, M.; Liu, L.-Y.; Wang, H.; Renneckar, S. Refining the Properties of Softwood Kraft Lignin with Acetone: Effect of Solvent Fractionation on the

- Thermomechanical Behavior of Electrospun Fibers. *ACS Sustain. Chem. Eng.* **2021**, *9*, 458–470.
- (206) Crestini, C.; Lange, H.; Sette, M.; Argyropoulos, D. S. On the Structure of Softwood Kraft Lignin. *Green Chem.* **2017**, *19* (17), 4104–4121.
- (207) Kubo, S.; Kadla, J. F. Hydrogen Bonding in Lignin: A Fourier Transform Infrared Model Compound Study. *Biomacromolecules* **2005**, *6* (5), 2815–2821.
- (208) Cho, M. Electrospinning of Lignin Based Composite Nanofibres With Nanocrystalline Celluloses, 2018.
- (209) Faix, O.; Rodrigues, J.; Pereira, H. Determination of Lignin Content of Eucalyptus Globulus Wood Using FTIR Spectroscopy. *Holzforschung* **1998**, *52* (1), 46–50.
- (210) Shi, F.; Zhao, H.; Liu, G.; Ross, P. N.; Somorjai, G. A.; Komvopoulos, K. Identification of Diethyl 2,5-Dioxahexane Dicarboxylate and Polyethylene Carbonate as Decomposition Products of Ethylene Carbonate Based Electrolytes by Fourier Transform Infrared Spectroscopy. *J. Phys. Chem. C* **2014**, *118* (27), 14732–14738.
- (211) Brežný, R.; Mihalov, V.; Kováčik, V. Low Temperature Thermolysis of Lignins -I. Reactions of  $\beta$ -O-4 Model Compounds. *Holzforschung* **1983**, *32*, 199–204.
- (212) Kun, D.; Pukánszky, B. Polymer/Lignin Blends: Interactions, Properties, Applications. *Eur. Polym. J.* **2017**, *93* (April 2017), 618–641.
- (213) Chen, R.; Abdelwahab, M. A.; Misra, M.; Mohanty, A. K. Biobased Ternary Blends of Lignin, Poly(Lactic Acid), and Poly(Butylene Adipate-Co-Terephthalate): The Effect of Lignin Heterogeneity on Blend Morphology and Compatibility. *J. Polym. Environ.* **2014**, *22* (4), 439–448.
- (214) Wang, H. M.; Wang, B.; Yuan, T. Q.; Zheng, L.; Shi, Q.; Wang, S. F.; Song, G. Y.; Sun,

- R. C. Tunable, UV-Shielding and Biodegradable Composites Based on Well-Characterized Lignins and Poly(Butylene Adipate-: Co-Terephthalate). *Green Chem.* **2020**, 22 (24), 8623–8632.
- (215) Maldhure, A. V.; Ekhe, J. D.; Deenadaylan, E. Mechanical Properties of Polypropylene Blended with Esterified and Alkylated Lignin. *J. Appl. Polym. Sci.* **2012**, 116 (5), 1701–1712.
- (216) Ouyang, W.; Huang, Y.; Luo, H.; Wang, D. Poly(Lactic Acid) Blended with Cellulolytic Enzyme Lignin: Mechanical and Thermal Properties and Morphology Evaluation. *J. Polym. Environ.* **2012**, 20 (1), 1–9.
- (217) Zhou, X.; Mohanty, A.; Misra, M. A New Biodegradable Injection Moulded Bioplastic from Modified Soy Meal and Poly (Butylene Adipate-Co-Terephthalate): Effect of Plasticizer and Denaturant. *J. Polym. Environ.* **2013**, 21 (3), 615–622.
- (218) Bova, T.; Tran, C. D.; Balakshin, M. Y.; Chen, J.; Capanema, E. A.; Naskar, A. K. An Approach towards Tailoring Interfacial Structures and Properties of Multiphase Renewable Thermoplastics from Lignin-Nitrile Rubber. *Green Chem.* **2016**, 18 (20), 5423–5437. <https://doi.org/10.1039/c6gc01067a>.
- (219) Galeja, M.; Hejna, A.; Kosmela, P.; Kulawik, A. Static and Dynamic Mechanical Properties of 3D Printed ABS as a Function of Raster Angle. *Materials (Basel)*. **2020**, 13 (2).
- (220) Maphutha, S.; Moothi, K.; Meyyappan, M.; Iyuke, S. E. A Carbon Nanotube-Infused Polysulfone Membrane with Polyvinyl Alcohol Layer for Treating Oil-Containing Waste Water. *Sci. Rep.* **2013**, 3.
- (221) Hilburg, S. L.; Elder, A. N.; Chung, H.; Ferebee, R. L.; Bockstaller, M. R.; Washburn, N.

- R. A Universal Route towards Thermoplastic Lignin Composites with Improved Mechanical Properties. *Polymer (Guildf)*. **2014**, 55 (4), 995–1003.
- (222) Sun, J.; Wang, C.; Stubbs, L. P.; He, C. Carboxylated Lignin as an Effective Cohardener for Enhancing Strength and Toughness of Epoxy. *Macromol. Mater. Eng.* **2017**, 302 (12), 1–8.
- (223) Lou, C.; Xu, J.; Liu, S.; Wang, T.; Ren, W. Effects of External Environments on the Fixed Elongation and Tensile Properties of the VAE Emulsion-Cement Composite Joint Sealant. *Materials (Basel)*. **2020**, 13 (14).
- (224) Maldhure, A. V.; Chaudhari, A. R.; Ekhe, J. D. Thermal and Structural Studies of Polypropylene Blended with Esterified Industrial Waste Lignin. *J. Therm. Anal. Calorim.* **2011**, 103 (2), 625–632.
- (225) Wilkes, G. L. Polymers, Mechanical Behavior. In *Encyclopedia of Physical Science and Technology*; 2002; pp 697–721.
- (226) Yarusso, D. J. The Mechanics of Adhesion - Polymer Characterization. *Adhes. Sci. Eng.* **2002**, 1, 499–533.
- (227) Wang, B.; Utzeri, R.; Castellano, M.; Stagnaro, P.; Müller, A. J.; Cavallo, D. Heterogeneous Nucleation and Self-Nucleation of Isotactic Polypropylene Microdroplets in Immiscible Blends: From Nucleation to Growth-Dominated Crystallization. *Macromolecules* **2020**, 53 (14), 5980–5991.
- (228) Lin, Z.; Renneckar, S. Nanocomposite-Based Lignocellulosic Fibers 2: Layer-by-Layer Modification of Wood Fibers for Reinforcement in Thermoplastic Composites. *Compos. Part A Appl. Sci. Manuf.* **2011**, 42 (1), 84–91.
- (229) Hammer, A. DSC Analysis of Thermoplastics. In *Thermal Analysis of Polymers*; 2010; pp

10–15.

- (230) Berlin, H. U. of. Investigation of Polymers with Differential Scanning Calorimetry. In *Advanced Lab: DSC Investigation of Polymers*; 2009; pp 1–17.
- (231) Tavares, L. B.; Ito, N. M.; Salvadori, M. C.; dos Santos, D. J.; Rosa, D. S. PBAT/Kraft Lignin Blend in Flexible Laminated Food Packaging: Peeling Resistance and Thermal Degradability. *Polym. Test.* **2018**, 67 (January), 169–176.
- (232) Kubo, S.; Kadla, J. F. Lignin-Based Carbon Fibers: Effect of Synthetic Polymer Blending on Fiber Properties. *J. Polym. Environ.* **2005**, 13 (2), 97–105.
- (233) Pouteau, C.; Baumberger, S.; Cathala, B.; Dole, P. Lignin-Polymer Blends: Evaluation of Compatibility by Image Analysis. *Comptes Rendus - Biol.* **2004**, 327 (9–10), 935–943.
- (234) Steiner, T.; Koellner, G. Hydrogen Bonds with  $\pi$ -Acceptors in Proteins: Frequencies and Role in Stabilizing Local 3D Structures. *J. Mol. Biol.* **2001**, 305 (3), 535–557.
- (235) Polymer stress-strain curve <https://www.doitpoms.ac.uk/tlplib/polymers/stress-strain.php>.



## Appendices

### Appendix A Supporting calculations

#### A.1 Moisture content

44.66% moisture content (for as received Grade A Lignoforce softwood kraft lignin)

$$\text{Lignin (150g)} = m(1 - 0.4466)$$

$$m_{\text{lignin dry weight}} = \frac{150g}{(1 - 0.4466)}$$

$$m_{\text{lignin dry weight}} = 271.05g$$

$$m_{\text{water}} = 1500g - (m_{\text{lignin dry weight}} - 150g)$$

$$m_{\text{water}} = 1500g - (271.05g - 150g)$$

$$m_{\text{water}} = 1378.95g = 1400 \text{ mL distilled water for 150g lignin}$$

#### A.2 Ethylene carbonate

$$\text{Molar mass of EC} = 88 \text{ g/mol}$$

$$\left[ (\text{AROH} + \text{COOH}) \frac{\text{mmol}}{g} * 15g \text{ lignin} * 88 \frac{g}{\text{mol}} * \frac{1 \text{ mol}}{1000 \text{ mmol}} \right]$$

$$= \text{necessary grams EC for reaction} * 15$$

where 15 is excess amount of EC

### A.3 Real time control

The theoretical molar amount of CO<sub>2</sub> was calculated based on the change of ArOH and COOH groups. It was assumed that the molar amount of ArOH and COOH groups is equal to the sum of the molar amount of these groups in modified lignin and the molar amount of CO<sub>2</sub> produced.<sup>191</sup>

$$m * [N]_u = \left( m + 44 * m * \frac{[N]_{tg}}{1000} \right) * [N]_m + m * [N]_{tg}$$

Where m is the weight of unmodified lignin (g), [N]<sub>u</sub> is the molar sum of ArOH + COOH groups in unmodified lignin (mmol/g), [N]<sub>tg</sub> is the theoretical molar amount of gas (mmol/g), [N]<sub>m</sub> is the molar sum of ArOH + COOH in modified lignin (mmol/g) and the molar mass of hydroxyethyl is 44 g/mol. It was shown in the real time control manuscript that the actual amount of CO<sub>2</sub> [N]<sub>ag</sub> (mmol/g) had a linear correlation with the theoretical amount of CO<sub>2</sub> [N]<sub>tg</sub> (mmol/g).<sup>191</sup>

$$[N]_{ag} = 0.7487 * [N]_{tg} + 0.3269$$

Using the ideal gas law PV=nRT, the molar amount of CO<sub>2</sub> can be converted to volume for a specific weight of lignin. The atmosphere pressure (P) in Vancouver, BC is 102.2 kPa, (V) is the volume of CO<sub>2</sub> (mL), R is the gas constant 8.314 J/(mol\*K), the absolute temperature (T) is room temperature (296.14K), and n is the molar amount of CO<sub>2</sub> (mol). By combining these equations, the resulting equation is used to predict the actual amount of CO<sub>2</sub> (V) (mL) necessary to complete the modification:

$$V = 1.804 * 10^4 * m * \frac{[N]_u - [N]_m}{44 * [N]_m + 1000} + 7.875 * m$$

For all samples m=15g. The UF\_UN [N]<sub>u</sub>=4.55 mmol/g and the [N]<sub>m</sub>=0.006, the AIKL\_UN [N]<sub>u</sub>=4.03 mmol/g and the [N]<sub>m</sub>=0.009, and the ASKL\_UN [N]<sub>u</sub>=5.6 mmol/g and the [N]<sub>m</sub>=0.006.

#### A.4 <sup>31</sup>P NMR functional groups

$$\text{Density of IS} = 179.173 \frac{g}{mL}$$

$$\text{Concentration of IS} = 10 \frac{mg}{mL}$$

$$\text{Amount of IS} = 100\mu L$$

$$\text{Mass of same (m)} \sim 20 \text{ mg}$$

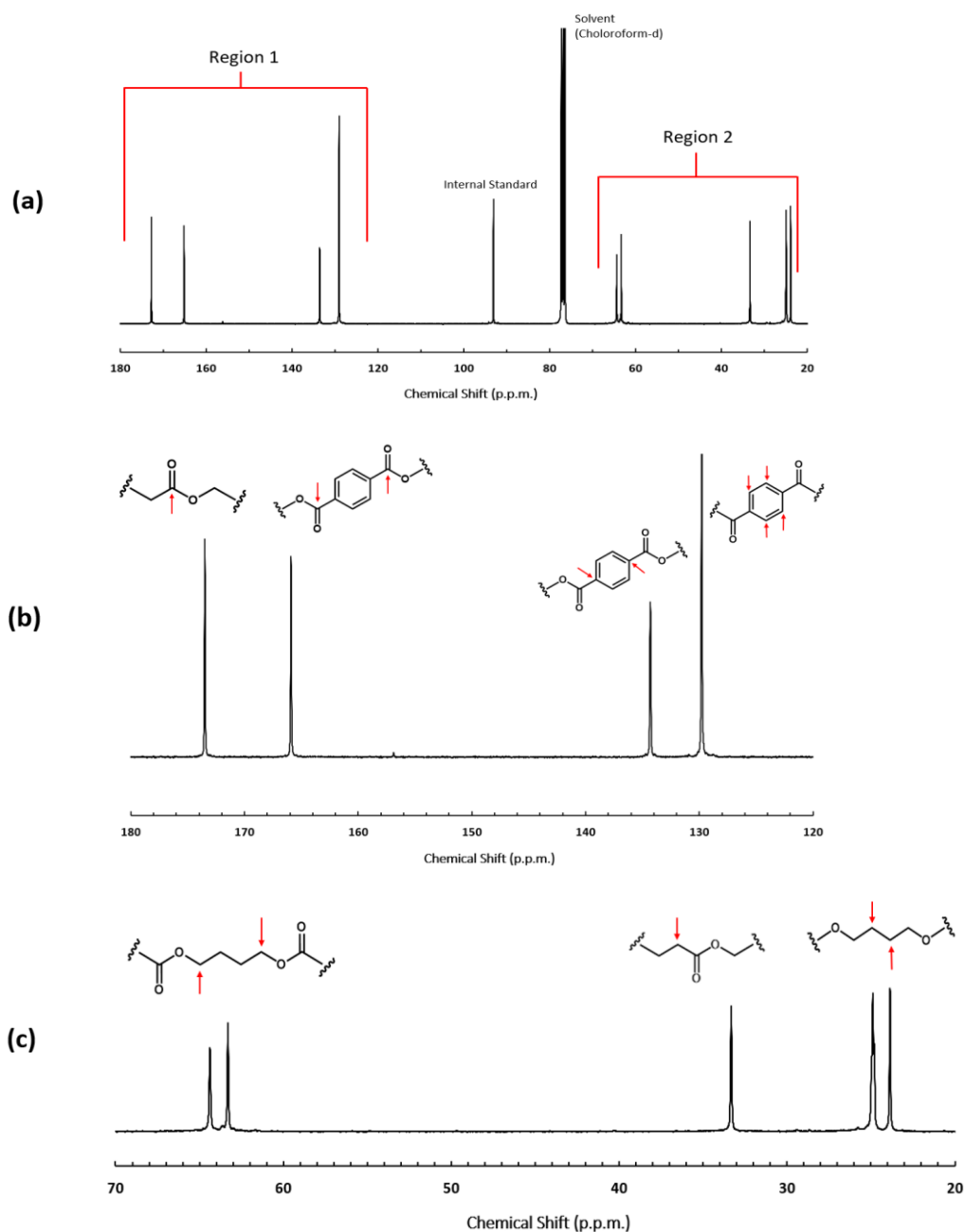
$$R = \frac{I_{OH}}{I_{NHMD}} = \frac{\text{Integration of spectral region of interest}}{\text{Integration of NHND region}}$$

**Table 24 Chemical shifts used for qualitative <sup>31</sup>P NMR analysis of lignin functional groups**

Lignin functional group	Chemical Shift (p.p.m.)
Aliphatic OH (AlOH)	~145.4-150.0
Phenolic OH (ArOH)	~137.6-144.0
Carboxylic acid OH (COOH)	~133.6-136.0
C5 condensed aromatics	~140-145

$$AlOH, ArOH, COOH \left( \frac{mmol}{g} \right) = \frac{R * 100 * 10}{179.173} \frac{1}{m}$$

## Appendix B $^{13}\text{C}$ NMR spectrum for as received Ecoflex<sup>TM</sup> blend F C1200

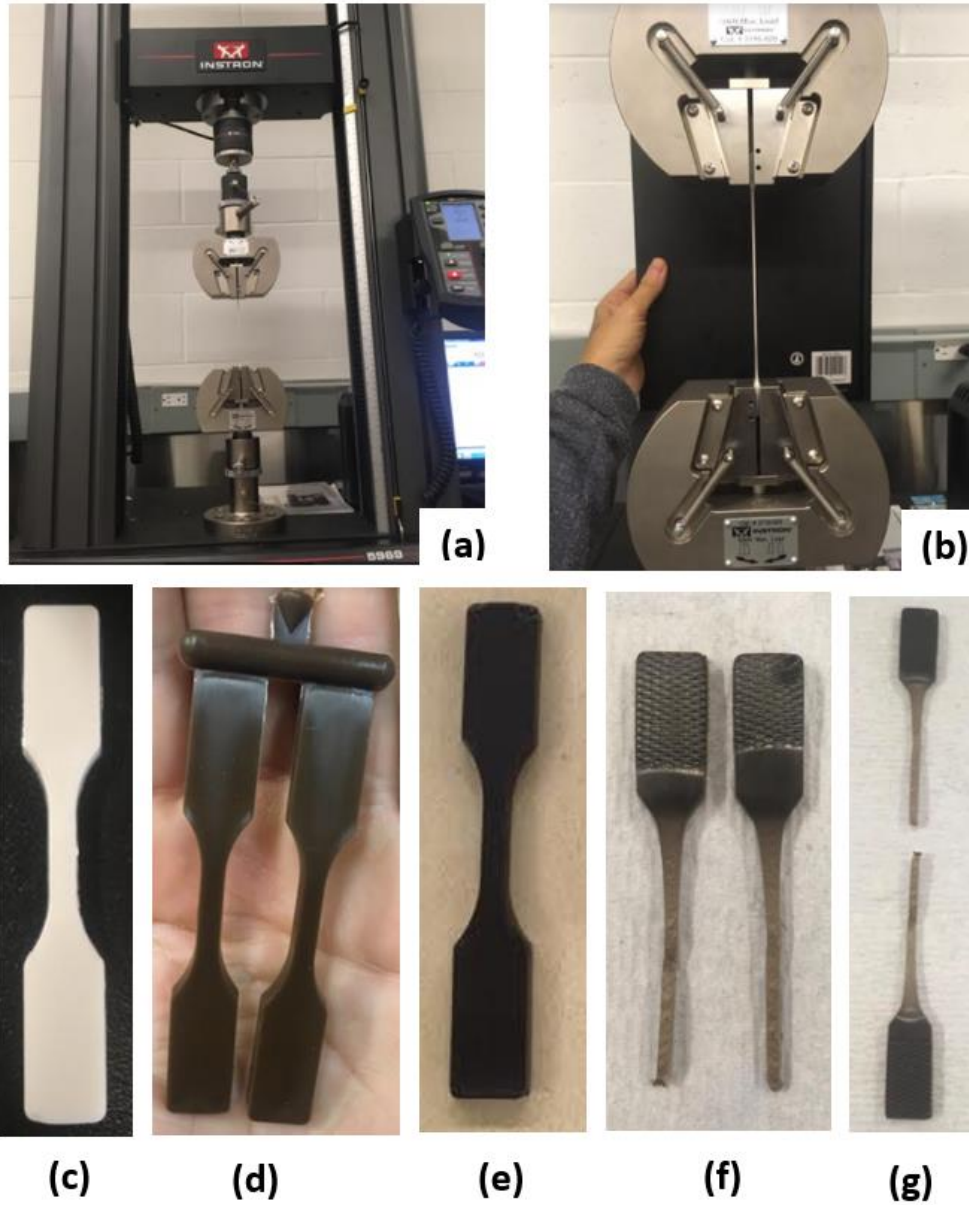


**Figure 82** Complete  $^{13}\text{C}$  NMR spectra for as received Ecoflex<sup>TM</sup> (a), the enlarged region 1 with structures and specific carbons pointed out (b) and the enlarged region 2 with structures and specific carbons pointed out (c) used to confirm the Ecoflex<sup>TM</sup> chemical structure prior to melt-processing

## Appendix C Melt processing equipment and sample imagery



**Figure 83** Overall equipment set up used to make lignin-Ecoflex™ thermoplastic blends (a), the twin screws used for melt processing (b), and the mould used for dumbbell shaped specimens (c)



**Figure 84 Instron load frame used for tensile testing (a), the grips elongating neat Ecoflex™ in vertical test direction (b) neat Ecoflex™ type V dumbbell shaped specimen (c), 10 wt% ASKL\_UN – Ecoflex™ thermoplastic blend after mould injection (d), 40 wt% ASKL\_E – Ecoflex™ thermoplastic blend after mould injection and removed from top piece (e), fracture of 40 wt% ASKL\_E – Ecoflex™ thermoplastic blend after tensile testing (f) and fracture of 40 wt% ASKL\_E – Ecoflex™ thermoplastic blend after tensile testing (g)**